Methods in Molecular Biology 1109

Springer Protocols

Meral Beksaç *Editor*

# Bone Marrow and Stem Cell Transplantation

*Second Edition*

Humana Press

# METHODS IN MOLECULAR BIOLOGY

*Series Editor*
**John M. Walker**
**School of Life Sciences**
**University of Hertfordshire**
**Hatfield, Hertfordshire, AL10 9AB, UK**

For further volumes:
http://www.springer.com/series/7651

# Bone Marrow and Stem Cell Transplantation

## Second Edition

Edited by

**Meral Beksaç**

*Department of Hematology, School of Medicine, Ankara University, Ankara, Turkey*

Humana Press

*Editor*
Meral Beksaç
Department of Hematology
School of Medicine
Ankara University
Ankara, Turkey

ISSN 1064-3745 ISSN 1940-6029 (electronic)
ISBN 978-1-4614-9436-2 ISBN 978-1-4614-9437-9 (eBook)
DOI 10.1007/978-1-4614-9437-9
Springer New York Heidelberg Dordrecht London

Library of Congress Control Number: 2013955604



Printed on acid-free paper

Humana Press is a brand of Springer
Springer is part of Springer Science+Business Media (www.springer.com)

# Preface

Hematopoietic stem cells have been introduced to treatment of more than 40 diseases and are being used successfully, thanks to the developments in molecular techniques and biotechnology. Recognition of the histocompatibility complex and development of immunosuppressive drugs constitute the major steps leading to almost 50,000 transplants worldwide every year. However perfect donor–recipient matching requires typing at non-HLA loci and natural killer cell receptors too. The purpose of this book when published in 2007 was to gather molecular methods related to stem cell transplantation from hematopoietic stem cell molecular profiling to in vivo tracking, donor–recipient matching and post-transplant monitorization as well from molecular genetics to proteomics under one roof. In the following years, stem cells have become the core of regenerative medicine, and the scope of stem cell transplantation has expanded from transplantation of hematopoietic stem cells to transplantation of progenitors of many non-hematopoietic tissues, i.e., neurons, myocardium, bone, and cartilage. Furthermore today, differentiated cells can be de-differentiated to behave as embryonic stem cells. In this era, there is a need to update the first edition. Thus we have revised the continuously evolving transplantation immunology methods on HLA, minor-HLA, and Killer Immunoglobulin-Like Receptor Typing. In addition, new chapters on immunophenotyping and functional characterization of stem cells are included. Suffice to say, the authors are eminent experts in this field and we are grateful for their most valuable contributions. Also I need to acknowledge the editorial assistance of Dr. Pinar Yurdakul.

This book may serve as a guide in the application of molecular methods for routine or investigational purposes. As spoken by M. K. Atatürk 80 years ago in Ankara "The truest guide in life is Science." We hope that the book will be a reference for scientists who are planning to start or are already advanced in stem cell transplantation studies. Every effort towards optimal use of stem cells will bring hope to patients who are in desperate need.

*Ankara, Turkey* *Meral Beksaç*

# Contents

# Contributors


Amaya Albalat • *BHF Glasgow Cardiovascular Research Centre, University of Glasgow, Glasgow, UK*

J. Alejandro Madrigal • *Anthony Nolan Research Institute, University College London, London, UK*

Meral Beksaç • *Department of Hematology, School of Medicine, Ankara University, Ankara, Turkey*

Cristiana Carniti • *Division of Hematology, Bone Marrow Transplantation Unit, Fondazione IRCCS Istituto Nazionale Tumori Milano, University of Milano, Milan, Italy*

Sule Colakoglu • *Department of Microbiology and Clinical Microbiology, Baskent University Faculty of Medicine Adana Hospital, Adana, Turkey*

Christopher H. Contag • *Department of Pediatrics, Stanford University School of Medicine, Stanford, CA, USA*

Paolo Corradini • *Division of Hematology, Fondazione IRCCS Istituto Nazionale Tumori Milano, University of Milano, Milan, Italy*

Klara Dalva • *Department of Hematology, Tissue Typing Laboratories, Ibni Sina Hospital, Ankara University, Ankara, Turkey*

Michelle E. DeLelys • *Department of Pathology, Massachusetts General Hospital, Boston, MA, USA*

Richard Charles Duggleby • *Anthony Nolan Research Institute, Royal Free Hospital, London, UK*

Y. Murat Elçin • *Faculty of Sciences and Stem Cell Institute, Ankara University, Ankara, Turkey*

A. Eser Elçin • *Faculty of Sciences and Stem Cell Institute, Ankara University, Ankara, Turkey*

Ahmet H. Elmaagacli • *Department of Bone Marrow Transplantation, University Hospital of Essen, Hufelandstr, Germany*

Michelle Escobedo-Cousin • *Anthony Nolan Research Institute, University College London, London, UK*

Katia Gagne • *Etablissement Français du Sang and Université de Nantes, Immunovirologie et Polymorphisme Génétique, Nantes, France*

Daniela S. Krause • *Department of Pathology, Massachusetts General Hospital, Boston, MA, USA*

Sophie Kusy • *Department of Pediatrics, Stanford University School of Medicine, Stanford, CA, USA*

Katy Latham • *Anthony Nolan Research Institute, University College London, London, UK*

Thomas Lion • *Children's Cancer Research Institute (CCRI), Vienna, Austria*

Ann-Margaret Little • *Histocompatibility and Immunogenetics, Greater Glasgow and Clyde, Gartnavel General Hospital, Glasgow, UK*

Steven G.E. Marsh • *Laboratoire HLA-EFS, Nantes, France*

William Mullen • *BHF Glasgow Cardiovascular Research Centre, University of Glasgow, Glasgow, UK*
Sedat Odabas • *Faculty of Sciences and Stem Cell Institute, Ankara University, Ankara, Turkey*
Fausto Palusci • *Department of Transplantation Immunology, Tissue Typing Laboratory, Maastricht University Medical Center, Maastricht, The Netherlands*
Frederic I. Preffer • *Department of Pathology, Massachusetts General Hospital, Boston, MA, USA*
Sandra Preuner • *Children's Cancer Research Institute (CCRI), Vienna, Austria*
Aurore Saudemont • *Anthony Nolan Research Institute, University College London, London, UK*
Jennifer Schellekens • *Anthony Nolan Research Institute and UCL Cancer Institute, London, UK*
Eric Spierings • *Laboratory for Translational Immunology, University Medical Center Utrecht, Utrecht, The Netherlands*
Marcel G.J. Tilanus • *Department of Transplantation Immunology, Tissue Typing Laboratory, Maastricht University Medical Center, Maastricht, The Netherlands*
Christina E.M. Voorter • *Department of Transplantation Immunology, Tissue Typing Laboratory, Maastricht University Medical Center, Maastricht, The Netherlands*
Eva M. Weissinger • *Department of Hematology, Hannover Medical School, Hemostasis and Oncology, Hannover, Germany*
Pinar Yurdakul • *Ankara University Faculty of Medicine, Cord Blood Bank, Ankara, Turkey*

# Chapter 1

# Reporter Gene Technologies for Imaging Cell Fates in Hematopoiesis

**Sophie Kusy and Christopher H. Contag**

## Abstract

Advances in noninvasive imaging technologies that allow for in vivo dynamic monitoring of cells and cellular function in living research subjects have revealed new insights into cell biology in the context of intact organs and their native environment. In the field of hematopoiesis and stem cell research, studies of cell trafficking involved in injury repair and hematopoietic engraftment have made great progress using these new tools. Stem cells present unique challenges for imaging since after transplantation, they proliferate dramatically and differentiate. Therefore, the imaging modality used needs to have a large dynamic range, and the genetic regulatory elements used need to be stably expressed during differentiation. Multiple imaging technologies using different modalities are available, and each varies in sensitivity, ease of data acquisition, signal to noise ratios (SNR), substrate availability, and other parameters that affect utility for monitoring cell fates and function. For a given application, there may be several different approaches that can be used. For mouse models, clinically validated technologies such as magnetic resonance imaging (MRI) and positron emission tomography (PET) have been joined by optical imaging techniques such as in vivo bioluminescence imaging (BLI) and fluorescence imaging (FLI), and all have been used to monitor bone marrow and stem cells after transplantation into mice. Photoacoustic imaging that utilizes the sound created by the thermal expansion of absorbed light to generate an image best represents hybrid technologies. Each modality requires that the cells of interest be marked with a genetic reporter that acts as a label making them uniquely visible using that technology. For each modality, there are several labels to choose from. Multiple methods for applying these different labels are available. This chapter provides an overview of the imaging technologies and commonly used labels for each, as well as detailed protocols for gene delivery into hematopoietic cells for the purposes of applying these specific labels to cell trafficking. The goal of this chapter is to provide adequate background information to allow the design and implementation of an experimental system for in vivo imaging in mice.

**Key words** Molecular imaging, Hematopoiesis, Bioluminescence, Reporter genes, Transcription, Biophotonic imaging

## 1 Introduction

In vivo imaging of labeled transplanted cells has made it possible to observe cell movement and to visualize cell function over time in the intact animal. Previous techniques have required sacrificing animals in order to analyze specific tissues and tissue compartments

Meral Beksaç (ed.), *Bone Marrow and Stem Cell Transplantation*, Methods in Molecular Biology, vol. 1109,
DOI 10.1007/978-1-4614-9437-9_1, © Springer Science+Business Media New York 2014

of interest for the presence of the rare labeled cells. Although these sorts of analyses certainly have yielded valuable information, their two major limitations are (1) each animal can only be analyzed at a single time point and (2) tissues of interest must be preselected such that potentially informative data on cell trafficking in other regions is lost. Alternatively, biopsies can be taken to address the first limitation; however, the second limitation remains. Sampling limitations exist for all ex vivo assays, and the lack of temporal information can introduce biases into a study. Therefore, a number of investigators have been developing and advancing novel noninvasive imaging approaches that can be performed repeatedly in a given animal over time. The use of such approaches in our group has revealed features of biological processes that were unexpected including the apparent tropism of *Listeria monocytogenes* to the lumen of the gall bladder, an otherwise sterile environment [1]; the restriction of which malignant cells metastasize and the unique sites of metastasis [2]; and the dynamic nature of hematopoietic reconstitution during the earliest stages after stem cell transplantation (Figs. 1 and 2) [3]. In the stem cell studies, it was observed that transplantation of a single hematopoietic stem cell would result in a single focus of engraftment and expansion; however, some of these foci led to reconstitution and others did not (Fig. 2). These types of discoveries are only possible because of the ability to make longitudinal observations of the whole mouse after the transfer of labeled cells.

A number of powerful imaging techniques have been described and are now being used to understand when, where, and which cells move, in many different mouse models of human biology and disease, and what cells do under a given set of circumstances. Imaging has been applied to the study of injury repair, infectious processes, host response to infection, hematopoietic reconstitution, tumor vascularization, response to chemotherapy, and antitumor immune response. This chapter will focus on the labeling and imaging of murine bone marrow cells for the purpose of transplantation and analysis using in vivo imaging technologies. These types of studies can serve as a demonstration of how imaging can improve the study of biology and reveal the nuances of complex biological processes and the subtlety of therapeutic responses.

### 1.1 Imaging Modalities

Several imaging modalities have been used for the investigation of stem cell fates and function, and a number of useful tools have been developed by each of these [4]. The ideal imaging modality is the one that has excellent spatial resolution and cell detection sensitivity, can guide the delivery of cells, and can serially follow stem cells and their fates and function. Currently, no such imaging modality exists. An appropriate imaging modality therefore needs to be selected based on the question that is being asked and the

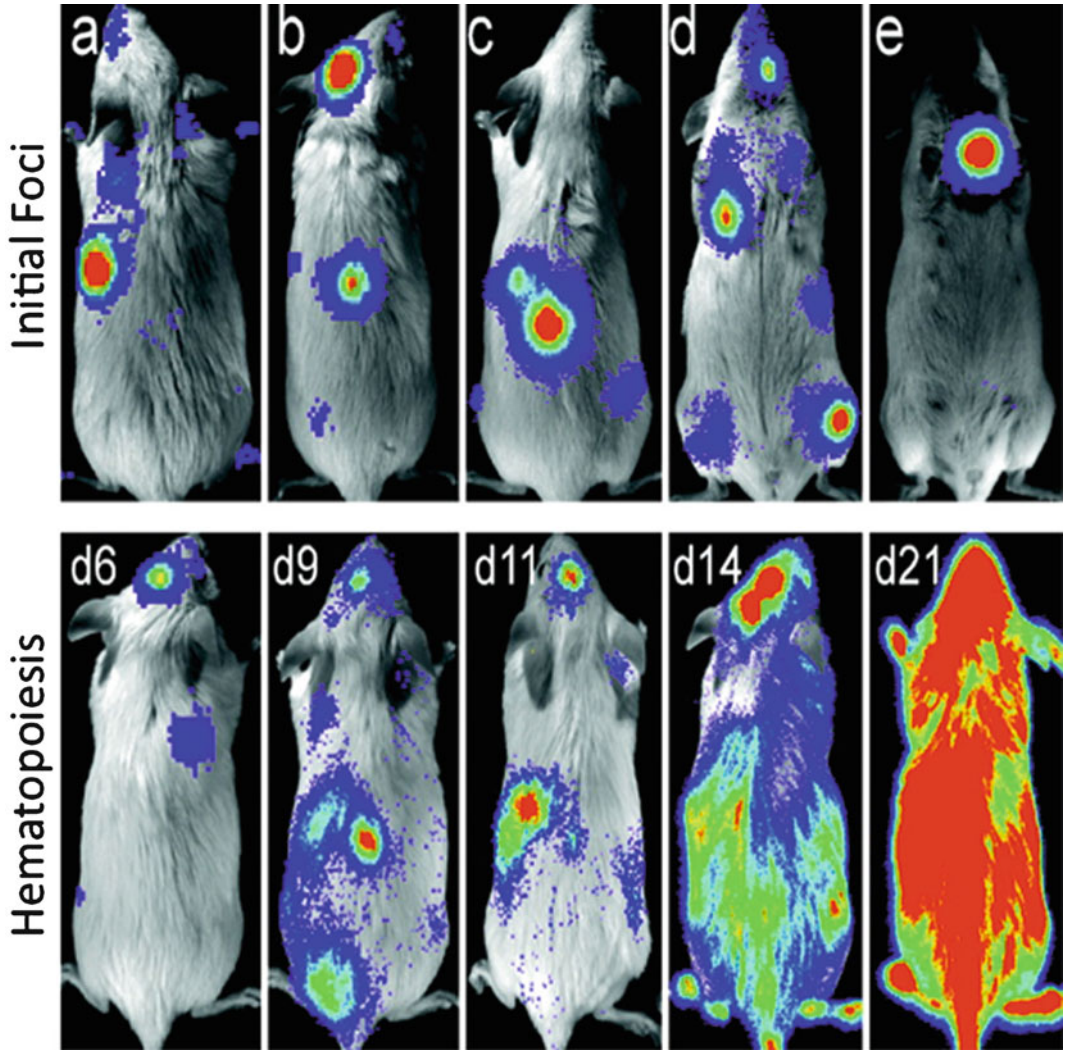


**Fig. 1** Location of bioluminescent foci following transplantation of transgenic luc+ hematopoietic stem cells. Foci were apparent in individual animals at anatomic sites corresponding to the location of the spleen, skull, vertebrae, femurs, and sternum (**a**–**e**, respectively) at 6–9 days after transfer. The patterns of engraftment were dynamic with formation and expansion or formation and loss of the bioluminescent foci. One recipient of 250 HSCs that was monitored over time is shown (*second row*). In this animal, two initial foci were apparent on day 6. By day 9, one was no longer detectable and another remained at nearly the same intensity as on day 6. New foci were apparent on day 9, and then the intensity at these sites weakened or disappeared by day 11. Pseudo-colored images reflecting optical signal intensity are overlaid upon a gray scale reference image of the animal. (Reproduced from Ref. [3], with permission)

nature of the study. For example, is the objective of the study to image the delivery and short-term homing of stem cell or to perform a long-term monitoring of stem cells viability? Other consideration, will this approach only be used in animal models or is there a need to extend this to human studies? Images of bone marrow and immune cell trafficking have been obtained by magnetic

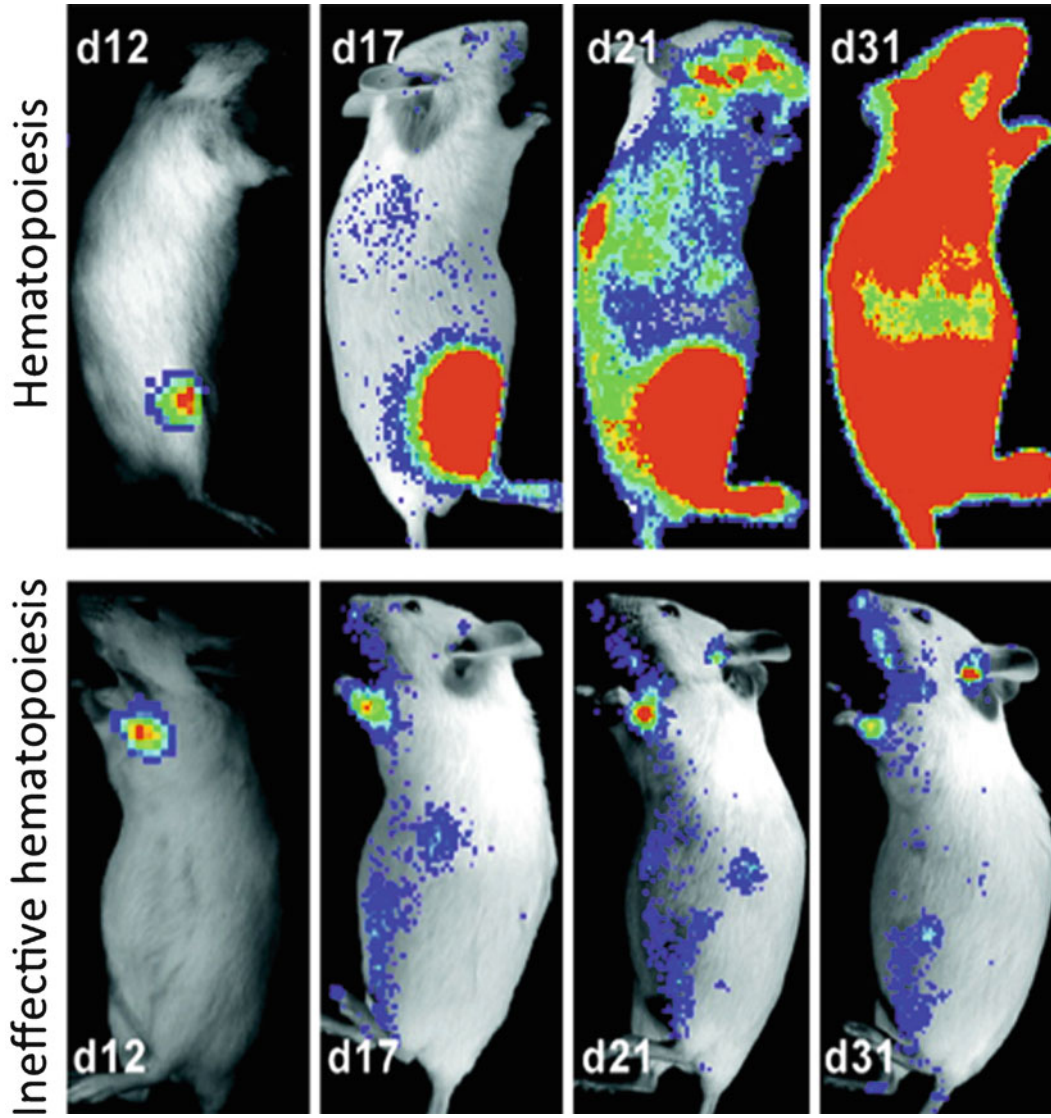


**Fig. 2** Temporal analyses of hematopoiesis following single cell transplants. These mice demonstrate the variability in contribution to reconstitution that was observed following the establishment of initial foci of hematopoietic engraftment after transplantation of single transgenic luc+ hematopoietic stem cells. Pseudo-colored images reflecting optical signal intensity are overlaid upon a gray scale reference image of the animal. (Reproduced from Ref. [3], with permission)

resonance imaging (MRI), positron emission tomography (PET), and single-photon emission computed tomography (SPECT) [5–8]. Each of these is used clinically for diagnostic applications and could be used for stem cell tracking and function. The availability of specialized MRI, PET, and SPECT scanners for small animal imaging has increased dramatically as well as the performance and capabilities of these tools. Their increased use in animal models will likely

lead to translational approaches, and they hold great promise for advances in a number of fields where there are clinical needs. In vivo bioluminescence (BLI) and fluorescence imaging have their greatest application in the study of small animal models and have been used to assess the trafficking patterns of cells in vivo [1, 3, 9]. There are a number of additional optical imaging approaches that have been developed for sensing and imaging in the living body, including diffuse optical tomography (DOT) and optical coherence tomography (OCT), but only in vivo BLI and fluorescence have been used to study long-term cell trafficking patterns, and these are amenable to reporter gene approaches. Despite the strengths of each of the available imaging modalities, the relatively greater accessibility, ease of use, and throughput capabilities have contributed greatly to the widespread use of BLI for animal studies. BLI is now routinely used as an initial step in the development of novel cell transfer protocols, and once the efficacy of the protocol is established, the BLI data serve as a guide for its adaptation into the clinic. Clinically, however, useful imaging modalities do not typically include optical imaging approaches.

One strategy for MR imaging of transplanted cells is based on the concept of the imaging of highly magnetic particles, named super paramagnetic iron oxide (SPIOs). In a direct labeling strategy, SPIOs are incorporated into the cells prior to transplantation to the living subject, and MRI is performed. This technique uses magnetic fields and radio frequency pulses to induce and measure signals from hydrogen atoms in the body. The image resolution is excellent in animal and human subjects, but the sensitivity to molecular changes is in the micromolar range and may not be sensitive enough to detect low signal levels from small numbers of cells [10]. MRI can be used to label stem cells for their localization immediately after delivery [11], but it is not well suited for long-term stem cell monitoring due to the dilution of the label through cell division and retention of magnetic particles in cells of the reticuloendothelial system [10]. That is, the particles may not stay in the transplanted cells over time but rather be taken up by macrophages [12].

PET and SPECT imaging can be performed on cells after the direct introduction of a radiolabel into the cells prior to transplantation. Recently, these techniques have been applied to the labeling of stem cells, using different isotopes (e.g., $^{18}$F-Fluoro-Dexyglucose ($^{18}$F-FDG) for PET, $^{111}$In for SPECT) [13–16]. Use of isotopes like $^{18}$F-FDG may allow tracking of cells for 6–8 h after transplantation, while use of $^{111}$In may allow cell tracking longer periods of time (up to 14 days). One of the major advantages of SPECT and PET imaging is their high sensitivity (nano- and femto-molar, respectively), which permits the detection of relatively low amounts of signal [17–19]. However, SPECT and PET have relatively low spatial resolution, which may be a relative disadvantage for signal

**Table 1**
**Commonly used, and emerging, genetically encoded reporter proteins and their corresponding reporter probes or substrates**

| Modality | Label | Reporter probe |
|---|---|---|
| MRI | Transferrin, ferritin | Magnetic iron oxides |
| | Lysine rich protein (LRP) | None |
| | Cytosine deaminase | 5-Fluorocytosine |
| | Tyrosinase | Iron (Fe) |
| PET/SPECT | HSV1-tk | [$^{124}$I]-FIAU, [$^{131}$I]-FIAU, [$^{18}$F]-FHBG |
| | $D_2R$ | [$^{18}$F]-FESP |
| | NIS | $^{123}$I, $^{124}$I, $^{125}$I, $^{131}$I, $B^{18}F_4$(tetrafluoroborate), $^{99m}TcO_4$ or $^{94m}TcO_4$(pertechnetate), $^{188}ReO_4$ or $^{186}ReO_4$(perrhenate), $^{211}$At(astatide) |
| | hSSTR2 | [$^{131}$I]-DTPA |
| BLI | Fluc | D-luciferin |
| | CBRluc | D-luciferin |
| | Rluc | Coelenterazine |
| | Gluc | Coelenterazine |
| | NanoLuc | Furimazine (coelenterazine analog) |
| Fluorescence | Fluorescent proteins (e.g., GFP) | Excitation light |
| Photoacoustic | Beta galactosidase | X-gal |
| | Tyrosinase | Fe |
| | Ferritin | Fe |

localization. The recent development of integrated PET-computed tomography (CT) and SPECT-CT provides a better anatomical guide for the location of the detected signal [20, 21]. The use of PET- and SPECT-based reporter genes (*see* Table 1) may compensate for the short half-lives of the isotope used for imaging, and the development of reporter genes is an area of intense investigation.

Whole-body imaging using bioluminescence and fluorescence is possible for small animal models of human physiology and disease. In general, these technologies are rapid and sensitive, and they can be used with molecular markers that are quite versatile. BLI is typically used to generate planar projection data and is displayed as pseudo-colored images to represent signal intensity that is localized over gray scale reference images of the subjects (Figs. 1 and 2). Optimal detection of bioluminescent or fluorescent signals requires the use of imaging systems that are sensitive to the weak signals that escape the scattering and absorbing environment of the mammalian body. These systems are typically based on charge-coupled device (CCD) detectors and lenses that operate in the visible to near-infrared regions of the spectrum. Anatomic resolution is relatively poor in whole-body images, but when necessary, a high-magnification

lens can be directed at sites in the body where labeled cells have been localized by whole-body imaging to produce high-resolution images that complement the lower resolution images taken noninvasively of the whole animal. This intravital microscopy approach has been published for a number of cell trafficking studies, and tremendous insights have been gained in this manner [22–27]. The lack of radioactivity and relatively lower costs make optical modalities more accessible and more available technologies for studies in small animal models. Moreover, significant efforts are being devoted to the development of tomographic BLI, either by rotating the subject under study or detecting light using two or more cameras or by spectral imaging [28, 29]. Efforts to generate tomographic fluorescence-based images have been reported [30–32]. In addition, novel developments, such as time-domain imaging, incorporate the time domain in the analysis and have the potential to provide in-depth information of the fluorescent signal [33–35].

### 1.2 Labels

In order to be tracked using any of the imaging modalities, cells of interest must be labeled for detection. A number of studies have used exogenous fluorescent dyes to label cells outside the body prior to transplantation (i.e., fluorescent semiconductor nanocrystals, known as quantum dots [36], or different fluorophores [37]). Although these dyes can have a relatively intense signal, a disadvantage of such techniques is that these dyes can be short-lived, and as labeled cells divide, the progeny cells, depending on the dye, may not be labeled and thus the signal is lost over time due to dilution through cell division. Some fluorescent dyes do not produce sufficient signal to be detectable by cameras placed outside the body, necessitating euthanasia of the animal and tissue sampling for analysis. For these reasons, the in vivo imaging techniques, by and large, have required the application of genetic labels. These "labels" are genes that must be introduced into cells and encode proteins that interact with "reporter probes," applied substrates (bioluminescence), or exogenous excitation light sources (fluorescence) to generate a signal that can be localized from outside the body (*see* Table 1).

MRI-based reporter genes are based on the production of proteins, mostly intracellular metalloproteins (transferrin, ferritin—*see* Table 1) [38]. They have high affinity for iron, leading to increased relaxivity that can be monitored by MR imaging. The signal is based on the accumulation of iron in the transfected cells, which may result in toxicity to the cell, and it gets diluted when cells divide. Tyrosinase and cytosine deaminase have also been used as an MR reporter gene (*see* Table 1).

There are predominantly three reporter gene systems for PET or SPECT that have been used for cell imaging (*see* Table 1). The most commonly used is the herpes simplex virus thymidine kinase (HSV1-tk). At the time of imaging, [$^{18}$F]-FHBG or [$^{124}$I]-FIAU is administered to the animal as a radioactive reporter probe that has

specificity for this TK enzyme. The probe is transported into cells and is phosphorylated by the TK protein only in the genetically labeled cells. The phosphorylated probe becomes trapped in the transfected cell and accumulates there, preferentially flagging the genetically labeled cells for detection. Because it has a viral origin, it has the potential to trigger an immunological response, resulting in a reaction in the organism with decreased overall signal. Attempts to circumvent this problem have included use of a mammalian mitochondrial tk [39], or a destabilized HSV1-tk [40]. A second reporter gene imaging strategy is based on the imaging of dopamine receptor using PET ($D_2R$ wild type [41] or $D_2R$ mutant [42, 43] version). The reporter gene encodes for a cell membrane protein that binds to an exogenously given probe ($^{18}$F-FESP), and the bound probe is imaged with PET. A third approach consists on the encoding of the sodium-iodide symporter (NIS) [44–48]. NIS is a thyroid transmembrane protein that transports iodine into the cells in exchange for sodium. It can be used for PET (with $^{124}$I) and SPECT (with $^{123}$I) imaging. Other less frequent reporter genes include the somatostatin receptor (hSSTR2), neurotensin receptor subtypes, and cytosine deaminase.

Bioluminescence optical imaging modalities require the generation of light by the cells of interest. Genetic labels for BLI are genes that encode luciferases. The reporter probes for these proteins are substrates that are oxidized and chemically consumed by the luciferases in reactions that generate light. In choosing a label for optical imaging, a few key parameters must be considered. Specifically, absorption and substrate biodistribution significantly influence the behavior of the experimental system. In the intact animal, absorption of light by tissue, and in particular absorption by hemoglobin, attenuates the detectable signal generated by cells of interest. Red and infrared light (wavelengths >600 nm) suffers less signal attenuation in the body due to absorption than does light with shorter wavelengths (<600 nm). This is an advantage to firefly luciferase (Fluc; derived from the North American firefly *Photinus pyralis*) and click beetle red luciferase (CBRluc; derived from *Pyrophorus plagiophalam*) over Renilla luciferase (Rluc; derived from the sea pansy *Renilla reniformis*) and Gaussia luciferase (Gluc; derived from the copepod *Gaussia princeps*). A related enzyme to Gluc called NanoLuc has also been recently reported [49], and an alternate substrate was described for use with this enzyme [49]. Both Fluc and CBRluc show emission peaks at approximately 620 nm at body temperature (37 °C), whereas the emission peak of Rluc and Gluc is at 480 nm, in a region where absorption by hemoglobin is relatively high. Recently, red-shifted Rluc variants have been developed with increased light emission with slight improvement sensitivity and detection capabilities, but the shift was not sufficient to extend beyond the hemoglobin absorption peak [50]. No red-shifted Gluc mutants have been reported;

however, there are brighter variants with a prolonged half-life [51–53]. An advantage of Renilla and Gaussia luciferases is the fact that they do not require ATP as a cofactor during bioluminescent reaction and thus can be used for imaging cells independent of their metabolic state.

The biodistribution of the administered substrate is also an important consideration for interpreting BLI data. To obtain quantitative information from BLI data, the substrate must not be limiting in the oxidation reaction that generates light. Therefore, proper imaging technique requires appropriate timing from the administration of substrate to the acquisition of data. The optimal time from administration to acquisition depends upon both the route of administration and the rate of clearance of the substrate in the body. The substrate for Fluc and CBRluc, D-luciferin, is relatively stable in the body and has a relatively long circulation time. It can be injected intraperitoneally or intravenously [54], and its biodistribution peaks at 15–20 min with a bioluminescence signal relatively stable for another 15–20 min before degrading as a result of substrate clearance. In contrast, the substrate for Rluc, Gluc, and NanoLuc, coelenterazine, is rapidly cleared from the body and binds to serum proteins [55]. Therefore, it can only be administered intravenously, and data acquisition must be complete within a few seconds to a minute after injection, since the peak of light emission occurs at about 1 min and decreases rapidly [56]. Challenges in designing dual-reporter systems, such as finding adequate means for separating the two bioluminescent signals while retaining sensitivity, remain [57–60]. BLI has been recently used for tracking and monitoring different types of stem cells after transplantation, such as hematopoietic stem cells (HSCs) [61] and embryonic stem cells [62, 63].

Fluorescence imaging, like detection of any optical signal through mammalian tissues, also requires consideration of light absorption by tissues. In this case, the wavelengths of both the excitation source and emitted light must be considered. The most commonly used genetic label for fluorescence imaging is enhanced green fluorescent protein (eGFP). The excitation and emission peaks for eGFP occur well below 600 nm, and light at these wavelengths is subject to severe signal attenuation by hemoglobin. Moreover, whole-body imaging of labeled cells in deep tissues can be difficult, and the use of fluorescent reporter gene imaging is usually restricted to the imaging of superficial tissues (up to 2 mm) such as skin and subcutaneous tissues [64–66]. Several fluorescent proteins with longer emission wavelengths are available (i.e., yellow-green fluorescent proteins mCitrine, Venus and YPet; red fluorescent proteins mCherry and tdTomato; far-red protein mPlum), but these have excitation peaks below 600 nm [67]. For these reasons, detection of these labels for deep tissue in vivo fluorescence imaging requires high levels of reporter gene expression

from a large number of cells. Despite limited penetration of light through tissues, an advantage of fluorescent reporter genes is that there is a range of different fluorescent proteins and dyes that can be used to label different cell populations permitting concomitant imaging of different cell populations and cell functions [68]. Multiplexing is limited in vivo and perhaps the important application of fluorescent reporter genes in cell tracking is the confirmatory ex vivo analysis, when they are used for cell sorting or histology. The creation of a triple fusion reporter gene that has a fluorescent reporter gene, a bioluminescent reporter gene, and a PET reporter gene, resulting in a fusion protein [69, 70], enables multimodality imaging and validation. Indeed, mouse embryonic stem cells have been engineered, using the fluorescent protein mRFP to identify the cells that have been effectively transduced with the fusion protein (using fluorescent-activated cell sorting), and then those cells were transplanted to the myocardium [62, 71]. Subsequently, the bioluminescent Fluc and PET reporter gene HSV1-tk were used for long-term monitoring of cell viability after transplantation [62, 71]. Using a similar approach to the one previously described (bi- or trifusion genes), one can label cells with a fluorescent reporter gene, and then, when the tissue is excised, the remaining cells can be easily identified using histological methods. Combinations of probes and indicators can link cell culture in vivo and ex vivo analysis for a more complete description of cell tracking.

Recent works have also suggested a new approach to imaging X-gal reporter gene expression in vivo using photoacoustic tomography (PAT) based on optical absorption [72, 73].

Imaging enables the in vivo study of cell biology and, when integrated with thorough studies in culture and ex vivo analyses, can reveal the nuances of disease mechanisms and therapeutic responses. Visible animal models of human biology and disease comprise one of the most important contributions of molecular imaging to human health as they serve to accelerate and refine the analyses of mammalian biology and offer rapid readouts for the development of new therapies.

### 1.3 Strategies

There are several strategies for introducing genetic labels into cells of interest for the purpose of tracking using in vivo imaging techniques. Different cells are variably amenable to the different labeling methods so the appropriate labeling method for any given experimental system will vary based on the cell types involved. This chapter includes detailed protocols for retroviral and lentiviral transduction. Although other methods, such as electroporation and liposome-mediated transfection, have been tried, viral transduction and transgenesis have proven to be the most effective methods for labeling bone marrow cells.

Labeling cells using classical transgenesis involves the generation of a plasmid encoding the genetic label of interest driven by an appropriate promoter. The plasmid is stably transfected (using conventional methods such as electroporation or liposome-mediated or calcium phosphate-mediated transfection) into an embryonic stem cell line, and those cells are microinjected into murine blastocysts. The blastocysts are transferred into pseudopregnant females, and chimeric pups are selected and bred until the transgene is found in all progeny tissues. This process can be time-consuming and labor intensive and usually requires the technical expertise of an available transgenic core facility. Genetic labels applied in this way exhibit a relatively predictable expression pattern but can be subject to the vagaries of random chromosomal integration. They may integrate into a site that is subject to transcriptional regulation that is not dictated by the originally designed plasmid. This is a so-called founder effect or contextual influence and is best screened for by examining the behavior of the transgene in multiple sibling chimeric lines.

Retroviral transduction is accomplished by replication-incompetent viral vectors that insert the genetic label directly into the genome of the target cell. The genetic label is first cloned into a plasmid that contains the viral packaging sequence (ψ) and promoter sequences (long terminal repeat [LTR] sequences). The plasmid is then transfected into a packaging cell line. The packaging line is a cell line that has been stably transfected with genes for viral envelope and packaging proteins. When these proteins are present in the same cell as DNA flagged with the ψ packaging sequence, viral particles are generated that contain the genetic label. Because the genes encoding envelope and packaging proteins are not present in the segment of DNA that is flagged by the viral packaging sequence, they are not included in the resulting viral particles. Those particles are, thus, replication-incompetent. Once they have infected a target cell, they insert the appropriate DNA into the target genome, and then, because no packaging or envelope proteins are present in the target cell, no further virus is generated.

An alternative to using a stably transfected "viral packaging cell line" is to use a second plasmid that contains only the genes encoding envelope and packaging proteins. This second plasmid can be co-transfected along with the plasmid containing the genetic label into an unmodified highly transfectable cell line of choice (e.g., 293T, as the lentiviral transduction protocol below uses). In the cells that receive both plasmids, the presence of ψ-flagged DNA along with envelope and packaging proteins leads to the generation of viral particles. As with the stably transfected packaging line, the fact that the genes encoding envelope and packaging proteins are not present on the ψ-flagged DNA means that those genes will not be included in the viral particles and will not be present in the target cell. Again, no virus will be generated in the target cell, but the genetic label will be inserted into its genome.

Retroviral and lentiviral transduction protocols are available, and an example of each is included in this chapter. The retroviral transduction protocol is optimized for mouse bone marrow and stem cells, and the lentiviral transduction protocol is specific for sorted HSCs. Both human and mouse cells can be transplanted into mice for optical imaging of cell trafficking patterns, but the human cells must be transplanted into immunocompromised mice (e.g., severe combined immunodeficient [SCID]-hu). Although lentiviral transduction can be used to label murine bone marrow cells, retroviral transduction systems have been used more extensively with mouse cells, and the reagents are readily available. On the opposite, human HSCs are less amenable to retroviral transduction, and the best success with transduction of human HSCs has been achieved using lentiviral systems.

The disadvantage to using retroviral transduction is that retroviral particles are only able to insert their DNA into the genomes of cells that are actively dividing. Protocols for retroviral labeling of bone marrow cells are thus carefully optimized for activation and stimulation of HSCs while preventing lineage differentiation. Lentiviral transduction systems do not require the target cells to be in cycle so are more appropriate for labeling cells that may not be actively dividing. However, if the target cells are HSCs, the same issues of maintaining the cells in culture while preventing lineage differentiation still arise. Genetic labels applied through viral transduction (either retroviral or lentiviral) have the advantage of being easier to apply than transgenic labels. The disadvantage is the unpredictable impact of cell culture and viral transduction on the biological behavior of the target cells.

## 2 Materials

### *2.1 Retroviral Transduction of Murine Bone Marrow and Stem Cells*

1. 5-Fluorouracil (5-FU; for human injection), American Pharmaceutical Partners, Inc. NDC 63323-117-10 (50 mg/mL, 10 mL). Stock concentration 25 mg/mL in phosphate-buffered saline (PBS), aliquot, and store at –20 °C.
2. Retroviral packaging cell line.
3. Retroviral expression plasmid.
4. Lipofectamine 2000 transfection reagent (Invitrogen, cat. no. 11668-027) (0.75 mL) (*see* **Note 1**).
5. Opti-MEM I reduced serum medium (Invitrogen, cat. no. 31985-070) (500 mL).
6. RBC lysing buffer (Sigma, cat. no. R7757) (100 mL).
7. rmIL-3 (Peprotech, cat. no. 213-13 (10 μg). Stock concentration 100 μg/mL in sterile water, aliquot, and store at –20 °C.
8. rmIL-6 (Peprotech, cat. no. 216-16 (10 μg). Stock concentration 100 μg/mL in sterile water, aliquot, and store at –20 °C.

9. rmSCF (Peprotech, cat. no. 250-03 (10 μg). Stock concentration 100 μg/mL in sterile water, aliquot, and store at –20 °C.
10. Fetal calf serum, heat inactivated to 56 °C for 45 min (Invitrogen, cat. no. 16000-044) (500 mL).
11. Dulbecco's modified Eagle's medium (DMEM; Invitrogen, cat. no. 10569-010) (500 mL), or StemSpan SFEM (Stem Cell Technologies, cat. no. 09650) (500 mL).
12. Hexadimethrine bromide (polybrene; Aldrich, cat. no. 107689-100G). Stock concentration 5 mg/mL in PBS, store at 4 °C.
13. HEPES buffer solution (1 M; Invitrogen, cat. no. 15630-080) (100 mL).

### 2.2 Lentiviral Transduction of Human HSCs and Progenitor Cells

1. Highly transfectable cell line to be used as packaging cells. This protocol describes conditions optimized for 293T cells.
2. Growth media for packaging cells. For 293T: DMEM with 10 % heat-inactivated fetal bovine serum, 100 U/mL penicillin and 100 U/mL streptomycin, 2 mM L-glutamine, 50 μg/mL 2-mercaptoethanol.
3. Calcium phosphate transfection kit (Invitrogen, cat. no. K2780-01) (*see* **Note 2**).
4. Lentiviral expression plasmid (e.g., pWPTS, pWPXL, pWPI, pLVTH).
5. Lentiviral packaging plasmid (e.g., pCMV-dR8.91, pCMV-dR8.74, psPAX2).
6. Lentiviral envelope plasmid (e.g., pMD2G).
7. Hexadimethrine bromide (polybrene; Aldrich, cat. no. 107689-100G). Stock concentration 5 mg/mL in PBS, store at 4 °C.
8. Myelocult H5100 media (Stem Cell Technologies, cat. no. 05150) (500 mL).
9. rh IL-6 (R&D Systems, cat. no. 206-IL-050) (50 μg).
10. rh TPO (R&D Systems, cat. no. 288-TP-025) (25 μg).
11. rh Flt-3L (R&D Systems, cat. no. 308-FKN-025) (25 μg).
12. rh SCF (R&D Systems, cat. no. 255-SC-050) (50 μg).

### 2.3 Bone Marrow Transplantation into Mice

1. Irradiation source for use with mice.
2. Mouse irradiation chamber (Shadel, Inc., cat. no. 62419).
3. Labeled bone marrow cells in PBS.
4. 28-Gage, one-half-inch, 1 cc/U-100 insulin syringes (Becton-Dickenson, cat. no. 329424).
5. Heating lamp/restraining device.
6. Trimethoprim/Sulfamethoxazole suspension (40 mg Trimethoprim and 200 mg Sulfamethoxazole/5 cc), (Hi-Tech Pharmacal, cat. no. NDC 50383-823-16) (200 mL).

### 2.4 Bioluminescence Imaging (See Note 3)

1. Low-light imaging system for BLI.
2. Anesthetic agent.
3. Substrate:
   (a) Luciferin (Biosynth, Int, cat. no. L-8220; 1 g). Stock concentration 30 mg/mL in PBS, aliquot, and store at –20 °C.
   (b) Coelenterazine (Nanolight, cat. no. NFCTZFB; 5 mg). Stock concentration 10 mg/mL in ethanol, aliquot, and store at –80 °C. For working stock, dilute frozen stock 10 μL into 1.5 mL of PBS (working stock concentration 67 μg/mL). Do not store.

## 3 Methods

### 3.1 Retroviral Transduction of Murine Bone Marrow and Stem Cells

Day 1:

1. Inject 250 mg/kg 5FU intraperitoneally or intravenously into each donor mouse (*see* **Note 4**).

Day 3:

2. Split packaging cell line for transfection per protocol. For Lipofectamine 2000, seed $1–1.5 \times 10^6$ cells per 6-cm dish. Incubate at 37 °C/5 % $CO_2$ overnight.

Day 4:

3. Transfect packaging cell line per protocol. For Lipofectamine 2000, prepare DNA-Lipofectamine 2000 complexes, one tube for each sample:
   (a) Dilute 8 μg DNA in 0.5 mL of Opti-MEM I reduced serum medium. Mix gently.
   (b) Mix Lipofectamine 2000 gently before use and then dilute 20 μL in 0.5 mL Opti-MEM. Mix gently and incubate for 5 min at room temperature. The next step must be done within 30 min.
   (c) After 5–30 min of incubation, combine the diluted DNA with the diluted Lipofectamine 2000 reagent. The total volume should now be 1 mL. Mix gently and incubate for 20 min to 6 h at room temperature.
4. Add the prepared 1 mL of DNA-Lipofectamine 2000 complexes to each 6-cm plate containing cells and 5 mL of medium. Mix gently by rocking back and forth.
5. Incubate the cells at 37 °C/5 % $CO_2$ for 48 h before harvesting viral supernatant.

Day 5:

6. Euthanize donor mice according to approved animal protocols.
7. Harvest bilateral femurs and tibias from each mouse. Scrape bones with a razor blade to remove any attached muscle, cartilage, and connective tissue. Using razor blade or scissors, remove the ends of the bones (*see* **Note 5**).

8. Using a 3-cc syringe and a one-half-inch, 25-gage needle, insert the needle into each cut end of each bone and squirt the marrow from the center using sterile PBS. Squirt into a sterile dish and refill the syringe with fresh PBS if necessary. Squirt the marrow until the bones turn white.
9. Make a single cell suspension of marrow cells by aspirating the cells in the sterile dish once through the one-half-inch, 25-gage needle and then pushing them back out through the needle and into a sterile conical tube.
10. Spin at $300 \times g$ for 5 min at 4 °C.
11. Aspirate supernatant. Resuspend in 3–5 mL RBC lysis buffer (depending on the size and "redness" of the cell pellet).
12. Incubate at RT room temperature for 10 min.
13. Spin at $300 \times g$ for 5 min at 4 °C.
14. Resuspend in activation media (DMEM or StemSpan SFEM + 10 % HI FCS + 10 ng/mL IL-3 + 50 ng/mL IL-6 + 100 ng/mL SCF), $1.5 \times 10^6$ cells/mL (*see* **Note 6**).
15. Plate at $1.5 \times 10^6$ cells/well in a 24-well plate, 1 mL per well. Incubate at 37 °C/5 % $CO_2$ overnight.

Day 6:

16. Collect the supernatant from the transfected packaging cell line. Replace with fresh media and return the cells to the incubator (*see* **Note 7**).
17. To the supernatant, add polybrene to 5 μg/mL and HEPES to 10 mM. Mix thoroughly.
18. Filter supernatant through a 0.45-μm filter.
19. Centrifuge the bone marrow cells at $920 \times g$ for 5 min. Aspirate media.
20. Add 1 mL of filtered viral supernatant to each well of bone marrow cells.
21. Centrifuge the bone marrow cells at $920 \times g$ for 75 min at room temperature. Aspirate media.
22. Add 1 mL activation media to each well of bone marrow cells. Return the cells to the incubator.

Days 7 and 8:

23. Repeat d 6 protocol. On day 8, discard transfected packaging cells after removing the viral supernatant.

Day 9:

24. If there is a fluorescent protein, assess transduction efficiency using flow cytometry.
25. If transduction is adequate, decide on a cell dose and proceed to transplantation as described below (*see* **Note 8**). For tail vein injection, plan for an injection volume of 200–500 μL per mouse.

### 3.2 Lentiviral Transduction of Human HSCs and Progenitor Cells

Day 1:

1. Seed 2–3 × $10^6$ packaging cells per 10-cm dish in 10 mL of growth media. Incubate at 37 °C/5 % $CO_2$ for 24 h. The cells should be 80 % confluent at the time of transfection.

Day 2:

2. Remove the media from the packaging cells and wash the cells with serum-free media. Leave the cells under 5 mL of serum-free media.
3. For each 10-cm plate of cells to be transfected, dispense 0.5 mL of 2× HBS buffer (found in a calcium phosphate transfection kit) in a 15-mL tube.
4. In a separate 15-mL tube, dispense 100 μL of 2 M $CaCl_2$ (also found in the kit). Add 11 μg lentiviral expression plasmid, 3 μg lentiviral packaging plasmid, and 6 μg of LV envelope plasmid. Add deionized $H_2O$ to a final volume of 500 μL.
5. Slowly add the DNA/calcium mixture dropwise to the 2× HBS solution while gently vortexing the 15-mL tube. The mixture must not spill.
6. Gently vortex for 10–15 min to allow the formation of calcium phosphate/DNA precipitates.
7. Remove the packaging cells from incubator at the last moment. Add the mixture one drop at a time to the supernatant. Gently rock the culture dish to mix and return the cells to the incubator overnight.

Day 3:

8. Check the cells under a microscope. Small black particles should be visible.
9. Remove the transfection media. Replace with 10 mL fresh growth media.

Day 5:

10. Remove the supernatant and filter through 0.45-μm pores.
11. Centrifuge the supernatant at 22,000 × *g* for 2 h to concentrate the virus (*see* **Note 9**).
12. Resuspend the viral pellet in 250 μL/10-cm plate of packaging cells. Use myelocult media.
13. Test the concentrated virus for optimal dilution by adding it to the supernatant of 293T cells at dilutions of 1:1, 1:10, and 1:100. Plan to use the dilution that gives maximal transduction with minimal cell toxicity.
14. Sort the desired number of HSCs and progenitor cells into Eppendorf tubes, each containing 200 μL of PBS with 2 % calf serum. Spin at 750 × *g* in a microfuge for 5 min.

15. Remove the supernatant, then resuspend in myelocult media supplemented to a final concentration of 50 ng/mL SCF, 10 ng/mL IL-6, 10 ng/mL TPO, and 50 ng/mL Flt3 ligand. Keep in mind the volume of virus that you will be adding. Use a volume appropriate to cover the cells lying in a single cell layer on the bottom of a tissue culture dish.
16. Add the concentrated lentiviral supernatant to the dilution determined in **step 13** above. Remove the cells to a tissue culture dish with adequate surface area to allow the cells to lie in single cell thickness at the bottom. Incubate at 37 °C/5 % $CO_2$ for 24 h.

Day 6:

17. If there is a fluorescent protein, assess transduction efficiency using flow cytometry.
18. If transduction is adequate, proceed to transplantation as described later. Cell doses of 10,000–50,000 labeled cells into SCID-hu mice have been used.

### *3.3 Bone Marrow Transplantation into Mice*

1. Transfer the recipient mice to the mouse irradiation chamber for lethal irradiation.
2. Deliver 800–900 cGy total body irradiation 24 h before transplantation (*see* **Note 10**).
3. Warm the recipient mice under a heating lamp to encourage peripheral vasodilation.
4. One mouse at a time, transfer the mice into a restraining device for tail vein injection (*see* **Note 11**) and inject a rescuing dose of bone marrow cells.
5. After injection, mice should be maintained in autoclaved cages and bedding with autoclaved water supplemented with approximately two capfuls of Trimethoprim/Sulfamethoxazole per full water bottle (*see* **Note 12**). These living conditions should continue for the first month.

### *3.4 Bioluminescence Imaging Considerations*

1. Using an approved method of anesthesia, anesthetize the mice for imaging. Expect to need them to lie still for up to 15 min for multiple images using 1–5 min data acquisition times.
2. Initialize the camera. The user interface of Living Image has a command to initialize which resets all parameters.
3. Before imaging, administer the appropriate luciferase substrate by the chosen route. For luciferin, the dose for an adult mouse is usually 150 mg/kg body weight given intraperitoneally. For coelenterazine, this is typically 6.7 μg injected intravenously (*see* **Note 13**).

4. Approximately 15 min after an intraperitoneal injection of luciferin or immediately after intravenous injection of any substrate, take the initial image (in Living Image, click on the "Acquire" button), keeping in mind the following considerations:
   (a) Stage height should be adjusted such that the field of view fits the number of mice in the image. It should be at the highest setting that allows visualization of all mice to be imaged. In Living Image, the "Acquire Continuous Photos" button is helpful for adjusting this. It takes photographic images only.
   (b) Shorter exposure times (e.g., 1 s) are appropriate if the signal is expected to be strong. Longer times (e.g., 5–10 min) are required if the signal is predicted to be weak. If the signal strength is unknown, a 1-min initial exposure time is a reasonable place to start. These parameters are set in the user interface.
   (c) Binning pixels can be done with extremely weak signals to improve the apparent contrast. The total number of photons collected does not change when binning the pixels, so it is not an increase in sensitivity, but binning does result in a loss of resolution, as there are a smaller number of elements on the chip. Smaller binning numbers correspond to higher image resolution and lower contrast. Higher binning numbers correspond to better apparent contrast and lower image resolution. Medium binning is a good place to start.
   (d) "Saturated" images are nonquantitative, as the pixels that are saturated cannot collect more signals. The previously described parameters should be adjusted to collect an image that reflects a signal strength that is adequate for anatomic localization but not strong enough to saturate the camera.
5. In order to verify and localize a given signal, mice should be imaged in multiple positions. Conventional views include ventral, dorsal, and two lateral images.

## 4 Notes

1. Any transfection protocol can be used. This protocol will use the Lipofectamine 2000 conditions.
2. Both calcium phosphate and liposome-mediated transfection methods have been used. This protocol describes a modified calcium phosphate-based method.

3. Several options for imaging systems are commercially available. This protocol describes the use of the Xenogen IVIS system and associated Living Image software.
4. These 5-FU doses are optimized for B6 mice. Doses of 150 mg/kg have also been used with 48 h pretransduction activation times in vitro.
5. Try to remove as little bone as possible as most of the HSCs are found near the ends of the bones.
6. Some have found that StemSpan SFEM-based media supplemented with calf serum and cytokines result in superior viability and activation of the bone marrow cells.
7. Virus can be harvested again from the transfected packaging cells in 72 h. After collection, virus can be concentrated as above. Discard the supernatant and store the viral pellet in the Eppendorf tube at –80 °C.
8. The cell dose required to rescue will vary depending on the quality of the 5-FU enrichment as well as the quality of the response to the activation media. Plan on being able to rescue one or two mice per well, depending on the health of the cells in culture as assessed by light microscopy.
9. Some have generated high-titer viral preparations by concentration using successive rounds of ultracentrifugation [74].
10. Lethal doses of total body irradiation vary by background strain. Balb/C and FVBN mice typically use 800 cGy, whereas C57B6 mice require 900 cGy. For C57B6, the dose can also be fractionated into an 800-cGy dose followed by a 400-cGy dose approximately 3 h later.
11. Rescuing bone marrow cells can also be introduced by retro-orbital injection. In that case, the heating lamp and restraining device are not necessary, but anesthesia may be required, and the injection volume should be 100–200 μL per mouse.
12. A mixture of Neomycin (1.2 g/L) and Polymyxin-B ($1 \times 10^6$ U/L) in the drinking water can also be used.
13. Biodistribution and ultimately consumption of the substrate throughout the mouse will result in the bioluminescence signal strength changing over time. For luciferin given intraperitoneally, the signal increases slowly and appears to plateau at approximately 15–20 min after the injection. It remains relatively stable for an additional 15–20 min and then declines. The precise timing of the plateau in signal should be measured in each experimental system by taking several consecutive images and noting the time from injection to signal stability. Luciferin can also be given intravenously, and this is helpful for reaching anatomic sites like the brain, but clearance of the substrate will occur much more rapidly than when substrate is delivered intraperitoneally.

## References


1. Hardy J, Francis KP, DeBoer M et al (2004) Extracellular replication of Listeria monocytogenes in the murine gall bladder. Science 303:851–853
2. Liu H, Patel MR, Prescher JA et al (2010) Cancer stem cells from human breast tumors are involved in spontaneous metastases in orthotopic mouse models. Proc Natl Acad Sci U S A 107:18115–18120
3. Cao YA, Wagers AJ, Beilhack A et al (2004) Shifting foci of hematopoiesis during reconstitution from single stem cells. Proc Natl Acad Sci U S A 101:221–226
4. Gambhir SS, Yaghoubi SS (2010) Molecular imaging with reporter genes. Cambridge University Press, Cambridge/New York, p xiii, 321
5. Bennink RJ, Hamann J, de Bruin K et al (2005) Dedicated pinhole SPECT of intestinal neutrophil recruitment in a mouse model of dextran sulfate sodium-induced colitis. J Nucl Med 46: 526–531
6. Bennink RJ, van Montfrans C, de Jonge WJ et al (2004) Imaging of intestinal lymphocyte homing by means of pinhole SPECT in a TNBS colitis mouse model. Nucl Med Biol 31: 93–101
7. Jendelova P, Herynek V, Urdzikova L et al (2004) Magnetic resonance tracking of transplanted bone marrow and embryonic stem cells labeled by iron oxide nanoparticles in rat brain and spinal cord. J Neurosci Res 76:232–243
8. Paik JY, Lee KH, Byun SS, Choe YS, Kim BT (2002) Use of insulin to improve [18 F]fluorodeoxyglucose labelling and retention for in vivo positron emission tomography imaging of monocyte trafficking. Nucl Med Commun 23: 551–557
9. Wang X, Rosol M, Ge S et al (2003) Dynamic tracking of human hematopoietic stem cell engraftment using in vivo bioluminescence imaging. Blood 102:3478–3482
10. Bengel FM, Schachinger V, Dimmeler S (2005) Cell-based therapies and imaging in cardiology. Eur J Nucl Med Mol Imaging 32(Suppl 2): S404–S416
11. Dick AJ, Guttman MA, Raman VK et al (2003) Magnetic resonance fluoroscopy allows targeted delivery of mesenchymal stem cells to infarct borders in Swine. Circulation 108: 2899–2904
12. Li Z, Suzuki Y, Huang M et al (2008) Comparison of reporter gene and iron particle labeling for tracking fate of human embryonic stem cells and differentiated endothelial cells in living subjects. Stem Cells 26:864–873
13. Bindslev L, Haack-Sorensen M, Bisgaard K et al (2006) Labelling of human mesenchymal stem cells with indium-111 for SPECT imaging: effect on cell proliferation and differentiation. Eur J Nucl Med Mol Imaging 33: 1171–1177
14. Kraitchman DL, Tatsumi M, Gilson WD et al (2005) Dynamic imaging of allogeneic mesenchymal stem cells trafficking to myocardial infarction. Circulation 112:1451–1461
15. Zhou R, Thomas DH, Qiao H et al (2005) In vivo detection of stem cells grafted in infarcted rat myocardium. J Nucl Med 46:816–822
16. Doyle B, Kemp BJ, Chareonthaitawee P et al (2007) Dynamic tracking during intracoronary injection of 18F-FDG-labeled progenitor cell therapy for acute myocardial infarction. J Nucl Med 48:1708–1714
17. Bengel FM, Gambhir SS (2005) Clinical molecular imaging and therapy-moving ahead together. Eur J Nucl Med Mol Imaging 32 (Suppl 2):S323
18. Troy T, Jekic-McMullen D, Sambucetti L, Rice B (2004) Quantitative comparison of the sensitivity of detection of fluorescent and bioluminescent reporters in animal models. Mol Imaging 3:9–23
19. Beeres SL, Bengel FM, Bartunek J et al (2007) Role of imaging in cardiac stem cell therapy. J Am Coll Cardiol 49:1137–1148
20. Gildehaus FJ, Haasters F, Drosse I et al (2011) Impact of indium-111 oxine labelling on viability of human mesenchymal stem cells in vitro, and 3D cell-tracking using SPECT/CT in vivo. Mol Imaging Biol 13: 1204–1214
21. Kang WJ, Kang HJ, Kim HS et al (2006) Tissue distribution of 18F-FDG-labeled peripheral hematopoietic stem cells after intracoronary administration in patients with myocardial infarction. J Nucl Med 47:1295–1301
22. Olson JA, Zeiser R, Beilhack A, Goldman JJ, Negrin RS (2009) Tissue-specific homing and expansion of donor NK cells in allogeneic bone marrow transplantation. J Immunol 183: 3219–3228
23. Sipkins DA, Wei X, Wu JW et al (2005) In vivo imaging of specialized bone marrow endothelial microdomains for tumour engraftment. Nature 435:969–973
24. Stoll S, Delon J, Brotz TM, Germain RN (2002) Dynamic imaging of T cell-dendritic cell interactions in lymph nodes. Science 296: 1873–1876
25. Reichardt W, Durr C, von Elverfeldt D et al (2008) Impact of mammalian target of rapamycin inhibition on lymphoid homing and tolerogenic function of nanoparticle-labeled dendritic cells following allogeneic hematopoietic cell transplantation. J Immunol 181:4770–4779

26. Fujisaki J, Wu J, Carlson AL et al (2011) In vivo imaging of Treg cells providing immune privilege to the haematopoietic stem-cell niche. Nature 474:216–219
27. Park D, Spencer JA, Koh BI et al (2012) Endogenous bone marrow MSCs are dynamic, fate-restricted participants in bone maintenance and regeneration. Cell Stem Cell 10: 259–272
28. Soloviev VY (2007) Tomographic bioluminescence imaging with varying boundary conditions. Appl Opt 46:2778–2784
29. Lv Y, Tian J, Cong W et al (2007) Spectrally resolved bioluminescence tomography with adaptive finite element analysis: methodology and simulation. Phys Med Biol 52:4497–4512
30. Montet X, Figueiredo JL, Alencar H et al (2007) Tomographic fluorescence imaging of tumor vascular volume in mice. Radiology 242:751–758
31. Montet X, Ntziachristos V, Grimm J, Weissleder R (2005) Tomographic fluorescence mapping of tumor targets. Cancer Res 65: 6330–6336
32. Roy R, Thompson AB, Godavarty A, Sevick-Muraca EM (2005) Tomographic fluorescence imaging in tissue phantoms: a novel reconstruction algorithm and imaging geometry. IEEE Trans Med Imaging 24:137–154
33. Keren S, Gheysens O, Levin CS, Gambhir SS (2008) A comparison between a time domain and continuous wave small animal optical imaging system. IEEE Trans Med Imaging 27: 58–63
34. Kumar AT, Raymond SB, Dunn AK, Bacskai BJ, Boas DA (2008) A time domain fluorescence tomography system for small animal imaging. IEEE Trans Med Imaging 27: 1152–1163
35. Model R, Orlt M, Walzel M, Hunlich R (1998) Optical imaging: three-dimensional approximation and perturbation approaches for time-domain data. Appl Opt 37:7968–7976
36. Michalet X, Pinaud FF, Bentolila LA et al (2005) Quantum dots for live cells, in vivo imaging, and diagnostics. Science 307:538–544
37. Kalchenko V, Shivtiel S, Malina V et al (2006) Use of lipophilic near-infrared dye in whole-body optical imaging of hematopoietic cell homing. J Biomed Opt 11:050507
38. Gilad AA, Winnard PT Jr, van Zijl PC, Bulte JW (2007) Developing MR reporter genes: promises and pitfalls. NMR Biomed 20: 275–290
39. Ponomarev V, Doubrovin M, Shavrin A et al (2007) A human-derived reporter gene for noninvasive imaging in humans: mitochondrial thymidine kinase type 2. J Nucl Med 48: 819–826
40. Hsieh CH, Chen FD, Wang HE et al (2008) Generation of destabilized herpes simplex virus type 1 thymidine kinase as transcription reporter for PET reporter systems in molecular genetic imaging. J Nucl Med 49:142–150
41. MacLaren DC, Gambhir SS, Satyamurthy N et al (1999) Repetitive, non-invasive imaging of the dopamine D2 receptor as a reporter gene in living animals. Gene Ther 6:785–791
42. Chen IY, Wu JC, Min JJ et al (2004) Micropositron emission tomography imaging of cardiac gene expression in rats using bicistronic adenoviral vector-mediated gene delivery. Circulation 109:1415–1420
43. Liang Q, Satyamurthy N, Barrio JR et al (2001) Noninvasive, quantitative imaging in living animals of a mutant dopamine D2 receptor reporter gene in which ligand binding is uncoupled from signal transduction. Gene Ther 8:1490–1498
44. Kang JH, Lee DS, Paeng JC et al (2005) Development of a sodium/iodide symporter (NIS)-transgenic mouse for imaging of cardiomyocyte-specific reporter gene expression. J Nucl Med 46:479–483
45. Kim YH, Lee DS, Kang JH et al (2005) Reversing the silencing of reporter sodium/iodide symporter transgene for stem cell tracking. J Nucl Med 46:305–311
46. Miyagawa M, Anton M, Wagner B et al (2005) Non-invasive imaging of cardiac transgene expression with PET: comparison of the human sodium/iodide symporter gene and HSV1-tk as the reporter gene. Eur J Nucl Med Mol Imaging 32:1108–1114
47. Terrovitis J, Kwok KF, Lautamaki R et al (2008) Ectopic expression of the sodium-iodide symporter enables imaging of transplanted cardiac stem cells in vivo by single-photon emission computed tomography or positron emission tomography. J Am Coll Cardiol 52:1652–1660
48. Penheiter AR, Russell SJ, Carlson SK (2012) The sodium iodide symporter (NIS) as an imaging reporter for gene, viral, and cell-based therapies. Curr Gene Ther 12:33–47
49. Hall MP, Unch J, Binkowski BF et al (2012) Engineered luciferase reporter from a deep sea shrimp utilizing a novel imidazopyrazinone substrate. ACS Chem Biol 7:1848–1857
50. Loening AM, Wu AM, Gambhir SS (2007) Red-shifted Renilla reniformis luciferase variants for imaging in living subjects. Nat Methods 4:641–643
51. Tannous BA, Kim DE, Fernandez JL, Weissleder R, Breakefield XO (2005) Codon-optimized Gaussia luciferase cDNA for mammalian gene expression in culture and in vivo. Mol Ther 11:435–443
52. Welsh JP, Patel KG, Manthiram K, Swartz JR (2009) Multiply mutated Gaussia luciferases provide prolonged and intense bioluminescence. Biochem Biophys Res Commun 389: 563–568

53. Maguire CA, Deliolanis NC, Pike L et al (2009) Gaussia luciferase variant for high-throughput functional screening applications. Anal Chem 81:7102–7106
54. Zhao H, Doyle TC, Coquoz O et al (2005) Emission spectra of bioluminescent reporters and interaction with mammalian tissue determine the sensitivity of detection in vivo. J Biomed Opt 10:41210
55. Zhao H, Doyle TC, Wong RJ et al (2004) Characterization of coelenterazine analogs for measurements of Renilla luciferase activity in live cells and living animals. Mol Imaging 3:43–54
56. Bhaumik S, Lewis XZ, Gambhir SS (2004) Optical imaging of Renilla luciferase, synthetic Renilla luciferase, and firefly luciferase reporter gene expression in living mice. J Biomed Opt 9:578–586
57. Kwon H, Enomoto T, Shimogawara M et al (2010) Bioluminescence imaging of dual gene expression at the single-cell level. Biotechniques 48:460–462
58. Mezzanotte L, Que I, Kaijzel E et al (2011) Sensitive dual color in vivo bioluminescence imaging using a new red codon optimized firefly luciferase and a green click beetle luciferase. PLoS One 6:e19277
59. Na IK, Markley JC, Tsai JJ et al (2010) Concurrent visualization of trafficking, expansion, and activation of T lymphocytes and T-cell precursors in vivo. Blood 116:e18–e25
60. Vilalta M, Jorgensen C, Degano IR et al (2009) Dual luciferase labelling for non-invasive bioluminescence imaging of mesenchymal stromal cell chondrogenic differentiation in demineralized bone matrix scaffolds. Biomaterials 30: 4986–4995
61. Sheikh AY, Lin SA, Cao F et al (2007) Molecular imaging of bone marrow mononuclear cell homing and engraftment in ischemic myocardium. Stem Cells 25:2677–2684
62. Cao F, Lin S, Xie X et al (2006) In vivo visualization of embryonic stem cell survival, proliferation, and migration after cardiac delivery. Circulation 113:1005–1014
63. Li Z, Wu JC, Sheikh AY, Kraft D, Cao F et al (2007) Differentiation, survival, and function of embryonic stem cell derived endothelial cells for ischemic heart disease. Circulation 116: I46–I54
64. Contag CH (2007) In vivo pathology: seeing with molecular specificity and cellular resolution in the living body. Annu Rev Pathol 2: 277–305
65. Massoud TF, Gambhir SS (2003) Molecular imaging in living subjects: seeing fundamental biological processes in a new light. Genes Dev 17:545–580
66. Shah BS, Clark PA, Moioli EK, Stroscio MA, Mao JJ (2007) Labeling of mesenchymal stem cells by bioconjugated quantum dots. Nano Lett 7:3071–3079
67. Shaner NC, Steinbach PA, Tsien RY (2005) A guide to choosing fluorescent proteins. Nat Methods 2:905–909
68. Slotkin JR, Chakrabarti L, Dai HN et al (2007) In vivo quantum dot labeling of mammalian stem and progenitor cells. Dev Dyn 236: 3393–3401
69. Kesarwala AH, Prior JL, Sun J et al (2006) Second-generation triple reporter for bioluminescence, micro-positron emission tomography, and fluorescence imaging. Mol Imaging 5:465–474
70. Ray P, Tsien R, Gambhir SS (2007) Construction and validation of improved triple fusion reporter gene vectors for molecular imaging of living subjects. Cancer Res 67: 3085–3093
71. Cao F, Drukker M, Lin S et al (2007) Molecular imaging of embryonic stem cell misbehavior and suicide gene ablation. Cloning Stem Cells 9:107–117
72. Cai X, Li L, Krumholz A, Guo Z, Erpelding TN et al (2012) Multi-scale molecular photoacoustic tomography of gene expression. PLoS One 7:e43999
73. Li L, Zemp RJ, Lungu G, Stoica G, Wang LV (2007) Photoacoustic imaging of lacZ gene expression in vivo. J Biomed Opt 12:020504
74. Ichim CV, Wells RA (2011) Generation of high-titer viral preparations by concentration using successive rounds of ultracentrifugation. J Transl Med 9:137

# Chapter 2

# Flow Cytometry for Hematopoietic Cells

**Daniela S. Krause, Michelle E. DeLelys, and Frederic I. Preffer**

## Abstract

Within the last 25 years, flow cytometry and fluorescence-activated cell sorting have emerged as both routine diagnostic tools in clinical medicine and as advanced analytic tools critical in performing scientific research. This chapter aims at summarizing the use of flow cytometry in benign and malignant hematology and the monitoring of inherited and acquired immunodeficiency states. Numerous figures are provided from our laboratories at Massachusetts General Hospital that illustrate examples of these conditions. The chapter also describes novel flow cytometry-based imaging techniques, the combination of flow cytometry and mass spectrography, new software tools, and some future directions and applications of advanced instrumentation for flow cytometry.

**Key words** Flow cytometry, Diagnostic immunophenotyping, Hematopoietic malignancies, Hematopathology, Immunodeficiencies, Hematopoietic stem cells, Bone marrow transplantation, Paroxysmal nocturnal hemoglobinuria, Amnis imaging cytometry, CyTOF mass cytometry, Gemstone probability state model

## 1 Introduction

The fascination of humans by blood dates back to the ancient Greek physician Hippocrates (460–377 B.C.), who referred to blood (Greek: "haima") as one of the four humors besides black bile (Greek: "melan chole"), yellow bile (Greek: "chole"), and phlegm (Greek: "phlegma"). With the development of the first microscopes in the seventeenth century, the interest turned to the corpuscular elements of the blood and the first description of cells in cork by the English natural philosopher, scientist, and architect Robert Hooke. Via the "cell theory" proposed by Theodor Schwann, Matthias Jakob Schleiden, Rudolf Virchow, and others in the nineteenth century, we have now arrived in an age in which hematopoietic cells and their earliest precursor cells can be isolated by techniques such as flow cytometric cell sorting, analyzed on a molecular level, expanded in vitro, and used therapeutically for hematopoietic stem cell transplantation. Efforts are now even being made to generate hematopoietic stem cells from skin fibroblasts in

Meral Beksaç (ed.), *Bone Marrow and Stem Cell Transplantation*, Methods in Molecular Biology, vol. 1109,
DOI 10.1007/978-1-4614-9437-9_2, 

the form of induced pluripotent stem cells. The easy availability of hematopoietic cells has been beneficial for these developments over the centuries.

Flow cytometric immunophenotyping has become an indispensable part of the clinical laboratory, as it allows enumeration of specific cell types in different disease settings. This immunophenotyping, in conjunction with cytogenetics, molecular studies, and morphological assessment, is an essential diagnostic tool in hematopathology. In this chapter we will primarily present a broad overview of such possible immunophenotypic uses of flow cytometry in the clinical diagnostic laboratory.

## 2 Enumeration of Different Cell Types in Different Clinical Settings

### 2.1 Assessment of CD34+ Hematopoietic Stem Cells for Bone Marrow Transplantation

CD34+ cells are pluripotent hematopoietic stem cells (HSC) that via multiple precursor cell types are able to differentiate into the lymphoid, myeloid, erythroid, and megakaryocytic lineages. HSC are able to reconstitute hematopoiesis in an individual who has received high-dose chemotherapy and/or radiation [1–4]. HSC are collected from healthy donors (allogeneic) or patients with hematological malignancies (autologous) after mobilization of HSC from the HSC niche in the bone marrow by granulocyte colony-stimulating factor (G-CSF) and/or the CXCR4-antagonist, plerixafor, apheresis, or direct harvesting from the bone marrow. CD34+ HSC are enumerated by flow cytometry in order to assess whether the amounts of HSCs which have been collected are sufficient for the patient's body weight, usually around that is generally around $2–5 \times 10^6$ cells/kg body weight. Accurate quantification of CD34+ HSC is critical, as they are often transfused into a myeloablated patient.

This test is performed using antibodies to CD34 and CD45 and quantitation has recently been automated utilizing a probability state model [5]. Red blood cells are lysed and acquisition of 100,000 total CD45+ cells or at least 100 CD34+ cells [6], in order to achieve statistical significance, and analysis are usually performed immediately. Viability of HSC may be determined by the nuclear dye 7-AAD, which is excluded in viable cells (Fig. 1).

### 2.2 Enumeration of Immune Cells in Acquired and Inherited States of Immunosuppression

Flow cytometry is a well-established and largely automated method for monitoring T-cell subsets in HIV infection or during immunosuppression with calcineurin inhibitors like tacrolimus. Peripheral blood leukocytes are stained with antibodies to CD3, CD8, CD45, and CD4 for T-cell-subset analysis and possibly CD16, CD56, and CD19 for a more comprehensive analysis of NK cells and B-lymphocytes. The test may be performed as a single-platform technology using an internal bead standard to obtain absolute

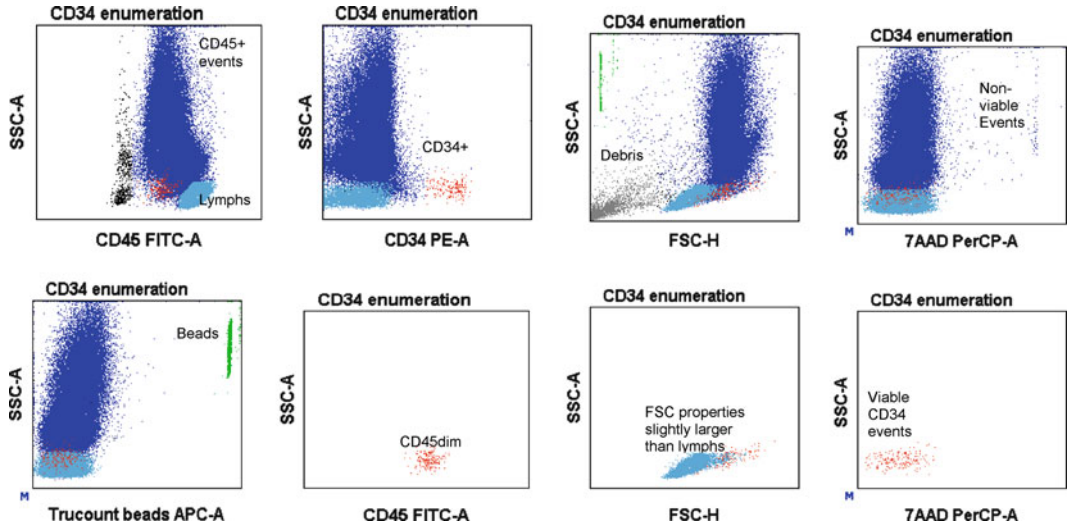


**Fig. 1** Representative dot plots from a patient's apheresis product post bone marrow stem cell mobilization using the BD™ Stem Cell Enumeration Kit and the ISHAGE stem cell gating method [6]. The stem cells are gated sequentially first by gating on CD45+ events, next by gating on CD34+SSC$^{low}$ events, and then by gating strictly on the CD45 dim events. Lastly it is ensured that the cells are similar in size (or slightly larger) to normal lymphocytes. The BD™ Stem Cell Enumeration Kit utilizes BD Trucount™ tubes, which allow for the determination of absolute numbers of stem cells as well as the viability dye 7AAD, to exclude nonviable events

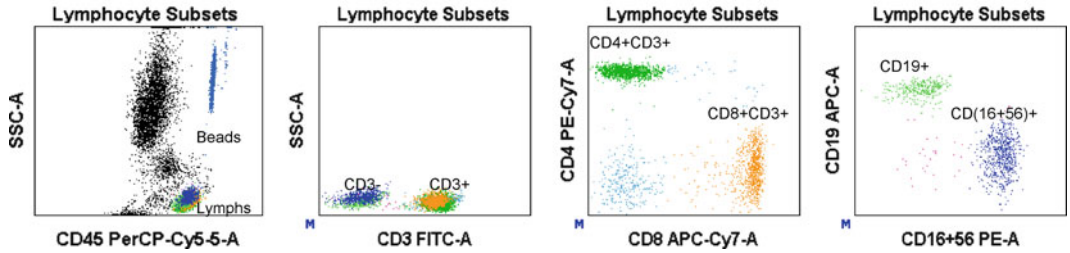


**Fig. 2** Representative dot plots from a patient's peripheral blood to determine absolute counts of lymphocyte subsets using the BD Multitest™ TBNK kit. First lymphocytes are gated using CD45 and low SSC. T-cell subsets are determined as CD3+CD4+ and CD3+CD8+ events, NK cells are determined by gating on CD3– CD(16+56+) events, and B cells are determined by gating on CD3– CD19+ events. BD Trucount™ tubes allow for the accurate determination of absolute numbers of cells in non-piston delivery fluidic systems

counts of CD4+ and CD8+ T cells, obviating the need for a concomitant blood sample to obtain the patient's white blood cell count [7] (Fig. 2).

Common variable immune deficiency (CVID) is a group of inherited immune disorders characterized by decreased levels of most or all of the immunoglobulin subclasses; a decreased number of B cells and plasma cells, both involved in the production of antibodies; and an increased frequency of bacterial infections [8].

The genetic abnormalities associated with CVID vary greatly among patients and may involve the genes encoding CD19, the transmembrane activator and calcium-modulating cyclophilin ligand interactor (TACI), and others. Flow cytometry can aid in the diagnosis of CVID by investigation of the expression of CD27, IgM, and IgD on B cells. In contrast, severe combined immunodeficiency (SCID) is a more severe immune defect, as individuals with this disorder have defects in both B- and T-cell lineages. Babies born with this defect usually die of severe infections before the age of 1 year. Most forms of the disease are due to mutations in the gamma chain ($\gamma_c$) common to the receptor for several interleukins or due to a defect in adenosine deaminase (ADA). Flow cytometry may be helpful in analyzing expression of CD45RA versus CD45RO on T cells. In the autoimmune lymphoproliferative syndrome (ALPS), increased numbers of lymphocytes are found in lymph nodes, spleen, and liver leading to enlargement of these organs. ALPS can be associated with autoimmune disorders such as anemia, thrombocytopenia, and neutropenia. Aberrant T cells in this disease may be CD4– CD8– CD3+ TCRαβ+ B220+.

### *2.3 Monitoring of B Cells During Anti-B-Cell Immunosuppressive Treatment*

An adequate response to the B-cell agent Rituxan (anti-CD20 therapeutic antibody) used for treatment of non-Hodgkin lymphoma and as immunosuppressant in several autoimmune disorders can be monitored by flow cytometry. The effects of Rituxan therapy are monitored by staining patient blood leukocytes with antibodies to CD45, CD19, and CD20 and observing the rapid and prolonged physical "clearance" of the B-cell lymphocyte subpopulation from the circulation (Fig. 3).

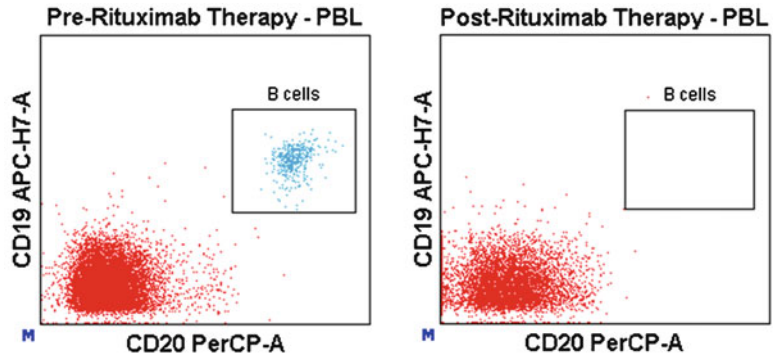


**Fig. 3** Representative dot plots from a patient's peripheral blood pre-rituximab treatment (*left*) and post-rituximab treatment (*right*)

## 3 Diagnostic Use of Flow Cytometry in Hematological Malignancies

### 3.1 Leukemia

Flow cytometry is considered an integral part of determining the diagnosis of different types of leukemia and lymphoma. A pathological diagnosis is now made based on a combination of morphological, cytogenetic, and immunophenotypic criteria. When a leukemia is suspected, immunophenotypic analysis of leukocytes is usually performed on a whole blood or bone marrow aspirate anticoagulated with acid-citrate-dextrose (ACD) or ethylenediaminetetraacetic acid (EDTA). Other body fluids like CSF, ascites, or pleuritic fluid as mentioned in Subheading 3.5, however, can also be used. To determine the presence or absence of an unusual or a clonal population of T, B, NK, or myeloid cells that potentially represent a leukemia, in our laboratory a patient sample is stained in three separate tubes using the following eight directly conjugated monoclonal antibodies:

Tube 1: CD7, CD16, CD3, CD2, CD8, CD14, CD4, CD45

Tube 2: kappa, lambda, CD19, CD10, CD23, CD20, CD5, CD45

Tube 3: CD71, myeloperoxidase (MPO), CD34, CD33, CD117, HLA-DR, CD13, CD45

The antigens these monoclonal antibodies are directed against are located on the external surface membrane of the target cell. However, the MPO antigen is found within the cytoplasm, which thus requires permeabilization of the cell membrane for monoclonal antibody access. Acute myeloid leukemia (AML) cells are usually positive for permutations of CD13, CD33, CD34, CD117, and/or MPO and might variably express HLA-DR, CD56, and/or CD15 (Table 1) (Fig. 4). When lacking CD34 and CD117 and expressing CD14 or CD64, monocytic differentiation is likely; aberrant myelomonocytic, megakaryoblastic, erythroblastic, or basophilic differentiation may also be identified utilizing antibodies specific for these cell lineages. Myeloid malignancies might also confusingly co-express B- or T-lymphoid markers such as CD19, CD7, CD2, and/or CD5.

If acute promyelocytic leukemia is suspected (APML), CD64, CD11c, CD45, and CD11b can be used with $CD33^{bright}+$ as additional markers to try to identify this malignancy with its diagnostic t(15;17)(q22;q12) translocation and penchant to be associated with disseminated intravascular coagulation (DIC) (Fig. 5). HLA-DR, CD11b, CD11c, CD18, and CD34 are usually negative in APML. This disease responds very favorably to all-*trans*-retinoic acid therapy, which acts therapeutically to differentiate the tumor; rapid diagnosis of this disease is essential, to avoid DIC.

While flow cytometry is not routinely used yet on a widespread basis to diagnose myelodysplastic syndrome (MDS), staining for CD13, CD16, and CD11b on neutrophils as well as a variety of other markers on lymphocytes and stem cells of patients with

**Table 1**
**Immunophenotype of selected hematological malignancies**

| Hematological malignancy | Common immunophenotypes |
|---|---|
| Acute myeloid leukemia | CD13+, CD33+, MPO+, CD117+, CD34+, HLA-DR+/–, CD14+/–, CD45$^{dim}$+ |
| Acute promyelocytic leukemia | CD13+, CD33$^{bright}$+, MPO+, CD117+, CD34–, HLA-DR–, CD64+/–, CD11c+/–, CD45+/–, CD11b+/– |
| B-acute lymphoblastic leukemia/lymphoma | CD19+, CD20–, CD10+, TdT+, CD34+, CD45$^{dim\text{-}to\text{-}negative}$, absent light chain expression |
| Burkitt's lymphoma | CD19+, CD20+, CD10+, TdT–, CD23–, CD43+, CD5–, surface light chain restricted expression |
| Follicular lymphoma | CD19+, CD20+, CD10+, CD23+, CD43–, surface light chain restricted expression |
| Diffuse large B-cell lymphoma | CD19+, CD20+, CD10+, CD23+, CD5–, surface light chain restricted expression |
| Mantle cell lymphoma | CD19+, CD20+, CD10–, CD23–, CD43+, CD5+, FMC7+ surface light chain restricted expression |
| Chronic lymphocytic leukemia | CD19+, CD20$^{dim}$+, CD5+, CD23+, CD43+, FMC7–, surface light chain$^{dim+}$ restricted expression |
| Hairy cell leukemia | CD19+, CD20$^{bright}$+, CD10–, CD5–, CD23–, CD103+, CD11c+, CD25+, surface light chain restricted expression |
| Marginal zone lymphoma | CD19+, CD20+, CD10–, CD23–, CD5–, CD43–, surface light chain restricted expression |
| Plasma cell myeloma | CD19–, CD38$^{bright}$+, CD138+, CD56+, CD45$^{dim+to\ neg}$ cytoplasmic light chain restricted expression |
| T-LGL | CD3+, CD2+, CD8+CD57+, CD56+, CD7+, CD16+, CD45+ |
| T acute lymphoblastic leukemia/lymphoma | CD1a+, CD2+, CD3+, CD4+8+, CD5+, CD7+, TdT+; CD99+, CD34+, CD10+ (variably) |
| T-NHL | CD3+, CD7+, CD2+, CD4+ or CD8+ |
| Cutaneous T-cell lymphoma | CD3+, CD2+, CD4+ and/or CD8+, CD5+/–, CD7+/– (CD26– in erythroderma) |

suspected MDS may be employed. Flow cytometry, however, is widely being used to enumerate the percentage of blasts in MDS and for estimation of minimal residual disease in AML and B- and T-cell acute lymphoblastic leukemia (B-ALL and T-ALL, respectively). Multiple strategies to more directly assess MDS by flow cytometry are currently under investigation [9–14].

B-ALL cells frequently express CD19, CD10, nuclear terminal deoxynucleotidyl transferase (TdT), and cytoplasmic CD79a and/or CD22 (Fig. 6). CD34 and CD20 are variably expressed and

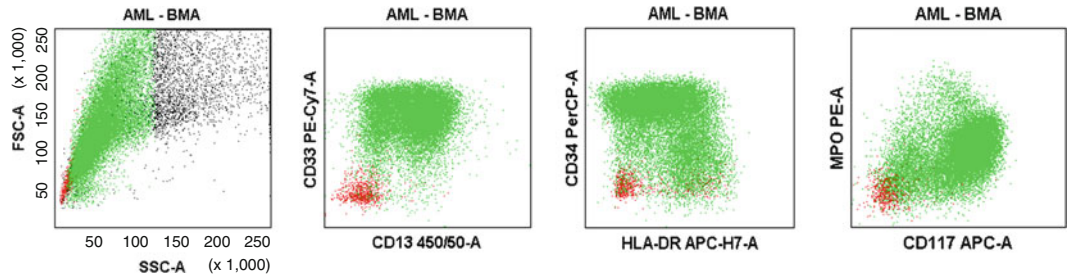


**Fig. 4** Representative dot plots from a patient's bone marrow aspirate demonstrating acute myeloid leukemia (AML). The myeloid blasts are depicted as the green dots and express the characteristic immunophenotype of CD13+CD33+CD34+HLA-DR+MPO+CD117+. There is obvious variation in the expression of CD34, CD117, CD13, and HLA-DR demonstrated in this example, showing the heterogeneity of immunophenotypic expression. Myeloid blasts are larger than normal lymphocytes in size and have increased side scatter

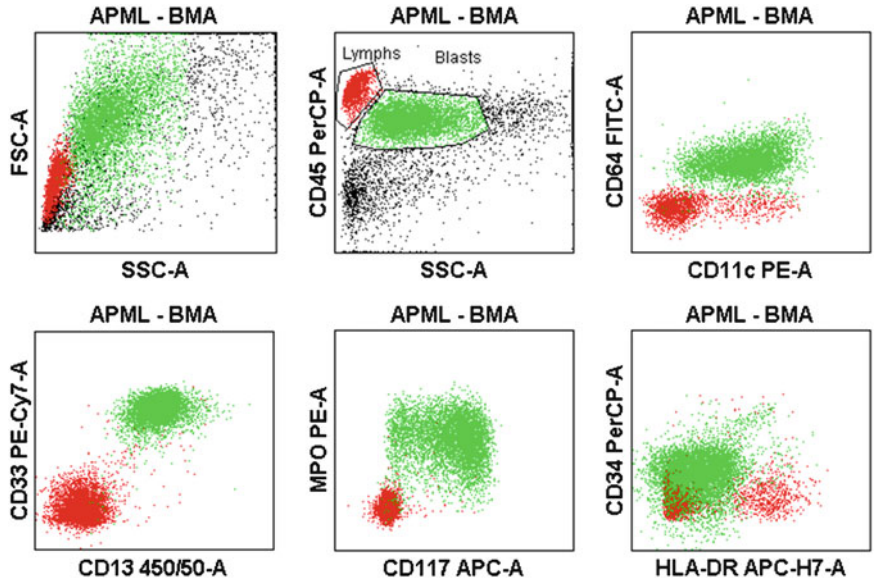


**Fig. 5** Representative dot plots from a patient's bone marrow aspirate demonstrating acute promyelocytic leukemia (APML). The malignant promyelocytes are depicted as the *green dots* and express the characteristic immunophenotype of CD13+CD33$^{bright}$+CD64+CD11c+MPO+CD117+CD34–HLA-DR–. Promyelocytes have forward and side scatter characteristics similar to monocytes

CD45 is usually reduced from that appreciated on normal B cells or possibly entirely absent. Expression of the myeloid markers CD13 and/or CD33 is also possible and with cytoplasmic MPO expression would suggest a biphenotypic leukemia rather than diagnosis [15].

B cells in chronic lymphocytic leukemia (CLL) can immunophenotypically be described as CD19+, CD20$^{dim}$+, CD5+, and CD23+

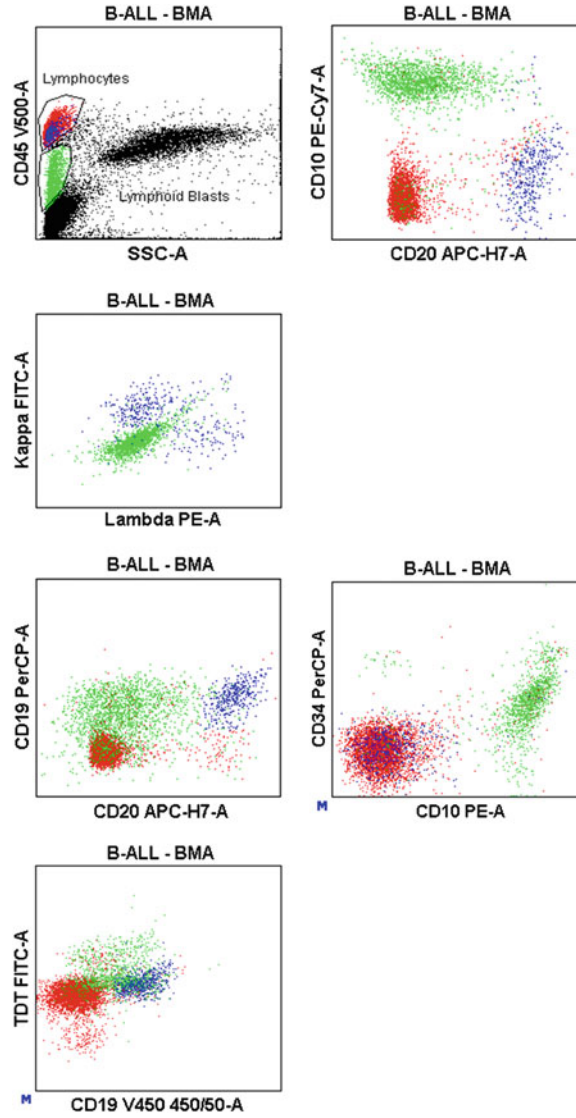


**Fig. 6** Representative dot plots from a patient's bone marrow aspirate demonstrating B-cell acute lymphoblastic leukemia (B-ALL). The B-ALL cells are depicted as the *green dots* and the population of comingling normal B cells are depicted as the *blue dots*. B-ALL cells express the characteristic immunophenotype of CD19+ $CD20^{dim}$+CD10+CD34+TdT+$CD45^{dim/negative}$ without surface or cytoplasmic immunoglobulin light chain. B-ALL cells are typically somewhat larger than normal lymphocytes in size, but have similar side scatter properties

and are either kappa or lambda restricted (Fig. 7). The clonal immunoglobulin light chain expression is characteristically surface "dim" or actually only apparent in the cytoplasm after permeabilization. Hairy cell leukemia is positive for pan-B-cell markers and CD103, CD11c, and CD25 and usually negative for CD5, CD10,

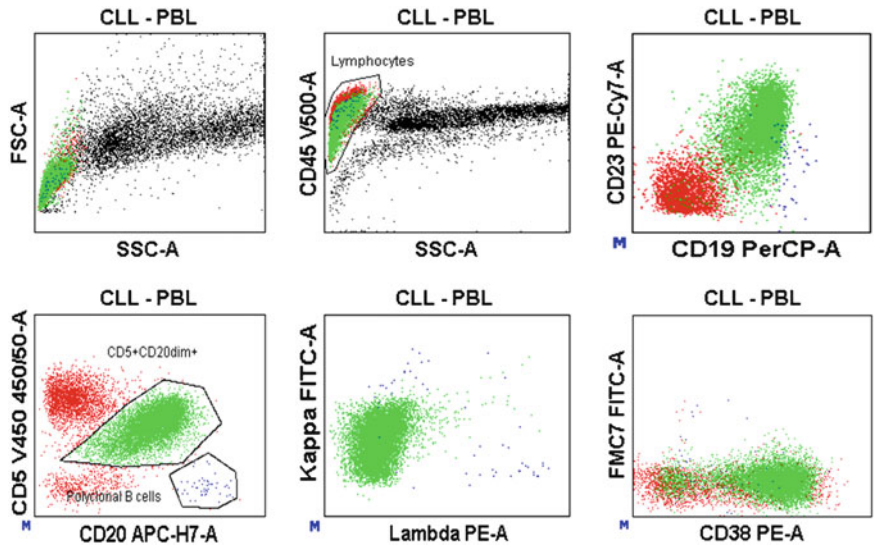


**Fig. 7** Representative dot plots from a patient's peripheral blood demonstrating chronic lymphocytic leukemia (CLL). The CLL cells are depicted as the *green dots* and the population of comingling normal B cells are depicted as the *blue dots*. CLL cells express the characteristic immunophenotype of CD19+CD20$^{dim}$+CD5$^{dim}$+ CD23+CD38+/−FMC7−CD10− with reduced expression of monotypic light chain. Note the contrast of CD5, CD20, and light chain expression of these cells to those demonstrated in mantle cell lymphoma in Fig. 12. CLL cells have similar forward and side scatter properties to that of normal lymphocytes

and CD23; these tumor cells often have increased forward light scatter (Fig. 8). Antibody combinations used to detect large granular lymphocyte (LGL) leukemia include CD57, CD7, CD3, CD2, CD56, CD8, CD16, and CD45 (Fig. 9).

A new flow cytometric assay for the detection of the *BCR-ABL1* oncogene, causative of chronic myelogenous leukemia (CML), has been developed. With this methodology mononuclear cells are lysed and the *BCR-ABL1* fusion protein is bound by anti-BCR antibodies adsorbed to capture beads. Subsequently, a phycoerythrin-tagged anti-ABL1 antibody is used as the detector reagent to determine the mean fluorescence intensity. This assay reached 100 % concordance with the polymerase chain reaction method for reliable detection of the *BCR-ABL1* fusion protein [16], but its value for clinical diagnosis of CML will need to be assessed in the future. Flow cytometry, however, is well established as a reliable method to enumerate blast counts.

Leukemic stem cells (LSC) are rare leukemic cells which are resistant to chemotherapy and have acquired the ability to self-renew and induce disease in immunosuppressed mice upon xenotransplantation. As they are thought to reside in an LSC niche, from where they are hypothesized to give rise to relapsed disease, they have not been accessible for flow cytometry and their exact immunophenotype is uncertain. However, they are thought to

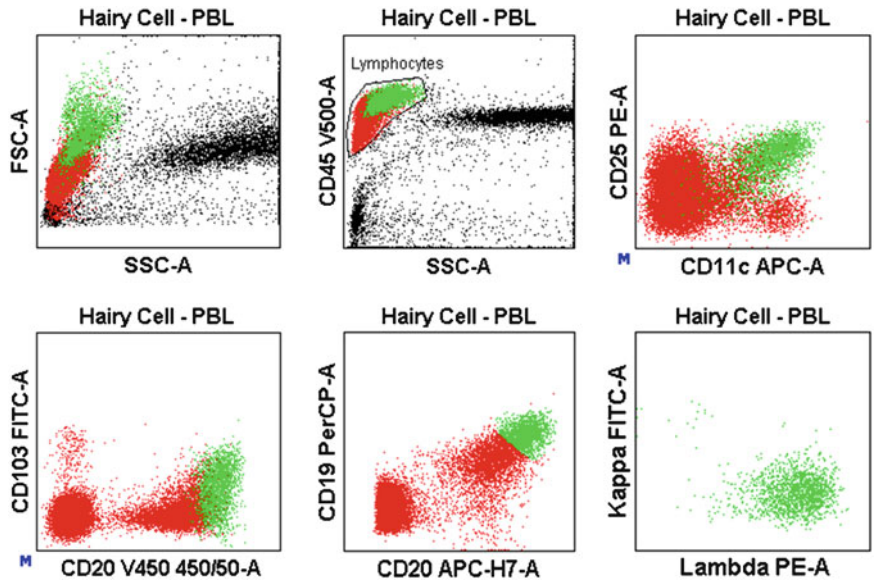


**Fig. 8** Representative dot plots from a patient's peripheral blood demonstrating hairy cell leukemia. The "hairy cells" are depicted as the *green dots* and express the characteristic immunophenotype of CD19+CD20$^{bright}$ +CD11c+CD25+CD103+ with monotypic light chain. Hairy cells are also larger than normal lymphocytes in size and have increased side scatter

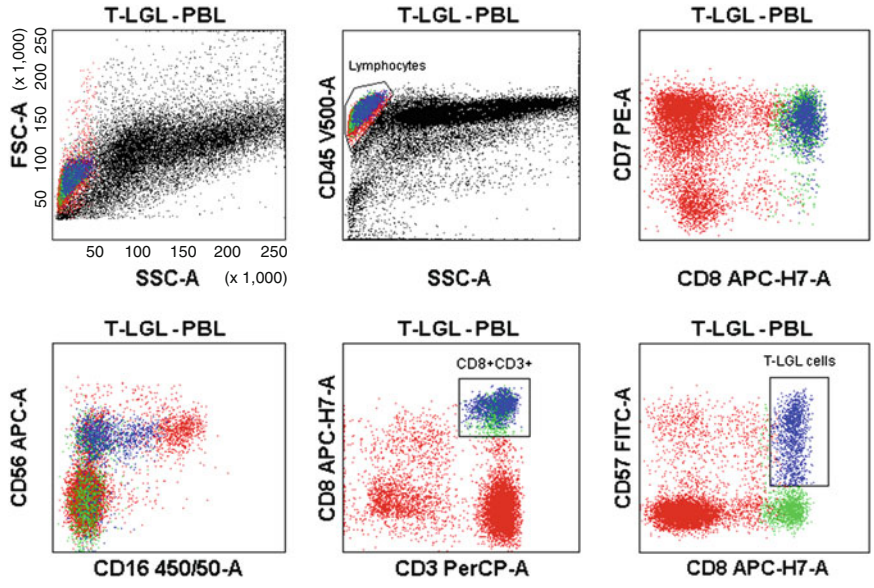


**Fig. 9** Representative dot plots from a patient's peripheral blood with T-cell large granular lymphocytosis (T-LGL). The T-LGLs are depicted as the *blue dots* and immunophenotypically co-express CD3+CD8+ CD57+CD7+CD56+. This particular case does not express CD16. T-LGLs are typically slightly larger than normal lymphocytes in size and may have slightly increased side scatter

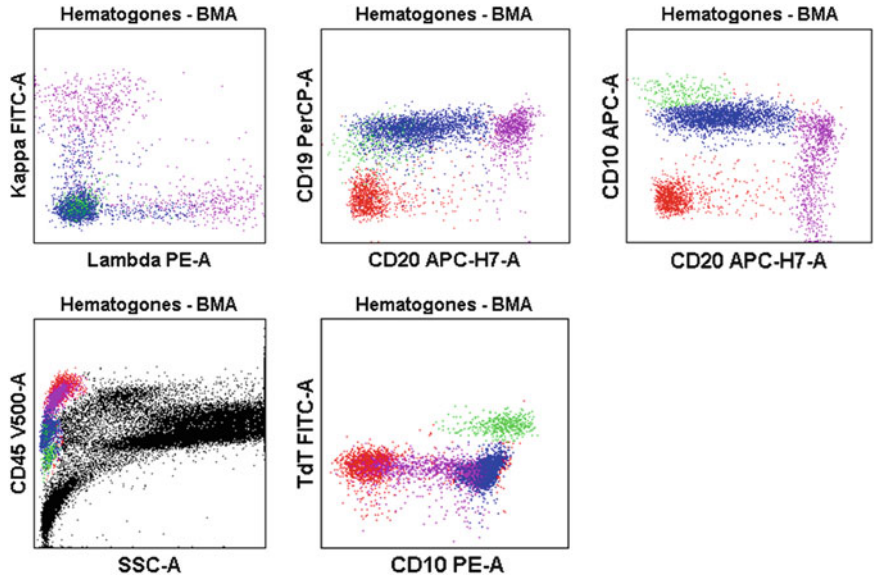


**Fig. 10** Representative dot plots from a patient's bone marrow aspirate demonstrating normal B-cell maturation (hematogones). The least mature B-cell population is depicted as *green dots*, with the highest levels of CD10+ $CD19^{dim}$+CD20−$CD45^{dim}$+ lacking surface or cytoplasmic light chain expression and exhibiting very low side scatter. These also have nuclear TdT+ expression as well as elevated levels of CD38 and CD43 (not shown). The *blue dots* are in an intermediate state where the aforementioned markers are downregulated, while CD19, CD20, and surface immunoglobulin are upregulated. The *purple dots* represent the mature B-cell population. As the B cells undergo the maturation process, the immunophenotype ultimately progresses to TdT-CD10-CD19+CD20+CD45+ with either kappa or lambda surface light chain expression. *See* also Figs. 18 and 19

reside in the CD34+ CD38− fraction in AML [17, 18] and CML [19, 20] and in the CD34+ CD38− CD19+ fraction in B-ALL [21] (reviewed in ref. 4). Hematogones, benign lymphoid precursor cells, are frequently found in bone marrow aspirates, especially of young patients after chemotherapy (Figs. 10, 18, 19). They should not be confused with B-ALL blasts, as their immunophenotype (CD19+ CD20+ CD10+) is similar.

### 3.2 Lymphoma

Flow cytometry is used to immunophenotype lymphocytes in peripheral blood, fine needle aspirates, ascites, pleuritic fluid, or solid tissue specimens using T-, B-, and NK-cell markers, if a clonal population which may be consistent with a non-Hodgkin lymphoma (NHL) is suspected.

Our laboratory utilizes the following two tubes with eight conjugated monoclonal antibodies:

Tube 1: CD7, CD16, CD3, CD2, CD8, CD14, CD4, CD45

Tube 2: kappa, lambda, CD19, CD10, CD23, CD20, CD5, CD45

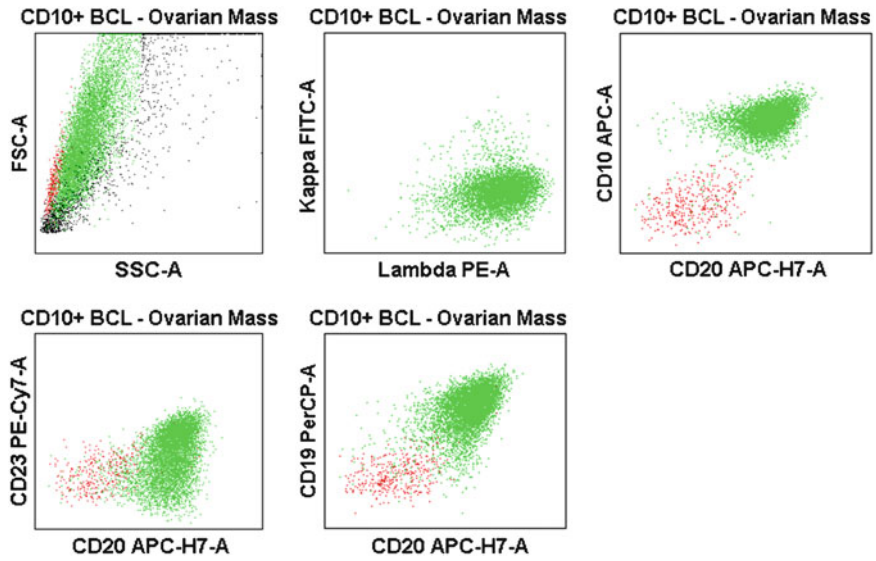


**Fig. 11** Representative dot plots from a patient's ovarian mass demonstrating a CD10+ B-cell lymphoma (this patient was diagnosed with Burkitt's lymphoma based on the finding of the t(8;14) karyotype. However, this immunophenotype could also be consistent with follicular lymphoma). The Burkitt's cells are depicted as the *green dots* and express the characteristic immunophenotype of CD19+CD20+CD10+CD5−CD23+/− with monotypic lambda light chain. Burkitt's lymphoma cells are often larger than normal lymphocytes in size and have slightly increased side scatter

Follicular lymphoma (FL) is generally positive for CD19, CD10, CD23, CD20, and clonal kappa or lambda, while diffuse large B-cell lymphoma (DLBCL) frequently contains larger cells with an increased forward scatter and exhibits a similar immunophenotype: CD19, CD10, cytoplasmic CD79a, CD23, CD20, and clonal kappa or lambda, although light chain expression may be absent. Several cases of DLBCL overlap immunophenotypically with FL. However, some DLBCLs lack germinal center markers (as assessed by immunohistochemistry), so the immunophenotype can aid in excluding FL. However, cell size and pattern are very important in distinguishing between FL and DLBCL. In addition, DLBCL almost always has a higher proliferation index. Epstein–Barr virus or human herpes virus 8 may be detectable in some uncommon cases of DLBCL, while these are absent in FL. Burkitt's lymphoma is positive for CD19, CD20, and CD10 and further distinction from DLBCL and FL is achieved by histomorphology and immunohistochemical stains such as bcl-2 (Fig. 11). Similar to CLL, CD5-expression on B cells is frequently found in mantle cell lymphomas (MCL), but MCL is typically CD23– and FMC7+ and expresses CD20 and clonal kappa or lambda light chain more brightly than CLL [22] (Fig. 12). For suspected NHL in cerebrospinal or vitreous fluids, our laboratory uses the following

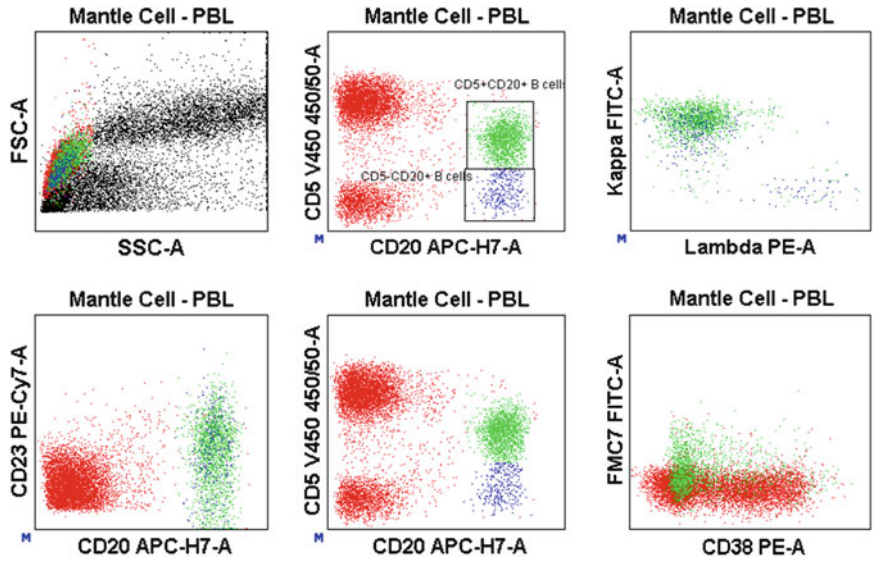


**Fig. 12** Representative dot plots from a patient's peripheral blood demonstrating mantle cell lymphoma (MCL). The MCL cells are depicted as the *green dots* and the population of comingling normal B cells are depicted as the *blue dots*. MCL cells express the characteristic immunophenotype of CD19+CD20+CD5+CD23+/–CD3–FMC7+CD10– with monotypic light chain. In contrast to CLL, note that the tumor cells of mantle cell lymphoma are quite similar in their CD20 expression to the comingling normal B cells but that their restricted light chain expression is enhanced. MCL cells have similar forward and side scatter properties to that of normal lymphocytes

combination of directly conjugated antibodies: kappa, lambda, CD19, CD3, CD4, CD8, CD20, and CD45.

Common markers in T-NHL are CD3, CD7, CD2, CD4, and/or CD8. Clonal T-cell receptor rearrangements may be found by molecular diagnostic techniques. Sezary syndrome/mycosis fungoides/cutaneous T-cell lymphoma (CTCL) is positive for CD3, CD2, CD4, and/or CD8 (Fig. 13). Expression of CD5 and/or CD7 may be variable in CTCL and loss of CD26 is frequent in erythroderma associated with Sezary syndrome [23]. Although usually found in tissue sections and formerly not a good candidate for diagnostic testing by flow cytometry, Hodgkin's lymphoma can also be identified by flow-based immunofluorescence techniques [24].

### 3.3 Plasma Cell Myeloma

Plasma cell myeloma (PCM) is a malignancy of plasma cells. A plasma cell is a fully differentiated manifestation of a B cell that functions to produce antibodies. Malignant plasma cells usually express $CD38^{bright}$+, CD138+, CD19–, and $CD45^{dim}$+. They demonstrate monotypic expression of kappa or lambda light chains detected by cytoplasmic staining, and many additional markers are being investigated for their contribution to diagnosis, management, and detection of minimal residual disease (Fig. 14) [25–29].

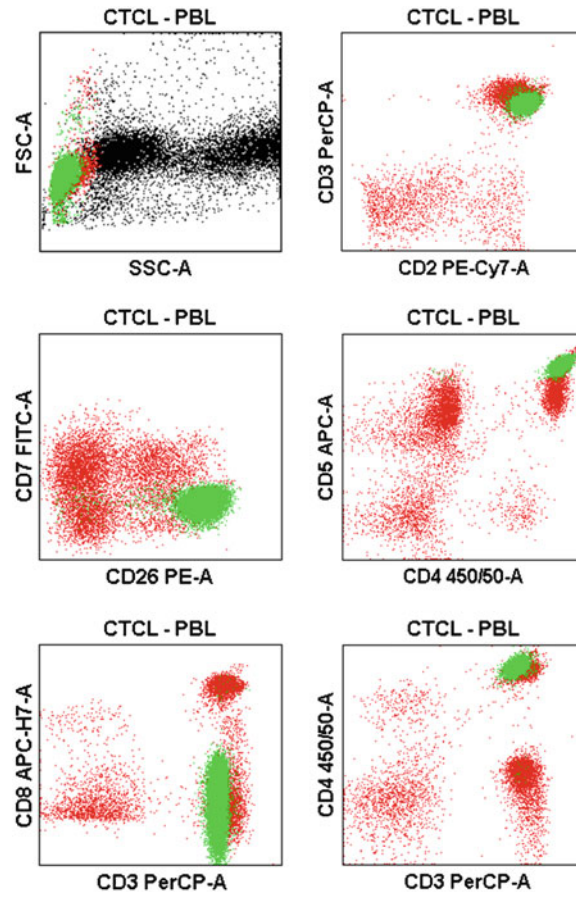


**Fig. 13** Representative dot plots from a patient's peripheral blood demonstrating cutaneous T-cell lymphoma (CTCL). The CTCL cells are depicted as the *green dots* expressing the immunophenotype CD3+CD2+CD7−CD26+CD4+CD5$^{bright}$+ CD8−. However, CTCL immunophenotypes can be variable. CTCL cells have similar forward and side scatter properties to that of normal lymphocytes

## *3.4 The Use of Flow Cytometry in Other Diseases/Tissue Sites*

### *3.4.1 Paroxysmal Nocturnal Hemoglobinuria*

Paroxysmal nocturnal hemoglobinuria (PNH) is a rare acquired hematopoietic disorder caused by a mutation in the gene encoding for phosphatidylinositol glycan A (PIGA) [30, 31]. PIGA is a protein necessary for producing glycosylphosphatidylinositol (GPI), which anchors proteins to the cell membrane, in particular proteins which protect the cell from destruction by the complement system, like CD55 and CD59. Thus, patients with PNH have a complement-induced hemolytic anemia, hemoglobinuria, and thrombosis. Flow cytometry allows analysis of the expression of GPI-linked proteins on red blood cells (CD59), monocytes (CD14), and neutrophils (CD24), as well as the specific GPI-linked protein aerolysin identified by the fluorescently linked aerolysin (FLAER), expressed by peripheral blood lymphocytes; similar to CD34 quantitation

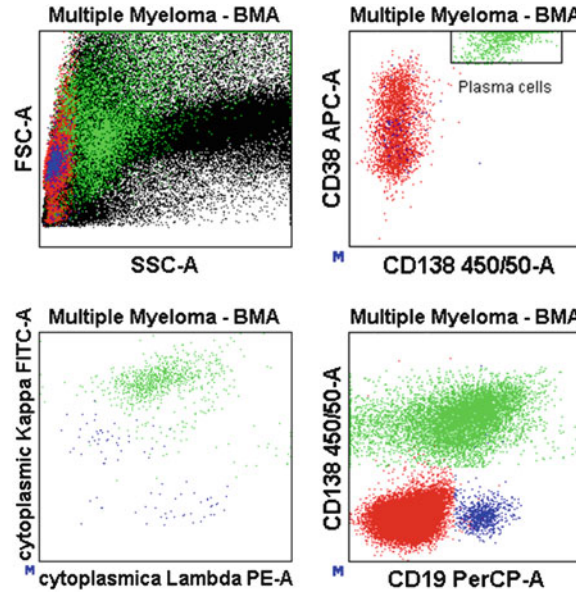


**Fig. 14** Representative dot plots from a patient's bone marrow aspirate demonstrating plasma cell myeloma. The malignant plasma cells are depicted as the *green dots* and the population of comingling normal B cells are depicted as the *blue dots*. Plasma cells in plasma cell myeloma express the characteristic immunophenotype of CD138+CD38+CD19−/+CD45$^{dim}$+ with monotypic cytoplasmic light chain. Plasma cells are larger than normal lymphocytes in size and have slightly increased side scatter

described in Subheading 2.1, this type of analysis has also been automated with a new software approach utilizing a probability state model (Fig. 15) [32]. The reagent pallet and method of analysis continue to expand, with the improvement of the assay with CD64 as a marker for monocytes [33, 34]. The expression of these proteins is decreased or absent in patients with PNH. Staining with directly conjugated monoclonal antibodies is performed as follows:

Red blood cells (1:100 dilution): glycophorin, CD59

Monocytes (undiluted blood): FLAER, CD64, CD14, CD45

Neutrophils (undiluted blood): FLAER, CD24, CD15, CD45 [35]

In order to detect abnormal T-cell populations in patients infected with human T-cell lymphotropic virus (HTLV)-1, antibodies to CD25, CD7, CD3, CD2, CD5, CD8, CD4, and CD45 are used. Abnormal populations of eosinophils can be detected by staining for CD49d, CD33, CD294, and CD45.

Although a less sensitive test for the detection of giardia in stool samples than conventional microcopy or direct immunofluorescence, flow cytometry may be beneficial in detecting giardia cysts, particularly

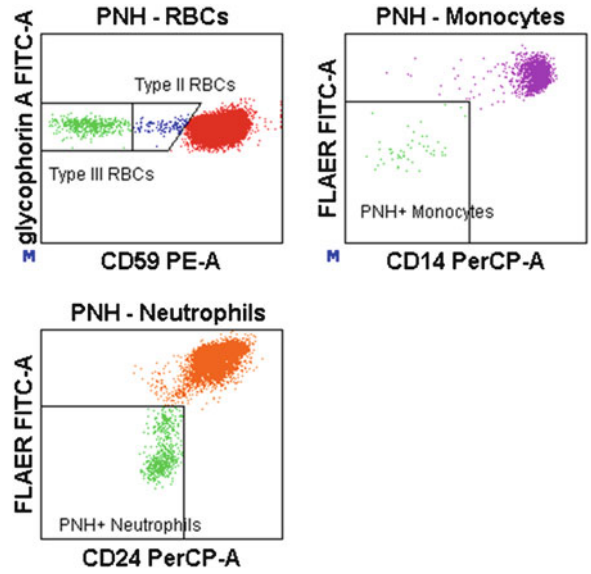


**Fig. 15** Representative dot plots from a patient's peripheral blood demonstrating paroxysmal nocturnal hemoglobinuria (PNH). The events characterizing PNH can be seen in the red blood cell lineage (as CD59 dim-to-negative events), the monocytic lineage (as fluorescent aerolysin-/CD14– events), and the neutrophilic lineage (as fluorescent aerolysin-/CD24– events)

in epidemiological settings or in the absence of an experienced microscopist [36]. Furthermore, flow cytometry showed good correlation with the standard Kleihauer-Betke assay for the detection of fetomaternal hemorrhage with the use of an anti-hemoglobin F antibody [37]. Used in conjunction with other techniques, flow cytometry is also useful in the detection of malignancy by the analysis of paucicellular bronchoalveolar lavage (BAL) specimens [38] and GIST tumors [39] and the analysis of cerebrospinal fluid [40].

### *3.5 Recent Developments and the Near Future of Flow Cytometry*

The field of flow cytometry continues to advance rapidly with exciting new developments. The technology may be thought of as a "three legged stool" that is supported by the synergy of hardware, software and fluorochrome biochemistry [41]. With respect to hardware, it has become obvious that high-resolution polychromatic flow cytometry (both for analysis and cell sorting) is greatly enhanced by both reducing the number of fluorochromes utilized per laser excitation beam and simultaneously increasing the number of excitation lines per instrument. This permits data production with little need for intra- or interlaser compensation and results in very clear concise data. This is presently far easier to do since the advent of extraordinarily small [relative to legacy water-cooled ion-gas lasers] fiber launched diode crystal lasers. With respect to these light sources, presently almost any line from the ultraviolet through

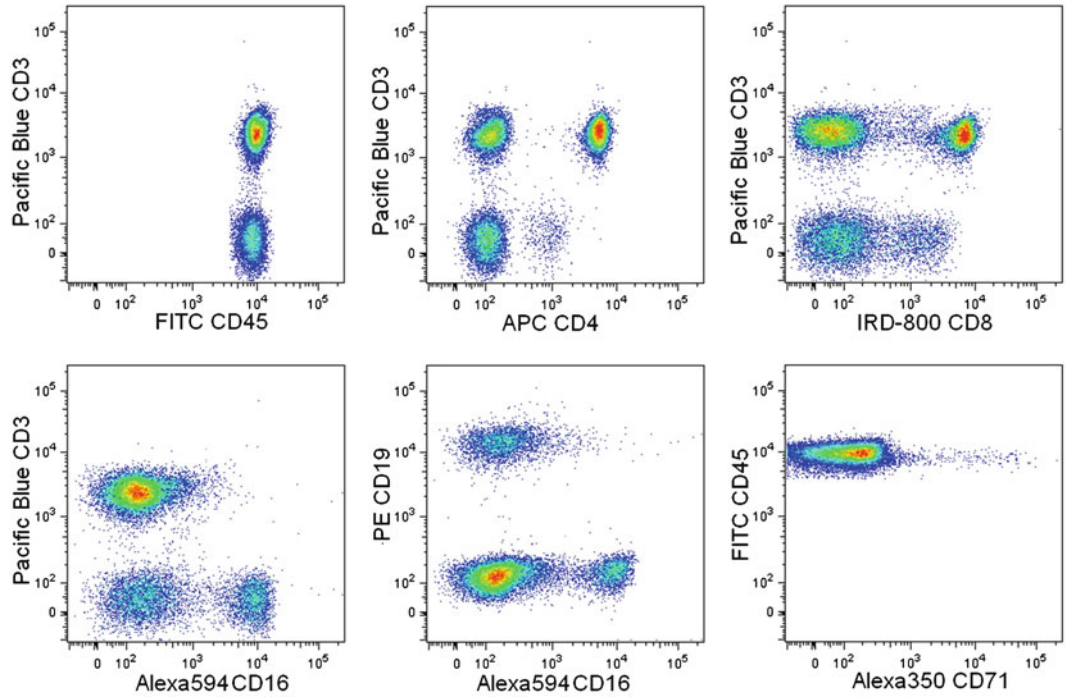


**Fig. 16** Seven lasers for seven fluorochromes. Individual laser excitation of conjugated monoclonal antibodies demonstrates high resolution data. The following reagent-fluorochrome combinations were utilized and excited by the indicated laser line: CD71 Alexa 350 (355 nm), CD3 Pacific Blue (405 nm), CD45 FITC (488 nm), CD19 PE (532 nm), CD16 Alexa 594 (594 nm), CD4 APC (641 nm), and CD8 IRD 800 (785 nm). This results in virtually no fluorescence spillover and almost entirely obviates the need for intra- and interlaser compensation which when applied negatively impacts data resolution. The data was produced on the eight-laser platform depicted in Fig. 17

the infrared can be obtained from laser vendors and can be placed in a benchtop cytometer (Fig. 16). Filters now transmit light with almost 95 % efficiency, over relatively "flat" passbands, with sharp nanometer cutoff specifications (Fig. 17). Electronics in flow cytometers have recently been produced that surpass a 20-parameter limit, permitting up to 50 parameters to be monitored. Scalable software such as GemStone™ (Verity Software, Topsham ME) which is unrestricted regarding the number of parameters it can handle is available from a variety of sources (Fig. 18). Presently, the "bottleneck" in this tripartite paradigm is limitations in the organic-dye fluorochromes available. These dyes increase the spill-over between capture channels and require "compensation" which reduces data resolution. While not yet fully mature, it is hoped that increased flexibility in fluorochrome options will soon be forth-coming from companies such as Sirigen and their High Sensitivity Fluorescence™ technology that will not only expand the utility

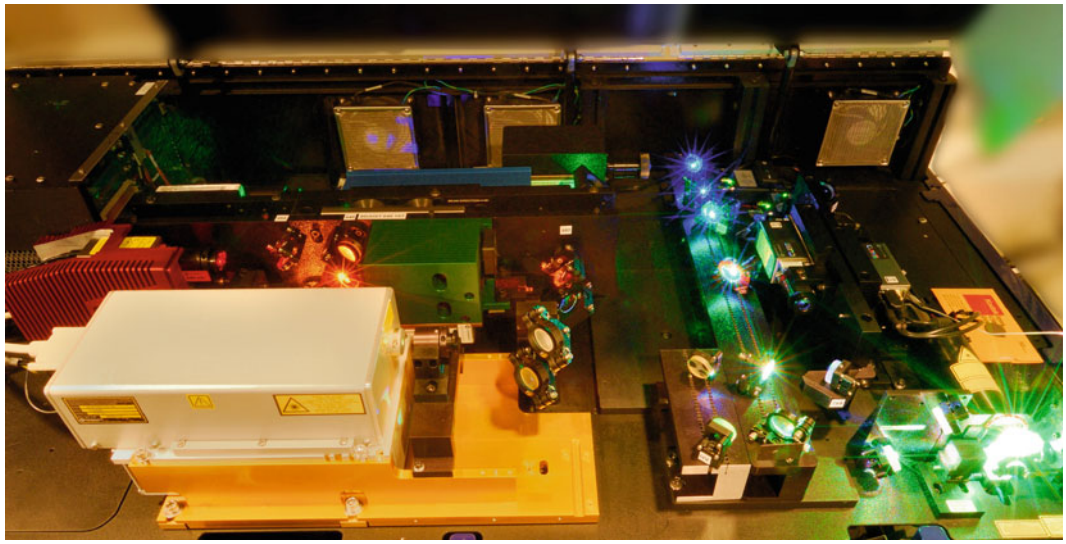

| Wavelength | Power mw | Label |
|---|---|---|
| 355 | 40 | Coherent Genesis |
| 405 | 100 | Coherent Cube |
| 488 | 100 | Coherent Sapphire |
| 532 | 150 | Coherent Sapphire |
| 552 | 100 | Coherent Sapphire |
| 594 | 200 | MPB |
| 641 | 100 | Coherent Cube |
| 785 | 40 | Coherent Cube |

**Fig. 17** Eight-laser SORP LSR (Becton-Dickinson) flow cytometer. The benchtop flow cytometer depicted contains eight lasers with the indicated power characteristics. This provides highly flexible excitation capacity to the laboratory. When the appropriate fluorochromes are available, for the highest data resolution, it is best to reduce the numbers of fluorochromes excited per laser and increase the numbers of lasers used. Future versions of this platform will have the capacity to incorporate additional excitation lines and acquire up to 50 distinct parameters simultaneously

of the violet beam but lower energy beams further into the red spectrum as well.

Mass cytometry, utilizing the CyTOF™ platform (DVS Sciences, Sunnyvale CA), is another emerging technology that combines the analytical power of mass spectrometry with multiparameter flow cytometry. Antibodies or DNA intercalators are labeled with isotopes of transition elements and are mass analyzed and counted together with stained, vaporized, atomized, and subsequently ionized cell samples. Similar to immunofluorescence-based flow cytometry, the atomic ions and the tagging isotopes are counted in real time and can be analyzed on conventional flow cytometric software after having been converted to the FCS 3.0 format. With mass-tag cellular barcoding, mass cytometry throughput has been increased significantly, which will be invaluable for drug discovery, immunology,

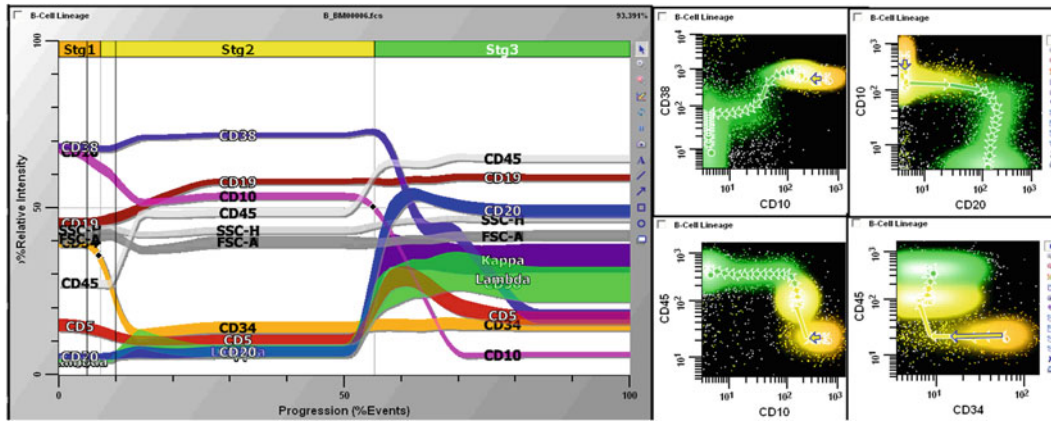


**Fig. 18** This representation of normal human marrow B-cell maturation is depicted simultaneously both as a parameter profile plot (*left*) and four more conventional bivariate dot plots (*right*) by Gemstone™ Software (Verity Software House, Topsham, ME). B-cell maturation is initiated in human bone marrow by $CD19^{dim}$+ $CD45^{dim}$+ CD34+ CD38+ $CD10^{bright}$+ cells which downregulate CD10+, CD34+, and then CD38+ as they upregulate CD45, CD20, and surface immunoglobulin expression. While the dot-plot format shown is familiar to all flow cytometrists, interpreting high numbers of them becomes problematic for polychromatic analysis. The parameter profile plots are "scalable" and can display as many data points as the user wishes and are far more comprehensible to the non-cytometrist

preclinical analysis, and the understanding of the mechanisms of diseases and their treatments [42–45].

A breakthrough technology is found in the form of the Amnis instrument where flow cytometry can now be integrated with the power of visual microscopy. The Amnis platform fills an important gap in existing technology. While flow cytometry provides great statistical power, it provides relatively little information content per cell (results are based essentially on intensity only). On the other hand, fluorescence microscopy provides extremely high information per cell (as it is an image), but typically provides very poor statistical power.

The Amnis ISX platform couples important attributes of these two technologies on the same platform. The high acquisition rates obtained by "imaging in flow" enable the ability to utilize population statistics to assess differences in appearance rather than solely differences in fluorescence expression/intensity.

By leveraging the same basic fluidics (and fluorochrome excitation/emission) principles as traditional flow cytometry, statistically robust numbers of cells can be acquired for analysis on the Amnis platform. Unlike flow cytometry, images are taken of each cell in bright-field and fluorescent channels and intensity information is collected, enabling "statistical microscopy" to be performed on large populations of cells (Fig. 19).

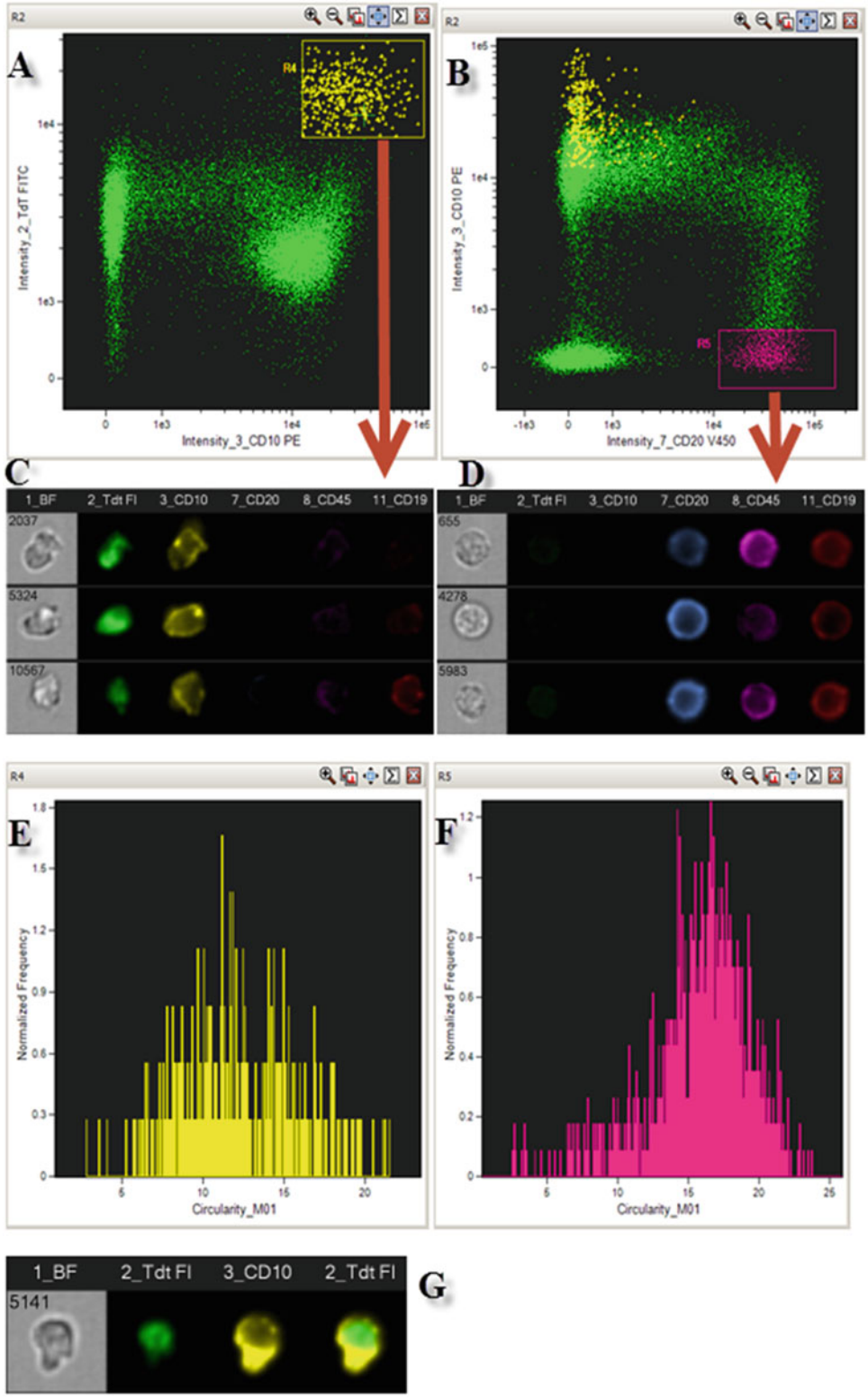


**Fig. 19** Image-based flow cytometry. Specimens introduced into the Amnis ISX platform were initially assessed to be in focus (high gradient root mean square, in bright field), single cells (area vs. high aspect ratio, in bright field), and CD45+ with low side scatter characteristics. These human bone marrow cells were stained by standard techniques with TdT-FITC, CD10-PE, CD20-V450, CD19-APC, and CD45-V500. A bivariate dot plot (*panel a*) depicts TdT versus CD10 expression, with the brightest CD10+TdT+ cells identified in the R4 yellow gate.

Individual cells are captured on one to two cameras and can be displayed by both bright-field and fluorescence features. This capacity to localize the staining provides not only information on basic immunofluorescence but additionally the analysis of internalization and co-localization of proteins, cell death and autophagy, cell signaling, cell cycling, apoptosis, and DNA damage and repair. Furthermore, the imaging of cell-cell interactions and discrimination of cells from debris are also now far more accessible. These features are already being used in the research setting and could be exploited clinically in order to assess specific killing of a malignant cell in response to drug treatment, for example [46]. One exciting, novel clinical application of the Amnis instrument is rapid detection of intracellular promyelocytic leukemia (PML) protein in abnormal myeloid cells in patients with acute promyelocytic leukemia [47, 48]. In these patients, a rapid diagnosis is essential in order to initiate treatment with all-trans retinoic acid and cytostatic therapy, in order to prevent life-threatening coagulopathy, rapid disease progression, and death.

### 3.6 Summary

In summary, flow cytometry and its associated technologies are powerful aids in the evaluation and diagnosis of human disease states. Not only is flow cytometry helpful in the assessment and continuous monitoring of inherited or acquired immune disorders, but it is also invaluable in the monitoring of clinical response to various immunomodulatory therapies. This is in addition to the critical role it continues to play in basic and applied research. This is an exciting time in which our knowledge of human disease is rapidly growing, yet is becoming more and more complex, due to improved genome sequencing methods and technologies to understand epigenetic regulation of genes and finally personalized medicine. Flow cytometry and its more recent developments will, therefore, be instrumental in demonstrating to us the effects of genetic, epigenetic, and pharmacological alterations on a cellular, morphological, and more functional level.

**Fig. 19** (continued) These cells are also shown to be CD20– in the CD10 versus CD20 plot (*panel b*). Each of the cells analyzed by the ISX is then individually assessed for their expression of each of the indicated markers and their bright-field image, as shown in the next row. For example, in *panel c*, the R4-gated CD10+TdT+ cells are seen to express nuclear TdT and bright membrane expression of CD10; there is only trace expression of CD20 and CD45 and CD19 is present, but this is relatively dimly expressed. The TdT+CD10$^{bright}$+CD19$^{dim}$ +CD20– immunophenotype is characteristic of the least mature cells on the B-cell differentiation path in the bone marrow. In *panel d*, all the TdT and CD10 expression is downregulated, while the cells fully express CD45 and B-lineage associated CD19 and CD20. Completely novel and specific to ISX analysis is that the shape of the cells can be both visually inspected, and assessed statistically, and shown to be distinct; that is, the most mature B cells are seen to be "round" (bright-field column, *panel d*) compared to the least mature cells which are distinctly "not round" (bright-field column, *panel c*). This was enumerated and graphed on 1,143 and 361 cells, in *panels f* and *g*, respectively; the biological significance of this observation is not presently understood. Finally, the nuclear staining of TdT and CD10 membrane expression are overlaid in the last column of *panel g*

## Acknowledgements

The authors would like to thank Laura Dillon, David Dombkowski, Abby Kelliher, and Scott Mordecai for their gracious help and specific contributions to this chapter.

## Disclaimers

The authors have no conflicts of interest to disclaim.

*Source of support*: K08 CA138916-02 to DSK and grants 1S10OD012027-01A1 and 1S10RR020936-01 to FIP.

### References

1. Spitzer TR, Dey BR, Chen YB, Attar E, Ballen KK (2012) The expanding frontier of hematopoietic cell transplantation. Cytometry B Clin Cytom 82:271–279
2. Preffer FI (2012) Issue highlights. Cytometry B Clin Cytom 82:343–344, November 2012
3. Rosko A, Lazarus HM (2012) Refining hematopoietic cell transplant: a concise review. Cytometry B Clin Cytom 82:266–267
4. Krause DS, Scadden DT, Preffer FI (2013) The hematopoietic stem cell niche—home for friend and foe? Cytometry B Clin Cytom 84: 7–20
5. Herbert DJ, Miller DT, Bruce Bagwell C (2012) Automated analysis of flow cytometric data for CD34+ stem cell enumeration using a probability state model. Cytometry B Clin Cytom 82:313–318
6. Whitby A, Whitby L, Fletcher M et al (2012) ISHAGE protocol: are we doing it correctly? Cytometry B Clin Cytom 82:9–17
7. Schnizlein-Bick CT, Spritzler J, Wilkening CL, Nicholson JKA, O'Gorman MRG (2000) Evaluation of TruCount absolute-count tubes for determining CD4 and CD8 cell numbers in human immunodeficiency virus-positive adults. Clin Diagn Lab Immunol 7:336–343
8. Warnatz K, Schlesier M (2008) Flow cytometric phenotyping of common variable immunodeficiency. Cytometry B Clin Cytom 74:261–271
9. van de Loosdrecht AA, Ireland R, Kern W et al (2013) Rationale for the clinical application of flow cytometry in patients with myelodysplastic syndromes: position paper of an International Consortium and the European LeukemiaNet Working Group. Leuk Lymphoma 54(3): 472–475
10. Bellos F, Alpermann T, Gouberman E et al (2012) Evaluation of flow cytometric assessment of myeloid nuclear differentiation antigen expression as a diagnostic marker for myelodysplastic syndromes in a series of 269 patients. Cytometry B Clin Cytom 82:295–304
11. Monaghan SA, Surti U, Doty K, Craig FE (2012) Altered neutrophil maturation patterns that limit identification of myelodysplastic syndromes. Cytometry B Clin Cytom 82:217–228
12. Della Porta MG, Lanza F, Del Vecchio L (2011) Flow cytometry immunophenotyping for the evaluation of bone marrow dysplasia. Cytometry B Clin Cytom 80:201–211
13. Kern W, Bacher U, Schnittger S, Alpermann T, Haferlach C, Haferlach T (2013) Multiparameter flow cytometry reveals myelodysplasia-related aberrant antigen expression in myelodysplastic/myeloproliferative neoplasms. Cytometry B Clin Cytom 84(3):194–197. doi:10.1002/cyto.b.21068
14. Sandes AF, Kerbauy DMB, Matarraz S, Chauffaille MD, López A, Orfao A, Yamamoto M (2013) Combined flow cytometric assessment of CD45, HLA-DR, CD34, and CD117 expression is a useful approach for reliable quantification of blast cells in myelodysplastic syndromes. Cytometry B Clin Cytom. doi:10.1002/cyto.b.21087
15. Swerdlow S, Campo E, Lee Harris N et al (2008) WHO classification of tumors of haematopoietic and lymphoid tissues, 4th edn. IARC, Lyon
16. Hevessy Z, Hudak R, Kiss-Sziraki V et al (2011) Laboratory evaluation of a flow cytometric BCR-ABL immunobead assay. Clin Chem Lab Med 50:689–692
17. Lapidot T, Sirard C, Vormoor J et al (1994) A cell initiating human acute myeloid leukaemia after transplantation into SCID mice. Nature 367:645–648

18. Bonnet D, Dick JE (1997) Human acute myeloid leukemia is organized as a hierarchy that originates from a primitive hematopoietic cell. Nat Med 3:730–737
19. Wang JCY, Lapidot T, Cashman JD et al (1998) High level engraftment of NOD/SCID mice by primitive normal and leukemic hematopoietic cells from patients with chronic myeloid leukemia in chronic phase. Blood 91: 2406–2414
20. Eisterer W, Jiang X, Christ O et al (2005) Different subsets of primary chronic myeloid leukemia stem cells engraft immunodeficient mice and produce a model of the human disease. Leukemia 19:435–441
21. Castor A, Nilsson L, Astrand-Grundstrom I et al (2005) Distinct patterns of hematopoietic stem cell involvement in acute lymphoblastic leukemia. Nat Med 11:630–637
22. Medd PG, Clark N, Leyden K et al (2011) A novel scoring system combining expression of CD23, CD20, and CD38 with platelet count predicts for the presence of the t(11;14) translocation of mantle cell lymphoma. Cytometry B Clin Cytom 80:230–237
23. Campbell SM, Peters SB, Zirwas MJ, Wong HK (2010) Immunophenotypic diagnosis of primary cutaneous lymphomas. J Clin Aesthet Dermatol 3:21–25
24. Fromm JR (2011) Flow cytometric analysis of CD123 is useful for immunophenotyping classical Hodgkin lymphoma. Cytometry B Clin Cytom 80:91–99
25. Cannizzo E, Bellio E, Sohani AR et al (2010) Multiparameter immunophenotyping by flow cytometry in multiple myeloma: the diagnostic utility of defining ranges of normal antigenic expression in comparison to histology. Cytometry B Clin Cytom 78:231–238
26. Paiva B, Almeida J, Pérez-Andrés M et al (2010) Utility of flow cytometry immunophenotyping in multiple myeloma and other clonal plasma cell-related disorders. Cytometry B Clin Cytom 78:239–252
27. Frébet E, Abraham J, Geneviève F et al (2011) A GEIL flow cytometry consensus proposal for quantification of plasma cells: application to differential diagnosis between MGUS and myeloma. Cytometry B Clin Cytom 80:176–185
28. Drain S, Catherwood MA, Bjourson AJ, Drake MB, Kettle PJ, Alexander HD (2012) Neither P-gp SNP variants, P-gp expression nor functional P-gp activity predicts MDR in a preliminary study of plasma cell myeloma. Cytometry B Clin Cytom 82:229–237
29. Peceliunas V, Janiulioniene A, Matuzeviciene R, Griskevicius L (2011) Six color flow cytometry detects plasma cells expressing aberrant immunophenotype in bone marrow of healthy donors. Cytometry B Clin Cytom 80:318–323
30. Sutherland DR, Keeney M, Illingworth A (2012) Practical guidelines for the high-sensitivity detection and monitoring of paroxysmal nocturnal hemoglobinuria clones by flow cytometry. Cytometry B Clin Cytom 82: 195–208
31. Marinov I, Kohoutova M, Tkacova V et al (2013) Intra- and interlaboratory variability of paroxysmal nocturnal hemoglobinuria testing by flow cytometry following the 2012 Practical Guidelines for high-sensitivity paroxysmal nocturnal hemoglobinuria testing. Cytometry B Clin Cytom 84(4):229–236
32. Miller DT, Hunsberger BC, Bagwell CB (2012) Automated analysis of GPI-deficient leukocyte flow cytometric data using GenStoneTM. Cytometry B Clin Cytom 82:319–324
33. Dalal BI, Khare NS (2013) Flow cytometric testing for paroxysmal nocturnal hemoglobinuria: CD64 is better for gating monocytes than CD33. Cytometry B Clin Cytom 84:33–36
34. Wong L, Davis BH (2013) Monochromatic gating method by flow cytometry for high purity monocyte analysis. Cytometry B Clin Cytom 84:119–124
35. Borowitz MJ, Craig FE, Digiuseppe JA et al (2010) Guidelines for the diagnosis and monitoring of paroxysmal nocturnal hemoglobinuria and related disorders by flow cytometry. Cytometry B Clin Cytom 78:211–230
36. El-Nahas HA, Salem DA, El-Henawy AA, El-Nimr HI, Abdel-Ghaffar HA, El-Meadawy HA (2013) Giardia diagnostic methods in human fecal samples: a comparative study. Cytometry B Clin Cytom 84:44–49
37. Pastoret C, Le Priol J, Fest T, Roussel M (2013) Evaluation of FMH QuikQuant for the detection and quantification of fetomaternal hemorrhage. Cytometry B Clin Cytom 84: 37–43
38. Song JY, Filie AC, Venzon D, Stetler-Stevenson M, Yuan CM (2012) Flow cytometry increases the sensitivity of detection of leukemia and lymphoma cells in bronchoalveolar lavage specimens. Cytometry B Clin Cytom 82: 305–312
39. Bozzi F, Conca E, Manenti G, Negri T et al (2011) High CD133 expression levels in gastrointestinal stromal tumors. Cytometry B Clin Cytom 80:238–247
40. Stacchini A, Demurtas A, Aliberti S (2012) Flow cytometric detection of liposomal cytarabine in cerebrospinal fluid of patients treated with intrathecal chemotherapy. Cytometry B Clin Cytom 82:280–282
41. Preffer FI, Dombkowski D (2009) Advances in complex multiparameter flow cytometry

technology: applications in stem cell research. Cytometry B Clin Cytom 76:295–314
42. Bodenmiller B, Zunder ER, Finck R et al (2012) Multiplexed mass cytometry profiling of cellular states perturbed by small-molecule regulators. Nat Biotechnol 30:858–867
43. Bandura DR, Baranov VI, Ornatsky OI et al (2009) Mass cytometry: technique for real time single cell multitarget immunoassay based on inductively coupled plasma time-of-flight mass spectrometry. Anal Chem 81:6813–6822
44. Bendall SC, Simonds EF, Qiu P et al (2010) Single-cell mass cytometry of differential immune and drug responses across a human hematopoietic continuum. Science 332:687–696
45. Wang L, Abbasi F, Ornatsky O et al (2012) Human CD4+ lymphocytes for antigen quantification: characterization using conventional flow cytometry and mass cytometry. Cytometry 81:567–575
46. Samsel L, Dagur P, Raghavachari N, Seamon C, Kato G, McCoy JP Jr (2013) Flow cytometry for morphologic and phenotypic characterization of rare circulating endothelial cells. Cytometry B Clin Cytom (in press). doi: 10.1002/cyto.b.21088
47. Grimwade L, Gudgin E, Bloxham D, Scott MA, Erber WN (2011) PML protein analysis using imaging flow cytometry. J Clin Pathol 64:447–450
48. Mirabelli P, Scalia G, Pascariello C et al (2012) ImageStream promyelocytic leukemia protein immunolocalization: in search of promyelocytic leukemia cells. Cytometry 81:232–237

# Chapter 3

# Isolation and Characterization of Mesenchymal Stem Cells

**Sedat Odabas, A. Eser Elçin, and Y. Murat Elçin**

## Abstract

Mesenchymal stem cells (MSCs) have drawn great interest in the field of regenerative medicine, for cell replacement, immunomodulatory, and gene therapies. It has been shown that these multipotent stromal cells can be isolated from tissues such as bone marrow, adipose tissue, trimester amniotic tissue, umbilical cord blood, and deciduous teeth and can be expanded in adherent culture. They have the capacity to differentiate into cells of the connective tissue lineages in vitro and contribute to tissue parenchyma in vivo. However, proper in vitro manipulation of MSCs is a key issue to reveal a potential therapeutic benefit following transplantation into the patients. This chapter summarizes some of the essential protocols and assays used at our laboratory for the isolation, culture, differentiation, and characterization of mesenchymal stem cells from the bone marrow and adipose tissue.

**Key words** Mesenchymal stem cells, Bone marrow, Adipose, Isolation, Culture, Differentiation, Gene expression, Microarray

## 1 Introduction

In the last decade, mesenchymal stem cells (MSCs) which also may refer to as the multipotent stromal cells have generated considerable excitement for their potential use as universal donor cells in the regenerative medicine field as a whole. With their unique immune-tolerant nature, they give hope for their therapeutic use in cell replacement, gene therapy, and immunomodulatory therapy.

Friedenstein first described MSCs in the bone marrow as fibroblast-like colony-forming units in the late 1960s [1]. Later, these plastic-adhering, extensively replicating clonogenic somatic cells were found to have multipotent character both under in vitro [2–4] and in vivo settings [5–7]. MSCs are known to maintain stem cell niches and have several endogenous roles [8, 9].

To date, MSCs have been isolated from a wide range of adult tissues including the bone marrow, lipo-aspirated adipose, skeletal muscle, synovium, and synovium fat pad [10–15]. They can be

Meral Beksaç (ed.), *Bone Marrow and Stem Cell Transplantation*, Methods in Molecular Biology, vol. 1109,
DOI 10.1007/978-1-4614-9437-9_3, 

isolated from the deciduous teeth, from the trimester amniotic tissue, and from placental tissues as well [16–19].

In 2006, the International Society for Cellular Therapy (ISCT) described in a position article the minimal set of standards for defining MSCs to diminish the ambiguity in their identification based on adherence to plastic in standard culture, expression of a specific surface antigen set (must express CD105, CD73, and CD90 and must lack expression of CD45, CD34, CD14, CD19, and HLA-DR), and the trilineage mesoderm (namely, osteogenic, chondrogenic, and adipogenic) differentiation in vitro (Fig. 1) [20]. We now know that MSCs also have the ability to differentiate into non-mesodermal tissues [21–23]. Besides, the exact lineage and the set of surface antigen markers defining MSCs are not in concurrence, a feature largely dependent to tissue source, as well as to donor age and gender, passage number and seeding density, etc. [24]. However, this set of standards is a beneficial guide to investigators evaluating the extent of plasticity of the heterogenous fibroblast-like cell population.

Yet, already, a number of protocols concerning the isolation, culture, and characterization of MSCs can be found in the literature [25–29], investigators still keep digging to identify these cells and strive to standardize related protocols. We believe that proven isolation and characterization methodologies and well-established protocols and regulations are still necessary to facilitate the data exchange among researchers that will lead mesenchymal stem cells to become prevalent in regenerative medicine. This chapter presents some of the essential and useful protocols for bone marrow- and adipose tissue-derived MSCs.

## 2 Materials

### 2.1 Equipments

The list given below is common for all protocols:

1. Class II biological safety cabinet.
2. Carbon dioxide incubator, humidified.
3. Bench-top centrifuge.
4. Circulating water bath at 37 °C.
5. Hemocytometer or automatic cell counter.
6. Electronic transfer pipette controller (Gilson, cat. no. F110751).
7. Serological pipettes (Corning Inc.).
8. Pipette dispenser (a complete set for dispensing 0.1–1,000 μL; Eppendorf AG).
9. Sterile-barrier, RNase-free pipette tips (Eppendorf AG).
10. Tissue culture polystyrene (TCPS) flasks or multi-wells (Corning Inc.).

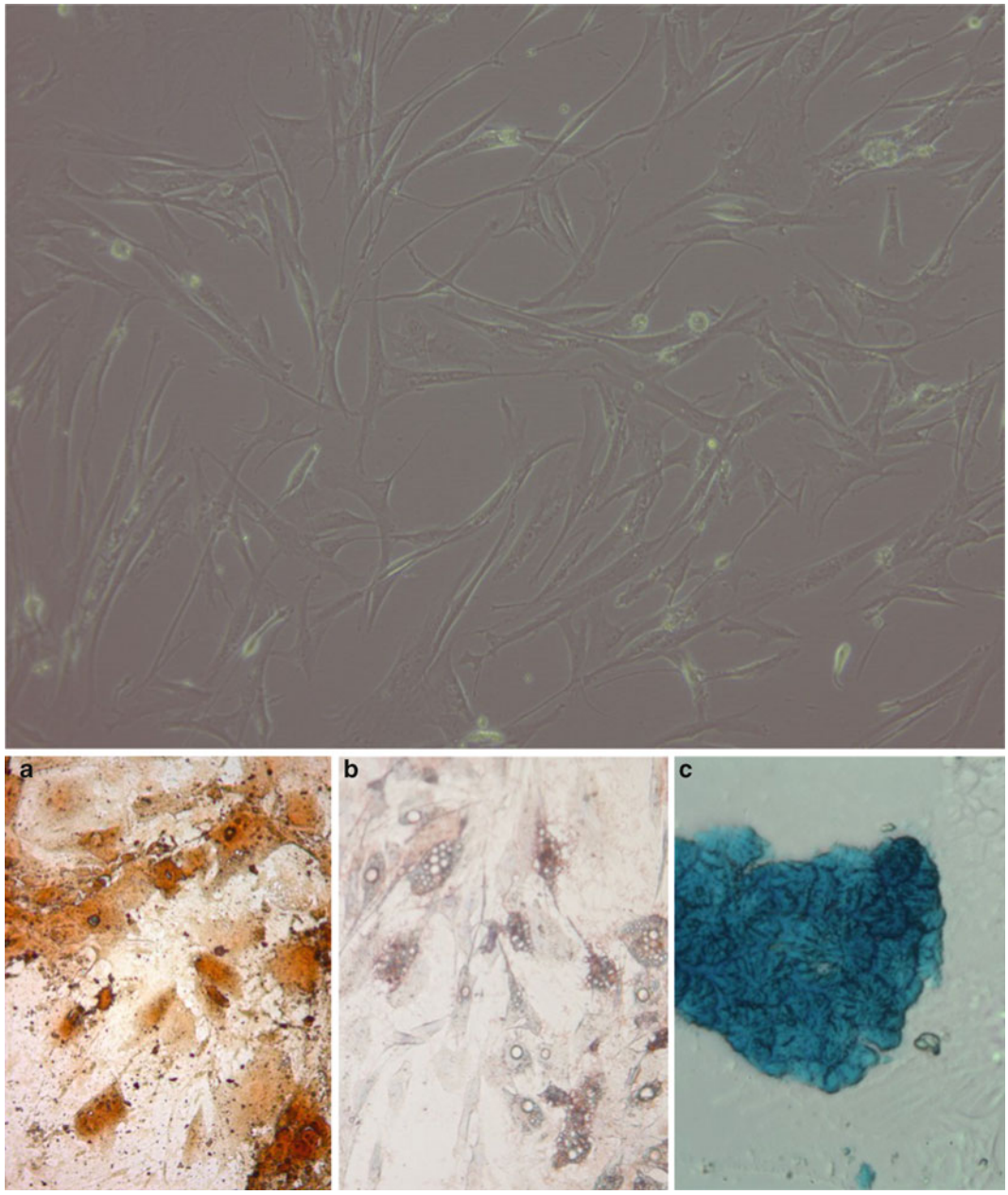


**Fig. 1** Mesenchymal stem cells in culture and their trilineage differentiation. (**a**) Osteogenic induction (Alizarin Red S staining); (**b**) adipogenic induction (Oil Red O staining); (**c**) chondrogenic induction (Alcian blue staining) (*from Elcin Lab*)

11. Conical tubes (Corning Inc.).
12. Cryostat.

### *2.2 Isolation of Mesenchymal Stem Cells*

1. Complete growth medium may consist of: Dulbecco's modified Eagle's medium/F12 (DMEM/F12) with L-glutamine (Lonza, cat. no. 12-604F).

Fetal bovine serum, 20 % (FBS, heat inactivated for 30 min at 56 °C; Lonza, cat. no. 14-502F).

Penicillin/streptomycin solution, 1 % (Lonza, cat. no. 17-602F) (*see* **Note 1**).

2. Transfer medium: DMEM (Lonza, cat. no. 12-708F) with 10 % FBS (heat inactivated, Lonza, cat. no. 14-502F) and 5 % penicillin/streptomycin solution (Lonza, cat. no. 17-602F) (*see* **Note 1**).
3. Heparinized tubes (Sarstedt S-Monovette).
4. Collagenase, type IA (Sigma cat. no. C9891).
5. Syringes with 25G needles (BD, cat. no. 305787).
6. Phosphate buffered saline (PBS), w/o $Ca^{2+}$ and $Mg^{2+}$ (Sigma, cat. no. D5662) for washings.
7. Cell strainers: 70 μm (BD, cat. no. 352350).

### 2.3 Growth, subculture, and cryopreservation of MSCs

1. A complete growth medium may consist of:
   DMEM F/12 with L-glutamine (Lonza, cat. no. 12-604F).
   FBS, 10 % (heat inactivated; Lonza, cat. no. 14-502F).
   Penicillin/streptomycin solution, 1 % (Lonza, cat. no. 17-602F).
2. Trypsin (Sigma, cat. no. T0646).
3. EDTA (Sigma, cat. no. E6511).
4. PBS, w/o $Ca^{2+}$ and $Mg^{2+}$ (Sigma, cat. no. D5662).
5. Cell freezing medium-dimethyl sulfoxide (DMSO) 1× (Sigma, cat. no. C6164).
6. Cryogenic vial (Corning Inc., cat. no. CLS430662).
7. Freezing container (Nalgene Cryo 1 °C, cat. no. 5100-0036).
8. Isopropyl alcohol, ≥99.5 % (Sigma Aldrich, cat. no. 190764).

### 2.4 Osteogenic Differentiation

The osteogenic differentiation medium may consist of:

1. DMEM F/12 with L-glutamine (Lonza, cat. no. 12-604F).
2. FBS, 10 % (heat inactivated; Lonza, cat. no. 14-502F).
3. Dexamethasone, 10 nM (Sigma, cat. no. D4902).
4. β-Glycerophosphate, 10 mM (Sigma, cat. no. 50020).
5. L-Ascorbic acid 2-phosphate, 50 μM (Sigma, cat. no. A4544).
6. Penicillin/streptomycin solution, 1 % (Lonza, cat. no. 17-602F).
   [For adipose-derived MSCs, add 10 ng/mL BMP-2 (Sigma cat. no. B3555) into the osteogenic medium.]

### 2.5 Chondrogenic Differentiation

The chondrogenic differentiation medium may consist of:

1. DMEM F/12 with high glucose (4,500 g/L) (Lonza, cat. no. 12-604F).

2. FBS, 10 % (heat inactivated; Lonza, cat. no. 14-502F).
3. Dexamethasone, $10^{-7}$ M (Sigma, cat. no. 4902).
4. L-Ascorbic acid 2-phosphate, 50 μM (Sigma, cat. no. A4544).
5. ITS-Premix, 1 % (insulin-transferrin-selenium supplement; Lonza, cat. no. 17-838Z).
6. Transforming growth factor-β1, 10 ng/mL (TGF-β1, Sigma, cat. no. T7039).
7. Penicillin/streptomycin solution, 1 % (Lonza, cat. no. 17-602F). [For adipose-derived MSCs, switch TGF-β1 with 10 ng/mL TGF-β3 (Sigma cat no. T9705) and 10 ng/mL BMP-7 (Sigma cat. no. B0814).]

### 2.6 Adipogenic Differentiation

The adipogenic differentiation medium may consist of:

1. DMEM F/12 with L-glutamine (Lonza, cat. no. 12-604F).
2. FBS, 10 % (heat inactivated for 30 min at 56 °C; Lonza, cat. no. 14-502F).
3. Dexamethasone, 50 nM (Sigma, cat. no. D4902).
4. Isobutylmethylxanthine, 0.5 mM (IBMX; Sigma, cat. no. I5879).
5. Indomethacin, 50 μM (Sigma, cat. no. I7378).
6. Penicillin/streptomycin solution, 1 % (Lonza, cat. no. 17-602F).
7. PBS, w/o $Mg^{2+}$and $Ca^{2+}$ (Sigma, cat. no. D5662) for washings.

### 2.7 CFU Assay

1. Complete growth medium.
2. PBS, w/o $Mg^{2+}$and $Ca^{2+}$ (Sigma, cat. no. D5662).
3. Trypsin (Sigma, cat. no. T0646).
4. Ethylenediaminetetraacetic acid (EDTA) (Sigma, cat. no. E6511).
5. Crystal violet (Merck, cat. no. 102543).
6. Methanol (Sigma, cat. no. 676780).

### 2.8 Histochemical Staining

1. Hematoxylin (Sigma Aldrich, cat. no. H3136).
2. Eosin Y-Na salt (Serva, cat. no. 21005).
3. Alizarin Red S (Sigma Aldrich, cat. no. A5533).
4. Alcian blue (Sigma Aldrich, cat. no. A3157).
5. Aluminum sulfate (Sigma Aldrich, cat. no. 202614).
6. Absolute ethanol (Sigma Aldrich, cat. no. 32221).
7. Nuclear Fast Red (Sigma, cat. no. 60700).
8. Glacial acetic acid (Sigma Aldrich, cat. no. 320099).
9. Sodium iodide (Sigma Aldrich, cat. no. 383112).
10. Citric acid (Sigma Aldrich, cat. no. C0759).
11. Sodium bicarbonate ($Na_2CO_3$) (Sigma, cat. no. S5761).
12. Oil Red O stain (Sigma Aldrich, cat. no. O0625).

13. Methanol (Sigma, cat. no. 676780).
14. Isopropanol (Bioreagent, cat. no. I9516).
15. Hydrochloric acid (Sigma, cat. no. H1758).
16. Whatman filter paper (Aldrich, cat. no. Z274852).
17. Ammonium hydroxide ($NH_4OH$) solution for pH adjustment (Sigma Aldrich, cat. no. 221228).
18. Glutaraldehyde solution (Sigma Aldrich, cat. no. G5882).
19. Tissue freezing solution, Tissue-Tek OCT Compound (Sakura, cat. no. 4583).
20. Microscope slide, polysine adhesion (Fischer Scientific, cat. no. 10219280).

### 2.9 RNA Isolation

1. peqGOLD TriFast reagent kit (PEQLAB Gmbh, cat. no. 30-2020). Alternatively TRIzol reagent (Invitrogen, cat. no. 15596-026) can be used for total RNA isolation.
2. RNase-free DNase I (Roche Applied Science, cat. no. 04716728001).
3. Absolute ethanol (Sigma Aldrich, cat. no. 32221).
4. DNase-free water (Sigma, cat. no. W4502).
5. Diethylpyrocarbonate (DEPC)-treated water (Fischer Bioreagents, cat. no. BP5611).
6. Microvolume spectrophotometer (Thermo Scientific, NanoDrop 2000).
7. Microcentrifuge.

### 2.10 cDNA Synthesis

1. Transcriptor First Strand cDNA Synthesis Kit (Roche Applied Science, cat. no. 04379012001).
2. UPL Probes (Roche Applied Science).
3. Thermal cycler with heated lid.
4. Sterile-barrier, RNase-free pipette tips (Corning Inc.).

### 2.11 Expression Analysis

1. Gene-specific primers (Roche Applied Science).
2. LightCycler TaqMan Master Mix solution (Roche Applied Science, cat. no. 04535286001).
3. Reaction plates, 96-well (Roche Applied Science, cat. no. 05102413001).
4. Real-time PCR.
5. Sterile, low-binding barrier pipette tips, RNase-/DNase-free (Corning Inc.).

### 2.12 Microarray Analysis

1. GeneChip HT 3′ IVT Express Kit (Affymetrix, cat. no. 901253) (*see* **Note 2**).

2. GeneChip® Hybridization, Wash, and Stain Kit (Affymetrix, cat. no. 900720).
3. Quant-iT™ RiboGreen® (Life Technologies, cat. no. R11490).
4. Absolute ethanol (Sigma Aldrich, cat. no. 32221).
5. GeneChip Hybridization Oven 640 (Affymetrix, cat. no. 800139).
6. GeneChip Fluidics Station 450 (Affymetrix, cat. no. 00-0079).
7. GeneChip Scanner 3000 (Affymetrix, cat. no. 00-0213).
8. Thermal cycler with heated lid.
9. Microcentrifuge (with an adapter for PCR strip-tubes or plates).
10. Magnetic stand for 96-well plates.
11. Orbital shaker for 96-well plates.
12. Sterile-barrier, RNase-free pipette tips (Corning Inc.).
13. Bioanalyzer.
14. Nonstick RNase-free microfuge tubes: 0.5 mL, 1.5 mL (Ambion, cat. nos. 12350, 12450).

### 2.13 Flow Cytometry

1. Flow cytometer (BD FACSAria II).
2. Primary and secondary antibodies (BD Biosciences).
3. Bovine serum albumin, BSA (Sigma, cat. no. A2153).
4. Sodium azide (Sigma Aldrich, cat. no. S2002).
5. Formaldehyde (Merck, cat. no. 1.04003).
6. Fetal bovine serum (Lonza, cat. no. 14-502F).

## 3 Methods

### 3.1 Isolation of MSCs from Bone Marrow

1. Under aseptic conditions, collect the marrow aspirate from the bone into heparinized tubes (to prevent blood coagulation), prefilled with transport medium.
2. Transfer the tubes immediately to the laboratory.
3. Rinse the aspirates twice with PBS plus 1 % penicillin/streptomycin solution.
4. Transfer the solution into a new sterile tube and centrifuge at $300 \times g$ for 7 min at room temperature.
5. Discard the supernatant and add enough amount of complete growth medium. Invert the tube with gently tapping 3–5 times.
6. Perform Ficoll density gradient centrifugation (Sigma, cat. no. F2637) for cell enrichment (*see* **Note 3**).
7. Transfer and split the mononuclear cells into culture flasks and incubate in a humidified incubator adjusted to 37 °C and 5 % $CO_2$ for 24 h to allow adherent cells to attach.

8. Discard the media that may include nonadherent cells and add enough amount of warm (37 °C) PBS to wash the surface of the culture flask. Wash the surface and discard PBS.
9. Add enough amount of complete growth medium and incubate the cells at 37 °C with 5 % humidified $CO_2$.

### 3.2 Isolation of MSCs from Adipose Tissue

1. Weigh the suctioned adipose tissue and wash several times with sterile PBS plus 1 % penicillin/streptomycin.
2. Clean out the tissue from any remaining blood vessels and skin residues and cut into thin pieces with a sterile scissors or a scalpel.
3. Add freshly prepared collagenase solution to the minced tissue suspension to reach an enzyme concentration of ~0.1 % (*see* **Note 4**).
4. Stir the mixture on a magnetic stirrer at 37 °C for 1 h.
5. To stop the enzyme activity, add equal amount of growth medium and centrifuge at 300 × *g* for 7 min.
6. Discard the upper part of the supernatant and filter the rest of the mixture through a 70 μm cell strainer.
7. Centrifuge the filtrate at 300 × *g* for 7 min.
8. Discard the supernatant and add 20 mL of erythrocytes lysis buffer and disrupt by pipetting and remain 10 min at room temperature.
9. Centrifuge the mixture at 300 × *g* for 7 min.
10. Discard the supernatant and add 1 mL of DMEM/F-12 plus containing 10 % FBS and 1 % penicillin/streptomycin solution onto the pellet and mix gently.
11. Count the cells using a hemocytometer or an automatic cell counter and seed the cells at desired density.

### 3.3 Growth, Subculture, and Cryopreservation of MSCs

1. After isolation of the cells according to Subheading 3.1 or 3.2, continue to incubate the cells at 37 °C with 5 %$CO_2$—95 % air—and >90 % humidity, and change the medium twice a week until 70–80 % confluence is reached (*see* **Note 5**).
2. Discard the medium and rinse the flask/plate surface with pre-warm PBS in order to remove traces of serum which could inhibit the trypsin action.
3. Expose cells to a sufficient volume of readily prepared and sterile-filtered 0.05 % trypsin/0.5 mM EDTA solution to completely cover the monolayer to detach from the surface. Place the culture flask/plate at 37 °C.
4. Wait until cells round up. Gently tapping the flask may help cell detachment. Timing is critical.

**Table 1**
**Practical numbers for *h*MSC culture**

| Culture substrate | Average medium volume | Average volume for trypsin/EDTA | Average cell number at confluence | Surface area[a] ($cm^2$) |
|---|---|---|---|---|
| 96-well plate (well) | 100 µL | 10 µL | $4 \times 10^3$ | 0.14 |
| 24-well plate (well) | 500 µL | 25 µL | $4 \times 10^4$ | 0.33 |
| 6-well plate (well) | 2 mL | 500 µL | $4 \times 10^5$ | 4.65 |
| T-25 flask | 5 mL | 1–2 mL | $5 \times 10^5$–$1 \times 10^6$ | 25 |
| T-75 flask | 10–12 mL | 3–5 mL | $1 \times 10^6$–$3 \times 10^6$ | 75 |
| T-150 flask | 15–20 mL | 5–7 mL | $3 \times 10^6$–$5 \times 10^6$ | 150 |

[a]Data may slightly vary between different commercial brands

5. Add growth medium with 2 times volume of trypsin/EDTA solution. Serum in the complete growth medium will neutralize the activity of the trypsin enzyme.
6. Collect all the solution into a conical tube and centrifuge at $300 \times g$ for 5 min.
7. Remove the supernatant, add 1 mL of complete medium, and mix gently.
8. Count the cells using a hemocytometer or an automatic cell counter; dilute and reseed cells in appropriate concentration into new flasks/plates for subculturing.
9. For cell freezing, resuspend the cells in the freezing medium composed of complete medium containing 10 % DMSO at about $1–2 \times 10^6$ cells/mL in a cryovial.
10. Gently mix the cell suspension inside the cryovial; then, place the vial in a cryofreezing container containing isopropyl alcohol and transfer to a deep freezer at −80 °C.
11. Next day, quickly transfer the cryovial to liquid nitrogen for cryopreservation (Table 1).

### *3.4 Osteogenic Lineage Differentiation*

1. For differentiation studies use cells from passages 2–5 (P2–P5) for bone marrow-derived MSCs and from passages 5–9 (P5–P9) for adipose-derived MSCs. Trypsinize MSC culture at 70–80 % confluence and centrifuge for 5 min at $300 \times g$.
2. Discard the supernatant and resuspend the cells in growth medium. The inoculation concentration should be adjusted close to confluence.
3. Distribute the cell suspension to any appropriate plate or wells.

4. Discard the culture medium on the following day and replace with an equal volume of osteogenic medium.
5. Replace the osteogenic medium twice a week and culture the cells for 21–28 days.
6. Evaluate differentiation with Alizarin Red S staining for osteogenic lineage (*see* **Note 6**).

### 3.5 Chondrogenic Lineage Differentiation

1. Trypsinize MSCs at 70–80 % confluence (between P2–P5 for bone marrow-derived MSCs and P5–P9 for adipose-derived MSCs) and centrifuge $2.5 \times 10^5$ cells in a 15 mL conical tube at $300 \times g$ for 5 min to form the cell micropellet.
2. Discard the supernatant and culture the micropellet inside the conical tube in the presence of the chondrogenic medium (different for bone marrow and adipose MSCs).
3. Replace chondrogenic medium twice a week and culture cells for 21–28 days.
4. Evaluate differentiation with Alcian blue staining for chondrogenic lineage.

### 3.6 Adipogenic Lineage Differentiation

1. Trypsinize MSCs at 70–80 % confluence (between P2–P5 for bone marrow-derived MSCs and P5–P9 for adipose-derived MSCs) and centrifuge at $300 \times g$ for 5 min.
2. Discard the supernatant and resuspend the cells in growth medium. The inoculation concentration should be adjusted close to confluence.
3. Distribute the cell suspension to any appropriate plate or wells.
4. The following day decant the culture medium and replace with an equal volume of adipogenic differentiation medium.
5. Replace the adipogenic medium twice a week and culture cells for 21–28 days.
6. Evaluate differentiation with Oil Red O staining for adipogenic lineage.

### 3.7 CFU Assay

1. Harvest expanded MSCs with trypsin/EDTA (Subheading 3.2) and count the cells using a hemocytometer or an automatic cell counter.
2. Resuspend cells in complete medium at $10^7$ cells/mL.
3. Distribute cells into 35 mm culture dish as 100 cells/2 mL complete medium.
4. Incubate for 14 days by changing the medium twice a week at 37 °C in 5 % humidified $CO_2$. Two weeks of culture is ideal for maximum colony size that can be observed.
5. Remove the medium and rinse the culture flask/plate with PBS twice and discard it.

6. Add 1 mL of methanol and wait for 5 min to fix the cells. Discard the methanol and allow the dish to air-dry at room temperature.
7. Add 1 mL of 0.5 % crystal violet stain solution (in methanol; w/v) and wait for 5 min at room temperature. Remove the stain solution and rinse the dish with water.
8. Discard the water and allow to air-dry.
9. Count the colonies by a microscope using the 4× objective.

### 3.8 Hematoxylin and Eosin Staining

There are several protocols (Harris, Mayer, Gills) for H&E staining. Here we follow the modified Mayer's protocol.

1. Remove the medium and rinse the culture flask/plate with PBS for twice and discard it.
2. Add enough milliliter of ice-cold methanol to the flask/plate and wait for 5 min to fix the cells. Discard methanol and allow the flask/plate to air-dry at room temperature.
3. Wash briefly in distilled water.
4. Add freshly prepared Mayer's hematoxylin stain solution (dissolve 50 g/L aluminum sulfate, 1 g/L hematoxylin, 0.2 g/L sodium iodide, and 1 g/L citric acid in distilled water, respectively) and wait at room temperature for 8–10 min.
5. Rinse in distilled water followed by rinsing in 95 % ethanol for 5 min.
6. Discard ethanol and counterstain with 0.25 % eosin Y solution (in 80 % ethanol; w/v) (or eosin-phloxine B solution) for 1 min.
7. Dehydrate through 95 % ethanol, 2 changes of absolute ethanol, 10 min each.
8. Analyze microscopically immediately after staining.

### 3.9 Alizarin Red S Staining

This stain indicates extracellular calcium deposition around the cells as in orange-red color stain that is a characteristic indication of osteogenic differentiation. Briefly:

1. Dissolve 2 g Alizarin Red S stain in 100 mL distilled water. Mix the solution.
2. Adjust pH to 4.2 by using 0.1 % $NH_4OH$ solution.
3. Filter the dark-brown solution from Whatman filter paper. Store the stain solution in the dark. The solution can be stored up to 1 month in the dark if pH is stable.
4. For staining, discard the medium and wash the cells with PBS w/o $Mg^{2+}$ and $Ca^{2+}$.
5. Discard PBS and add enough ice-cold methanol to cover the surface of the flask or the culture dish. Wait for 10 min at room temperature.

6. Aspirate the methanol solution and wash the cells with PBS.
7. Add enough volume of Alizarin Red S stain and wait 45 min at room temperature in the dark.
8. Discard the stain solution and wash the cells with PBS.
9. Examine microscopically after staining.

### 3.10 Alcian Blue Staining

This method is used to stain in blue color the glycosaminoglycans and some of the mucopolysaccharide types in the cartilage tissue and also indicates chondrogenic differentiation of cell cultures. Briefly:

1. Dissolve 0.1 g Alcian blue in 10 mL 0.1 N HCl.
2. Dissolve 0.1 g Nuclear Fast Red in 5 wt-% solution of aluminum sulfate. Cool down the solution and filter through a Whatman filter paper.
3. Remove the medium from the conical tube and add 5 mL of 2.5 % glutaraldehyde solution onto the micropellet for fixation and wait for 30 min.
4. Remove the fixative solution and wash the micropellet using PBS with care.
5. Remove the micropellet, place inside the tissue freezing solution, and put up into deep freezer at −80 °C.
6. Cryosection the micropellet into 5–6 μm-thick sections, the next day.
7. Place cryosections on the slides.
8. Add enough Alcian blue stain solution and wait 2 min at room temperature.
9. Wash the cells with distilled water and aspirate all.
10. Wash the cells with 0.1 N HCl for 3 s and aspirate all.
11. Wash the sections with 0.3 % $Na_2CO_3$ for 30 s.
12. Add enough Nuclear Fast Red stain and wait for 5 min.
13. Discard the stain solution and wash the sections twice with 95 % ethanol solution.
14. Examine microscopically after staining.

### 3.11 Oil Red O Staining

This stain indicates lipid vesicles in the cell cytoplasm in bright red color, which is a characteristic indication of adipogenic differentiation. Briefly:

1. Dissolve 0.3 % (w/v) Oil Red O in isopropyl alcohol. This stock solution can be stored in dark up to a year.
2. Discard the medium and wash the cells with PBS.
3. Discard the PBS and add enough ice-cold methanol to cover the surface of the flask or the culture dish. Wait for 10 min at room temperature.

4. Dilute Oil Red O stock solution with distilled water to 2:3 (v/v) ratio.
5. Discard the formalin solution and wash the cells with enough 60 % isopropyl alcohol to cover the surface of the flask. Wait for 5 min at room temperature.
6. Discard the isopropanol solution and add enough Oil Red O working solution to cover the surface of the flask. Wait for 15 min at room temperature.
7. Discard the Oil Red O stain solution and wash the cells several times with distilled water to remove the excess stain residues.
8. Examine microscopically after staining.

### 3.12 Flow Cytometry Analysis for MSCs

Protocols have close similarity for most cell types and antibodies. For additional information regarding staining or binding, follow the instructions of the antibody and kit providers.

1. Discard the medium and rinse cells with sterile PBS.
2. Detach cells with trypsin-EDTA solution prepared in PBS according to Subheading 3.3.
3. Centrifuge the cell suspension at $300 \times g$ for 5 min.
4. Add enough PBS plus 2 % FBS solution to the cell pellet to obtain a final concentration of $2 \times 10^5$ cells/100 μL. Mix gently.
5. Add 10 μL specific dye-conjugated antibody to each tube and wait 20 min at room temperature. For purified antibodies, an extra 20 min is needed for dye-conjugated secondary antibody staining.
6. Add enough amount of rinse solution containing BSA and 2 % FBS and centrifuge at $300 \times g$ for 5 min. Wash twice.
7. Discard the supernatant and add 200 μL rinse solution to each tube containing 1 % formaldehyde, 0.1 % sodium azide, and 0.5 % BSA. Mix gently.
8. Perform flow cytometry according to defined analysis program (Table 2).

### 3.13 RNA Isolation

1. Harvest MSCs according to previously described protocol (Subheading 3.2).
2. Isolate the total RNA from the cell pellet by using the peqGOLD TriFast kit or by TRIzol, according to manufacturer's instructions.
3. Wash the pellet twice with 80 % ethanol and air-dry before resuspending into DEPC-treated water.
4. Determine the RNA concentration by using a microvolume spectrophotometer at 260 and 280 nm. A260/A280 absorbance ratio should be between 1.9 and 2.1 to obtain a pure RNA sample.

**Table 2**
**Surface antigen expression[a] of cultured human mesenchymal stem cells between passages 2 and 5**

| Surface markers | Bone marrow-derived MSCs | Adipose-derived MSCs[b] |
|---|---|---|
| CD 29 | +++ | +++ |
| CD 31 | – | – |
| CD 34 | – | –/± |
| CD 44 | +++ | ++/+++ |
| CD 45 | – | – |
| CD 73 | +++ | +++ |
| CD 90 | +++ | +++ |
| CD 105 | +++ | ++/+++ |
| CD 106 | ++ | – |
| CD 166 | +++ | ++/+++ |
| HLA ABC (class I) | +++ | +++ |
| HLA DP, DQ, DR (class II) | – | – |

[a]Indication of marker expression levels: –, 0–5 %; ± , 5–25 %; +, 25–50 %; ++, 50–75 %; +++, 75–100 %
[b]Some of the surface antigen expressions change in subsequent passages (P5–P9)

### 3.14 cDNA Synthesis

1. Perform cDNA synthesis with a commercially available cDNA synthesis kit by following the manufacturer's instructions. You should consider correlation between kits which mostly depends on personal experience.

### 3.15 Expression Analysis

1. Perform quantitative real-time PCR analysis using previously designed primers for related genes. There are several platforms for designing the primers and probes for gene expression analysis; one good example is *Roche Assay Design Center* (http://www.roche-applied-science.com/sis/rtpcr/upl/index.jsp?id=UP030000).
2. Run real-time PCR with a defined program. For instance, 1 μL cDNA and 1 μL TaqMan Master Mix (10×) solution and at a condition of 2 min at 50 °C, 50 cycles of 10 s at 95 °C, and 20 s at 60 °C. Conditions may vary between different instructions.

### 3.16 Microarray Analysis

1. Isolate total RNA from the cells; check the amount and purity. RNA samples should be free of contaminating proteins, DNA, and other materials.
2. Use poly-A RNA control stock and poly-A control Dil buffer provided by the kit. A total RNA amount of 100 ng is usually recommended. Dilutions are critical.

3. Proceed with the instructions described in the kit. The main steps of the microarray analysis are as follows:
   (a) Reverse transcription to synthesize cDNA: This includes several steps comprising of the first- and the second-strand cDNA assembly.
   (b) In vitro transcription to synthesize biotin-modified aRNA with IVF labeling master mix (4–16 h): This step sets up the conversion of cDNA into dye-binding aRNA.
   (c) aRNA purification (0.75 h): This includes several steps to purify aRNA by magnetic separation techniques.
   (d) Fragmentation of the labeled aRNA (1 h).
   (e) Hybridization (16 h/overnight): This step includes several sub-steps for the hybridization of fragmented and labeled aRNA with defined probes.
   (f) Following hybridization, the washing, staining, and scanning steps should be performed according to manufacturer's instructions.

## 4 Notes

1. Media compositions may vary between laboratories. This mostly depends on personal experience. Alpha MEM (Life Technologies, Carlsbad, CA) can be used as an alternative.
2. Other commercial kits, such as Ambion MessageAmp II Amino Allyl with Cy Dyes (Life Technologies cat. no. 1753), and Cy3 and Cy5 mono-reactive dye packs (Amersham Biosciences, cat. no. PA 23001, PA25001) can be used as alternatives.
3. Alternatively, you can use ammonium chloride solution (Sigma, cat. no. A9434) to lyse erythrocytes and separate the mononuclear cells.
4. Since the activity of enzyme lots has discrepancies, you should optimize tissue digestion according to the collagenase lot that is being used.
5. Recent findings suggest the positive influence of hypoxic conditions (<2 % oxygen) on the motility and propagation of MSC cultures [30, 31]. However, the standard condition (5 % $CO_2$—95 % air containing ~20 % oxygen) is still extensively used.
6. Osteogenic differentiation can also be evaluated by immunohistochemistry, using osteonectin, osteopontin, bone sialoprotein, and osteocalcin antibodies [32].

## Acknowledgments

YME acknowledges the support of The Turkish Academy of Sciences (TÜBA), Ankara.

### References

1. Friedenstein AJ, Chailakhjan RK, Lalykina KS (1970) The development of fibroblast colonies in monolayer cultures of guinea-pig bone marrow and spleen cells. Cell Tissue Kinet 3: 393–400
2. Pittenger MF, Mackay MA, Beck SC et al (1999) Multilineage potential of adult human mesenchymal stem cells. Science 284:143–147
3. Jiang Y, Jahagirdar BN, Reinhardt RL et al (2002) Pluripotency of mesenchymal stem cells derived from adult marrow. Nature 418:41–49
4. Lennon DP, Haynesworth SE, Young RG et al (1995) A chemically defined medium supports *in vitro* proliferation and maintains the osteochondral potential of rat marrow-derived mesenchymal stem cells. Exp Cell Res 219:211–222
5. Gussoni E, Soneoka Y, Strickland CD et al (1999) Dystrophin expression in the mdx mouse restored by stem cell transplantation. Nature 401:390–394
6. Quarto R, Mastrogiacomo M, Cancedda R et al (2001) Repair of large bone defects with the use of autologous bone marrow stromal cells. N Engl J Med 344:385–386
7. Minguell JJ, Erices A, Conget P (2001) Mesenchymal stem cells. Exp Biol Med 226: 507–520
8. Baksh D, Song L, Tuan RS (2004) Adult mesenchymal stem cells: characterization, differentiation, and application in cell and gene therapy. J Cell Mol Med 8:301–316
9. Götherström C (2007) Immunomodulation by multipotent mesenchymal stromal cells. Transplantation 84:35–37
10. Jones EA, Kinsey SE, English A et al (2002) Isolation and characterization of bone marrow multipotential mesenchymal progenitor cells. Arthritis Rheum 46:3349–3360
11. Celebi B, Elcin YM (2009) Proteome analysis of rat bone marrow mesenchymal stem cell subcultures. J Proteome Res 8:2164–2172
12. Dicker A, Le Blanc K, Astrom G et al (2005) Functional studies of mesenchymal stem cells derived from adult human adipose tissue. Exp Cell Res 308:283–290
13. Jankowski RJ, Deasy BM, Huard J (2002) Muscle-derived stem cells. Gene Ther 9: 642–647
14. De Bari C, Dell'Accio F, Vandenabeele F et al (2003) Skeletal muscle repair by adult human mesenchymal stem cells from synovial membrane. J Cell Biol 160:909–918
15. Wickham MQ, Erickson GR, Gimble JM et al (2003) Multipotent stromal cells derived from the infrapatellar fat pad of the knee. Clin Orthop 412:196–212
16. Lee OK, Kuo TK, Chen WM et al (2004) Isolation of multipotent mesenchymal stem cells from umbilical cord blood. Blood 103: 1669–1675
17. In't Anker PS, Scherjon SA, van der Keur CK et al (2004) Isolation of mesenchymal stem cells of fetal or maternal origin from human placenta. Stem Cells 22:1338–1345
18. Miura M, Gronthos S, Zhao M et al (2003) SHED: stem cells from human exfoliated deciduous teeth. Proc Natl Acad Sci U S A 100:5807–5812
19. Tsai MS, Lee JL, Chang YJ, Hwang SM (2004) Isolation of human multipotent mesenchymal stem cells from second-trimester amniotic fluid using a novel two-stage culture protocol. Hum Reprod 19:1450–1456
20. Dominici M, Le Blanc K, Mueller I et al (2006) Minimal criteria for defining multipotent mesenchymal stromal cells. The International Society for Cellular Therapy position statement. Cytotherapy 8:315–317
21. Prockop DJ (1997) Marrow stromal cells as stem cells for nonhematopoietic tissues. Science 276:71–74
22. Kolf CM, Cho E, Tuan RS (2007) Mesenchymal stromal cells. Biology of adult mesenchymal stem cells: regulation of niche, self-renewal and differentiation. Arthritis Res Ther 9: 204–213
23. Barry FP, Murphy JM (2004) Mesenchymal stem cells: clinical applications and biological characterization. Int J Biochem Cell Biol 36: 568–584
24. Bruder SP, Jaiswal N, Haynesworth SE (1997) Growth kinetics, self-renewal, and the osteogenic potential of purified human mesenchymal stem cells during extensive subcultivation and following cryopreservation. J Cell Biochem 64:278–294

25. Jaiswal N, Haynesworth SE, Caplan AI, Bruder SP (1997) Osteogenic differentiation of purified culture-expanded human mesenchymal stem cells in vitro. J Cell Biochem 64: 295–312
26. Koc A, Emin N, Elcin AE, Elcin YM (2008) *In vitro* osteogenic differentiation of rat mesenchymal stem cells in a microgravity bioreactor. J Bioact Compat Polym 23:244–261
27. Nakahara H, Bruder SP, Haynesworth SE et al (1990) Bone and cartilage formation in diffusion chambers by subcultured cells derived from the periosteum. Bone 11:181–188
28. Majumdar MK, Thiede MA, Mosca JD et al (1998) Phenotypic and functional comparison of cultures of marrow derived mesenchymal stem cells (MSCs) and stromal cells. J Cell Physiol 176:57–66
29. Majumdar MK, Keane-Moore M, Buyaner D et al (2003) Characterization and functionality of cell surface molecules on human mesenchymal stem cells. J Biomed Sci 10:228–241
30. Grayson WL, Zhao F, Bunnell B, Ma T (2007) Hypoxia enhances proliferation and tissue formation of human mesenchymal stem cells. Biochem Biophys Res Commun 358:948–953
31. Rosova I, Dao M, Capoccia B et al (2008) Hypoxic preconditioning results in increased motility and improved therapeutic potential of human mesenchymal stem cells. Stem Cells 26:2173–2182
32. Inanc B, Elcin AE, Koc A et al (2007) Encapsulation and osteoinduction of human periodontal ligament fibroblasts in chitosan-hydroxyapatite microspheres. J Biomed Mater Res A 82:917–926

# Chapter 4

# Methods for Functional Analysis of Stem Cells

**Michelle Escobedo-Cousin, J. Alejandro Madrigal, and Aurore Saudemont**

## Abstract

Hematopoietic stem cells (HSC) are rare, multipotent cells characterized by their ability to self-renew and to generate all blood cells throughout life. Major advances have been made in the area of HSC research as a result of the development of different techniques that allowed HSC identification, purification, and analysis of biological functions. This chapter presents methods that are currently used to analyze HSC functions in vitro based on their characteristics.

**Key words** Hematopoietic stem cells, Self-renewal, Differentiation, Reconstitution, In vitro assays

## 1 Introduction

Following the observation in 1961 by Till and McCulloch [1] of the production of colony-forming units in the spleen (CFU-S) of irradiated mice after infusion of bone marrow (BM) cells, different studies focused on the discovery of hematopoietic stem cells (HSC) in the BM of humans and other animals [2, 3]. HSC are rare, multipotent cells capable to self-renew, produce, and maintain all blood and immune cells of an individual throughout life [4]. HSC are found in a quiescent state in the BM, in the endosteal and perivascular BM compartments that form the HSC niche [5]. In the niche HSC self-renew and undergo differentiation into all blood cell lineages. Nevertheless, it has been reported that in steady state conditions, a small number of HSC will circulate from the BM to the periphery and back [6, 7]. This physiological process has facilitated the translation of HSC to the clinic, as HSC injected intravenously will thus home back to niches into the BM. It is noteworthy that self-renewal of HSC has only been observed in transplantation conditions and that their self-renewal capacities seem to decrease after in vitro culture.

Hematopoiesis is maintained due to HSC capacity to differentiate into mature blood cells on a daily basis. This process occurs in a

Meral Beksaç (ed.), *Bone Marrow and Stem Cell Transplantation*, Methods in Molecular Biology, vol. 1109,
DOI 10.1007/978-1-4614-9437-9_4, 

tightly regulated manner, with HSC at the top of this hierarchy. HSC differentiates into common lymphoid progenitors (CLP) or common myeloid progenitors (CMP) [8]. These progenitors have no or low self-renewal ability and have limited differentiation, as they will only differentiate into mature cells of a specific lineage. CLP can differentiate into T cells, B cells, natural killer cells, as well as antigen-presenting cells [9]. CMP differentiate into granulocyte-/monocyte-committed progenitors (GMP) or megakaryocyte-committed progenitors (MEP). GMP then give rise to granulocytes, monocytes, and dendritic cells and MEP to erythrocytes and platelets [8, 10]. Notably it has been shown that HSC can differentiate into myeloerythroid or myelolymphoid progenitors before differentiating into a specific lineage [11] and for some myeloid-like progenitors to generate lymphoid cells such as NK cells in vitro [12–14]. All these studies have been performed using in vitro systems, and further studies are needed in order to fully elucidate whether CMP and CLP are strictly committed to one specific lineage in vitro and in vivo in particular in humans.

It has been described using animal models of HSC transplantation that HSC are heterogeneous and exhibit short-term or long-term repopulating capacities [15, 16]. It was later demonstrated that HSC with long-term repopulating capacities (LT-HSC), also termed long-term repopulating cells (LTRC), were capable to repopulate all blood cell types in vitro and in vivo as well as generating cells that could themselves exhibit the same properties when transferred to another recipient, properties that could be repeated upon secondary or even tertiary transfer [17–19]. In contrast, some HSC could demonstrate similar functions but only reconstitute the myeloid and lymphoid compartments after transfer to a host for a limited period of time [20], typically up to 4 months. These cells are termed short-term repopulating cells (ST-HSC).

The fields of HSC biology and hematopoiesis have greatly evolved. Nowadays it is possible to isolate with high purity HSC populations, human stem/progenitor cells (HSPC), and even single HSC. This has been possible as a result of techniques being developed such as isolation using magnetic beads, fluorescence-activated cell sorting, and the identification over the years of different surface and intracellular markers expressed by HSC. Notably, a lot of effort has been dedicated to identify markers that will allow discriminating specifically between LT-HSC and ST-HSC. Currently a combination of markers can be used in order to specifically identify mouse or human HSC [21, 22]. Mouse HSC were first defined as lineage $(Lin)^-$, Sca-$1^+$, c-$kit^+$, referred as LSK cells [23, 24]. Later, it was reported that the absence of CD34 antigen on mouse HSC correlated with HSC abilities to self-renew and provide long-term reconstitution [25]. In addition, it was shown that LT-HSC activity resides in the $CD150^+$ $CD48^-$ HSC population in mice [26] but not in humans and in macaques [27]. In humans, CD34 was the first marker reported to be expressed on

HSC and HSPC [28]. Over the years different markers have been described to identify HSC; in humans HSC can be characterized by the expression of CD34 and Thy1 [29, 30] and the lack of expression of CD38 [31, 32] and CD45RA [33] with the latest markers being progressively expressed on HSC while they differentiate and therefore being more specific of HSPC. In addition to CD34, CD133 can be used to identify HSC (*see* **Note 1**); it has been reported that HSC are contained within the $CD133^{+}CD34^{+}CD38^{-}/^{lo}$ population (*see* **Note 2**). Importantly other markers such as CXCR4 or the lack of expression of lineage markers can also be used to identify HSC, but as they are also expressed on other cell types, these markers have to be analyzed in conjunction with other markers. Metabolic properties of HSC such as HO3342, Rh123, in vivo resistance to 5-fluorouracil, or high activity of aldehyde dehydrogenase have also been utilized for their identification. Lastly, integrin expression such as CD49b in mice [34] or CD49f in humans [35] has been used to analyze or isolate LT-HSC.

Different assays have been developed in order to assess HSC functions in vitro and in vivo and are summarized in Fig. 1. The colony-forming unit (CFU) also called colony-forming cell (CFC)

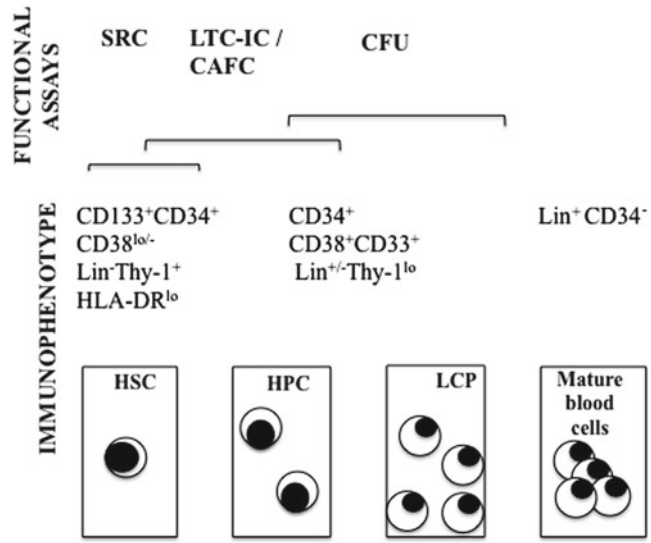


**Fig. 1** Functional assays to identify HSC. The diagram shows the most commonly used assays to study HSC. In vivo mouse repopulating cell assay identifies HSC in vivo *on* their capacity to self-renew, proliferate, and differentiate into all blood lineages. Long-term culture-initiating cells (LTC-IC) and cobblestone area-forming cells (CAFC) are useful to identify similar populations of HSC and primitive hematopoietic progenitor cells (HPC) in vitro. Colony-forming unit assay (CFU) allows the identification of HPC and lineage-committed progenitors (LCP) that will lead to the formation of colonies. Finally, mature cells derived from HSC can be assessed by different assays, such as immunophenotype and functional assays

assay tests the ability of HSC and progenitor cells to form colonies in a methylcellulose culture medium containing growth factors [36, 37]. In these conditions HSC and HSPC will be able to proliferate and differentiate into mature hematopoietic cells that can then be enumerated and characterized based on their morphology. This assay is used to assess the capacity of HSC and HSPC to differentiate into erythroid, granulocytic, monocytic, and megakaryocytic lineages. Each colony indicates the proliferation and differentiation of a progenitor cell.

Cobblestone area-forming cell (CAFC) and long-term culture-initiating cell (LTC-IC) assays assess long-term repopulating capacities of HSC in vitro [38–40]. For both assays, HSC are cultured using stromal feeder layer cells for 3–5 weeks, as only "true" HSC will maintain their properties during that time. LTC-IC assay measures the self-renewal ability of HSC over several weeks. In this assay HSC maintain their clonogenic capacity and will thus be able to proliferate and produce colonies of differentiated cells. CAFC assays only assess the ability of HSC to self-renew and proliferate during weeks; however, it does not analyze the capacity of HSC to differentiate [41]. The name of CAFC is due to the fact that areas of cluster of cells will look like cobblestone when visualized using a microscope. CAFC assays have only a visual readout, while LTC-IC assays are a CAFC assay followed by CFU assays.

The gold standard assay to analyze all HSC biological functions is the SCID-repopulating cell (SRC) assay, which consists in analyzing engraftment and immune reconstitution of lethally irradiated mice following injection of HSC. Different mouse strains support engraftment of human cells and immune reconstitution. This has been reviewed extensively elsewhere [42, 43] and will not be discussed in detail in this chapter. Typically this assay allows assessing different characteristics of HSC such as short-term or transient repopulation and long-term repopulation by analyzing engraftment around 5 weeks and from 12 weeks post-infusion, respectively. Multi-lineage reconstitution can be evaluated in the recipient mice at different time points posttransplant according to the lineage studied.

## 2 Materials

### 2.1 CFU Assay

1. MethoCult GF H-84434 medium (Stem Cell Technologies, cat. no. 84434).
2. 10 mm × 15 mm Petri dish (BD, cat. no. 351029).
3. Culture dishes for optimal colony growth in methylcellulose.
4. Blunt needle.
5. 1 mL syringe.
6. Sterile water (Sigma, cat. no. W3500).

### 2.2 CAFC / LTC-IC

1. MS-5 cell line.
2. Alpha-MEM (Lonza, cat. no. BE12-169F).
3. Heat-inactivated filtered FBS (Lonza, cat. no. 9SB018).
4. 2 mM L-glutamine (Lonza, cat. no. 17-605C).
5. 2 mM sodium pyruvate (Lonza, cat. no. BE13-115E).
6. Penicillin-streptomycin (Lonza, cat. no. 17-602E).
7. 75 $cm^2$ flask (BD, cat. no. 353136).
8. Trypsin 0.25 % with EDTA (Invitrogen, cat. no. 25200-056).
9. Tissue-culture-treated flat-bottom 96-well plates (BD, cat. no. 353296).
10. $10^{-5}$ M hydrocortisone (Sigma, cat. no. HO88).
11. 50 mM β-mercaptoethanol (Lonza, cat. no. M/P200/05).
12. Sterile water (Sigma, cat. no. W3500).

## 3 Methods

### 3.1 CFU Assay

1. Use approximately 200 HSC per culture dish for optimal colony growth.
2. Plate cells using the 1 mL syringe and blunt needle, in duplicate or triplicate in MethoCult GF H-84434 medium, and culture at 37 °C in a humidified, 5 % $CO_2$ air-controlled atmosphere. If duplicates are performed, fill in a third of the culture dish with 5 mL of sterile water.
3. After 2 weeks score all colonies using an inverted microscope. Colonies can be defined as (*see* **Note 3**):
   (a) CFU-GM: colonies with at least 40 granulocyte macrophage (GM) cells
   (b) CFU-GEMM: colonies with at least 20 cells of GM lineage in close proximity to the erythroid component. GEMM stands for granulocyte, erythrocyte, monocyte, and megakaryocyte (*see* **Note 4**).

### 3.2 CAFC

1. Culture MS-5 cells in 90 % alpha-MEM, 10 % heat-inactivated filtered FBS, 2 mM L-glutamine, 2 mM sodium pyruvate, and 1 % penicillin-streptomycin at a concentration of $1–2 \times 10^6$ in 25 mL in a 75 $cm^2$ flask and incubate at 37°C in a humidified, 5 % $CO_2$ incubator.
2. When 80–90 % cell confluence is achieved, detach the cells with trypsin 0.25 % with EDTA. Collect the cells and centrifuge at $300 \times g$ for 10 min. MS-5 cells can then be used for LTC-IC assays.

3. Irradiate MS-5 cells at 30 Gy for 7 min.
4. Plate $2 \times 10^4$ irradiated MS-5 cells per well of a tissue-culture-treated flat-bottom 96-well plate. Plate the cells into the 60 inner wells of the plate in 200 µL of cobblestone medium (alpha-MEM, 20 % FBS, $10^{-5}$ M hydrocortisone, 50 mM β-ME, 1 % pen-strep). Add sterile water to the outer wells of the plate. Incubate the cells at 37 °C in a humidified, 5 % $CO_2$ incubator for 48–72 h to create a feeder layer in each well.
5. Add 500 HSC in each well with feeder layer cells. Prepare ten replicates per condition, in a volume of 200 µL. Incubate the plate at 37 °C in a humidified, 5 % $CO_2$. Change the medium weekly by hemi-depletion.
6. Score the wells after 4 weeks using an inverted microscope. A cobblestone area is defined as a group of at least six cells in proximity to each other growing underneath the stroma. Score each well containing one or more cobblestone areas as positive and those containing no cobblestone areas as negative.

### 3.3 LTC-IC

1. Long-term culture-initiating cells assay consists of cobblestone assay followed by CFUs.
2. After 4 weeks of cobblestone assays, rinse adherent cells with PBS 1× and detach the cells using trypsin 0.25 % with EDTA for 2 min. Centrifuge the cells at $300 \times g$ for 10 min and resuspend in IMDM to perform CFU assays as previously described.
3. Score the colonies after 2 weeks of culture at 37 °C in a humidified, 5 % $CO_2$ air-controlled atmosphere.

## 4 Notes

1. Different methods are currently available to isolate HSC from different sources. HSC can be isolated on the basis of expression of only one marker such as CD34 or CD133. The method should be optimized according to which cell source is used, BM, mobilized peripheral blood, or umbilical cord blood.
2. We recommend to follow the International Society of Hematotherapy and Graft Engineering (ISHAGE) guidelines when analyzing HSC using flow cytometry [44].
3. One limitation of the CFU assay is that this assay does not allow differentiating between true HSC and committed progenitors.
4. The results obtained from CFU, CAFC, and LTC-IC assays are subject to interobserver error; therefore, it is recommended to standardize CFU/cobblestone counting to have homogeneous results.

5. The in vitro assays described mostly support myeloid differentiation. However, different systems—that use different feeder stromal cell lines and cytokine cocktails—are now available that also support lymphoid differentiation [45–48].

## Acknowledgements

Research in the laboratory is funded by Anthony Nolan. M. Escobedo-Cousin is the recipient of a CONACyT and SEP fellowship.

### References

1. Till J, McCulloch EA (1961) A direct measurement of the radiation sensitivity of normal mouse bone marrow cells. Radiat Res 14:213–222
2. Lemischka I, Raulet D, Mulligan R (1986) Developmental potential and dynamic behavior of hematopoietic stem cells. Cell 45:917–927
3. Wu A, Siminovitch L, Till J et al (1968) Evidence for a relationship between mouse hemopoietic stem cells and cells forming colonies in culture. Proc Natl Acad Sci USA 59:1209–1215
4. Weissman I (2000) Stem cells: units of development, units of regeneration, and units in evolution. Cell 100:157–168
5. Schofield R (1978) The relationship between the spleen colony-forming cell and the haemopoietic stem cell. Blood Cells 4:7–25
6. Wright D, Wagers A, Gulati A et al (2001) Physiological migration of hematopoietic stem and progenitor cells. Science 294:1933–1936
7. Massberg S, Schaerli P, Knezevic-Maramica I et al (2007) Immunosurveillance by hematopoietic progenitor cells trafficking through blood, lymph, and peripheral tissues. Cell 131: 994–1008
8. Manz M, Miyamoto T, Akashi K (2002) Prospective isolation of human clonogenic common myeloid progenitors. Proc Natl Acad Sci USA 99:11872–11877
9. Kondo M, Weissman I, Akashi K (1997) Identification of clonogenic common lymphoid progenitors in mouse bone marrow. Cell 91:661–672
10. Akashi K, Traver D, Miyamoto T et al (2000) A clonogenic common myeloid progenitor that gives rise to all myeloid lineages. Nature 404:193–197
11. Arinobu Y, Mizuno S, Chong Y et al (2007) Reciprocal activation of GATA-1 and PU.1 marks initial specification of hematopoietic stem cells into myeloerythroid and myelolymphoid lineages. Cell Stem Cell 1:416–427
12. Grzywacz B, Kataria N, Kataria N et al (2011) Natural killer-cell differentiation by myeloid progenitors. Blood 117:3548–3558
13. Pinho M, Marques C, Carvalho F et al (2012) Genetic regulation on ex vivo differentiated natural killer cells from human umbilical cord blood CD34+ cells. J Recept Signal Tranduct Res 32:238–249
14. Perez S, Sotiropoulou P, Gkika D et al (2003) A novel myeloid-like NK cell progenitor in human umbilical cord blood. Blood 101:3444–3450
15. Glimm H, Eisterer W, Lee K et al (2001) Previously undetected human hematopoietic cell populations with short-term repopulating activity selectively engraft NOD/SCID-beta2 microglobulin-null mice. J Clin Invest 107: 199–206
16. Spangrude G, Brooks D, Tumas D (1995) Long-term repopulation of irradiated mice with limiting numbers of purified hematopoietic stem cells: in vivo expansion of stem cell phenotype but not function. Blood 85:1006–1016
17. Jordan C, Lemischka I (1990) Clonal and systemic analysis of long-term hematopoiesis in the mouse. Genes Dev 4:220–232
18. Keller G, Snodgrass R (1990) Life span of multipotential hematopoietic stem cells in vivo. J Exp Med 171:1407–1418
19. Iscove N, Nawa K (1997) Hematopoietic stem cells expand during serial transplantation in vivo without apparent exhaustion. Curr Biol 7:805–808
20. Morrison S, Weissman I (1994) The long-term repopulating subset of hematopoietic stem cells is deterministic and isolatable by phenotype. Immunity 1:661–673
21. Ratajczak M (2008) Phenotypic and functional characterization of hematopoietic stem cells. Curr Opin Hematol 15:293–300

22. Bryder D, Rossi D, Weissman I (2006) Hematopoietic stem cells: the paradigmatic tissue-specific stem cell. Am J Pathol 169: 338–346
23. Ikuta K, Weissman I (1992) Evidence that hematopoietic stem cells express mouse c-kit but do not depend on steel factor for their generation. Proc Natl Acad Sci USA 89:1502–1506
24. Spangrude G, Heimfeld S, Weissman I (1988) Purification and characterization of mouse hematopoietic stem cells. Science 241:58–62
25. Osawa M, Hanada K, Hamada H et al (1996) Long-term lymphohematopoietic reconstitution by a single CD34-low/negative hematopoietic stem cell. Science 273:242–245
26. Kiel M, Yielmaz Y, Iwashita T et al (2005) SLAM family receptors distinguish hematopoietic stem and progenitor cells and reveal endothelial niches for stem cells. Cell 121:1109–1121
27. Larochelle A, Savona M, Wiggins M (2011) Human and rhesus macaque hematopoietic stem cells cannot be purified based only on SLAM family markers. Blood 117:1550–1554
28. Civin C, Strauss L, Brovall C et al (1984) Antigenic analysis of hematopoiesis. III. A hematopoietic progenitor cell surface antigen defined by a monoclonal antibody raised against KG-1a cells. J Immunol 133:157–165
29. Baum C, Weissman I, Tsukamoto A et al (1992) Isolation of a candidate human hematopoietic stem-cell population. Proc Natl Acad Sci USA 89:2804–2808
30. Murray L, Chen B, Galy A et al (1995) Enrichment of human hematopoietic stem cell activity in the CD34+Thy-1+Lin- subpopulation from mobilized peripheral blood. Blood 85:368–378
31. Bhatia M, Wang J, Kapp U et al (1997) Purification of primitive human hematopoietic cells capable of repopulating immune-deficient mice. Proc Natl Acad Sci USA 94:5320–5325
32. Conneally E, Cashman J, Petzer A et al (1997) Expansion in vitro of transplantable human cord blood stem cells demonstrated using a quantitative assay of their lympho-myeloid repopulating activity in nonobese diabetic-scid/scid mice. Proc Natl Acad Sci USA 94:9836–9841
33. Lansdorp P, Sutherland H, Eaves C (1990) Selective expression of CD45 isoforms on functional subpopulations of CD34+ hemopoietic cells from human bone marrow. J Exp Med 172:363–366
34. Benveniste P, Frelin C, Janmohamed S et al (2010) Intermediate-term hematopoietic stem cells with extended but time-limited reconstitution potential. Cell Stem Cell 6:48–58
35. Notta F, Doulatov S, Laurenti E et al (2011) Isolation of single human hematopoietic stem cells capable of long-term multilineage engraftment. Science 333:218–221
36. Moore M, Williams N, Metcalf D (1973) In vitro colony formation by normal and leukemic human hematopoietic cells: characterization of the colony-forming cells. J Natl Cancer Inst 50:603–623
37. Pike B, William R (1970) Human bone marrow colony growth in agar-gel. J Cell Physiol 76:77–84
38. Gartner S, Kaplan H (1980) Long-term culture of human bone marrow cells. Proc Natl Acad Sci USA 77:4756–4759
39. Sutherland H, Eaves C, Eaves A et al (1989) Characterization and partial purification of human marrow cells capable of initiating long-term hematopoiesis in vitro. Blood 74: 1563–1570
40. Sutherland H, Eaves C, Lansdorp P et al (1991) Differential regulation of primitive human hematopoietic cells in long-term cultures maintained on genetically engineered murine stromal cells. Blood 78:666–672
41. Hao Q, Thiemann F, Petersen D et al (1996) Extended long-term culture reveals a highly quiescent and primitive human hematopoietic progenitor population. Blood 88:3306–3316
42. Doulatov S, Notta F, Laurenti E et al (2012) Hematopoiesis: a human perspective. Cell Stem Cell 10:120–136
43. Shultz L, Brehm M, Garcia-Martinez J et al (2012) Humanized mice for immune system investigation: progress, promise and challenges. Nat Rev Immunol 12:786–798
44. Keeney M, Chin-Yee I, Weir K et al (1998) Single platform flow cytometric absolute CD34+ cell counts based on the ISHAGE guidelines. International Society of Hematotherapy and Graft Engineering. Cytometry 34:61–70
45. Collins L, Dorshkind K (1987) A stromal cell line from myeloid long-term bone marrow cultures can support myelopoiesis and B lymphopoiesis. J Immunol 138:1082–1087
46. Itoh K, Tezuka H, Sakoda H et al (1989) Reproducible establishment of hemopoietic supportive stromal cell lines from murine bone marrow. Exp Hematol 1989(17):145–153
47. La Motte-Mohs R, Herer E, Zúñiga-Pflücker J (2004) Induction of T-cell development from human cord blood hematopoietic stem cells by Delta-like 1 in vitro. Blood 105:1431–1439
48. Grzywacz B, Kataria N, Sikora M et al (2006) Coordinated acquisition of inhibitory and activating receptors and functional properties by developing human natural killer cells. Blood 108:3824–3833

# Chapter 5

# An Overview of HLA Typing for Hematopoietic Stem Cell Transplantation

**Katy Latham, Ann-Margaret Little, and J. Alejandro Madrigal**

## Abstract

The selection of a related or an unrelated hematopoietic stem cell donor for a patient requires accurate matching of human leukocyte antigen (HLA) genes in order to maximize the beneficial effects of the transplant. There are various different factors a laboratory must consider in order to achieve an HLA type including the number of samples being processed, level of resolution to be achieved, cost of providing the various tests, and turnaround time required. Each method has its advantages and disadvantages, and in most laboratories, a combination of methods may be used.

**Key words** HLA typing, PCR-SSP, PCR-SSO, PCR-SBT, NGS

## 1 Introduction

Polymorphic human leukocyte antigen (HLA) genes are encoded within the human major histocompatibility complex (MHC) on chromosome 6 (Table 1). These genes encode components of HLA molecules involved in antigen presentation to the immune system. Determination of HLA polymorphism (referred to as "HLA typing" or "tissue typing") is performed in clinical laboratories in order to aid the selection of potential organ and stem cell donors for patients and also as an aid in diagnosis of various diseases that are associated with a particular HLA genotype [1]. Stem cell donor registries and cord blood banks provide HLA typing on their donors and cord units that are available to search for use in stem cell transplantation. In addition, polymorphisms within HLA genes and other genes linked to HLA genes within the MHC are now known to play a role in the responsiveness of individuals to vaccines and other pharmaceutical drugs [2]. HLA typing is also used as a tool to aid genetic and anthropological studies of human populations [3].

HLA typing methods have evolved significantly since the discovery of the first HLA antigens from studies with sera from multiparous women [4]. Originally serological and cellular methods

Meral Beksaç (ed.), *Bone Marrow and Stem Cell Transplantation*, Methods in Molecular Biology, vol. 1109,
DOI 10.1007/978-1-4614-9437-9_5, 

**Table 1**
**Human leukocyte antigen (HLA) genes and number of alleles, January 2013**

| **Number of HLA class I alleles** | **6,919** | |
|---|---|---|
| **Number of HLA class II alleles** | **1,875** | |
| **Total number of HLA alleles** | **8,794** | |
| **HLA locus** | **Alleles** | **Expressed proteins** |
| HLA-A | 2,188 | 1,571 |
| HLA-B | 2,862 | 2,156 |
| HLA-C | 1,746 | 1,252 |
| HLA-DRA | 7 | 2 |
| HLA-DRB1 | 1,285 | 959 |
| HLA-DRB3 | 58 | 46 |
| HLA-DRB4 | 15 | 8 |
| HLA-DRB5 | 20 | 17 |
| HLA-DQA1 | 49 | 31 |
| HLA-DQB1 | 193 | 137 |
| HLA-DPA1 | 39 | 18 |
| HLA-DPB1 | 159 | 136 |

*See* ref. 31

were applied to determine HLA type. However, since the application of DNA-based methods, particularly after the introduction of the PCR, the sophistication of the methods available for HLA typing has increased significantly. This technology has taken the next step recently with the development of next-generation sequencing (NGS). This chapter focuses on the currently available DNA-based methods, their applicability for different tests, and their advantages and disadvantages.

### *1.1 HLA Typing Methods*

The many HLA alleles found are the product of multiple single-nucleotide polymorphisms (SNPs) distributed singly or in group "motifs" via recombinatorial mechanisms generating what is often referred to as a "patchwork" pattern of polymorphism. This extensive polymorphism of HLA makes this genetic system one of the most complex to analyze (Fig. 1). A combination of techniques is often required to resolve ambiguities arising from a single method which is unable to discriminate how polymorphisms are linked on a gene, referred to as cis/trans polymorphisms. However advances in sequencing technology have the potential to resolve these ambiguities and are beginning to enter clinical HLA typing laboratories.

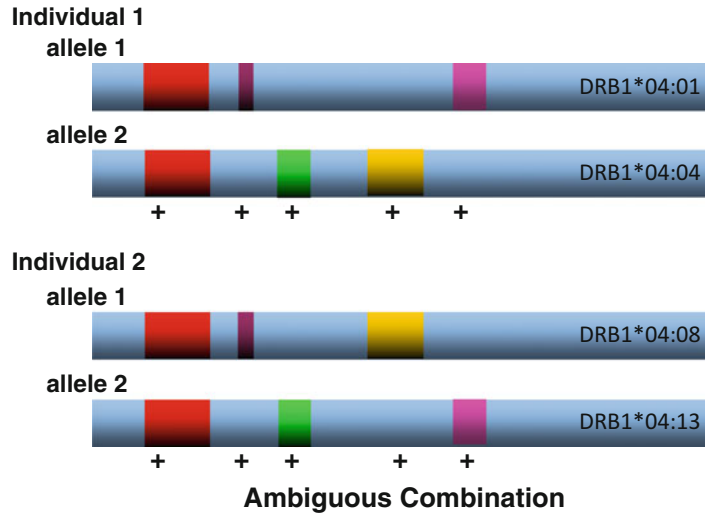


**Fig. 1** Example of HLA ambiguity. There are four different HLA-DRB1*04 alleles present in the two individuals. Both individuals are heterozygous and do not share either of their HLA-DRB1 alleles. The polymorphic positions that distinguish those alleles are represented by the *colored blocks*. In PCR-SSO where each polymorphic area is targeted individually the reaction pattern will be identical for the two individuals. In generic PCR-SBT the heterozygous peaks in the electropherogram traces will be identical. Resolution of this ambiguity requires methods to link the polymorphic areas together or a combination of techniques that are able to link the polymorphisms differently, the results of which can be combined

*The four main molecular methodologies for HLA typing are:*

1. PCR using sequence-specific oligonucleotides (PCR-SSO).
2. PCR using sequence-specific primers (PCR-SSP).
3. PCR sequence-based typing (PCR-SBT).
4. NGS.

### 1.1.1 PCR-SSO

PCR-SSO involves a PCR producing an amplicon from an HLA locus, e.g., HLA-A, which is then hybridized against a panel of oligonucleotide probes that have sequences complementary to stretches of polymorphisms within the target HLA region e.g., exon 2 and 3. Originally, denatured PCR products were immobilized to multiple nitrocellulose or nylon membranes, the number of membranes equating with the number of oligonucleotide probes to be used. After hybridization of each membrane with a different oligonucleotide probe (which may involve different hybridization temperatures for different probes), bound probes were visualized using detection systems such as radioisotopes or later chemiluminescence. The process was best suited for large batches [5] rather than individual samples and was extremely labor intensive. Although modifications were made to this method it has mostly

**Table 2**
**An example of the different resolution of HLA typing that can be achieved through the use of different bead and oligonucleotide probe profiles**

| LABType® SSO assay details | HLA-A alleles defined using LABType® SSO and analyzed using Fusion (One Lambda, part of Thermo Fisher, Canoga Park, California, USA) |
|---|---|
| Intermediate assay RSSO1A_12R_00 | 01:01/01:01N/01:02/01:04N/01:06/01:09/01:11N/01:16N/01:18N/01:20/01:22N/01:24/01:25/01:29/01:30/01:32/01:33/01:34N/01:35/01:36/01:37/01:38/01:39/01:40/01:41/01:42/01:44/01:45/01:47/01:50/01:52N/01:53N/01:54/01:55/01:56N/01:57N/01:58/01:59/01:62/01:65/01:66/01:67/01:69/01:70/01:74/01:75/01:76/01:77/01:78/01:79/01:80/01:81/01:82/01:83/01:84/01:85 |
| High-definition assay RSSO1HA _007_001 | 01:01/01:01N/01:04N/01:22N/01:32/01:34N/01:37/01:45/01:56N/01:81 |

Both these assays follow the same work flow allowing flexibility of the procedure

been superseded by the introduction of "reverse" PCR-SSO methods which are the predominant HLA typing methodology in use today.

The reverse PCR-SSO methods involve immobilization of the oligonucleotide probes on a solid-phase support and subsequent hybridization of the solid-phase immobilized oligonucleotide probes with liquid-phase PCR. The introduction of reliable automation for PCR-SSO, flexibility in the level of resolution achieved, e.g., low, intermediate, and in some cases high (Table 2), plus a single procedure for all HLA loci and resolutions have allowed these systems to be extremely flexible for both small clinical laboratories and large-scale donor registries alike [6]. Solid-phase supports most widely in use include the following:

1. Oligonucleotide-coated polystyrene microspheres (Luminex® xMAP technology, Luminex Corp, Austin, TX; LIFEMATCH™, Hologic Gen-probe, San Diego CA; and LABType® SSO, One Lambda Inc., Los Angeles, CA).
2. Nitrocellulose membrane strips (INNOLiPA line probe assay, Innogenetics, Ghent, Belgium).

One of the limitations of PCR-SSO methods has been the inability to link cis and trans polymorphisms. However, with the design of longer probes that discriminate multiple polymorphisms, this problem can be reduced.

A brief overview of PCR-SSO: After DNA extraction, locus-specific PCR product is produced, e.g., HLA-A. To enable subsequent detection biotin is incorporated into the PCR primers. The presence of correct sized PCR product without contamination is determined by separating an aliquot of the amplicon by agarose

gel electrophoresis; this check allows the procedure to be halted prior to the hybridization phase. The PCR amplicon is denatured (chemically or heat) to produce single-stranded DNA for both sense and antisense strands. The single-stranded amplicons are hybridized to the immobilized oligonucleotide probe, which is attached to a solid support, e.g., membrane, microplate well, and bead. Amplicons that do not hybridize are washed away. The presence of bound amplicon to oligonucleotide probe is measured using an enzymatic color reaction, e.g., addition of streptavidin conjugated to an enzyme, e.g., horseradish peroxidase or alkaline phosphatase which will catalyze the formation of a colored complex in the presence of appropriate substrate or alternatively the addition of fluorescently labelled streptavidin allows identification of bound PCR product. For systems using a membrane-bound strip format the physical location of the oligonucleotide probe on the strip acts as an identifier. For microbead assays each bead has a unique spectral signature determined by its red/infrared mixture which is detected by the analyzer upon excitation by a light source. The analyzer interprets the bead's signature and the presence of the reporter indicating a positive reaction. The absence of the reporter indicates a negative meaning that the oligonucleotide probe has no complementary sequence present in the DNA template (xMap®, Luminex Corporation). Interpretation of the results is the most complex aspect of the PCR-SSO test and requires the use of specific software if all known HLA alleles are included in the analysis.

#### 1.1.2 PCR-SSP

PCR-SSP involves the use of multiple PCR reactions targeting the presence and absence of polymorphisms within the target HLA gene [7, 8]. Each PCR primer pair is designed to be either complementary to the target polymorphism or a mismatch through substitution of the complementary nucleotide at the 3′-end of either or both primers with a noncomplementary nucleotide. This approach is also called the amplification refractory mutation system (ARMS) [9]. As the *Taq* polymerase enzyme used in the PCR reaction does not have a 3–5 exonuclease proofreading ability, mismatched priming does not result in production of a PCR amplicon. In order for this approach to be successful and for PCR-SSP to be used routinely for HLA typing, it is necessary to optimize the annealing and other PCR conditions including buffer components, for each primer pair utilized. The amplicons produced, which are indicative of the presence of the target polymorphism within the sample DNA being tested, are visualized after agarose gel electrophoresis and staining, usually with ethidium bromide. Most PCR-SSP protocols include, within each amplification mix, primers for amplification of a segment from a housekeeping gene. The presence of this additional amplicon serves as an internal control, as it should be amplified from all human samples tested (Fig. 2).

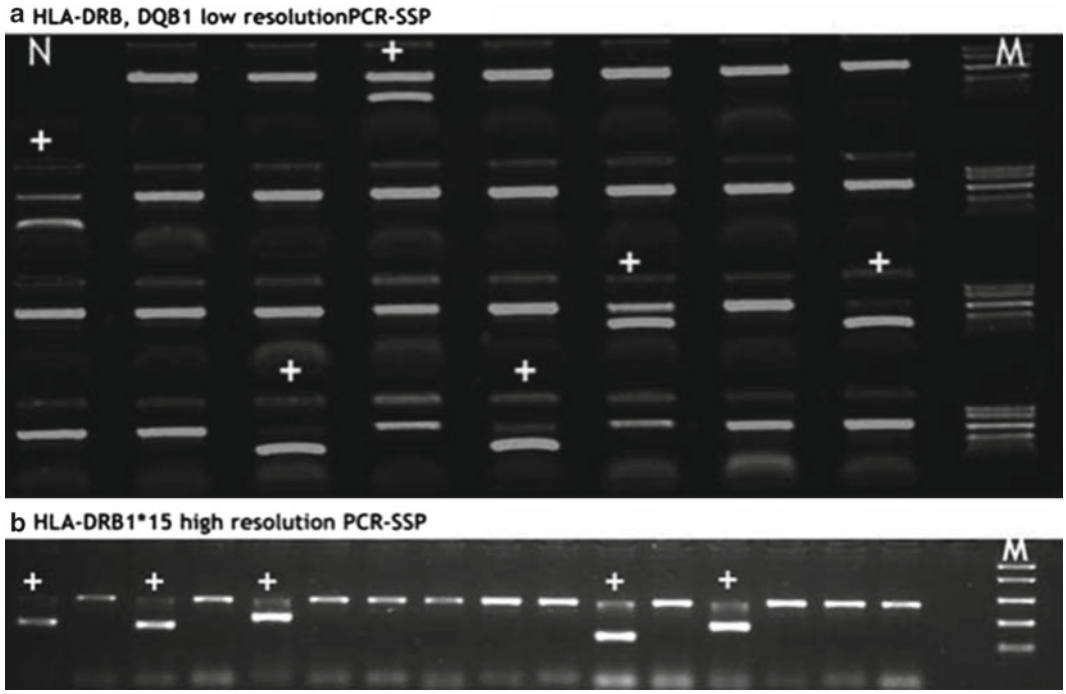


**Fig. 2** PCR using sequence-specific primers (PCR-SSP) results for low- and high-resolution typing. *N* = negative control; *M* = molecular weight marker; + = positive reaction. The band present in all lanes except the negative control is the positive internal control amplicon. An example of a low-resolution human leukocyte antigen (HLA)-DRB and -DQB1 PCR-SSP typing result is given in (**a**). All HLA-DRB1, 3, 4, 5, and DQB1 specificities are covered by this test, which uses 31 primer pairs. The positive reactions in lanes 4, 9, 22, 24, 27, and 29 (numbering of lanes is from top left-hand corner, reading from left-hand side to right-hand side) indicate the presence of HLA-DRB1*04, *15; DRB4*01; DRB5*01; and DQB1*03, *05. The results of further PCR-SSP testing of the same sample for high-resolution (allele level) HLA typing of the DRB1*15 allele only are given in (**b**). Using 16 primer pairs, the four-digit alleles of the DRB1*15/*16 group can be distinguished. Positivity in lanes 1, 3, 5, 11, and 13 indicate the presence of DRB1*15:01

PCR-SSP is an extremely flexible method that can be performed in laboratories with minimum molecular biology equipment (thermal cycler, agarose gel electrophoresis unit, ultraviolet transilluminator, and system for documenting gel image). Depending on the design and number of primer mixes prepared, PCR-SSP can be used to provide a low- to medium-resolution type for each locus. If the low-resolution type is known, additional PCR-SSP testing can target the HLA allele group giving allelic level typing.

PCR-SSP is currently the quickest of the DNA-based methodologies and therefore can be used to provide fast HLA typing in urgent clinical scenarios within a few hours of sample receipt. The cost of PCR-SSP can be kept low with in-house-developed primer mixes used, but this requires the laboratory to ensure that allele lists and interpretation tables are kept up to date. The laboratory must also have the ability to search primer sequences against

current alleles as more alleles are defined. There are many commercially available HLA PCR-SSP solutions. PCR-SSP is not used for large-scale HLA typing such as that undertaken by the larger hematopoietic stem cell registries because of the rate-limiting step of agarose gel electrophoresis. This step could be improved by the use of fluorescence detection systems such as that used in real-time PCR, which allows both detection and quantification of PCR amplicons and may allow discrimination of homozygous and heterozygous polymorphisms. Real-time PCR is also more open to automation as a result of the nonrequirement for electrophoresis. This approach has been developed commercially for HLA typing by Inno-Train (HLA FluoGene). Simpler systems involving the addition of PicoGreen® dye, which binds to the minor groove of double-stranded DNA molecules produced during the extension phases of the PCR reaction, can also be used. As the quantity of double-stranded DNA increases, the fluorescent emissions from the PicoGreen also increase, and this can be detected using a fluorescence reader. Such fluorescent systems, however, do not directly allow discrimination of molecular weights, and therefore false-negative results may be missed.

One of the advantages of PCR-SSP is the reduction in the number of ambiguous results compared with PCR-SSO. Cis polymorphisms can be linked by the generation of a product using primers designed to amplify from sequences containing both mutations.

### *1.1.3 PCR Sequence-Based Typing*

The resolution of results obtained with both PCR-SSO and PCR-SSP is limited by the number of oligonucleotide probes and primer mixes used, respectively. Current protocols do not cover the full genomic region of the HLA genes, and therefore it is always possible that novel mutations may not be observed. HLA gene sequencing was originally described using cloned PCR products to allow unambiguous identification of allele sequences, and the data generated from these studies led to the establishment of sequence databases that are used to develop reagents used in methods such as PCR-SSO and PCR-SSP. Improvements in automated DNA sequencing in the 1990s, concomitant with the introduction of robust dye-terminator chemistry protocols to allow accurate distinction between homozygous and heterozygous sequences, have permitted the establishment of routine HLA sequencing protocols from PCR-produced amplicons. Current PCR sequencing protocols have been described for all HLA loci using generic PCR amplification systems (the most widely used approach targets exons 2, 3, and 4 of the HLA class I loci and exon 2 of the class II loci), and also group-specific PCR sequencing protocols are described [10–12]. The latter approach has been most useful for analysis of the HLA-DRB1 locus, as it is difficult to amplify all HLA-DRB1 alleles in a single PCR reaction without coamplification of other HLA-DRB alleles as a result of sequence similarities [13].

Sequencing heterozygous PCR products necessitates the use of dedicated software to allow identification of all heterozygous positions and to allow comparison of the various possible sequences obtained against a database of known HLA sequences [14, 15].

### 1.1.4 Next-Generation Sequencing

NGS technology has been used to generate vast amounts of whole-genome data quickly and cheaply; however, the amount of data generated and the ability to interpret this data have identified the need to develop robust bioinformatics alongside any NGS approach. NGS is becoming more widely used clinically for example in oncology where utilization of whole-genome data can aid diagnosis. In the HLA setting the mega base amounts of sequence data generated has been successfully used to target the HLA genes. This can be achieved by targeting specific exons or by amplifying the whole gene using long-range PCR followed by a fragmentation and library preparation whereby the resulting sequence fragments are aligned to provide the genomic sequence. The benefits to HLA typing are the ability to produce allelic level typing incorporating exonic and intronic data [16, 17]. The uptake of this technology is expected to further increase the detection of novel HLA alleles. The current NGS platforms produce data through massively parallel clonal amplification of DNA molecules allowing the sequence to be generated to be unambiguous as the polymorphisms are aligned in phase. The ability to apply a DNA barcode to the amplicon and fragments enables multiplexing of many individual samples. Many commercially available platforms now provide high- and low-throughput options making this a realistic option for a clinical laboratory. Consideration of the platform capacity, cost, throughput, ability to automate, read length, accuracy, GC-rich and homopolymer presence in the template, output reads, and time to prepare the library and perform a run are important considerations. A summary of currently available systems that are being used for HLA typing is given here:

Roche 454 system (GS Junior and GS FLX+): This system utilizes pyrosequencing to monitor the pyrophosphate released during DNA polymerization. Single-stranded DNA templates are generated either from specific size amplicon incorporating fusion primers with 454 sequencing adaptor primers or by ligation of library adaptors to DNA fragments. These adaptors enable ligation to capture beads followed by an emulsion PCR step. This results in clonal amplification of the single-stranded DNA fragment; following breaking of the emulsion a single bead with the clonally amplified product attached is applied to a picotiter plate, and dNTPs are flowed over the plate in a sequential order. Incorporation of a dNTP triggers the release of pyrophosphatase (PPi) equal to the dNTP. Through the transformation of luciferin into oxyluciferin via the action of ATP and PPi visible light is generated proportional to the number of the specific dNTPs incorporated.

The remaining dNTPs are degraded through the flowing of apyrase over the picotiter plate, and the process is repeated [18]. The use of microfluidics and the development of automation means that scalability is an option for this system [19].

Illumina TruSeq (Miseq and Hiseq): Following generation of a sample library with fixed adapters single-stranded DNA is grafted to the surface of the flow cell. Cluster amplification allows clonal amplification of the DNA fragments. The addition of paired end reads allows the sequencing of both the forward and the reverse templates allowing for more accurate aligning in the analysis phase. The sequencing by synthesis technology utilizes a reversible terminator-based method that allows detection of single dNTPs as they are incorporated. During each flow cycle all four fluorescently labelled dNTPs are present. Detection of the incorporated base is via a charge-coupled device, and the incorporated terminator is cleaved allowing the synthesis to continue.

Life Technologies (Ion Torrent PGM): This platform utilizes semiconductor sequencing technology detecting the proton released during nucleotide incorporation. This results in a slight change in pH which is detected as a change in voltage. dNTPs are flowed over the chip in a known order allowing the DNA sequence to be elucidated. The voltage will increase in relation to the number of homologous bases incorporated, e.g., AA and AAA. Development of automation to support the emulsion PCR step and flow cell loading and the small footprint of the platform opens up NGS to smaller scale HLA typing laboratories.

### 1.2 Third Generation

Even though NGS platforms are only just being to be embraced by clinical HLA typing laboratories the so-called third-generation technologies are emerging. Although currently they are not being widely used they should be noted as a potential for HLA typing in the future. These technologies have developed strategies for the direct sequencing of a single DNA molecule, rather than requiring clonal expansion, and represent an opportunity to resolve HLA ambiguity across both exons and introns by analysis of long DNA fragments, up to 3 kb currently and likely to increase.

Third-generation sequencing platforms: Pacific Biosciences (single-molecule real-time (SMRT) cell): This exploits the rapid processivity of DNA polymerase and interprets fluorescently labelled dNTP incorporation in a real-time setting. In principle a single template DNA molecule is captured per reaction well with a modified DNA polymerase. A phospholinked nucleotide is incorporated as part of DNA synthesis; fluorescent elevation following this event is captured by a corresponding color channel. Separation of the fluorescent dye following incorporation and diffusion out of the capture well ends the fluorescent detection allowing a new nucleotide to be incorporated. The addition of adapted linkers (SMRTBell) allows the circulation of the single DNA molecule

| | Father | Mother | |
|---|---|---|---|
| HLA-A | *02:01, 02:01 | *01:01, 03:01 | |
| HLA-B | *44:02, 44:03 | *08:01, 07:02 | |
| HLA-C | *05:01, 16:02 | *07:01, 07:02 | |
| HLA-DRB1 | *04:01, 04:02 | *03:01, 15:01 | |
| HLA-DQB1 | *03:01, 03:02 | *02:01, 06:02 | |
| | Patient | Sibling 1 | Sibling 2 |
| HLA-A | *02:01, 01:01 | *02:01, 01:01 | *02:01, 01:01 |
| HLA-B | *44:02, 08:01 | *44:02, 08:01 | *44:03, 08:01 |
| HLA-C | *05:01, 07:01 | *05:01, 07:01 | *16:02, 07:01 |
| HLA-DRB1 | *04:01, 03:01 | *04:01, 03:01 | *04:02, 03:01 |
| HLA-DQB1 | *03:01, 02:01 | *03:01, 02:01 | *03:02, 02:01 |

**Fig. 3** Identification of a matched related donor may require extended and high-resolution human leukocyte antigen (HLA) typing. This example of HLA typing within a family highlights the potential for error when only first-field (low resolution) HLA-A, -B, and -DRB1 typing is performed (the HLA type before the : delimiter). At first-field HLA typing, the father appears to be homozygous for HLA-A, -B, and -DRB1, and both siblings appear to match the patient. However, extending the HLA type to include HLA-C and -DQB1 and performing second-field HLA typing (numbers after the ":" delimiter) demonstrate the father to possess two different haplotypes, and only one of the two siblings is a true match for the patient

which allows strand displacement of the growing replicated strand [20]. Good-quality DNA template to allow long-range sequencing is essential and likely to be an area targeted for improvement. The cost–benefit from the large scale of the throughput may be more suited to larger HLA typing facilities such as stem cell registries.

Oxford Nanopore Technologies: Oxford Nanopore Technologies Strand Sequencing is a technique that passes intact single DNA polymers through a protein nanopore, sequencing in real time as the DNA translocates the pore by electrophoresis [21]. By measuring the disruption of that current, it is possible to identify the nucleotide that has passed through. Although in the early stages of development for clinical use the potential for cheap sequencing in a platform as small as a key ring makes this an exciting area of future development.

### *1.3 HLA Typing Resolution Requirements for Hematopoietic Stem Cell Transplantation*

Usually, the search for a hematopoietic stem cell donor begins within the patient's family, and the identification of a matched related donor can be made with a minimum HLA-A, -B, and -DRB1 type when the haplotypes present are unique. However when similar haplotypes exist (e.g., if one of the parents is apparently homozygous by low-resolution typing (Fig. 3)), or if the four parental haplotypes cannot be established in the available family members, it is advisable to perform more extended typing at high resolution and to include HLA-C and DQB1. Where there is no fully matched related donor, extended familial typing may result in

the identification of a single antigen mismatched donor. This has been reported to have favorable outcomes post transplant compared to a fully matched unrelated donor and should be considered [22]. HLA-DPB1 typing is also informative as recombination between HLA-DPB1 and -DQB1 has been observed in as many as 5 % of related cases as a result of a lack of linkage disequilibrium between HLA-DPB1 and other HLA loci [23].

When a search is extended to unrelated donors, it is an increasing requirement to perform high-resolution or allele-level typing for both patient and selected unrelated donor. The largest volunteer donor registry, the national marrow donor program (NMDP), since June 2005 requires high-resolution typing of all unrelated donors and patients for HLA-A, -B, -C, and -DRB1 prior to releasing the donor for stem cell harvest, and other registries have followed suit [24]. There are now extensive data supporting the importance of matching at high resolution for HLA-A, -B, -C, and -DRB1 loci vs. low resolution [25]. There are also data to support the use of single-allele mismatched donors when a perfect match cannot be found [26]. In order to know if a donor is only mismatched for one allele, high resolution is required to eliminate mismatches not detected by lower resolution typing methods. The role of HLA-DQB1 and -DPB1 matching has been more difficult to ascertain. As a result of linkage disequilibrium between HLA-DRB and -DQB1 loci, there are few cases of donor and patient pairs mismatched for HLA-DQB1 in the presence of no other mismatches; however, the presence of DQB1 mismatches in addition to other HLA mismatches was associated with increased mortality in a study published by the Fred Hutchinson Cancer Research Center [26]. Yet, the NMDP did not find a negative contribution of HLA-DQB1 mismatching in their analysis [25]. The differences in these studies are likely a reflection of differences in the cohorts used and analyses performed. HLA-DPB1 is not in linkage disequilibrium with other HLA loci, presenting the scenario where a 10/10 HLA matched donor (HLA-A, -B, -C, -DRB1, -DQB1) may not be matched for HLA-DPB1. DPB1 mismatches based on T-cell epitope groups do indicate the potential for permissive and non-permissive mismatches, whereby avoiding non-permissive mismatches decreases the mortality risk post transplant [27]. This indicates that HLA-DPB1 typing should be performed in certain clinical settings [28].

The number of banked cord blood units is increasing worldwide with bone marrow donors worldwide reporting 563,082 available [29]. Current HLA typing requirements are to consider HLA matching at HLA-A and -B at low resolution (antigen level) and HLA-DRB1 at allele level (second field level). However the effect of high-resolution typing and matching at other HLA loci is being reported [30].

### 1.4 Patient and Donor Testing

Selecting a method for patient and donor testing depends on various factors including the number of samples that the laboratory tests, the type of sample obtained, and also the level of resolution to be achieved. The patient and related donor may initially be tested to low/medium resolution (PCR-SSO or PCR-SSP) with additional high/allele-level resolution (PCR-SSP and/or PCR-SBT) performed if required to resolve ambiguities. All potentially matching unrelated donors selected from the various volunteer donor registries must have their HLA type confirmed by repeat testing, and this should always include extension of the original HLA type to include additional loci: e.g., if donor is HLA-A, -B, and -DRB typed on the register, further testing for HLA-C, -DQB1, and -DPB1 is warranted, and loci (HLA-A, -B, -C, and -DRB1 as a minimum) should be tested to high/allele level of resolution (PCR-SSP and/or PCR sequencing). HLA genes are very polymorphic, and determination of accurate HLA types can be complex and may necessitate the use of more than a single method. The development of DNA-based HLA typing assays has made reliable, reproducible, and sensitive assays available for all laboratories supporting a hematopoietic stem cell transplantation program.

## Acknowledgments

Dr. Raymond Fernando and Mr. Franco Tavarozzi are thanked for providing Fig. 2.

### References

1. Warrens A, Lechler R (eds) (2000) HLA in health and disease. Academic, London, pp 139–146
2. Mallal S, Nolan D, Witt C et al (2002) Association between presence of HLA-B*5701, HLA-DR7, and HLA-DQ3 and hypersensitivity to HIV-1 reverse transcriptase inhibitor abacavir. Lancet 359:727–732
3. Abi-Rached L, Jobin MJ, Kulkarni S et al (2011) The shaping of modern human immune systems by multiregional admixture with archaic humans. Science 334:89–94
4. Klein K (1986) Natural history of the major histocompatibility complex. Wiley, Toronto, ON
5. Cao K, Chopek M, Fernandez-Vina MA (1999) High and intermediate resolution DNA typing systems for class I HLA-A, B, C genes by hybridization with sequence-specific oligonucleotide probes (SSOP). Rev Immunogenet 1:177–208
6. Trajanoski D, Fidler SJ (2012) HLA typing using bead-based methods. Methods Mol Biol 882:47–65
7. Olerup O, Zetterquist H (1992) HLA-DR typing by PCR amplification with sequence-specific primers (PCR-SSP) in 2 hours: an alternative to serological DR typing in clinical practice including donor-recipient matching in cadaveric transplantation. Tissue Antigens 39:225–235
8. Bunce M, O'Neill CM, Barnardo MC et al (1995) Phototyping: comprehensive DNA typing for HLA-A, B, C, DRB1, DRB3, DRB4, DRB5 & DQB1 by PCR with 144 primer mixes utilizing sequence-specific primers (PCR-SSP). Tissue Antigens 46:355–367

9. Newton CR, Graham A, Heptinstall LE et al (1989) Analysis of any point mutation in DNA. The amplification refractory mutation system (ARMS). Nucleic Acids Res 17:2503–2516
10. van der Vlies SA, Voorter CE, van den Berg-Loonen EM (1998) A reliable and efficient high resolution typing method for HLA-C using sequence-based typing. Tissue Antigens 52:558–568
11. Turner S, Ellexson ME, Hickman HD et al (1998) Sequence-based typing provides a new look at HLA-C diversity. J Immunol 161: 1406–1413
12. Swelsen WT, Voorter CE, van den Berg-Loonen EM (2005) Sequence-based typing of the HLA-A10/A19 group and confirmation of a pseudogene coamplified with A*3401. Hum Immunol 66:535–542
13. Kotsch K, Wehling J, Blasczyk R (1999) Sequencing of HLA class II genes based on the conserved diversity of the non-coding regions: sequencing based typing of HLA-DRB genes. Tissue Antigens 53:486–497
14. Sayer DC, Goodridge DM, Christiansen FT (2004) Assign 2.0: software for the analysis of Phred quality values for quality control of HLA sequencing-based typing. Tissue Antigens 64: 556–565
15. Rozemuller EH, Tilanus MG (2000) Bioinformatics: analysis of HLA sequence data. Rev Immunogenet 2:492–517
16. Shiina T, Suzuki S, Ozaki Y et al (2012) Super high resolution for single molecule-sequence-based typing of classical HLA loci at the 8-digit level using next generation sequencers. Tissue Antigens 80:305–316
17. Lind C, Ferriola D, Mackiewicz K et al (2012) Filling the gaps—the generation of full genomic sequences for 15 common and well-documented HLA class I alleles using next-generation sequencing technology. Hum Immunol 74:318–324
18. Liu L, Li Y, Li S et al (2012) Comparison of next generation sequencing systems. J Biomed Biotechnol 2012:251364. doi:10.1155/2012/251364
19. Moonsamy PV, Williams T, Bonella P et al (2013) High throughput HLA genotyping using 454 sequencing and the Fluidigm Access Array™ system for simplified amplicon library preparation. Tissue Antigens 81:141–149
20. Eid J, Fehr A, Gray J et al (2009) Real-time DNA sequencing from single polymerase molecules. Science 323:133–138
21. Maitra RD, Kim J, Dunbar WB (2012) Recent advances in nanopore sequencing. Electrophoresis 33:3418–3428
22. Valcarcel D, Sirra J, Wang T et al (2011) One antigen mismatched related versus HLA matched unrelated donor haematopoietic stem cell transplantation in adults with acute leukemia: center for International Blood and Marrow Transplant Research results in the ERA or molecular HLA typing. Biol Blood Marrow Transplant 17:640–648
23. Buchler T, Gallardo D, Rodriguez-Luaces M, Pujal JM, Granena A (2002) Frequency of HLA-DPB1 disparities detected by reference strand-mediated conformation analysis in HLA-A, -B, and -DRB1 matched siblings. Hum Immunol 63:139–142
24. Bioinformatics.NMDP.Org. Policies (www.nmdpresearch.org/HLA/hla_policies.html)
25. Flomenberg N, Baxter-Lowe LA, Confer D et al (2004) Impact of HLA class I and class II high-resolution matching on outcomes of unrelated donor bone marrow transplantation: HLA-C mismatching is associated with a strong adverse effect on transplantation outcome. Blood 104:1923–1930
26. Petersdorf EW, Anasetti C, Martin PJ et al (2004) Limits of HLA mismatching in unrelated hematopoietic cell transplantation. Blood 104:2976–2980
27. Shaw BE, Potter MN, Mayor NP et al (2003) The degree of matching at HLA-DPB1 predicts for acute graft-versus-host disease and disease relapse following haematopoietic stem cell transplantation. Bone Marrow Transplant 31:1001–1008
28. Fleischauer K, Shaw BE, Gooley T et al (2012) Effect of T-cell-epitope matching at HLA-DPB1 in recipients of unrelated donor haemopoietic cell transplantation: a retrospective study. Lancet Oncol 13:366–374
29. Bone Marrow Donors Worldwide (http://www.bmdw.org/). Accessed Feb 2013
30. Eapen M, Klein JP, Sanz GF et al (2011) Effect of donor–recipient HLA matching at HLA A, B, C, andDRB1 on outcomes after umbilical-cord blood transplantation for leukaemia and myelodysplastic syndrome: a retrospective analysis. Lancet Oncol 12: 1214–1221
31. Robinson J, Mistry K, McWilliam H, Lopez R, Parham P, Marsh SGE (2011) The IMGT/HLA database. Nucleic Acids Res 39: 1171–1176

# Chapter 6

# HLA Typing with Sequence-Specific Oligonucleotide Primed PCR (PCR-SSO) and Use of the Luminex™ Technology

**Klara Dalva and Meral Beksac**

## Abstract

The hybridization products obtained by PCR using sequence-specific oligonucleotides can be traced either by colorimetric (streptavidin–biotin)-, X-ray (digoxigenin–CSPD)-, or fluorescence (FITC, PE)-based detection systems. To achieve a faster, reliable, automated typing technique microbead and fluorescence detection technology have been combined and introduced to this field (XMAP™ technology). For each locus, a series of microspheres, which are recognizable by their specific color originating from two internal fluorescent dyes, are used. Each microsphere is coupled with a single probe that is capable of hybridizing with the biotin-labeled complementary amplicon. Once hybridization occurs, it can be quantified by measuring the fluorescence signal originating from fluorescently (streptavidin–PE) labeled amplicons captured by the beads. Currently, there are two commercially available systems that differ in the scale of probes and the methods used for amplification and denaturation. One of these is described in detail in this chapter.

**Key words** PCR-SSO, Luminex™, XMAP™ technology, HLA typing

## 1 Introduction

The first applications of PCR using sequence-specific oligonucleotides (PCR-SSO) in the field of human leukocyte antigen (HLA) were started with the DQA1 locus and followed by class I and other class II specificities [1–8]. In order to eliminate ambiguities, protocols that use PCR primers designed to amplify the entire hypervariable region of a particular HLA locus (group-specific primers) were introduced. These PCR products are incubated in the presence of a panel of labeled oligonucleotides designed for the detection of different polymorphic positions specific for an allele or an allelic group [9]. The primers for HLA-A, -B, and -C loci usually give a locus-specific product covering exons 2 and 3. Primer for HLA-DR gives a product from exon 2 [1, 8, 10].

The introductory chapter on molecular HLA typing authored by Katy Latham, Ann-Margaret Little, and J Alejandro Madrigal (Chapter 5) summarizes the main features of PCR-SSO typing and

Meral Beksaç (ed.), *Bone Marrow and Stem Cell Transplantation*, Methods in Molecular Biology, vol. 1109,
DOI 10.1007/978-1-4614-9437-9_6, 

compares it with the other methods. Here, we describe an automated system, Luminex™ technology, that is capable of typing of multiple individuals simultaneously. The xMAP™ technology developed by Luminex (Austin, TX) is a microsphere-based, multiplexed, flow cytometric analysis system that makes it possible to combine hybridization with fluorescence detection [11, 12]. Classification of HLA alleles by Luminex system was first described by Fulton et al. [13]. The xMAP™ technology employs simultaneous applications of up to 100 probes, which are already coated on microspheres. To be able to recognize these probes, 100 shades of two colors that are formed by the ratio of two internal fluorescent dyes are assigned for each probe. The fluoroanalyzer contains a red laser that excites the dyes in the microspheres and categorizes them based on their dye content. The microspheres are coated with carboxyl groups in order to achieve a covalent bridge between the oligonucleotides that contain terminal amino groups and the beads. Thus, the bound oligonucleotides also become color coded. In addition to the red laser, the instrument contains a green laser that is used to quantify fluorescently (streptavidin–PE (SA–PE)) labeled amplicons captured by the beads. Each probe mix contains one or more oligonucleotides that react with all alleles within the locus of interest, which also serves as an internal control. They are used in the normalization of the values during the calculation of reaction patterns. If the minimum fluorescent intensity values defined for this control probes are not achieved, the sample test must be repeated. All probe-coated beads can be applied within a well. For an enhanced resolution an additional well is used to add a new set of probe-coated beads. This unique feature enables one locus typing of 96 samples or more loci on smaller number of samples. Currently, there are two commercially available kits, namely, One-Lambda LabType-SSO and Gen-Probe Lifecodes HLA-SSO typing kits. The probe number, specificity, and cutoff levels may vary between lots and commercial sources. In this chapter, we focus on Gen-Probe Lifecodes HLA-SSO typing kits.

## 2 Materials

### 2.1 Specimen

#### 2.1.1 Patient/Donor Sample

DNA is usually obtained from EDTA- or ACD-anticoagulated venous blood samples. Heparin interferes with Taq polymerase activity and should not be used as an anticoagulant. Final DNA concentration must be 10–200 ng/μL.

#### 2.1.2 Controls

A previously run DNA sample can be used as a positive control. Purified DNA/RNA-free water can be used as a negative control.

### 2.2 DNA Extraction

*Reagents*

#### 2.2.1 Isolation with EZ1 Advanced XL Instrument

1. EZ1 DNA Blood 350 μL kit (the kit includes prefilled reagent cartridges, 2-mL screw-cap Eppendorf tubes required for

distribution of blood samples, 1.5-mL screw-cap Eppendorf tubes for the elution of extracted DNA, plugged pipet tips, and pipet tip holders sufficient for DNA isolation from 48 samples).

*Equipment*

1. EZ1 Advanced XL instrument (or GenoM™ 6 Robotic Workstation).

### 2.2.2 Salting-Out Technique

This method is a modification of Miller's salting-out procedure, with the omission of proteinase K and addition of a chloroform extraction phase [4].

*Reagents*

1. Red cell lysis buffer (RCLB): 0.144 M ammonium chloride ($NH_4Cl$), 1 mM sodium bicarbonate ($NaHCO_3$): 15.4 g of $NH_4Cl$ and 1.68 g of $NaHCO_3$ are dissolved in 2 L of double-distilled (dd) $H_2O$.
2. Nuclear lysis buffer (NLB): 10 mM Tris–HCl pH 8.2, 0.4 M sodium chloride (NaCl), 2 mM disodium EDTA ($Na_2EDTA$) pH 8.0: Dissolve 23.37 g of NaCl in 900 mL of $ddH_2O$. Add 10 mL 1 M Tris–HCl pH 8.2 and 10 mL $Na_2EDTA$ pH 8.0 and adjust to 1 L with $ddH_2O$.
3. 10 % w/v sodium dodecyl sulfate (SDS): Dissolve 100 g of SDS in 1 L $ddH_2O$. Store at room temperature to prevent the formation of precipitates.
4. NLB + SDS buffer: 300 mL of NLB and 20 mL of 10 w/v SDS are mixed. Store at room temperature.
5. 95 % Ethanol: Dilute 950 mL of absolute ethanol with 50 mL of $ddH_2O$.
6. 70 % Ethanol: Dilute 700 mL of absolute ethanol with 300 mL of $ddH_2O$.
7. 6 M NaCl: 350.64 g sodium chloride was dissolved in 800 mL $ddH_2O$ by warming the solution and the volume adjusted to 1 L by $ddH_2O$. As 6 M NaCl is a saturated solution, not all of the NaCl will dissolve into the solution.

*Equipment*

1. Centrifuge.
2. Plastic tubes (15 mL, 2 mL).

## 2.3 PCR Amplification

*Reagents*

1. Lifecodes HLA-SSO typing kits (HLA-A, -B, -C, -DRB1, -DQB typing kits): Each kit contains the appropriate master mix (MX) including 10× PCR buffer, 10× dNTPs, locus-specific biotin-conjugated primers (MX-A, -B, -C, -DRB1, -DQB), an appropriate fluorescently coded probe mix (BM), a dilution solution

**Table 1**
**Number of probes for HLA typing (IVD certified) (March 2013)**

| Locus | Lifecodes HLA-SSO | Lifecodes HLA-SSO (eRES) |
|---|---|---|
| A | 72 | 140 (72 + 68) |
| B | 92 | 166 (92 + 64) |
| C | 55 | 77 |
| DRB1 | 93 | 138 (93 + 45) |
| DRB3,4,5 | 52 | – |
| DQB | 56 | – |

*eRES* enhanced resolution, *IVD* in vitro diagnostic use

(DS) necessary for the hybridization step and the threshold table, probe hit chart(s) (store at +4 °C).

2. Recombinant Taq polymerase (5 U/μL) (store at –20 °C).
3. Nuclease-free water.

*Equipment*

1. Microcentrifuge.
2. Vortex mixer.
3. Cooling block or melting ice.
4. DNase/RNase-free tubes (2 mL).
5. DNase/RNase-free thin-wall tubes/strips (0.2 mL).
6. PCR thermocycler(s): Model with a 96-well format (e.g.: LabCycler—Sensoquest, CGI-960 Corbett Research).
7. Dispensing equipment: Adjustable pipet(s), plastic tips.

### 2.4 Hybridization

*Reagents*

1. Lifecodes HLA-SSO typing kits (HLA-A, -B, -C, DRB, -DQB) (keep at +4 °C): Each kit contains an appropriate fluorescently coded probe mix (BM), a dilution solution (DS) necessary for the hybridization step. If you want to increase the resolution of the results you may select the eRES kits for loci-A, -B, and -DRB1 which contain an additional probe mix within the kit. Examples for the available probe numbers in these kits are presented in Table 1.
2. SA–PE (1 mg/mL, GenProbe).

*Equipment*

1. Heating block.
2. Ultrasonic bath.
3. Vortex mixer with adjustable speed.
4. PCR plates (thin-wall, 96-well, 250 μL/well).

5. Polyethylene sealing tape.
6. Dispensing equipment, adjustable pipette(s), plastic tips.

### 2.5 Data Collection

*Reagents*

1. Sheath fluid (store at room temperature).
2. Daily maintenance reagents (70 % isopropanol, $ddH_2O$).

*Equipment*

1. Luminex100 Instrument and XY Platform.
2. Luminex100 IS software, Quick Type for Lifematch 2.6 software.

### 2.6 Analysis

Quick Type for Lifematch 2.6 software.

## 3 Method

### 3.1 DNA Extraction

Extracted, highly pure DNA is required for PCR-SSP typing. Because the class I amplicon is larger than the class II amplicon, the DNA preparation method is critical for the success of the PCR. Here, two different methods are described. The optimal DNA concentration for EZ1 isolations is 15 and 30 μg/mL for the other methods. High-quality DNA results in an optical density (OD) 260/280 ratio greater than 1.6 (*see* **Notes 1** and **2**).

#### 3.1.1 Isolation with EZ1 Advanced XL Instrument

The EZ1 Advanced XL instrument can be used for an easy, automated nucleic acid isolation and purification. The procedure involves binding of GenoPrep magnetic beads to the nucleic acids. The EZ1 Advanced XL instrument performs all the steps involved in sample preparation, including sample lysis, binding of nucleic acids to the beads, and washing and elution in an automated system. Protocols can be scaled up and down according to the needs of the user.

*Principle*

Isolation of the DNA relies upon its binding to the silica surface of the paramagnetic beads in the presence of a chaotropic salt solution such as sodium iodide.

The addition of chaotropic solutions (GTC) and silica magnetic beads results in complete cell lysis and release of DNA. DNAses are denaturated and inactivated during this step. Magnetic beads are mixed with the sample, resulting in binding of the DNA to the GenoPrep DNA magnetic beads. Subsequently, immobilized DNA bound to magnetic beads are collected by application of a magnetic force. Three consecutive washing steps are performed during the application of magnetic force. During the first wash, a chaotropic solution removes any unbound material.

In the second wash, ethanol is applied and removes GTC, followed by a third wash, in which water removes the ethanol. DNA is released from the GenoPrep DNA magnetic beads via thorough resuspension in $ddH_2O$.

*Operation*

1. Select and insert the program card, "DNA Blood Card," into the card inlet located on the front of the EZ1 Advanced XL instrument.
2. Switch on the main power of the EZ1 Advanced XL instrument.
3. Choose the desired volume from the top menu. 350 μL protocol is selected for a low-resolution typing of HLA-A, -B, -C, -DR, and -DQ.
4. Load disposables on the instrument platform (1.5-mL elution tubes to the first row, tips to the second row, and 2-mL sample tubes to the fourth row). Prefilled cartridges are inserted in the predefined positions.
5. Place the sample tubes that include a minimum of 1 mL of a homogenized anticoagulated blood sample on the instrument platform.
6. Close the instrument, and start the extraction procedure. The Menu Screen will indicate at which stage the isolation process is in.
7. Retrieve the isolated DNA from the elution row (first row).
8. Proceed with the PCR amplification step immediately or otherwise store the DNA at +4 °C for up to 7 days or at −20 °C for several months.

### *3.1.2 Salting-Out Technique*

*Operation*

1. Centrifuge 5 mL of EDTA or ACD-A-anticoagulated blood to obtain a buffy coat.
2. Aspirate the buffy coat into a 15-mL polypropylene tube.
3. Add 10 mL of RCLB, invert several times, and leave to stand for 5 min at room temperature.
4. Centrifuge the tube at 1,000 × *g* for 10 min. Discard the supernatant, and gently rinse the pellet with 2 mL of RCLB buffer. The pellet will appear white with a pink halo. If there is excess hemoglobin, resuspend the pellet in RCLB and gently agitate, continuing with further centrifugation (10 min, 1,000 × *g*).
5. Resuspend the pellet in 3 mL of NLB + SDS buffer. Add 1 mL of 6 M NaCl, and vortex. At this stage, the precipitate should be visible.
6. Add 2 mL of chloroform, and gently mix until a homogenous milky solution is obtained. Centrifuge the tube (10 min, 1,000 × *g*).

**Table 2**
**Reaction components of an amplification mix**

| Component | Amount sufficient for 1 reaction (prepare for $n+1$ reactions) |
|---|---|
| Master mix (MX) | 15.0 µL |
| $ddH_2O$ | 24.5 µL |
| Taq polymerase | 0.5 µL (2.5 U) |
| Total | 40 µL |

7. Aspirate the top phase containing the DNA into a 20-mL tube. Avoid aspirating protein from the interphase. If the DNA phase is not clear, transfer the aspirate into a clean polypropylene tube, and repeat the chloroform extraction step.
8. Add 2 mL of 95 % ethanol, and gently invert the tubes until all of the DNA is precipitated.
9. Centrifuge the tubes (5 min, 700 × *g*), and resuspend the pellet in 2 mL of 70 % ethanol. Repeat once more.
10. Transfer the DNA precipitate into a sterile 0.5-mL microcentrifuge tube, and centrifuge the tubes in order to obtain a DNA pellet. Remove the excess ethanol by a further centrifugation step.
11. Resuspend the DNA in 0.3 mL of sterile $ddH_2O$. A DNA yield of 0.2–1.0 mg/mL is expected.

### *3.2 PCR Amplification*

The Lifecodes kits utilize an asymmetric PCR that increase the amount of one primer approx 10× and allow to generate single-stranded DNA products in addition to the double-stranded products (*see* **Note 3**).

1. Allow the master mix to warm to room temperature.
2. Gently vortex for 10 s, and centrifuge briefly to ensure that salts are in solution (*see* **Note 4**).
3. Prepare the amplification mix sufficient for $n+1$ samples (Table 2) (*see* **Notes 5** and **6**).
4. Pipette 10 µL of genomic DNA isolated by GenoPrep™ (approx 200 ng of DNA) into the PCR tubes (except the negative control tube, in which DNA–RNA-free water is added instead of DNA).
5. Dispence 40 µL of the amplification mix into the PCR tubes containing the DNA.
6. Close the tubes tightly to prevent evaporation during PCR.
7. Place samples in the thermal cycler, and run program (Table 3). Identical PCR cycling conditions are used for all applications (*see* **Notes 7** and **8**).

**Table 3**
**PCR cycling conditions**

| Number of cycles | Condition |
|---|---|
| 1 Cycle | 95 °C for 5 min, denaturation |
| 8 Cycles | 95 °C for 30 s, denaturation<br>60 °C for 45 s, annealing<br>72 °C for 45 s, extension |
| 32 Cycles | 95 °C for 30 s, denaturation<br>63 °C for 45 s, annealing<br>72 °C for 45 s, extension |
| 1 Cycle | 72 °C for 15 min |

### 3.3 Hybridization

This technique excludes the prehybridization denaturation step. Single-stranded DNA is achieved by asymmetric PCR and by the addition of a 5-min incubation at 97 °C prior to the hybridization (*see* **Notes 9** and **10**).

Before starting with the hybridization, turn on the Luminex100 instrument and XY platform to allow warming of the laser at least for 30 min prior to the analysis.

1. Warm probe mix to 55 °C in a 55–60 °C heat block for 7 min [5–10] to obtain the solubilization of the components thoroughly. Protect from light to avoid photobleaching, do not refreeze bead mixture after thawing, and store at 2–8 °C (*see* **Note 11**).
2. Sonicate the probe carrier beads briefly for 15 s and then vortex it for another 15–30 s to thoroughly suspend the beads (*see* **Note 11**).
3. Aliquot 5 μL of locus-specific PCR product (amplicon) into a thermal cycler 96-well plate (*see* Fig. 1).
4. Aliquot 15 μL of appropriate probe mix into each well (*see* **Note 12**). When aliquoting probe mix to more than ten wells, gently vortex the probe mix for each set of 10 (*see* **Note 13**).
5. Seal the plate with a polyethylene sealing tape (*see* **Note 14**).
6. Hybridize the samples under the following incubation conditions in a thermocycler:

   97 °C for 5 min.

   47 °C for 30 min.

   56 °C for 10 min.

   56 °C hold.

| Sample(s) | 1 | 2 | 3 | 4 | 5 | 6 | 7 | 8 | 9 | 10 | 11 | 12 |
|---|---|---|---|---|---|---|---|---|---|---|---|---|
| Locus | | | | | | | | | | | | |
| HLA-A | | | | | | | | | | | | |
| HLA-B | | | | | | | | | | | | |
| HLA-C | | | | | | | | | | | | |
| HLA-DRB1 | | | | | | | | | | | | |
| HLA-DQB1 | | | | | | | | | | | | |
| | | | | | | | | | | | | |
| | | | | | | | | | | | | |
| | | | | | | | | | | | | |

**Fig. 1** Sample of hybridization data sheet prepared for this application

7. While hybridization is in progress, prepare the working SA–PE solution by mixing 0.85 μL of SA–PE and 170 μL of DS per sample.

   Prepare the solution for $n+1$ samples. SA–PE is light sensitive, so keep the DS/SA–PE solution in the dark, at room temperature. Do not reuse; discard any remaining solution (*see* **Note 15**).
8. While the tray is still on the thermocycler at the 56 °C "hold" step, serially aliquot 170 μL of SA–PE/DS mixture to each well containing the hybridized sample(s). It is critical to dilute all of the samples within 5 min following the 10-min incubation at 56 °C (*see* **Note 16**).
9. Remove the samples from the thermocycler and place in the Luminex100 instrument to analyze the samples.
10. Turn off the thermal cycler.

Assay the samples immediately using the prewarmed Luminex100 instrument. If immediate reading is not possible, protect samples from light. Samples can be read within 30 min following the addition of SA–PE/DS mixture.

Prior to data acquisition and analysis steps, set up a "batch run" by which the samples will be analyzed.

### 3.4 Data Acquisition

The steps described next are a general guide for data acquisition. Daily startup, calibration, maintenance, and shutdown procedures may be found in the user's manual.

1. Turn on the Luminex100 30 min to 4 h before acquisition of the samples.
2. Prior to acquisition, check the level of the sheath fluid, tighten the cap, empty the waste tank, perform a "prime" and a wash with 70 % isopropanol, and proceed with a wash using the sheath fluid.

3. Set up a "batch run" by which the samples will be analyzed. For each locus, follow the directions for the analysis.
4. Open Luminex100 IS software from desktop, and open "submitted batch." Follow directions. To analyze multiple loci in one plate, "Create Multi-batch" by adding batches, and click "finish" after naming the multi-batch.
5. Eject the plate holder, and place the 96-well plate containing the samples in the XYP heater block present on the plate holder. Click the "retract" icon to start the acquisition.
6. Once the sample tray has been placed into the XY Platform of the Luminex100 instrument, click the "Start Plate" icon to start with acquisition.
7. After running of the samples, perform a sanitization wash by rinsing two times with 70 % isopropanol and perform "soak" with dd$H_2O$.
8. Release the pressure on the sheath fluid tank.
9. Turn off the instrument. Completed batches are exported automatically as comma-separated values (csv), and named as "output.csv," and saved in a folder with batch name defined on the third step. This data are available for the assignments of the results.

### 3.5 Interpretation of Results

Interpretation of the results is performed by using the Quick Type for Lifematch 2.6 software with which the opened csv files may be analyzed. The steps described next are only a general guide to data analysis.

1. Select "Final Typing Assignments."
2. Select file(s) to be analyzed.
3. Verify the number of counted events to be greater than 60 for each probe including the controls in each sample (this information is present in "data type" and count section of csv files).
4. The values for the consensus probes(con) for each sample must exceed the minimum median fluorescent intensity (MFI) (*see* **Notes 4** and **8**). These values can be found on the threshold tables supplied with each kit or can be loaded to the analyzer by the technical services during updating process. The minimum thresholds are lot specific.
5. For each probe, compare the normalized value with the threshold values supplied with the kits. The software makes this assignment automatically. However, the current result must be validated before continuing to the next step. Normalized values are calculated as
[MFI(probe) – MFI(controlblankorprobe)]/[MFI(consensus) – MFI (control blank or consensus)].

6. If the measured value for a particular probe falls above the maximum threshold of a negative assignment and below the minimum value of a positive assignment, the software evaluates this value as "undetermined" (*see* **Note 17**).
7. Save and print the results.

## 4 Notes

1. Poor-quality, degraded, or insufficient amount of DNA may lead to reaction failures. Reisolate DNA. The DNA quality should be checked. WBC counts less than 1,000 μL may lead to an insufficient amount of DNA. Repeat the isolation with buffy coat collected from 10 mL instead of 350 μL of blood. The DNA extracted by the GenoPrep kits is highly purified. If a DNA sample was isolated with a different extraction method, repeat the extraction with the GenoPrep kits by using diluted DNA which is adjusted to 350 μL with $ddH_2O$. If degradation or poor-quality DNA is suspected, increase the amount of Taq (50 % more) and reduce DNA volume.
2. A sample contamination may lead to failure to yield an HLA typing result.
3. The differences between Lifecodes and LabType are the amplification policy (asymmetric PCR vs. regular PCR) and the availability of ready-to-use mixtures and the amplification conditions; the number of probes is also currently different.
4. Pipetting errors owing to poor homogenization of reagents (master mix) may result in reaction failures (low MFI for the control probes). This can be avoided by prewarming the master mix at 37 °C for 5 min.
5. Poor-quality Taq polymerase may result in reaction failures. Use only recombinant Taq.
6. Before adding to the amplification mix the Taq polymerase gently to protect from denaturation (mix by low-speed vortex or by flicking the tube with fingers).
7. Before proceeding to hybridization, check sample amplification by gel electrophoresis.
8. PCR program errors, temperature failures, and poor contact with the PCR block may lead to multiple SSO failures. Perform gel electrophoresis to be sure of sample amplification.
9. For LabType SSO, there is a separate 10-min denaturation/neutralization step prior to hybridization that is applied by the addition of denaturation buffer and neutralization buffers, respectively.

10. For LabType SSO, the hybridization conditions are different. There are three wash steps prior to labeling with SA–PE and one wash step after labeling in order to eliminate unbound probes.
11. A probe mix that is not suspended thoroughly may lead to low bead counts and, as a result, interpretation failures.
12. The eRES kits require two wells per sample, one for the standard probe mix and one for eRES probe mix.
13. Poor-quality tubes/pipet tips may lead to the adhesion of the beads to their surface and may cause too low bead counts.
14. Evaporation during hybridization may lead to random failures in various samples within a batch or batches. In situations in which partial use of plates is planned, keep one row empty on each side of the samples to allow space for tight sealing. Layer a silicone pad over the sealing tape to prevent evaporation.
15. Warm DS at 45 °C for 5 min upon arrival. Before the labeling, warm the DS to room temperature, vortex, and store at room temperature until pipetting. DS/SA–PE mixture must be protected from light.
16. Do not cancel hybridization program before removing the tray from the thermal cycler.
17. If more than two probes are indeterminate, repeat the assay. If less than two probes are indeterminate, analyze the sample with the probe as negative and repeat with the probe as positive.
    (a) One of the choices provides a match, continue to the next step.
    (b) Both choices provide matches, reassay the sample.
    (c) Neither choices produce a match, check for the other possible incorrectly assigned probes, check for an amplification failure, and repeat the assay.

## References

1. Blasczyk R (1998) New HLA typing methods. In: Huhn D (ed) New diagnostic methods in oncology and hematology. Springer, Berlin, pp 143–195
2. Saiki RK, Bugawan TL, Horn GT, Mullis KB, Erlich HA (1986) Analysis of enzymatically amplified beta globin and HLA-DQ alpha DNA with allele specific oligonucleotide probes. Nature 324:163–166
3. Kostyu DD, Pfohl J, Ward FE, Lee J, Murray A, Amos DB (1993) Rapid HLA-DR oligotyping by an enzyme-linked immunosorbent assay performed in microtiter trays. Hum Immunol 38:148–158
4. Olerup O, Zetterquist H (1992) HLA-DRB1*01 subtyping by allele specific pcr amplification: a sensitive, specific and rapid technique. Tissue Antigens 37:197–204
5. Bugawan TL, Apple R, Erlich HA (1994) A method for typing polymorphism at the HLA-A Locus using PCR amplification and immobilized oligonucleotide probes. Tissue Antigens 44:137–147
6. Middleton D, Williams F, Cullen C, Mallon E (1995) Modification of an HLA-B PCR-SSOP typing system leading to improved allele determination. Tissue Antigens 45:232–236
7. Kennedy LJ, Poulton KV, Dyer PA, Ollier WE, Thomson W (1995) Definition of HLA-C alleles using sequence specific oligonucleotide probes (PCR-SSOP). Tissue Antigens 46: 187–195

8. Cereb N, Maye P, Lee S, Kong Y, Yang SY (1995) Locus specific amplification of HLA Class I genes from genomic DNA: locus specific sequences in the first and third introns of HLA-A, -B and -C, alleles. Tissue Antigens 45: 1–11
9. Robinson J, Malik, Parham P, Bodmer JG, Marsh SGE (2000) IMGT/HLA database a sequence database for the human major histocompatibility complex. Tissue Antigens 55: 280–287
10. Erlich H (2012) HLA-EDNA typing: past, present and future. Tissue Antigens 80:1–11
11. Wu YY, Csako G (2006) Rapid and/or high throughput genotyping for human red blood cell, platelet, and leukocyte antigens, and forensic applications. Clin Chim Acta 363: 165–176
12. Dunbar AS (2006) Applications of Luminex® MAP technology for rapid, high throughput multiplexed nucleic acid detection. Clin Chim Acta 363:71–82
13. Fulton RJ, McDade RL, Smith PL, Kienker LJ, Kettman JR Jr (1997) Advanced multiplexed analysis with FlowMetrix system. Clin Chem 43:1749–1756

# Chapter 7

# Sequence-Based Typing of HLA: An Improved Group-Specific Full-Length Gene Sequencing Approach

**Christina E.M. Voorter, Fausto Palusci, and Marcel G.J. Tilanus**

## Abstract

Matching for HLA at the allele level is crucial for stem cell transplantation. The golden standard approach for allele definition of full gene polymorphism, the so-called high-resolution HLA typing, is sequence-based typing (SBT). Although the majority of the polymorphism for class I is located in exons 2 and 3 and for class II in exon 2, for allele definition it is necessary to unravel the complete coding and intron sequences leading to an ultrahigh HLA typing resolution at the allele level, i.e., a full-length gene polymorphism identification.

This chapter describes our recently developed SBT method for HLA-A, -B, -C, and -DQB1, that is based on full-length hemizygous Sanger sequencing of the alleles, separated by group-specific amplification using the low-resolution typing result as reference starting point. Group-specific amplification has already been established for DRB. This method enables a cost-efficient, user-friendly SBT approach resulting in a timely unambiguous HLA typing to an ultrahigh resolution level with minimal hands-on time.

**Key words** Sequence-based typing, Human leukocyte antigen, HLA class I, HLA class II, Full-length HLA gene polymorphism, Group-specific sequencing, Unambiguous HLA typing

## 1 Introduction

The human leukocyte antigen (HLA) is one of the most polymorphic gene systems present in the human genome. The function of HLA molecules to eliminate foreign intruders is complicating transplantation. For stem cell transplantation matching of HLA-A, -B, -C, -DRB1, and -DQB1 at the allele level is determined as crucial [1, 2]. Furthermore, recent studies have shown that also DPA1 and DPB1 matching might play an important role in correct engraftment of donor stem cells [3–5], based on cellular reactivity in response to permissible and non-permissible mismatches. Also in cord blood transplantation high-resolution allele definition is relevant for at least HLA-DRB1 [6], and the need for high-resolution allele

Meral Beksaç (ed.), *Bone Marrow and Stem Cell Transplantation*, Methods in Molecular Biology, vol. 1109,
DOI 10.1007/978-1-4614-9437-9_7, 

identification for other loci is currently evaluated. In disease association, drug hypersensitivity association, and HLA antibody studies the identification of epitopes rather than alleles becomes more and more predictive for the associations with diseases and specificity of the HLA antibodies [7–10].

Due to the high polymorphism of HLA, the golden standard for typing at the allele level has been and still is sequence-based typing (SBT). Sequencing determines the full nucleotide sequence of the alleles present [11]. Although the clinical relevance of polymorphism outside the peptide-binding groove is under discussion, it is clear that allele definition depends on the full-gene polymorphism and the so-called ultrahigh-resolution typing results [12]. Although exons 2 and 3 have a high polymorphic index, at least exons 1, 4, and 5 of class I show high polymorphic indexes as well (M. Groeneweg, personal communication) based on IMGT 3.9.0.

Since 1990 the HLA SBT method has evolved from sequencing only exons 2 and 3 for class I and exon 2 for class II, using amplification primers that were already located in the exons of interest, to sequencing all exons needed using primers located in the introns [13–21]. However, with the increasing number of HLA alleles identified [22], also the number of ambiguities increased using the heterozygous way of sequencing.

Three different types of ambiguities can occur: a genotype ambiguity, an allele ambiguity, and ambiguities that occur from allele combinations with unknown parts of the allele sequences.

A genotypic ambiguity includes a combination of two alleles that has an identical heterozygous sequence to another or more combinations of two alleles. For instance the sequence of HLA-A*23:01 with A*24:03 is identical to the sequence of HLA-A*23:04 with A*24:02 (IMGT/HLA database, [22]). For resolving this kind of ambiguity the cis–trans location of the nucleotides involved needs to be identified. An allelic ambiguity includes an HLA class I allele that has an exon 2 and 3 sequence identical to another HLA class I allele or a class II allele that has an exon 2 sequence identical to another class II allele; the difference between the alleles is located outside of these exons. For example the exon 2 and 3 sequence of HLA-A*02:01:01 is identical to A*02:09, A*02:43N, and 19 other HLA-A*02 alleles. To resolve these ambiguities other exons need to be sequenced. A third type of ambiguity occurs when the sequence of an allele is not completely known, and this can be resolved by identifying the complete genomic sequence of the allele.

In 2008–2009 the percentage of ambiguities found in our laboratory by heterozygous SBT was 66 % for HLA-A, 71 % for HLA-B, and 58 % for HLA-C. In all these cases additional sequencing was needed to obtain an unambiguous result. Null alleles often are identified by polymorphism in introns, for instance by defining

alternative splice sites. Full sequence characterization adds to the understanding of the mechanisms that lead to null alleles [23].

Next-generation sequencing (NGS) methods have been a promising tool for sequencing whole genomes. Detailed reviews have been recently published [24–26]. Since it is based on emulsion PCR with only one sequence being present per bead, alleles will be separated if different alleles are present. Therefore, this method has been thought to give the solution for the increasing list of ambiguities obtained with heterozygous sequencing of HLA. Although the method has been used [27, 28] there are some major drawbacks. The individual length of sequence that can be obtained with NGS is limited; thus, either overlapping sequences (using shotgun library method) or different PCR reactions (using the amplicon method) are needed to obtain a complete gene. Since the polymorphism of HLA originated evolutionarily by gene amplification, inter-allelic and intergenic recombinations, point mutations, deletions, and insertions [29], resulting in different combinations of existing sequence motifs, both methods (shotgun library and amplicon method) have the possibility of connecting the wrong sequences to each other, resulting in a different allele. Furthermore, another drawback of NGS is the long turnaround time, before individual results can be analyzed. Due to these two drawbacks, NGS is less suitable for HLA typing in routine diagnostics and patient care.

In this chapter we describe our recently developed unambiguous SBT Sanger method for HLA-A, -B, -C, and -DQB1 typing, based on group-specific amplification and sequencing of full-length HLA genes, using the low-resolution typing result as reference starting point. The method has been validated, using selected samples covering all different allele groups as available, and has been implemented since 2011 in the routine laboratory diagnostic setting. With this improved method, ambiguities were reduced to 4.4 % for HLA-A, 4.4 % for HLA-B, and 0 % for HLA-C. Current available analysis software can be used once individual sequence analysis for one sample can be combined into an allele assignment as applicable with SeqPilot (JSI medical systems, Kirpenstein). Other analysis software mostly is adjusted on the industrial SBT kits available [30]. Furthermore, an approach for HLA-DRB1 and -DRB345 is being developed to simultaneously amplify exons 2, 3, and 4. Our individual group-specific DRB1 and DRB345 strategy with separately amplifying the exons is still full applicable and routinely used [15, 31].

Overall, the method described here enables a cost-efficient, user-friendly SBT approach resulting in a timely unambiguous HLA typing to an ultrahigh-resolution level with minimal hands on time.

## 2 Materials

### 2.1 Reagents

#### 2.1.1 Amplification and Sequencing

1. Expand High Fidelity PCR kit (Roche, 11759078001), containing 10× Expand High Fidelity buffer (including 15 mM $MgCl_2$) and Expand High Fidelity enzyme mix, store at temperatures between −15 and −25 °C.
2. HLA-A, -B, -C, and -DQB1 group-specific amplification mixes will be provided with the Maastricht SBT reagents (*see* **Note 1**).
3. HLA-A, -B, -C, and -DQB1 generic and specific sequencing primers for the different exons will be provided with the Maastricht SBT reagents.
4. ExoSAP-IT (USB corporation, 78202), store at −20 °C.
5. BigDye Terminator v1.1 Cycle Sequencing kit (Applied Biosystems, 4337451) consisting of:
   - 5× BigDye Terminator v1.1/3.1 sequencing buffer, store at 2–8 °C.
   - BigDye Terminator v1.1 cycle sequencing mix RR-2500 (BDT) in 2.5× sequencing buffer, store at temperatures between −15 and −25 °C.
6. 10× 3730 buffer with EDTA (Applied Biosystems, 4335613), store at 2–8 °C, prepare 1× solution daily by adding 16 mL of buffer to 144 mL MilliQ water.
7. POP-7 (Performance optimized polymer) (Applied Biosystems, 4332241), store at 2–8 °C, change weekly.
8. Sephadex G50 DNA grade (GE Healthcare, 17-0573-02), store at room temperature.
9. Aqua Dest (Braun, 756030599), store at RT.

Reagents 6 and 7 are specifically for sequencing with a 3730 automated DNA analyzer; for other analyzers different reagents might be needed.

#### 2.1.2 Agarose Gel Electrophoresis

1. Agarose electrophoresis grade (Invitrogen, 16500100). Store at room temperature (RT).
2. 10× TBE buffer (Invitrogen, 15581044), dilute 20× with MilliQ to obtain 0.5× TBE, store at RT.
3. Ethidium Bromide (Fluka Biochemika, 46067), 10 mg/mL in water, store at 2–8 °C.
4. 500 bp molecular ruler (Biorad 170–8203), dilute 20 μL DNA marker with 80 μL Aqua Dest and 20 μL loading buffer (dissolve in 10 mL AD 100 mg Orange G, 10 mg SDS, 200 μL 0.5 M EDTA, 500 μL 1 M Tris–HCl pH 8.0, 1 g Ficoll 400, add 6 mL glycerol and Aqua Dest to a final volume of 20 mL). Store at 4 °C for max. 1 year.

### 2.2 Laboratory Design

The PCR setup (Subheading 3.1) must be performed in a pre-PCR laboratory, preferably in a biohazard, with dedicated equipment, pipettes, and disposables. Amplification to obtain the template for sequencing and all further steps (Subheadings 3.2–3.8) are performed in a post-PCR lab, including the PCR machines.

### 2.3 Equipment (Apparatus and Software)

#### 2.3.1 Amplification and Sequencing Reaction

1. 96-well Optical Reaction plate with barcode (Applied Biosystems, 4306737).
2. 3730 Trayholder (Applied Biosystems, 4334869 and 4334873).
3. Septa overlay 96 well (Applied Biosystems, 4315933).
4. Multiscreen column loader 45 μL (Millipore, MACL09645).
5. Multiscreen HV filterplate (Millipore, MAHVN4550).
6. Multiscreen column loader scraper (Millipore, MACL0SC03).
7. Multiscreen centrifuge alignment frame (Millipore, MACF09604).
8. Vortex.
9. Centrifuge with swing bucket rotor for 96-well microplate.
10. Micropipettes for the appropriate volumes.
11. Pipette tips.
12. 1.5 mL microfuge tubes (sterile).
13. PCR tubes and trays (sterile).
14. Thermocycler.
15. 3730 DNA analyzer (Applied Biosystems) or other automated DNA analyzers able to detect the BigDye Terminator-labelled nucleotides and to read lengths of approximately 500 bp with data collection software.
16. Software SeqPilot (JSI medisys).
17. Optional: Biohazard.

Equipment 1, 2, and 3 are specifically for sequencing with a 3730 automated DNA analyzer; for other analyzers different equipment might be needed.

#### 2.3.2 Agarose Gel Electrophoresis

1. Gel electrophoresis system (e.g., Biorad), including gel tray and combs.
2. Microgram scale.
3. 50 °C water bath.
4. Electrophoresis power supply.
5. UV transilluminator (e.g., Geldoc system, Biorad).

## 3 Methods

For unambiguous HLA class I typing the HLA-A, -B, and -C genes are amplified using group-specific primers located in the 5′ UT and 3′ UT region or intron 7 (*see* **Note 2**). For HLA-DQB1 typing,

exons 2 and 3 are amplified, using group-specific primers located in intron 1 and intron 3 or exon 4. The low-resolution typing result is used as starting point to determine which primer mixes need to be used. The HLA-A alleles were clustered into 8 groups, for HLA-B 15 different groups were distinguished, for HLA-C 13 groups were distinguished, and HLA-DQB1 alleles were clustered into 5 different groups. Furthermore, also gene-specific primer mixes are available for heterozygous amplification and sequencing for those individuals that show homozygosity at the low-resolution level to confirm this homozygosity with SBT. After amplification, the PCR products can be analyzed by agarose gel electrophoresis to determine the quality and quantity (*see* **Note 3**). PCR amplicons are purified by ExoSAP treatment to remove excess amplification primers and dNTPs that can disturb in the sequencing process. For cycle sequencing with dye terminator chemistry, different generic sequencing primers are available for all exons and intervening introns, resulting in a full-length sequence. The sequencing reaction products are purified before capillary electrophoresis on an automated DNA analyzer. The sequences obtained are analyzed using the SeqPilot software program (*see* **Note 4**), enabling analysis of both hemizygous sequences simultaneously. Due to the hemizygosity of the sequences the manual analysis time has been 10–15× reduced compared to heterozygous sequencing and analysis is suitable for automation.

### *3.1 Preparing Sequencing Template (Amplification)*

1. Provide a clean work environment, e.g., a biohazard. Keep the reaction mixes on ice throughout the entire protocol.
2. Transfer PCR tubes with the HLA-A, -B, -C, and -DQB1 mixes, according to the low-resolution typing of the individual, to a PCR tray, centrifuge briefly, and put on ice. Include appropriate negative controls.
3. Calculate the total number of reactions, and prepare an enzyme/water dilution, using 0.4 μL Expand High Fidelity enzyme mix with 2.6 μL Aqua Dest per reaction.
4. Add 3 μL of DNA (at a concentration of 100 ng/μL) per PCR tube.
5. Add 3 μL of enzyme/water dilution per PCR tube, and close tubes either by a lid or a rubber overlay.
6. Centrifuge PCR tray (pulse centrifugation until reaching 1,000 × *g*).
7. Move the PCR tray directly to the PCR thermocycler (in post-PCR lab).
8. Run PCR program:

   2 min 94 °C.

   7 min 68 °C Hold on 4 °C.

| | |
|---|---|
| 10 Cycles | 15 s 94 °C<br>30 s 63 °C<br>4 min 68 °C |
| 10 Cycles | 15 s 94 °C<br>30 s 60 °C<br>6 min 68 °C |
| 10 Cycles | 15 s 94 °C<br>30 s 60 °C<br>10 min 68 °C |

9. After the PCR reaction, 1–2 μL of the PCR products can be checked by agarose gel electrophoresis according to the protocol in Subheading 3.2. Store PCR tray at 2–8 °C overnight or at −25 to −35 °C for max. 1 month.

### 3.2 Agarose Gel Electrophoresis

1. Transfer 200 mL of 0.5× TBE to an Erlenmeyer, add 1.6 g agarose, and mix.
2. Transfer the Erlenmeyer with TBE and agarose to a microwave and boil until the agarose is fully solved (*see* **Note 5**).
3. Cool the solvent to ca. 50 °C by holding the Erlenmeyer under cold running water, swirling the Erlenmeyer to obtain an even temperature and to prevent partial solidification of the gel.
4. Put the Erlenmeyer covered with parafilm in a 50 °C water bath for a minimum of 10 min (*see* **Note 6**).
5. Add 10 μL ethidium bromide (final concentration 0.5 μg/mL), swirl the Erlenmeyer, and pour the gel solvent in a gel tray. Discard the air bubbles, and put combs in the gel.
6. Leave the gel for a minimum of 10 min at RT to solidify, followed by approximately 30 min at 4 °C.
7. Put sufficient 0.5× TBE buffer in the gel electrophoresis system and add 20 μL ethidium bromide (the gel must be completely covered by buffer).
8. Remove the combs from the gel tray, and put the gel tray in the electrophoresis system.
9. Take the PCR tray out of the thermocycler, and centrifuge the tray (pulse centrifugation until reaching 1,000 × *g*).
10. Load 1–2 μL of each PCR product in each lane of the gel and 10 μL of 500 bp molecular ruler (size marker) in one lane.
11. Close the electrophoresis lid, and run the gel for 3 h at 10 V/cm.

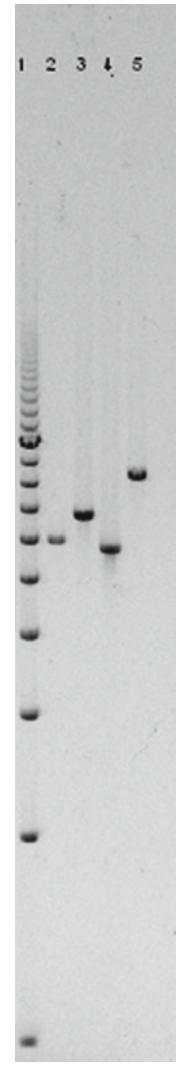


**Fig. 1** Example of agarose gel electrophoresis pattern for PCR products of HLA-A (*lane 2*), -B (*lane 3*), -C (*lane 4*), and -DQB1 (*lane 5*). 1 μL of PCR product was applied to a 0.8 % agarose gel and run for 3 h at 10 V/cm. The approximate length of the PCR products can be determined by comparison with the 500 bp marker (*lane 1*)

12. Following electrophoresis transfer the gel to a Geldoc system to visualize the ethidium bromide-stained bands under UV light. An example is shown in Fig. 1. The length of the PCR product depends on the alleles present and the primer mixes used. For HLA-A the length of the PCR products varies between 2.9 and 3.2 kb, for HLA-B between 2.8 and 3.8 kb, for HLA-C between 2.8 and 3.3 kb, and for HLA-DQB1 between 3.5 and 4.2 kb. The band intensity must be sufficient to obtain reliable sequencing patterns.

### 3.3 Purification of Sequencing Template

1. All steps need to be performed on ice. Pipette 1 part ExoSAP-IT and 2.5 parts PCR product in a PCR tube (e.g., 4 μL ExoSAP-IT and 10 μL of PCR product) and mix well with the pipette. Close tubes either by a lid or a rubber overlay.
2. Transfer the PCR tubes to the PCR thermocycler.
3. Run PCR program:

   15 min 37 °C.
   15 min 80 °C.
   Hold on 4 °C (*see* **Note 7**).

### 3.4 Sequencing Reaction

1. Prepare the sequencing mixes on ice; per sequencing primer one mix has to be prepared:

| | |
|---|---|
| Per reaction | 1.0 μL BDT sequencing mix (*see* **Note 8**) |
| | 1.5 μL BDT sequencing buffer (5×) |
| | 0.5 μL sequencing primer (5 pmol) |
| | 6.0 μL Aqua Dest |
| | 9.0 μL total volume |

2. Pipette 9 μL sequencing mix in a new PCR tube on ice and add 1 μL purified PCR product, mix well, and close tubes either by a lid or a rubber overlay.
3. Transfer the tubes to a PCR thermocycler.
4. Run PCR program:

| | |
|---|---|
| | 1 min 96 °C |
| 25 cycles | 10 s 96 °C |
| | 5 s 50 °C |
| | 4 min 60 °C |

   Hold on 4 °C

### 3.5 Purification of Sequencing Reaction Products

1. Following the sequencing reaction, purify the products by separation on Sephadex G50 columns (other purification methods to remove fluorescently labelled ddNTPs can be used).
2. Fill the Multiscreen column loader with Sephadex G50 powder using the multiscreen column loader scraper. Place an empty Multiscreen HV filterplate upside down on the column loader, turn around, and gently tap the Sephadex powder into the filter plate.
3. Pipette 300 μL Milli-Q water in each Sephadex-filled well of the filter plate.

4. Wrap the plate with parafilm and close with the lid. Leave the plate 3 h at room temperature before use (*see* **Note 9**).
5. Remove the parafilm, and centrifuge the plate for 5 min at 1,000 × *g* to remove the water, using the multiscreen centrifuge alignment frame and an empty waste plate underneath.
6. Add 20 μL of MilliQ water to the sequencing reaction products. Bring the total of 30 μL onto the Sephadex columns in the filter plate.
7. Use an empty 96-well optical reaction plate for the sequencer to put underneath the Sephadex filter plate. Centrifuge this combination for 5 min at 1,000 × *g*. The sequencing reaction products are now purified in the 96-well optical reaction plate.

### 3.6 Capillary Electrophoresis

The purified sequencing reaction products can be analyzed by any automated DNA sequencer that is able to detect the BigDye Terminator-labelled nucleotides and able to read lengths of approximately 500 bp.

For running the sequencing reaction products on a 3730 DNA analyzer, overlay the 96-well optical reaction plate (with the sequencing reaction products) with a septa overlay and place the plate into the tray holder. Place this combination in the 3730 DNA analyzer (*see* **Note 10**). Capillary electrophoresis is performed using 50 cm capillaries, POP7 (*see* **Note 11**), and the following conditions:

| | |
|---|---|
| Oven temperature | 60 °C |
| Prerun voltage | 15.0 KV |
| Prerun time | 180 s |
| Injection voltage | 1.5 V |
| Injection time | 15 s |
| First readout time | 300 ms |
| Second readout time | 300 ms |
| Run voltage | 8.5 KV |
| Voltage number of steps | 40 steps |
| Voltage step interval | 15 s |
| Voltage tolerance | 0.6 KV |
| Current stability | 30.0 μA |
| Ramp delay | 600 s |
| Data delay | 405 s |
| Run time | 5,640 s |

### 3.7 Analysis of Results

The sequence output is analyzed by the software SeqPilot or equivalents (*see* **Note 4**). Sequencing is always performed in the forward and reverse direction. An example of analysis of HLA-A is illustrated in Fig. 2. The quality of sequence data should be assessed by trained laboratory personnel to exclude those sequences that cannot be interpreted reliably. However, due to hemizygosity of sequences, background noise and poor separation of peaks will be less interfering with correct allele assignment, and the necessity for editing the sequence is drastically reduced.

## 4 Notes

1. Details of the group-specific and sequencing-defined primers are available on request, after signing a nondisclosure agreement. Enrolment in the user group for training and evaluation for this approach is still possible. Contact Dr. Christien Voorter for more information.
2. The procedure and reagents described here are owned by Maastricht University Medical Center+ (MUMC), Department of Transplantation Immunology, and are available after CE certification.
3. This step can be omitted in experienced laboratories.
4. SeqPilot is the only analysis software that is able to assign both hemizygous allele sequences of one sample simultaneously. With other programs (Assign, U-type) the hemizygous sequence of one allele is analyzed separately from the other allele.
5. It is important to boil long enough until all agarose particles are fully dissolved in the TBE buffer.
6. The temperature of the gel mixture must not exceed 60 °C when ethidium bromide is added, because at this temperature the ethidium bromide will be destroyed.
7. The purified PCR product can be stored for a maximum of 1 week at 4 °C.
8. BDT contains fluorescently labelled ddNTPs; keep the reagent in the dark as much as possible.
9. The Sephadex plate can be stored at 4 °C (after 3 h at room temperature) for a maximum of 1 week.
10. A sequencing standard can be run to check for any inconsistencies during the capillary electrophoresis and analysis procedure.
11. The POP7 solution has to be changed every week. Water, waste, and buffer are prepared fresh each day.

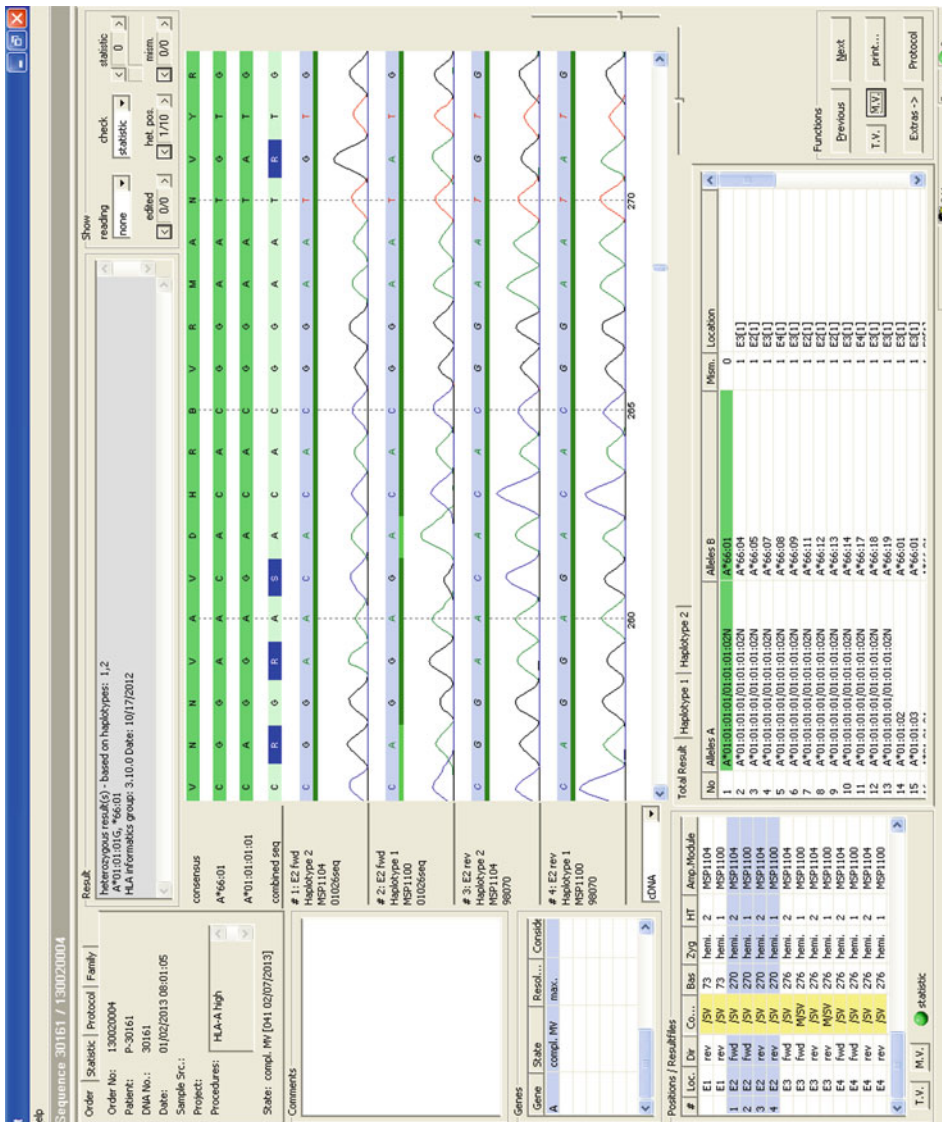


**Fig. 2** Example of simultaneous analysis of the hemizygous sequences of the two alleles. Each exon was sequenced forward and reverse for each allele. The HLA-A*01:01:01:02N was excluded by sequencing intron 2. Although the introns were sequenced as well, the software programs for analysis are not yet able to take this sequence into account due to the limited information available. Due to the hemizygosity of the sequences, the allele calling was unambiguous. If heterozygous sequencing was performed, the result would include five different allele combinations (see IMGT database [22])

## Acknowledgments

The co-workers of the department are acknowledged for successfully introducing this validated SBT approach in routine diagnostics. The authors thank Diana van Bakel for her excellent secretarial assistance and Mathijs Groeneweg for the polymorphic index information.

### References

1. Lee SJ, Klein J, Haagenson M et al (2007) High-resolution donor-recipient HLA matching contributes to the success of unrelated donor marrow transplantation. Blood 110: 4576–4583
2. Petersdorf EW (2008) Optimal HLA matching in hematopoietic cell transplantation. Curr Opin Immunol 20:588–593
3. Crocchiolo R, Zino E, Vago L et al (2009) Nonpermissive HLA-DPB1 disparity is a significant independent risk factor for mortality after unrelated hematopoietic stem cell transplantation. Blood 114:1437–1444
4. Fleischhauer K, Shaw BE, Gooley T et al (2012) Effect of T-cell-epitope matching at HLA-DPB1 in recipients of unrelated-donor haemopoietic-cell transplantation: a retrospective study. Lancet Oncol 13:366–374
5. Hollenbach JA, Madbouly A, Gragert L et al (2012) A combined DPA1~DPB1 amino acid epitope is the primary unit of selection on the HLA-DP heterodimer. Immunogenetics 64:559–569
6. Spellman SR, Eapen M, Logan BR et al (2012) A perspective on the selection of unrelated donors and cord blood units for transplantation. Blood 120:259–265
7. Amicosante M, Sanarico N, Berretta F et al (2001) Beryllium binding to HLA-DP molecule carrying the marker of susceptibility to berylliosis glutamate. Hum Immunol 62:686–693
8. Billen EV, Christiaans MH, Doxiadis II et al (2010) HLA-DP antibodies before and after renal transplantation. Tissue Antigens 75:278–285
9. Illing PT, Vivian JP, Dudek NL et al (2012) Immune self-reactivity triggered by drug-modified HLA-peptide repertoire. Nature 486:1–7
10. Sollid LM, Qiao SW, Anderson RP et al (2012) Nomenclature and listing of celiac disease relevant gluten T-cell epitopes restricted by HLA-DQ molecules. Immunogenetics 64: 455–460
11. Smith L, Fidler S (2010) HLA typing technologies. In: Mehra N (ed) The HLA complex in biology and medicine. Jaypee Brothers Medical Publishers Ltd, New Delhi, pp 175–187
12. Voorter CEM, Meertens C, Palusci F et al (2012) Rare HLA alleles within the CWD groups redefined by a new SBT typing strategy. Hum Immunol 79:545
13. McGinnis MD, Conrad MP, Bouwens AGM et al (1995) Automated, solid-phase sequencing of DRB region genes using T7 sequencing chemistry and dye-labeled primers. Tissue Antigens 46:173–179
14. Versluis LF, Rozemuller E, Tonks S et al (1993) High-resolution HLA-DPB typing based upon computerized analysis of data obtained by fluorescent sequencing of the amplified polymorphic exon 2. Hum Immunol 38:277–283
15. Voorter CEM, Rozemuller EH, de Bruyn-Geraets D et al (1997) Comparison of DRB sequence-based typing using different strategies. Tissue Antigens 49:471–476
16. Scheltinga SA, Johnston-Dow LA, White CB et al (1997) A generic sequencing based typing approach for the identification of HLA-A diversity. Hum Immunol 57:120–128
17. Tilanus MGJ, Eliaou JF (1997) HLA sequencing based typing. In: Charron D (ed) Genetic diversity of HLA: functional and medical implications. EDK Press, Paris, pp 237–266
18. Voorter CEM, Kik MC, Van den Berg-Loonen EM (1998) High-resolution HLA typing for the DQB1 gene by sequence-based typing. Tissue Antigens 51:80–87
19. van der Vlies SA, Voorter CEM, van den Berg-Loonen EM (1999) There is more to HLA-C than exons 2 and 3: sequencing of exons 1, 4 and 5. Tissue Antigens 54:169–177
20. Swelsen WTN, Voorter CEM, van den Berg-Loonen EM (2002) Sequence analysis of exons 1, 2, 3, 4 and 5 of the HLA-B5/35 cross-reacting group. Tissue Antigens 60:224–234
21. Swelsen WTN, Voorter CEM, van den Berg-Loonen EM (2004) Ambiguities of human leukocyte antigen-B resolved by sequence-based typing of exons 1, 4 and 5. Tissue Antigens 63:248–254
22. Robinson J, Halliwell JA, McWilliam H et al (2013) The IMGT/HLA database. Nucleic Acids Res 41:D1222–D1227

23. Reinders J, Rozemuller EH, Otten HG et al (2005) Identification of HLA-A*0111N: a synonymous substitution, introducing an alternative splice site in exon 3, silenced the expression of an HLA-A allele. Hum Immunol 66: 912–920
24. Erlich H (2012) HLA DNA typing: past, present, and future. Tissue Antigens 80:1–11
25. De Santis D, Dinauer D, Duke J et al (2013) 16(th) IHIW: review of HLA typing by NGS. Int J Immunogenet 40:72–76
26. Smith LK (2012) HLA typing by direct DNA sequencing. In: Christiansen F, Tait B (eds) Immunogenetics—methods and applications in clinical practice: methods in molecular biology. Humana, New York, pp 67–86
27. Bentley G, Higuchi R, Hoglund B et al (2009) High-resolution, high-throughput HLA genotyping by next-generation sequencing. Tissue Antigens 74:393–403
28. Lind C, Ferriola D, Mackiewicz K et al (2010) Next-generation sequencing: the solution for high-resolution, unambiguous human leukocyte antigen typing. Hum Immunol 71: 1033–1042
29. Parham P, Adams EJ, Arnett KL (1995) The origins of HLA-A, B, C polymorphism. Immunol Rev 143:141–180
30. Dunn PP (2011) Human leucocyte antigen typing: techniques and technology, a critical appraisal. Int J Immunogenet 38:463–473
31. Voorter CEM, de Bruyn-Geraets D, van den Berg-Loonen EM (1997) High-resolution HLA typing for the DRB3/4/5 genes by sequence-based typing. Tissue Antigens 50: 283–290

# Chapter 8

# Molecular Typing Methods for Minor Histocompatibility Antigens

Eric Spierings

## Abstract

Minor histocompatibility (H) antigen mismatching leads to clinically relevant alloimmune reactivity. Depending on the tissue expression pattern of the involved minor H antigens, the immune response may either cause graft-versus-host disease and a graft-versus-tumor effect or lead to only a graft-versus-leukemia effect. Thus, identification of recipient–donor pairs with minor H antigen mismatches has clinical importance. This chapter describes molecular typing methods for molecular typing of minor H antigens.

**Key words** Minor histocompatibility antigens, Transplantation, Stem cells, Solid organ, Graft-versus-host, Graft-versus-tumor, Graft rejection, Genotyping

## 1 Introduction

Minor histocompatibility (H) antigens have been defined as immunogenic peptides derived from polymorphic intracellular proteins and presented on the cell surface by MHC class I and class II molecules [1]. They induce human leukocyte antigen (HLA)-restricted T cell responses in the setting of HLA-matched stem cell transplantation (SCT). Minor H antigens have to be considered as key molecules in the alloimmune responses of the pathophysiology of graft-versus-host-disease (GvHD) and in the curative graft-versus-tumor (GvT) reactivity after HLA-matched SCT [2]. Minor H antigens have been shown to play a role in renal allograft tolerance; minor H antigen HA-1-specific regulatory T cells, HA-1-specific effector T cells, and HA-1 microchimerism were observed in renal allograft-tolerant recipients [3]. Interestingly, also in the physiological setting of pregnancy, minor H antigen-specific T cells could be identified in the mutual direction of mother and child [4–6]. Moreover, minor H antigen-specific antibody titers are increased in unexplained secondary recurrent

Meral Beksaç (ed.), *Bone Marrow and Stem Cell Transplantation*, Methods in Molecular Biology, vol. 1109,
DOI 10.1007/978-1-4614-9437-9_8, © Springer Science+Business Media New York 2014

miscarriage patients [7]. These increased titers are associated with low male:female ratios in subsequent live births.

The clinical usefulness of minor H antigen typing is evident in the area of SCT. As mentioned above, two clinically related components justify minor H antigen typing, i.e., GvHD and GvT. The mode of tissue expression, i.e., hematopoietic restricted or ubiquitous, of minor H antigens determines their role as target molecules in GvHD and/or GvT. The minor H antigens with ubiquitous expression including expression on the GvHD target organs are particularly relevant in the development and maintenance of GvHD. Minor H antigens with expression limited to cells of the hematopoietic system and to solid tumors are especially relevant for the GvT activity [8–10]. The latter minor H antigens can be exploited as curative tools for SCT-based immunotherapy of hematological malignancies and solid tumors. The therapeutic GvT effect of these minor H antigen disparities seems, however, to depend upon the presence of GvHD [11].

Nowadays, there are two options to exploit the differences in minor H antigen expression between donor and recipients. In both cases, HLA-matched minor H antigen-mismatched recipient/donor combinations are selected. One strategy is the adoptive transfer of in vitro-generated SCT donor-derived minor H antigen-specific CTLs. The other, more practical, and potentially efficient strategy is post-SCT "vaccination." In this concept, the relevant recipient-specific minor H peptides are administered to boost the donor-derived minor H antigen-specific T cells to achieve optimal GvT responses in vivo. Both strategies are currently ongoing in clinical phase I/II studies [2]. Although not frequently observed, minor H antigens have been shown to influence SCT graft rejection [12, 13]. In this respect, the expression of minor H antigens on the donor progenitor cells might be relevant in sensitized patients receiving a minor H antigen-disparate T cell-depleted SCT.

Minor H antigen typing is useful in the clinical-related research investigating the role of minor H antigen-specific T cells in HLA-matched solid organ transplants. The observation of coexistence of CD8+ memory T-effector and T-regulator cells, both specific for the same minor H antigen HA-1 in the context of renal allograft tolerance, validates further exploration of the relevance of minor H antigen mismatching in solid organ transplantation [3]. The relevance of minor H antigen typing recently further extended towards two types of SCT donors, i.e., the parous woman and the cord blood donor. Examination of multiparous women demonstrated that pregnancy can lead to alloimmune responses against the infant's paternal minor H antigens [4, 6]. Interestingly, a similar immunization status has been observed in cord blood samples, where minor H antigen-specific cytotoxic T cells directed at the non-inherited maternal minor H antigens could be demonstrated [5]. The minor H antigen immunization status of SCT donors raises important questions for clinical practice.

Next to minor H antigen geno- and phenotyping, quantification of the minor H antigen gene product at the RNA level may be useful. For some minor H antigens a quantitative real-time Taqman PCR method for the analysis of minor H RNA expression levels has been developed [14, 15]. Analysis of the membrane expression of minor H antigens by various cell types may be relevant. This analysis can be performed by functional assays such as cell-mediated lympholysis (CML), by growth inhibition of clonogenic normal and leukemic precursor cells (as reviewed in ref. 16), or by using the skin explant assay [17]. Tables 1 and 2 list all currently available information on the human autosomally and Y chromosome-encoded minor H genes, the immunogenic peptides they encode, and the minor H antigen tissue distribution.

In this chapter we summarize all methodologies for minor H antigen typing on the genomic and on the RNA level that have been described to date. With regard to the genomic typing, different technologies have been developed by the various laboratories.

## 2 Materials

1. 5–10 mL peripheral blood or $5–10 \times 10^6$ cells.
2. Phosphate-buffered saline (PBS).
3. Ficoll–Isopaque.
4. Reagents for DNA isolation.
5. Minor H antigen-specific oligonucleotide primers as listed.
6. Standard thin-wall PCR tubes.
7. Taq polymerase and buffers.
8. dNTPs.
9. PCR thermal cycler.
10. Real-time PCR equipment.
11. Restriction enzymes and buffers.
12. Agarose.
13. Gel electrophoresis equipment.
14. Agarose, molecular biology grade.
15. Gel Red.
16. Loading buffer (0.5 g Orange G and 40 g sucrose in 100 mL $H_2O$).
17. Tris–acetate–EDTA (TAE) buffer.
18. Exonuclease I.
19. SAP.
20. Big dye terminator (BDT) Cycle sequence kit v1.1.
21. Sephadex G-50 Superfine DNA Grade.

**Table 1**
**Autosomally encoded minor H antigens, ordered alphabetically**

| Original name | HLA restriction | Gene | Chromosome | Peptide | dbSNP | Reference |
|---|---|---|---|---|---|---|
| ACC-1 | HLA-A24 | BCL2A1 | 15 | DYLQYVLQI | rs1138357 | [43] |
| ACC-2 | HLA-B44 | BCL2A1 | 15 | KEFEDDIINW | rs3826007 | [43] |
| ACC-6 | HLA-B44 | HMSD | 18 | MEIFIEVFSHF | rs9945924 | [44] |
| C19orf48 | HLA-B7 | C19orf48 | 19 | TPNQRQNVC | rs5818907 | [45] |
| CD19 | HLA-DQA1*05/B1*02 | CD19 | 16 | RTLDKVLEV | rs2173904 | [41] |
| CTSH/A31 | HLA-A31 | CTSH | 15 | ATLPLLCAR | rs2289702 | [46] |
| CTSH/A33 | HLA-A33 | CTSH | 15 | WATLPLLCAR | rs2289702 | [46] |
| HA-1/A2 | HLA-A2 | HMHA1 | 19 | VLHDDLLEA | rs1801284 | [47] |
| HA-1/B60 | HLA-B60 | HMHA1 | 19 | KECVLHDDLL | rs1801284 | [48] |
| HA-2 | HLA-A2 | MYO1G | 7 | YIGEVLVSV | rs61739531 | [23] |
| HA-3 | HLA-A1 | AKAP13 | 15 | VTEPGTAQY | rs7162168 | [22] |
| HA-8 | HLA-A2 | KIAA0020 | 9 | RTLDKVLEV | rs2173904 | [29] |
| HB-1 | HLA-B44 | HMHB1 | 5 | EEKRGSLHVW | rs161557 | [15] |
| HEATR1 | HLA-B8 | HEATR1 | 1 | ISKERAEAL | rs2275687 | [49] |
| LB-ADIR-1 | HLA-A2 | TOR3A | 1 | SVAPALALFPA | rs2296377 | [50] |
| LB-APOBEC3B-1K | HLA-B7 | APOBEC3B | 22 | KPQYHAEMCF | rs2076109 | [42] |
| LB-ARHGDIB-1R | HLA-B7 | ARHGDIB | 12 | LPRACWREA | rs4703 | [42] |
| LB-BCAT2-1R | HLA-B7 | BCAT2 | 19 | QPRRALLFVIL | rs11548193 | [42] |
| LB-EBI3-1I | HLA-B7 | EBI3 | 19 | RPRARYYIQV | rs4740 | [42] |
| LB-ECGF-1 | HLA-B7 | TYMP | 22 | RPHAIRRPLAL | n.a. | [42] |

| | | | | | | |
|---|---|---|---|---|---|---|
| LB-ERAP1-1R | HLA-B7 | ERAP1 | 5 | HPRQEQIALLA | rs26653 | [42] |
| LB-GEMIN4-1V | HLA-B7 | GEMIN4 | 17 | FPALRFVEV | rs4968104 | [42] |
| LB-LY75-1K | HLA-DRB1*1301 | LY75 | 2 | GITYRNKSLM | rs12692566 | [51] |
| LB-MR1-1R | HLA-DRB3*0202 | MR1 | 1 | YFRLGVSDPIRG | rs2236410 | [51] |
| LB-MTHFD1-1Q | HLA-DRB1*0301 | MTHFD1 | 14 | SSIIADQIALKL | rs2236225 | [51] |
| LB-PDCD11-1F | HLA-B7 | PDCD11 | 10 | GPDSSKTFLCL | rs2986014 | [42] |
| LB-PI4K2B-1 | HLA-DQ6 | PI4K2B | 4 | SRSSSAELDRSR | rs313549 | [52] |
| LB-PRCP-1D | HLA-A2 | PRCP | 11 | FMWDVAEDLKA | rs2298668 | [42] |
| LB-PTK2B-1T | HLA-DRB3*0101 | PTK2B | 8 | VYMNDTSPL | rs751019 | [51] |
| LB-SSR1-1S | HLA-A2 | SSR1 | 6 | SLAVAQDLT | rs10004 | [42] |
| LB-WNK1-1I | HLA-A2 | WNK1 | 12 | RTLSPEIITV | rs12828016 | [42] |
| LRH-1 | HLA-B7 | P2RX5 | 17 | TPNQRQNVC | rs5818907 | [53] |
| PANE1 | HLA-A3 | CENPM | 22 | RVWDLPGVLK | n.a. | [54] |
| SLC1A5 | HLA-B61 | SLC1A5 | 19 | AEATANGGLAL | rs3027956 | [40] |
| SP110 | HLA-A3 | SP110 | 2 | SLPRGTSTPK | rs1365776 | [55] |
| UGT2B17 | HLA-A29/B44 | UGT2B17 | 4 | AELLNIPVLY | n.a. | [31] |
| UGT2B17 | HLA-A2 | UGT2B17 | 4 | CVATMIFMI | n.a. | [40] |
| UTA2-1 | HLA-A2 | C12orf35 | 12 | QLLNSVLTL | rs2166807 | [56] |

**Table 2**
**Y chromosome-encoded minor H antigens order by HLA restriction molecule**

| Minor H antigen | HLA restriction | Gene | Peptide | Reference |
|---|---|---|---|---|
| A1/HY | HLA-A1 | USP9Y | IVDCLTEMY | [57, 58] |
| A2/HY | HLA-A2 | KDM5D | FIDSYICQV | [59] |
| A33/HY | HLA-A33 | TMSB4Y | EVLLRPGLHFR | [60] |
| B27/HY | HLA-B27 | DDX3Y | RDSRGKPGY | [61] |
| B52/HY | HLA-B52 | RPS4Y1 | TIRYPDPVI | [62] |
| B60/HY | HLA-B60 | UTY | RESEEESVSL | [63] |
| B7/HY | HLA-B7 | KDM5D | SPSVDKARAEL | [64] |
| B8/HY | HLA-B8 | UTY | LPHNHTDL | [65] |
| DQ5/HY | HLA-DQ5 | DDX3Y | HIENFSDIDMGE | [66] |
| DR15/HY | HLA-DR15 | DDX3Y | SKGRYIPPHLR | [67] |
| DRB3*0301/HY | HLA-DRB3*0301 | RPS4Y1 | VIKVNDTVQI | [68] |

22. Sephadex 96-well matrix plate.
23. 96-wells MultiScreen filter plate (Millipore).
24. POP7 (Applied Biosystems).
25. 10× Genetic analyzer buffer with EDTA.
26. DNA size marker, ranging from 100 bp to at least 1,000 bp with a size interval of approximately 100 bp, e.g., the 1 kb+ ladder.

## 3 Methods

*The methods described below outline:*

1. The isolation of material for minor H typing.
2. Standard PCR procedures.
3. Methods for allele-specific PCR based on sequence-specific primers (SSP-PCR) for HA-1, HA-2, and HA-3.
4. PCR-RFLP for HA-1, HA-2, HA-8, and HB-1.
5. Gene-specific PCR for UGT2B17 and H-Y.
6. Real-time PCR for ACC-1 and H-Y.
7. PCR with melting curve analyses for HA-1.
8. Reference strand conformation analysis (RSCA) for HA-1.

### 3.1 Chromosomal DNA Isolation

Molecular typing for minor H antigens is preferentially performed on genomic DNA above cDNA. For cDNA, RNA has to be isolated and cDNA must be synthesized prior to the PCR amplifications. The use of RNA will require extra work and costs. Furthermore additional care has to be taken with the source of the cells used for RNA isolation since the expression of the, e.g., minor H antigens HA-1 and HB-1 can be restricted [18, 19].

All cell types are suitable for genomic DNA extraction. Furthermore genomic DNA is routinely prepared for HLA typing. Numerous kits and protocols are available for genomic DNA isolation, and they work all equally well. One should take into account that it is important that the isolated nucleic acid is free of contaminants and pure enough for PCR purposes. In most cases genomic DNA will be extracted from peripheral blood derived from peripheral blood mononuclear cells (PBMCs) isolated by Ficoll–Isopaque density gradient centrifugation. The use of reference material is strongly advised (*see* **Note 1**).

### 3.2 Polymerase Chain Reaction

Generally, a PCR mix contains a Taq polymerase, a buffer, $MgCl_2$, dNTPs, and primers. Bovine serum albumin can be included to improve performance. Since concentrations of reagents highly depend on the chosen buffers, enzymes, and methodology, the reader is referred to the original reports and the protocols of the enzyme manufacturer for detailed information. Primers, probes, and restriction enzymes used for minor H antigen typing are listed in separate tables for each methodology. Take appropriate measures to prevent contamination (*see* **Note 2**).

### 3.3 Allele-Specific SSP-PCR

SSP-PCR identifies the different alleles by using sequence-specific primers. For optimal performance, the polymorphic nucleic acid is generally located at the last 3′ position of the oligonucleotide primer. This method has been developed for the minor H antigens HA-1 [20], HA-2 [21], and HA-3 [22]. The primers for these loci are listed in Table 3. PCR amplifications are analyzed by agarose gel electrophoresis.

#### 3.3.1 HA-1 SSP-PCR

HA-1 was the first minor H antigen for which allele-specific SSP-PCR was described [20]. The two allele-specific primers, for HA-$1^H$ and HA-$1^R$, respectively, are derived from exon A of the HA-1-encoding gene KIAA0223. Polymorphic primer sets were designed both in the reverse direction (set 1) and in the forward direction (set 2) in combination with two different common primers (Table 3). Cycling condition for the HA-1 SSP-PCR are 1 cycle of 5 min at 95 °C, followed by 10 cycles of 1 min 95 °C and 1 min 65 °C, and finally 20 cycles of 95 °C for 1 min, 62 °C for 1 min, and 72 °C for 1 min. Amplification products of unknown samples are compared with individuals homozygous for either the HA-$1^H$ allele or the HA-$1^R$ allele. The product size for primer set 1 is 190 and 331 bp for set 2.

**Table 3**
**Oligonucleotide primers for allele-specific SSP-PCR**

| Minor H antigen | Allele | Forward primer | Reverse primer | Fragment size |
|---|---|---|---|---|
| HA-1 | H | CTTAAGGAGTGTGTGCTGCA | ACTCCTACACATCCCTCAGAG | 190 |
| | R | CTTAAGGAGTGTGTGTTGCG | ACTCCTACACATCCCTCAGAG | 190 |
| HA-2 | V | ACAGTCTCTGAGTGGCTCAG | GCAGCTCCTGGTAGGGGTTAAC | 271 |
| | M | ACAGTCTCTGAGTGGCTCAG | GCAGCTCCTGGTAGGGGTTAAT | 271 |
| HA-3 | M | GTCCTTCAGAGAGACTTGGGCAT | AGACTCAGCAGGTTTGTTAC | 129 |
| | T | GTCCTTCAGAGAGACTTGGGCAC | AGACTCAGCAGGTTTGTTAC | 318 |
| HA-8 | R | TGCAGTCAGCAGATCACCG | CTTCTGGGCAACAGTTATGGA | 186 |
| | P | TGCAGTCAGCAGATCACCC | CTTCTGGGCAACAGTTATGGA | 186 |
| HB-1 | Y | GCCATTCTTTTCTATAGGTTCTTTGT | AGGGCATATGTTCCACTTGCTT | 213 |
| | H | ATTCTTTTCTATAGGTTCTCTGC | AGGGCATATGTTCCACTTGCTT | 210 |
| ACC-1 | Y | CATTGCCTCAACAGCTTCAAG | GGTTGTGGTATCTGTAGGGCGT | 136 |
| | C | CATTGCCTCAACAGCTTCAAG | GGTTGTGGTATCTGTAGGGCGC | 136 |
| ACC-2 | D | GATGGAAAAGGAGTTTGAAGGCGA | CAGCCTCCGTTTTGCCTTATC | 197 |
| | G | GATGGAAAAGGAGTTTGAAGGCGG | CAGCCTCCGTTTTGCCTTATC | 197 |
| SP110 | R | AATGTGGTTTGAAGACCAAAAGT | CTTGTACTCTCATCTTACCTCC | 185 |
| | G | AATGTGGTTTGAAGACCAAAAGT | CTTGTACTCTCATCTTACCTCT | 185 |

| | | | | |
|---|---|---|---|---|
| PANE1 | R | AGGCAAGTCCCACACTCG | AATGGGGTAAATGACGTGCTG | 207 |
| | stop | CAGGCAAGTCCCACACTCA | AATGGGGTAAATGACGTGCTG1 | 207 |
| LB-ECGF | H | CCTGGCTCCGCGTGCACCG | GAGGGGGCGGCGAATGTCGT | 105 |
| | R | CCTGGCTCCGCGTGCACCG | AGGGGGCGGCGAATGGCGC | 105 |
| CTSH | R | TGCCGCTGCTCTGCGCCA | CAGAGTTCCTGGCCTCTCAC | 210 |
| | G | TGCCGCTGCTCTGCGCCG | CAGAGTTCCTGGCCTCTCAC | 210 |
| LRH1 | 5C | GCCCACACACACTCTGAGAA | ACCTGATTGTGACCCACAAC | 193 |
| | 4C | GCCCACACACACTCTGAGAA | AACCTGATTGTGACCACAAC | 193 |
| LB-ADIR | F | GCTGAAGAGCGTCCAAGTACC | GCGCCAGCTTTGGCTCTTTT | 183 |
| | S | GCTGAAGAGCGTCCAAGTACC | CGCCAGCTTTGGCTCTTTC | 183 |

#### 3.3.2 HA-2 SSP-PCR

The HA-2-encoding gene, designated as MYO1G, consists of two alleles: HA-$2^V$ and HA-$2^M$ [23]. SSP-PCR has been developed based upon the genomic sequences [21]. The PCR mix for HA-2 contains a common forward primer and polymorphic reverse primers. Cycling conditions are 1 cycle of 2 min at 95 °C, followed by 10 cycles of 1 min 95 °C and 1 min 70 °C, and finally 20 cycles of 1 min 95 °C, 1 min 67 °C, and 1 min 72 °C. Both primer combinations result in a PCR product with a size of 274 bp.

#### 3.3.3 HA-3 SSP-PCR

Genomic typing for HA-3 is based on the sequence of the Rho-GEF AKAP13 [22]. Polymorphic primers were designed at the same position within the HA-3 gene. They were, however, combined with different reverse oligonucleotides. Cycling conditions are 1 cycle of 2 min at 95 °C, followed by 10 cycles of 1 min 95 °C and 1 min 70 °C, and finally 20 cycles of 1 min 95 °C, 1 min 67 °C, and 1 min 72 °C. As a result of the use of different reverse primers, the HA-$3^T$ SSP-PCR yields a product of 129 bp, while its negative counterpart HA-$3^M$ has a size of 318 bp. Despite the fact that a single-tube analysis is still excluded by this design, misinterpretation of the results is avoided due to these differences in product size. Eventually, analysis of the PCR products on agarose gel can be performed by combining the two PCR products into one single lane.

#### 3.3.4 A Uniform Typing Methodology Using SSP-PCR

The abovementioned techniques have been merged into a single protocol, allowing typing for a large number of minor H antigens in a single PCR run [24]. The full primer set has been listed in Table 3. The PCR program used for this typing tray starts with 2 min at 94 °C, followed by 10 cycles of 10 s at 94 °C and 60 s at 65 °C. Subsequently, 20 cycles were run using the following conditions: 10 s at 94 °C, 50 s at 61 °C, and 30 s at 72 °C. Samples can be analyzed on a 2 % agarose gel.

Primers for human platelet antigen (HPA; 5′-ACCTAGATAGGTGCGAGCTCACC-3′ and 5′-CAGACTGAGCTTCTCCAGCTTGG-3′; 439 bp product) and the human growth hormone-2 (GH2; 5′-CAGTGCCTTCCCAACCATTCCCTTA-3′ and 5′-ATCCACTCACGGATTTCTGTTGTGTTTC-3; 504 bp product) can be used as an internal control, 0.125 μM each (*see* **Note 3**). To facilitate the analyses, include the HPA primers in the immunogenic amplification primer mix and the GH2 primers in the non-immunogenic primer mix.

### 3.4 Allele-Specific PCR-RFLP

The RFLP-PCR identifies point mutations [25] and polymorphisms [26] by using restriction endonucleases (*see* **Note 4**). In this methodology, the entire polymorphic region of the minor H gene is amplified by PCR first using non-polymorphic primers (Table 4). In a second step, an aliquot of the PCR products is digested with the appropriate restriction endonuclease. The products of the

**Table 4**
**Oligonucleotide primers and enzymes for allele-specific PCR-RFLP**

| Minor H antigen | Allele | Forward primer | Reverse primer | Restriction enzyme | Size |
|---|---|---|---|---|---|
| HA-1 | H | GACGTCGTCGAGGACATCTCCCATC | CTCTTGAGCCAGTGTACGCTCA | Fnu4HI | 82 + 213 |
| | | | | Tsp45I | 295 |
| | R | GACGTCGTCGAGGACATCTCCCATC | CTCTTGAGCCAGTGTACGCTCA | Fnu4HI | 295 |
| | | | | Tsp45I | 85 + 210 |
| HA-2 | V | AAGCTTTTCGAGAAGGGCCGCATCTA | GAATTCGAGATGACGATGCAGGTGTC | NlaIII or Hsp92 | 218 |
| | M | AAGCTTTTCGAGAAGGGCCGCATCTA | GAATTCGAGATGACGATGCAGGTGTC | NlaIII or Hsp92 | 163 + 55 |
| HA-8 | R | GGATATACAGCAGAGCTTTC | TCTAACACTTTGTCCCGGAATT | EcoRI | 165 + 22 |
| | P | GGATATACAGCAGAGCTTTC | TCTAACACTTTGTCCCAGAATT | EcoRI | 183 |
| HB-1 | H | GAGCCTTCTGACCTCACATC | TTGTCCCTGCTCATCCACACC | NlaIII | 99 + 135 |
| | Y | GAGCCTTCTGACCTCACATC | TTGTCCCTGCTCATCCACACC | NlaIII | 234 |

restriction digest are analyzed either by agarose gel electrophoresis or by electrophoresis on an acrylamide gel depending on the length of the resulting fragments. PCR-RFLP genomic typing of minor H antigens has been described for HA-1 [27], HA-2 [28], HA-8 [29], and HB-1 [15].

#### 3.4.1 HA-1 PCR-RFLP

HA-1 PCR-RFLP uses primers to produce a 295 bp product after PCR. Cycling conditions for the PCR are 40 cycles of 30 s 94 °C, 30 s 58 °C, and 1 min 72 °C. Products from the HA-$1^H$ allele are susceptible for cleavage by *Fnu4HI*, while the HA-$1^R$ product can be digested with *Tsp45I*. Digestions are performed at 37 °C for 2 h and analyzed by electrophoresis on 2.2 % agarose gels. Successful digestions result in fragments of 85 and 215 bp.

#### 3.4.2 HA-2 PCR-RFLP

For RFLP analysis of HA-2, a fragment with a size of 218 bp is generated by PCR. Cycle parameters are as follows: denaturation at 94 °C for 2 min; 36 cycles of denaturation at 94 °C for 1 min, annealing at 60.5 °C for 1 min, extension at 72 °C for 1 min, and final extension at 72 °C for 10 min. Samples are digested at 37 °C for 12 h with either *Hsp92 II* or *NlaIII*. The HA-$2^V$-derived sequence will not be digested under these conditions, whereas the HA-$2^M$ allele will result in fragments of 163 and 55 bp.

#### 3.4.3 HA-8 PCR-RFLP

Primers for amplifying the HA-8-encoding gene KIAA0020 have been designed to result in a 183 bp PCR product. The A at position 20 in the reverse primer has been introduced to artificially create an *EcoRI* site but only when the primer anneals to the HA-$8^R$ allele. The exact cycling conditions for amplification have not been described. PCR products are digested with *EcoRI* and analyzed on a 2.5 % agarose gel. The HA-$8^P$ polymorphism produces a single 183-bp band, whereas the HA-$8^R$ allele will result in bands of 165 and 22 bp.

#### 3.4.4 HB-1 PCR-RFLP

PCR-RFLP for HB-1 is performed on cDNA. The PCR is performed for 33 cycles (1 min at 94 °C, 1 min at 60 °C, and 1 min at 72 °C). The product has a length of 234 bp. PCR products are digested with *NlaIII* to discriminate between HB-$1^H$ and HB-$1^Y$ alleles. The *NlaIII* enzyme digests the HB-$1^Y$ allele into two fragments of 99 and 135 bp. The HB-$1^H$ allele will not be cut.

### 3.5 Gene-Specific PCR

Gene-specific PCR can be applied for the analysis of minor H antigens encoded by genes that lack a negative counterpart. For these minor H antigens the negative allele cannot be demonstrated directly. Its absence is indicated simply by a negative signal after PCR. Two minor H antigens of this type have been described.

#### 3.5.1 HY PCR

All HY minor H antigens are located on the Y chromosome Tables 2. Therefore presence of the Y chromosome implicates

**Table 5**
**Oligonucleotide primers for gene-specific PCR**

| Minor H antigen | Forward primer | Reverse primer | Size |
|---|---|---|---|
| UGT2B17 | | | |
| 5′ region | GGCAGTATCTTGCCAATGT | AGACTCCAAGTGCCAGTT | 341 |
| Exon 1a | TGTTGGGAATATTCTGACTATAA | CCCACTTCTTCAGATCATATGC | 352 |
| Exon 1b | AAATGACAGAAAGAAACAA | GCATCTTCACAGAGCTTATAT | 443 |
| Exon 6 | GAATTCATCATGATCAACCG | ACAGGCAACATTTTGTGATC | 201 |
| HY (SRY) | TGGCGATTAAGTCAAATTCGC | CCCCCTAGTACCCTGACAATGTATT | 136 |

positivity for all of the HY minor H antigens. The gene-specific PCR for HY is based on SRY [30]. Primers are identical to the ones used in the real-time PCR protocol described in Subheading 3.6.1, except for the fact that no probe is included in the procedure. Cycling conditions are 1 cycle of 2 min at 95 °C, followed by 10 cycles of 1 min 95 °C and 1 min 70 °C, and finally 20 cycles of 1 min 95 °C, 1 min 67 °C, and 1 min 72 °C. Product size for HY-positive samples is 136 bp.

#### *3.5.2 UGT2B17 PCR*

Individuals that are negative for UGT2B17 completely lack the *UGT2B17* gene on both chromosomes [31]. As a result of this, this minor H antigen resembles the HY antigens, and full genotyping cannot be performed. Three different primer sets have been designed to demonstrate the presence of at least one positive allele: two are located on exon 1, one on exon 6, and one set is designed to amplify the region 5′ to *UGT2B17*. Amplification is performed for 38 cycles for genomic DNA or cDNA synthesized from total RNA. Each cycle consists of denaturation (94 °C; 30 s), annealing (68 °C; 20 s), and elongation (72 °C; 30 s). PCR products are analyzed by electrophoresis on a 1.5 % agarose gel. The size of the PCR product depends on the selected primer set (Table 5).

### *3.6 Real-Time PCR*

The real-time PCR identifies polymorphisms by the usage of allele-specific fluorogenic hybridization probes (*see* **Note 5**). The method is based on the 5′–3′ exonuclease activity of the Taq DNA polymerase, which results in cleavage of fluorescent dye-labeled probes during PCR [32]. The hybridization probes emit a fluorescent signal that directly correlates with the amount of target sequence. Forward and reverse PCR primers and a probe, labeled with a reporter dye, e.g., FAM or VIC, and a quencher dye, e.g., TAMRA or MGB, bind to the DNA template. A 3′ phosphate

group prevents extension of the probe during PCR. The Taq polymerase enzyme enables extension of the primer displacing the probe. The displaced probe is cleaved by Taq DNA polymerase resulting in an increase in relative fluorescence of the reporter dye. The real-time PCR continuously measures the amount of hybridization probe annealing to the target sequence in every cycle.

Rapid genotyping by the real-time PCR method has been described for the detection of the alleles of ACC-1 [33] and for detection of HY [30, 34].

#### 3.6.1 ACC-1 Real-Time PCR

The fragment covering the ACC-1 polymorphic site of *BCL2A1* can be amplified by primers flanking the polymorphic region. Amplification is performed in the presence of probes complementary to the polymorphic region. These probes are labeled with a fluorescent dye and a quencher as described above. PCR cycling conditions are 95 °C for 10 min, followed by 35 cycles of 92 °C for 15 s and 60 °C for 1 min. Amplification and analyses are carried out in a real-time PCR cycler. Since two different fluorochromes are used for each allele, this assay can be performed in a single tube.

#### 3.6.2 HY Real-Time PCR

Y chromosome-specific real-time PCR was developed for measuring the concentration of fetal DNA in maternal plasma or serum [30] and for the detection of remaining male cells after sex-mismatched transplantation [34]. This methodology can also be applied for sex determination of individuals. Oligonucleotides for amplification are located on the SRY gene or the DFFRY gene, both situated on the Y chromosome. Amplification primers for SRY real-time PCR, which are identical to the gene-specific PCR primers described in Subheading 3.5.1, are combined with a dual-labeled FAM-TAMRA SRY probe containing a 3′-blocking phosphate group (Table 6). PCR is initiated with 2 min of 50 °C for uracil DNA glycosylase treatment [35] (*see* **Notes** for details), followed by 10 min of 95 °C and 40 cycles of 15 s 95 °C and 1 min 60 °C.

The described methodology to detect DFFRY is similar as for SRY. Amplification conditions were as follows: 95 °C for 2.5 min, then 30 cycles at 95 °C for 45 s, 58 °C for 30 s, and 72 °C for 1 min, followed by extension at 72 °C for 10 min.

### 3.7 PCR with Melting Curve Analysis

The PCR with melting curve analysis for HA-1 genotyping [36] uses fluorescence resonance energy transfer (FRET) occurring between two closely adjacent fluorescent oligonucleotides binding to the same strand of DNA [37]. A long oligonucleotide (5′-TTTCTCAAGGCCCTCAGCGAAGCGG-3′) is labeled with fluorescein as donor fluorophore, and the shorter one (5′-CTCTCACCGTCATGCAGCACACACTCCTT-3′) is labeled with acceptor fluorophore LightCycler Red 640 (RED640) on the adjacent sites. After binding, the fluorescein is excited by the light source of the LightCycler instrument. A part of this energy is

**Table 6**
**Oligonucleotide primers and probes for real-time PCR**

| Minor H antigen | Allele | Forward primer | Reverse primer | Probe | Size |
|---|---|---|---|---|---|
| ACC-1 | Y | ATTTACAGGCTGGCT CAGGACTA | GGACCTGATCCAGG TTGTGGTAT | CTGCAGTGCGTCCT | 65 |
| | C | ATTTACAGGCTGGCT CAGGACTA | GGACCTGATCCAGG TTGTGGTAT | TCTGCAGTACGTCCTA | 65 |
| HY (SRY) | + | TGGCGATTAAGTCAAA TTCGC | CCCCCTAGTACCCT GACAATGTATT | AGCAGTAGAGCAGTCA GGGAGGCAGA | 136 |
| HY (DFFRY) | + | AACTCACCTCCAACAC ATACTCCAC | TTCATGATGAAATCT GCTTTTTGTTT | CAGCCACCAGAATTATC TCCAAGCTCTCTGA | 84 |

transferred by FRET to RED640, which consecutively emits the measured light of a different wavelength.

Amplification with primers 5′-AGGACATCTCCCATCTG CTG-3′ and 5′-GCATTCTCTGTTTCCGTGTT-3′ is performed using the following conditions: 1 cycle of 30 s at 95 °C, followed by 40 cycles of 1 s 95 °C, 10 s 64 °C, and 20 s 72 °C. After amplification of the polymorphic region with flanking primers, melting curve analyses are executed. In this analysis, the PCR product is first denatured at 95 °C, followed by a probe annealing step at 59 °C for 15 s. Subsequently, the temperature is raised to 85 °C in steps of 0.1 °C/s. Since the RED640-labeled probe has a lower melting temperature, it will be released earlier than the fluorescein-labeled probe. This process can be measured in real time in FRET analyses. Since the RED640 probe is matched for the HA-$1^H$ allele and has two nucleotides mismatched with the HA-$1^R$ allele, the FRET signal of the HA-$1^R$ allele will show up earlier in the melting process than the HA-$1^H$ allele (67.8 °C versus 71.5 °C, respectively). Although complicated in design, this methodology allows rapid analysis in a single tube.

### 3.8 Reference Strand Conformation Analysis

The RSCA (*see* **Note 6**) uses fluorescent-labeled reference (FLR) DNA (sense strand) derived from a PCR of the locus of interest [38]. This fluorescent reference DNA is hybridized with a locus-specific PCR product from the sample to be tested. Duplexes are formed between the sense and antisense strands present in the mixture. Because only the sense strand is labeled, duplexes formed with this strand can be identified by a laser detection system after electrophoresis in an automated DNA sequencer. Each duplex generated has a unique mobility, and therefore each allele is represented. Initially, the RSCA method was used for the detection of new polymorphisms.

The RSCA method has been described as a reliable method for genomic typing of the minor H antigen HA-1 [39]. A fragment of 486 bp derived from the HA-1 locus-specific region is first amplified by PCR using a common forward primer (5′-GTGCTG CCTCCTTGGACACTG-3′) in combination with a common reverse primer (5′-GCATTCTCTGTTTCCGTGTT-3′). Cycling conditions are 1 cycle of 5 min at 95 °C, followed by 10 cycles of 1 min 95 °C and 1 min 65 °C, and finally 25 cycles of 95 °C for 1 min, 62 °C for 1 min, and 72 °C for 1 min. An FLR is generated using HA-$1^H$ and HA-$1^R$ homozygous material using a Cy5-labeled forward primer. Hybridization of the FLR with the PCR product from the samples with the FLR is performed at a ratio of 1:3. Electrophoresis is executed on 6 % non-denaturing polyacrylamide gels in an automated sequencer.

### 3.9 Sequencing-Based Typing

The sequencing-based typing (SBT) is a commonly used technique for determining high-resolution HLA typing. This methodology is highly flexible and allows identification of multi-SNPs on one gene

in one analysis. In this methodology, the entire polymorphic region of the minor H gene is amplified by PCR using non-polymorphic primers (Table 7). In a second step, an aliquot of the PCR products is preferentially sequenced in two directions using non-polymorphic gene-specific sequencing primers (forward and reverse sequencing primers). Alternatively, amplification primers can be tagged with, e.g., an M13 sequence. Although this latter approach facilitates uniform sequencing procedures with an M13 sequencing primer, it also increases the risk of sequencing PCR side products. Sequence analyses can be performed using regular analysis programs by hand. Homozygous typing results appear as single peaks, and heterozygous typing results can be identified by double peaks. Recently, automated minor H antigen typing analyses were implemented in the SBTEngine© Software (GenDx BV, Utrecht, The Netherlands).

Genomic SBT of minor H antigens has been developed for HA-1, HA-2, HA-3, HA-8, HB-1, ACC-1, ACC-2, SP110, PANE1, LB-ECGF, CTSH, LRH-1, LB-ADIR, and CD19. As ACC-1 and ACC-2 are located on the same gene, both polymorphisms can be determined by one single PCR followed by a single sequencing procedure. Below we describe in detail our local setup for minor H antigen typing by SBT.

### 3.9.1 SBT Methods

1. Prepare a PCR mix containing 80 ng genomic DNA, 0.25 U AmpliTaq, 0.8 mM dNTP, 0.5 μM specific primers, 1.5 mM $MgCl_2$, 50 mM KCl, and 10 mM Tris–HCl (pH 8.3) in a total volume of 50 μL. Sequences of the amplification primers for all minor H antigens have been listed in Table 7. Start the PCR with the following cycling conditions: 10 min at 95 °C, followed by 35 cycles of 30 s at 54 °C (56 °C for HA-1) and 30 s at 72 °C. Subsequently, run one cycle of 10 min at 72 °C.
2. Before continuing with the sequencing step, analyze the PCR products on a 2 % agarose gel. If the products display the correct size, purify the PCR product to remove the remaining enzyme. To this end, add 1 μL SAP (1 U/μL) and 0.5 μL ExoR1 (20 U/μL). Mix, spin down, and incubate for 30 min at 37 °C and 20 min at 80 °C in a PCR cycler.
3. Transfer 1 μL of the purified PCR product to a fresh tube and add 9 μL ready reaction sequence mix to it. This mix contains 0.2 μL BDT Ready Reaction V1.1 mix (enzyme; ABI), BDT Buffer (ABI), and 100 pmol/μL sequencing primer.
4. Prepare the sequencing mixes consisting of 1.0 μL BDT Ready Reaction V1.1 mix (enzyme), 9 μL BDT Buffer (5× stock), and sequencing primer (100 pmol/μL). Start the sequencing reactions in a PCR machine using the following cycling conditions: 10 s at 96 °C, followed by 25 cycles of 10 s at 96 °C, 10 s at 50 °C, and 2 min at 60 °C.

**Table 7**
**Oligonucleotide primers for sequencing-based typing**

| Minor H antigen | Type of primer | Primer sequence | Amplicon size |
|---|---|---|---|
| HA-1 | Forward PCR | AAGGACCGTTGTTTGTGAAAGC | |
| | Reverse PCR | **CAGGAAACAGCTATGA**CCCGTTGTCATGCCTTCATCCTAC | 523 bp |
| | Forward sequence | AAGGACCGTTGTTTGTGAAAGC | |
| | Reverse sequence | **CAGGAAACAGCTATGACC** | |
| HA-2 | Forward PCR | CCCCTTCTTCCTTCTCCACT | |
| | Reverse PCR | **CAGGAAACAGCTATGAC**CAGCCAGGTTCGCTCTCTTA | 526 bp |
| | Forward sequence | CACAGGAGATGCTCTAATGG | |
| | Reverse sequence | TGTGGGTGCCTGTAAG | |
| HA-3 | Forward PCR | GTGACTGACCCACAGGGAGT | |
| | Reverse PCR | CCCAGGTGGGAAAGTACTCA | 498 bp |
| | Forward sequence | TACCTCTTGATTGGGAGAAA | |
| | Reverse sequence | CTTGACTTGTTCGATGACAG | |
| HA-8 | Forward PCR | GCTACCTCTTCTGGGCAACA | |
| | Reverse PCR | **CAGGAAACAGCTATGAC**GCCTGGCTCTTTAAATGCAC | 402 bp |
| | Forward sequence | GCCATTGGAGTTAGAATCTG | |
| | Reverse sequence | TCAGCTAATCAGGTTACTCC | |
| HB-1 | Forward PCR | CCTGAGCCTTCTGACCTCAC | |
| | Reverse PCR | AAACTCTGGGCTTCGAGTCA | 215 bp |
| | Forward sequence | CACAGTGGAGAAACCAGAAC | |
| | Reverse sequence | AAGAGCTGTGCCTCAGATAC | |

| | | | |
|---|---|---|---|
| ACC-1 and -2 | Forward PCR | CATTGCCTCAACAGCTTCAA | |
| | Reverse PCR | **CAGGAAACAGCTATGAC**AGCCTCCGTTTTGCCTTATC | 478 bp |
| | Forward sequence | CTCAAGACTTTGCTCTCCAC | |
| | Reverse sequence | CATTATGAACTCCGCAAC | |
| PANE1 | Forward PCR | GCAGGCCACGGAGAT | |
| | Reverse PCR | GTCAAGCCCTGACTGGACAT | 308 bp |
| | Forward sequence | GGAAGGAGGAACAGC | |
| | Reverse sequence | ACCCTCACAGGTCCTCCA | |
| SP110 | Forward PCR | CCATCACCTAAGGTCACCAA | |
| | Reverse PCR | TGAAGAGTGGGCCTTGATTT | 573 bp |
| | Forward sequence | CAAGATTGGGAGATCAATGT | |
| | Reverse sequence | TAAAATTCAACCCTCCACAG | |
| CTSH | Forward PCR | GAGAACCCCCGCCTATAATG | |
| | Reverse PCR | GCCGACAGGTGAACTAGAGC | 507 bp |
| | Forward sequence | TCTGCGTACCTAAGGAGTTC | |
| | Reverse sequence | TCCCAGTTGACGCTC | |
| LRH-1 | Forward PCR | CCTTCATTCTGCCAGGAGAG | |
| | Reverse PCR | **CAGGAAACAGCTATGAC**CCTCAGTGCCTCTCTGGTTC | 378 bp |
| | Forward sequence | AGAATAGGGGTTCTTCTTCG | |
| | Reverse sequence | GGGTTCTTCTTCGCTT | |
| LB-ADIR-1 | Forward PCR | CTCCTCGTCCTCGTCACAGT | |
| | Reverse PCR | **CAGGAAACAGCTATGAC**AGGACCCCAGACAGGGTTT | 447 bp |
| | Forward sequence | GCTGAAGAGCGTCCAGTA | |
| | Reverse sequence | CCACAGCAACACCAAT | |
| CD19 | Forward PCR | CTCTCTCTGCGGGTCTTTGT | |
| | Reverse PCR | **CAGGAAACAGCTATGAC**TTCAGCTCTAGGCTCAGCAA | 557 bp |
| | Forward sequence | GTGTCTCTGCATTTGGTTCT | |
| | Reverse sequence | CACAGGACAGCCAGAG | |

Sequences in bold represent the M13 reverse primer sequence

5. Prepare a 96-well Millipore plate filled with Sephadex. Add 20 μL $H_2O$ to 30 μL PCR product. Add the mixture drop by drop to the Sephadex, place the Sephadex plate on top of a sequencing plate, and spin the plates for 5 min at 400 × *g*. The purified product can be applied to an automated sequence analyzer.

### 3.10 The Future of Minor H Antigen Typing: SNP Microarrays

As listed in Table 1 and 2, most minor H polymorphisms have been identified as being a single-nucleotide polymorphism (SNP) or deletion/insertion polymorphism (DIP). A large number of these SNPs and DIPs have been included in microarrays for typing of genomic variation. Novel high-throughput minor H antigen identification methods make use of these arrays [40–42]. Logically, these arrays are good tools to genotype patients and donors for their minor H alleles. Currently, the costs of setting up SNP typing facilities for the purpose of minor H antigen typing are high. It is, however, anticipated that costs will drop in the near future and that this methodology will provide a universal tool for typing.

## 4 Notes

1. Local validation of all protocols is essential. Control DNA can be obtained from the IHW cell panel. A large number of the cell lines in this panel have been typed for most of the known minor H antigens [24].
2. Carryover contamination from previous PCR can be a significant problem due to the abundance of PCR products and the ideal structure of the contaminant material for re-amplification. Therefore controls to detect contamination should always be included. An option to control carryover contamination with PCR products is using uracil DNA glycosylase in all PCR samples [35]. The procedure requires the following two steps: (1) incorporating dUTP in all PCR products by substituting dUPT for dTTP and (2) treating all subsequent fully preassembled starting reactions with uracil DNA glycosylase (UDG), followed by thermal inactivation of UDG. UDG cleaves the uracil base from uracil-containing DNA but has no effect on thymidine-containing DNA. This cleavage blocks replication by DNA polymerases. UDG does not react with dUTP and is inactivated during denaturation at 95 °C.
3. A disadvantage of SSP-PCR is the possibility to miss an allele when the amplification conditions are suboptimal. Internal controls should be included in the PCR reaction. In the above-described SSP-PCR protocol for the minor H antigen HA-1 an internal control has been introduced for the

one-tube assay. Here, the common reverse and the common forward primer must amplify a band of 486 bp in all samples. Alternatively, primers for a non-polymorphic gene can be included.

4. PCR-RFLP analysis is a reliable technique. However, it is laborious and time consuming, since multiple manipulations are required for each sample. Furthermore, different endonucleases are required for detecting the alleles of all minor H antigens.
5. The real-time PCR method is a rapid and reliable method without any post-PCR sample manipulation, allowing high-throughput analyses. The method, however, requires the use of expensive equipment. Furthermore, cross-reaction of allele-specific oligonucleotide primers can occur and give false-positive signals.
6. With the RSCA method a lot of samples can be processed at the same time. Major drawback is that the RSCA method needs special equipment and computer programs that are not available in each laboratory.

## Acknowledgments

Talitha de Hoop and Walter van Ginkel, University Medical Center Utrecht, are acknowledged for developing and validating the SBT protocols; Jos Pool and Jos Drabbels, Leiden University Medical Center, for developing and validating the uniform PCR-SSP protocols; and Erik Rozemuller, GenDx BV, Utrecht, for the implementation of automated allele assignment for minor H antigens after SBT in SBTEngine©.

### References

1. Goulmy E (1996) Human minor histocompatibility antigens. Curr Opin Immunol 8:75–81
2. Hambach L, Goulmy E (2005) Immunotherapy of cancer through targeting of minor histocompatibility antigens. Curr Opin Immunol 17:202–210
3. Cai J, Lee J, Jankowska-Gan E, Derks R et al (2004) Minor H antigen HA-1-specific regulator and effector CD8+ T cells, and HA-1 microchimerism, in allograft tolerance. J Exp Med 199:1017–1023
4. Verdijk RM, Kloosterman A, Pool J et al (2004) Pregnancy induces minor histocompatibility antigen-specific cytotoxic T cells: implications for stem cell transplantation and immunotherapy. Blood 103:1961–1964
5. Mommaas B, Stegehuis-Kamp JA, Van Halteren AG et al (2004) Cord blood comprises antigen-experienced T cells specific for maternal minor histocompatibility antigen HA-1. Blood 105:1823–1827
6. Van Halteren AG, Jankowska-Gan E, Joosten A et al (2009) Naturally acquired tolerance and sensitization to minor histocompatibility antigens in healthy family members. Blood 114: 2263–2272
7. Nielsen HS, Wu F, Aghai Z et al (2010) H-Y antibody titers are increased in unexplained secondary recurrent miscarriage patients and associated with low male: female ratio in subsequent live births. Hum Reprod 25: 2745–2752

8. Mutis T, Goulmy E (2002) Hematopoietic system-specific antigens as targets for cellular immunotherapy of hematological malignancies. Semin Hematol 39:23–31
9. Klein CA, Wilke M, Pool J et al (2002) The hematopoietic system-specific minor histocompatibility antigen HA-1 shows aberrant expression in epithelial cancer cells. J Exp Med 196: 359–368
10. Fujii N, Hiraki A, Ikeda K et al (2002) Expression of minor histocompatibility antigen, HA-1, in solid tumor cells. Transplantation 73:1137–1141
11. Mutis T, Brand R, Gallardo D, van Biezen A, Niederwieser D, Goulmy E (2010) Graft-versus-host driven graft-versus-leukemia effect of minor histocompatibility antigen HA-1 in chronic myeloid leukemia patients. Leukemia 24:1388–1392
12. Goulmy E, Termijtelen A, Bradley BA, van Rood JJ (1976) Alloimmunity to human H-Y. Lancet 2:1206
13. Voogt PJ, Fibbe WE, Marijt WA et al (1990) Rejection of bone-marrow graft by recipient-derived cytotoxic T lymphocytes against minor histocompatibility antigens. Lancet 335: 131–134
14. Wilke M, Dolstra H, Maas F et al (2003) Quantification of the HA-1 gene product at the RNA level; relevance for immunotherapy of hematological malignancies. Hematol J 4: 315–320
15. Dolstra H, Fredrix H, Maas F et al (1999) A human minor histocompatibility antigen specific for B cell acute lymphoblastic leukemia. J Exp Med 189:301–308
16. Goulmy E (1997) Human minor histocompatibility antigens: new concepts for marrow transplantation and adoptive immunotherapy. Immunol Rev 157:125–140
17. Dickinson AM, Wang XN, Sviland L et al (2002) In situ dissection of the graft-versus-host activities of cytotoxic T cells specific for minor histocompatibility antigens. Nat Med 8: 410–414
18. de Bueger MM, Bakker A, van Rood JJ, Van der Woude F, Goulmy E (1992) Tissue distribution of human minor histocompatibility antigens. Ubiquitous versus restricted tissue distribution indicates heterogeneity among human cytotoxic T lymphocyte-defined non-MHC antigens. J Immunol 149:1788–1794
19. Dolstra H, Fredrix H, Preijers F et al (1997) Recognition of a B cell leukemia-associated minor histocompatibility antigen by CTL. J Immunol 158:560–565
20. Wilke M, Pool J, den Haan JM, Goulmy E (1998) Genomic identification of the minor histocompatibility antigen HA-1 locus by allele-specific PCR. Tissue Antigens 52: 312–317
21. Wilke M, Pool J, Goulmy E (2002) Allele specific PCR for the minor histocompatibility antigen HA-2. Tissue Antigens 59:304–307
22. Spierings E, Brickner AG, Caldwell JA et al (2003) The minor histocompatibility antigen HA-3 arises from differential proteasome-mediated cleavage of the lymphoid blast crisis (Lbc) oncoprotein. Blood 102:621–629
23. den Haan JM, Sherman NE, Blokland E et al (1995) Identification of a graft versus host disease-associated human minor histocompatibility antigen. Science 268:1476–1480
24. Spierings E, Drabbels J, Hendriks M et al (2006) A uniform genomic minor histocompatibility antigen typing methodology and database designed to facilitate clinical applications. PLoS ONE 1:e42
25. Deng G (1988) A sensitive non-radioactive PCR-RFLP analysis for detecting point mutations at 12th codon of oncogene c-Ha-ras in DNAs of gastric-cancer. Nucleic Acids Res 16:6231
26. Mercier B, Ferec C, Dufosse F, Huart JJ (1992) Improvement in HLA-DQB typing by PCR-RFLP—introduction of a constant restriction site in one of the primers for digestion control. Tissue Antigens 40:86–89
27. Tseng LH, Lin MT, Martin PJ, Pei J, Smith AG, Hansen JA (1998) Definition of the gene encoding the minor histocompatibility antigen HA-1 and typing for HA-1 from genomic DNA. Tissue Antigens 52:305–311
28. Pierce RA, Field ED, Mutis T et al (2001) The HA-2 minor histocompatibility antigen is derived from a diallelic gene encoding a novel human class I myosin protein. J Immunol 167: 3223–3230
29. Brickner AG, Warren EH, Caldwell JA et al (2001) The immunogenicity of a new human minor histocompatibility antigen results from differential antigen processing. J Exp Med 193: 195–206
30. Lo YMD, Tein MSC, Lau TK et al (1998) Quantitative analysis of fetal DNA in maternal plasma and serum: implications for noninvasive prenatal diagnosis. Am J Hum Genet 62: 768–775
31. Murata M, Warren EH, Riddell SR (2003) A human minor histocompatibility antigen resulting from differential expression due to a gene deletion. J Exp Med 197:1279–1289
32. Heid CA, Stevens J, Livak KJ, Williams PM (1996) Real time quantitative PCR. Genome Res 6:986–994
33. Akatsuka Y, Warren EH, Gooley TA et al (2003) Disparity for a newly identified minor histocompatibility antigen, HA-8, correlates

with acute graft-versus-host disease after haematopoietic stem cell transplantation from an HLA-identical sibling. Br J Haematol 123: 671–675
34. Fehse B, Chukhlovin A, Kuhlcke K et al (2001) Real-time quantitative Y chromosome-specific PCR (QYCS-PCR) for monitoring hematopoietic chimerism after sex-mismatched allogeneic stem cell transplantation. J Hematother Stem Cell Res 10:419–425
35. Longo MC, Berninger MS, Hartley JL (1990) Use of uracil DNA glycosylase to control carry-over contamination in polymerase chain reactions. Gene 93:125–128
36. Kreiter S, Wehler T, Landt O, Huber C, Derigs HG, Hess G (2000) Rapid identification of minor histocompatibility antigen HA-1 subtypes H and R using fluorescence-labeled oligonucleotides. Tissue Antigens 56:449–452
37. Wittwer CT, Herrmann MG, Moss AA, Rasmussen RP (1997) Continuous fluorescence monitoring of rapid cycle DNA amplification. Biotechniques 22:130–131, and 134–138
38. Arguello JR, Little AM, Pay AL et al (1998) Mutation detection and typing of polymorphic loci through double-strand conformation analysis. Nat Genet 18:192–194
39. Arostegui JI, Gallardo D, Rodriguez-Luaces M et al (2000) Genomic typing of minor histocompatibility antigen HA-1 by reference strand mediated conformation analysis (RSCA). Tissue Antigens 56:69–76
40. Kamei M, Nannya Y, Torikai H et al (2009) HapMap scanning of novel human minor histocompatibility antigens. Blood 113:5041–5048
41. Spaapen RM, Lokhorst HM, van den Oudenalder K et al (2008) Toward targeting B cell cancers with CD4+ CTLs: identification of a CD19-encoded minor histocompatibility antigen using a novel genome-wide analysis. J Exp Med 205:2863–2872
42. van Bergen CA, Rutten CE, van der Meijden ED et al (2010) High-throughput characterization of 10 new minor histocompatibility antigens by whole genome association scanning. Cancer Res 70:9073–9083
43. Akatsuka Y, Nishida T, Kondo E et al (2003) Identification of a polymorphic gene, BCL2A1, encoding two novel hematopoietic lineage-specific minor histocompatibility antigens. J Exp Med 197:1489–1500
44. Kawase T, Akatsuka Y, Torikai H et al (2007) Alternative splicing due to an intronic SNP in HMSD generates a novel minor histocompatibility antigen. Blood 110:1055–1063
45. Tykodi SS, Fujii N, Vigneron N et al (2008) C19orf48 encodes a minor histocompatibility antigen recognized by CD8+ cytotoxic T cells from renal cell carcinoma patients. Clin Cancer Res 14:5260–5269
46. Torikai H, Akatsuka Y, Miyazaki M et al (2006) The human cathepsin H gene encodes two novel minor histocompatibility antigen epitopes restricted by HLA-A*3101 and -A*3303. Br J Haematol 134:406–410
47. den Haan JM, Meadows LM, Wang W et al (1998) The minor histocompatibility antigen HA-1: a diallelic gene with a single amino acid polymorphism. Science 279:1054–1057
48. Mommaas B, Kamp J, Drijfhout JW et al (2002) Identification of a novel HLA-B60-restricted T cell epitope of the minor histocompatibility antigen HA-1 locus. J Immunol 169: 3131–3136
49. Bleakley M, Otterud BE, Richardt JL et al (2010) Leukemia-associated minor histocompatibility antigen discovery using T-cell clones isolated by in vitro stimulation of naive CD8+ T cells. Blood 115:4923–4933
50. van Bergen CA, Kester MG, Jedema I et al (2007) Multiple myeloma-reactive T cells recognize an activation-induced minor histocompatibility antigen encoded by the ATP-dependent interferon-responsive (ADIR) gene. Blood 109: 4089–4096
51. Stumpf AN, van der Meijden ED, van Bergen CA, Willemze R, Falkenburg JH, Griffioen M (2009) Identification of 4 new HLA-DR-restricted minor histocompatibility antigens as hematopoietic targets in antitumor immunity. Blood 114:3684–3692
52. Griffioen M, van der Meijden ED, Slager EH et al (2008) Identification of phosphatidylinositol 4-kinase type II beta as HLA class II-restricted target in graft versus leukemia reactivity. Proc Natl Acad Sci U S A 105: 3837–3842
53. de Rijke B, van Horssens-Zoetbrood A, Beekman JM et al (2005) A frame-shift polymorphism in *P2X5* elicits an allogeneic cytotoxic T lymphocyte response associated with remission of chronic myeloid leukemia. J Clin Invest 115:3506–3516
54. Brickner AG, Evans AM, Mito JK et al (2006) The PANE1 gene encodes a novel human minor histocompatibility antigen that is selectively expressed in B-lymphoid cells and B-CLL. Blood 107:3779–3786
55. Warren EH, Gavin MA, Xuereb SM et al (2002) A single nucleotide polymorphism in the SP110 nuclear phosphoprotein gene creates a minor histocompatibility antigen whose expression is regulated by interferon-gamma. Blood 100:73A
56. Oostvogels R, Minnema MC, van Elk M et al (2013) Towards effective and safe

immunotherapy after allogeneic stem cell transplantation: identification of hematopoietic-specific minor histocompatibility antigen UTA2-1. Leukemia 27:642–649
57. Vogt MH, de Paus RA, Voogt PJ, Willemze R, Falkenburg JH (2000) DFFRY codes for a new human male-specific minor transplantation antigen involved in bone marrow graft rejection. Blood 95:1100–1105
58. Pierce RA, Field ED, den Haan JM et al (1999) Cutting edge: the HLA-A*0101-restricted HY minor histocompatibility antigen originates from DFFRY and contains a cysteinylated cysteine residue as identified by a novel mass spectrometric technique. J Immunol 163:6360–6364
59. Meadows L, Wang W, den Haan JM et al (1997) The HLA-A*0201-restricted H-Y antigen contains a posttranslationally modified cysteine that significantly affects T cell recognition. Immunity 6:273–281
60. Torikai H, Akatsuka Y, Miyazaki M et al (2004) A novel HLA-A*3303-restricted minor histocompatibility antigen encoded by an unconventional open reading frame of human TMSB4Y gene. J Immunol 173:7046–7054
61. Rosinski KV, Fujii N, Mito JK et al (2008) DDX3Y encodes a class I MHC-restricted H-Y antigen that is expressed in leukemic stem cells. Blood 111:4817–4826
62. Ivanov R, Aarts T, Hol S et al (2005) Identification of a 40S ribosomal protein S4-derived H-Y epitope able to elicit a lymphoblast-specific cytotoxic T lymphocyte response. Clin Cancer Res 11:1694–1703
63. Vogt MH, Goulmy E, Kloosterboer FM et al (2000) UTY gene codes for an HLA-B60-restricted human male-specific minor histocompatibility antigen involved in stem cell graft rejection: characterization of the critical polymorphic amino acid residues for T- cell recognition. Blood 96:3126–3132
64. Wang W, Meadows LR, den Haan JM et al (1995) Human H-Y: a male-specific histocompatibility antigen derived from the SMCY protein. Science 269:1588–1590
65. Warren EH, Gavin MA, Simpson E et al (2000) The human UTY gene encodes a novel HLA-B8-restricted H-Y antigen. J Immunol 164: 2807–2814
66. Vogt MH, van den Muijsenberg J, Goulmy E et al (2002) The DBY gene codes for an HLA-DQ5 restricted human male specific minor histocompatibility antigen involved in GvHD. Blood 99:3027–3032
67. Zorn E, Miklos DB, Floyd BH et al (2004) Minor histocompatibility antigen DBY elicits a coordinated B and T cell response after allogeneic stem cell transplantation. J Exp Med 199:1133–1142
68. Spierings E, Vermeulen C, Vogt MH et al (2003) Identification of HLA class II-restricted H-Y-specific T-helper epitope evoking CD4+ T-helper cells in H-Y-mismatched transplantation. Lancet 362:610–615

# Chapter 9

# Natural Killer Cells and Killer-Cell Immunoglobulin-Like Receptor Polymorphisms: Their Role in Hematopoietic Stem Cell Transplantation

**Jennifer Schellekens, Katia Gagne, and Steven G.E. Marsh**

## Abstract

Natural killer (NK) cells are important effector cells in the early control of infected, malignant, and "nonself" cells. Various receptor families are involved in enabling NK cells to detect and efficiently eliminate these target cells. The killer-cell immunoglobulin-like receptor (KIR) family is a set of receptors that are very polymorphic with regard to gene content, expression level, and expression pattern. KIRs are responsible for the induction of a NK cell alloreactive response through their interaction with HLA class I molecules. The role of NK cells in hematopoietic stem cell transplantation (HSCT) has been studied for many years, and induction of antileukemic responses by donor NK cells has been reported. Conflicting data still exist on the exact circumstances in which the KIR repertoire affects and influences clinical outcome after HSCT. More large-scale studies are needed on well-defined cohorts to unravel the mechanism of action of the NK cell-mediated alloresponse in an HSCT setting.

**Key words** NK cells, KIR, KIR genotyping, KIR polymorphism, HLA class I, HSCT

## 1 Introduction

Natural killer (NK) cells are a diverse population of granular, mononuclear lymphocytes, which account for 5–20 % of all circulating lymphocytes in humans. They are considered the key effector cells in the innate immune response because they are capable of rapidly lysing target cells without the need for prior sensitization or antibody recognition [1]. More recently, a role for NK cells in the adaptive immune response has also been defined as the existence of antigen-specific memory NK cells was established as well as adaptation of NK cell responsiveness to the environment [2–4]. NK cells are important for the early control of infected, malignant, and "nonself" cells and also play an important role in reproduction [5]. NK cells are tightly regulated by a sophisticated repertoire of cell surface receptors, which control NK cell activation, proliferation, and effector function [6, 7].

Meral Beksaç (ed.), *Bone Marrow and Stem Cell Transplantation*, Methods in Molecular Biology, vol. 1109,
DOI 10.1007/978-1-4614-9437-9_9, 

Effector function of NK cells was first defined by the missing-self hypothesis, based on the observation that tumor cells deficient of any surface MHC class I expression are susceptible to killing by NK cells [8, 9]. By monitoring the expression of sufficient levels of self-MHC class I on the membrane of the target cells, NK cells are capable of distinguishing between "self" and "nonself" and recognizing malignant or infected cells. This interaction between NK cell receptors and MHC class I is proving to be a major mechanism that influences both the developmental maturation of NK cells and the execution of their effector function [10].

NK cells are generally identified by their absence of CD3 and the expression of CD56 and NKp46 [11, 12]. No unique NK cell marker has been identified yet as CD56 and NKp46 are also present on a subset of T cells [13, 14]. Thus far, phenotypic identification of NK cells still relies on the unique combination of surface antigens that are non-NK cell restricted. Two distinct subsets of NK cells can be distinguished based on the expression level of the adhesion molecule CD56. In peripheral blood the majority, approximately 90 %, of human NK cells are $CD56^{dim}$ with the remainder being characterized as $CD56^{bright}$. The $CD56^{dim}$ NK cells express high levels of CD16, produce only low levels of cytokines, and are the dominant subset in mediating natural cytotoxicity [15]. The $CD56^{bright}$ subpopulation is either $CD16^{dim}$ or $CD16^{-}$ and has only limited cytotoxic ability. The main importance of $CD56^{bright}$ NK cells lies in their capacity to produce abundant levels of immunoregulatory cytokines, such as IFN-γ upon activation [16, 17]. This cytokine production is important to set off a proper innate immune response by providing early IFN-γ and other cytokines for macrophages and other antigen-presenting cells. Using this mechanism, a positive cytokine feedback loop is induced resulting in efficient control of infection. NK cells eliminate target cells by releasing granzyme and perforin or via the death receptor-related pathways, such as Fas or TRAIL [18].

Unlike T- and B-cell receptors, NK cell receptors do not require somatic gene rearrangements to generate receptor diversity and specificity. Instead, a wide variety of germline-encoded receptor families are expressed on the NK cell membrane. Four major families of inhibitory and activating NK cell receptors have been described, including killer-cell immunoglobulin-like receptors (KIRs), C-type lectin receptors such as CD94/NKG2, leukocyte immunoglobulin-like receptors (LILRs), and the natural cytotoxicity receptors such as NKp46 [19–21]. NK cell receptors are expressed in a variegated, stochastic way, which means that within every individual, a multitude of NK cell subsets exist each with their own receptor repertoire and specificity [22]. Each NK cell expresses at least one inhibitory receptor that is specific for the "self" MHC class I ligand present in that individual. This interaction means that autoreactivity of the NK cells against healthy,

"self" cells is avoided. The expression of both inhibitory and activating receptors on the NK cell membrane ensures a balance is maintained in which "nonself" or diseased cells will be efficiently eliminated yet healthy "self" cells are spared from killing [23]. Regulation of NK cell effector function is a dynamic process in which the NK cells will eliminate the target cell if either they have downregulated their cognate MHC class I expression or they have up-regulated stress-induced molecules [24].

### 1.1 Killer-Cell Immunoglobulin-Like Receptors

The KIR gene family is part of a broad family of NK cell receptors each with their own ligand specificities and function [25, 26]. KIRs encompass an important set of receptors that enable the NK cells to carry out a crucial role in immune defense, which allows individuals to survive infection and also contribute to reproduction allowing populations to survive to the next generation. For most of the inhibitory KIRs, HLA class I has been identified as the ligand. This allows NK cells to discriminate between healthy, "self" cells and cells that have lost HLA class I expression or present "nonself" HLA class I molecules.

KIRs are membrane-bound glycoproteins with either two or three extracellular domains, which are reflected in the name of each receptor as 2D or 3D, respectively. Variation in the intracellular part of the KIRs is caused by the length of the cytoplasmic tail, which is displayed in the name as an "L" for long or an "S" for a short tail. Two immunoreceptor tyrosine-based inhibitory motifs (ITIM) are present in the KIRs with a long cytoplasmic tail. Upon binding of its ligand, these receptors generate an inhibitory signal, which prevents killing of the target cell by these NK cells. The KIRs with a short cytoplasmic tail lack the presence of these ITIMs. Instead they have a positively charged residue in their transmembrane part. This enables the formation of a heterodimer with an adaptor molecule, usually DAP12 [27]. Two immunoreceptor tyrosine-based activating motifs are present in the DAP12 molecule that will generate an activating signal upon binding of the KIR with its ligand.

A total of 14 different KIRs have been identified. Seven KIRs, KIR2DL1, KIR2DL2, KIR2DL3, KIR2DL5, KIR3DL1, KIR3DL2, and KIR3DL3, generate an inhibitory signal upon ligand binding. An activating signal is generated by six KIRs, KIR2DS1, KIR2DS2, KIR2DS3, KIR2DS4, KIR2DS5, and KIR3DS1. KIR2DL4 is able to generate both inhibitory and activating signals upon binding of its ligand [28]. Also, two pseudogenes have been identified, KIR2DP1 and KIR3DP1, but these two KIRs do not play a role in NK cell immune surveillance as they do not encode a functional, membrane-bound receptor [29]. For KIR2DL5, two loci have been characterized each containing a copy of the KIR2DL5 gene with a 99.5–99.7 % similarity in their coding sequence [30]. KIR2DL5A is located in the telomeric

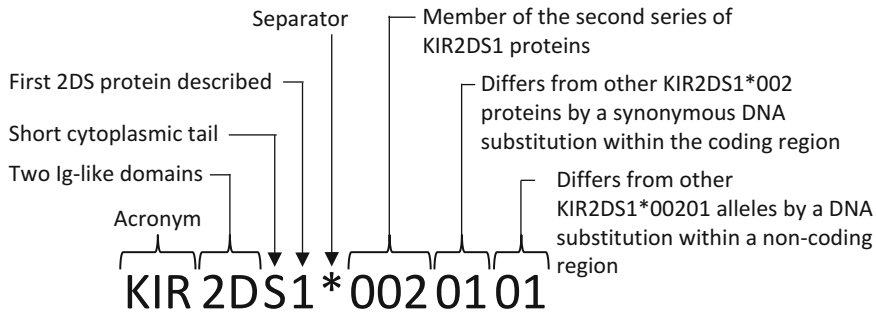


**Fig. 1** Nomenclature of KIR alleles. The number of extracellular domains and the length of the intracellular tail of the receptor are reflected in the gene name. After the gene name an asterisks is used as a separator before a numerical allele designation. The KIR allele sequences are named in a similar fashion to that used for HLA alleles

half of the haplotype and KIR2DL5B in the centromeric half. It has also been established that KIR2DL2 and KIR2DL3 segregate as alleles of a single locus on the centromeric half of the haplotype [31, 32]. In the telomeric half the inhibitory KIR3DL1 and its activating counterpart KIR3DS1 also behave as alleles of the same locus [29].

Allelic variants of the KIR genes are named in a similar system to that used for HLA alleles [29]. After the gene name an asterisk is used as a separator after which a total of seven digits indicate the different levels of polymorphism between alleles of the same gene (Fig. 1). The first three digits after the separator indicate alleles of the same gene that differ from each other by one or more amino acids present in the mature protein. The second two digits indicate alleles that differ by a synonymous substitution within the coding region. The last two digits indicate alleles that differ from each other in the noncoding region like the intron or the promoter region (Fig. 1) [29].

### *1.2 KIR Gene Organization*

A large cluster of closely related Ig-type receptor families including the KIR gene family is located in the leukocyte receptor complex (LRC). The LRC is located on chromosome 19q13.4 and spans an area of approximately 1 Mb [26]. The KIR gene cluster is flanked by the genes encoding Fc alpha receptor (CD89) and another family of NK cell receptors, LILR [26]. LILRs are predominately expressed on cells of the myeloid lineage. They recognize a broad range of classical and nonclassical HLA class I molecules and UL18 and are thought to exert an influence on the signalling pathway of both the innate and adaptive immune systems [19].

The KIR genes are clustered in a head-to-tail fashion covering approximately 150 kb. Two main haplotypes have been distinguished, referred to as haplotype A and B [33]. Each haplotype

varies in the number and combination of KIR genes present. Four framework genes are present on every haplotype which are KIR3DL3 and KIR3DP1 flanking the centromeric and KIR2DL4 and KIR3DL2 flanking the telomeric side of each haplotype [31, 34]. The group A haplotype carries a fixed gene content comprising KIR2DL3, KIR2DP1, KIR2DL1, KIR3DL1, and KIR2DS4 or any combination or fewer of these genes. The group B haplotype is much more variable in number and combination of KIR genes and is characterized by the presence of at least one of the group B-specific KIRs which are KIR2DS2, KIR2DL2, KIR2DL5, KIR2DS3, KIR2DS5, KIR3DS1, or KIR2DS1 [31, 33]. The presence of the group A-specific genes is not restricted to just the A haplotype as, for example, KIR2DL1 and KIR2DP1 are also present on many B haplotypes [35, 36].

A striking difference between A and B haplotypes is the variation in the number of activating KIR genes present. KIR2DS4 is the only activating KIR present on the A haplotype, but the most common variant is a variant allele with a 22 bp deletion rendering it nonfunctional [37]. As many as 75 % of A haplotypes do not possess a KIR gene encoding a functional, activating receptor [38]. For B haplotypes a total of between one and five activating KIRs can be present. The presence of activating KIRs in the mother has been linked with successful reproduction [39].

The frequency of the two haplotypes varies within different populations. For example, the A haplotype is the most common haplotype in the Japanese population with 56 % bearing the AA genotype [40]. The Aboriginal Australians have a predominance of B haplotypes with 77 % having at least one B haplotype [41]. For Caucasians the distribution of A and B haplotypes is relatively even [42]. Balancing selection has ensured that all human populations have retained the presence of both the A and the B haplotypes [43]. Overall it is believed that A haplotypes favor successful immune defense, whereas B haplotypes favor reproductive success [44]. This illustrates the complementary function that both haplotypes fulfill to ensure survival of a population.

It is believed that the KIR haplotypes we commonly encounter today have all originated from a small number of haplotypes. Multiple crossover and recombination events have diversified the gene content for KIR haplotypes. Copy number variation, even including the framework KIR genes, has been shown to be more frequent in B haplotypes compared to A haplotypes [45]. Reciprocal recombination in the central part of the KIR gene cluster, between KIR3DP1 and KIR2DL4, linked together different centromeric and telomeric KIR gene motifs. A total of four common centromeric (Cen) and two telomeric (Tel) KIR gene motifs have been identified which in various permutations are responsible for the vast majority of all haplotypes (Fig. 2) [46]. One A-specific and three B-specific Cen motifs were defined as well as one A- and one

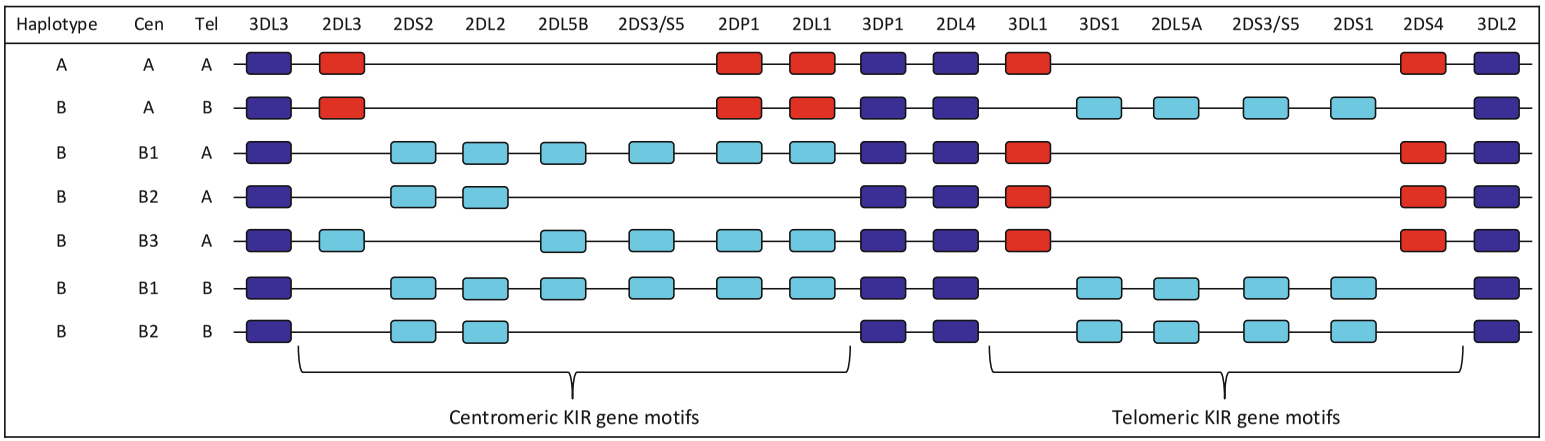


**Fig. 2** KIR haplotypes consist of a centromeric and telomeric KIR gene motif. Six common KIR gene motifs have been defined consisting of one A-specific and three B-specific, B1, B2, and B3, centromeric motifs and one A-specific and one B-specific telomeric KIR gene motif. KIR2DS3 and KIR2DS5 can be present in the centromeric and the telomeric half of the haplotype. KIR2DP1 and KIR2DL1 are present in both the A-specific and some B-specific centromeric KIR gene motifs. *Cen* Centromeric KIR gene motif, *Tel* Telomeric KIR gene motif, *dark blue boxes* framework KIR genes, *red boxes* A-specific gene motifs, *light blue boxes* B-specific gene motifs

B-specific Tel gene motif. A group A haplotype by definition consists of two A motifs in both the centromeric and telomeric parts. A group B haplotype is built up of either a Cen B motif or a Tel B motif combined with an A motif or consists of a Cen B and a Tel B gene motif (Fig. 2). A minority of haplotypes have been identified with aberrant KIR gene content caused by unequal crossing over events that has resulted in either loss or gain of KIR loci or the presence of fusion genes [47–50].

### 1.3 KIR Genotyping

An individual's KIR genotype can be determined by RT-PCR [51, 52], quantitative RT-PCR at the RNA level [53] or DNA level [54–56], or by a variety of methods at the DNA level such as polymerase chain reaction-sequence-specific primer (PCR-SSP), PCR-sequence-specific oligoprobe (PCR-SSO), reverse PCR-SSO Luminex-based technology, or sequence-based typing (SBT). A matrix-assisted laser/desorption ionization-time-of-flight mass spectrometer method using primer extension has also been described [57]. The choice of KIR genotyping technique depends on different parameters including the quality and/or quantity of material available (genomic DNA, mRNA) [58–60], the required laboratory equipment (thermocycler, Luminex platform, sequencer, incubator), the level of resolution desired (gene and/or allelic resolution), and the number of samples to be tested.

Numerous methods for KIR genotyping have been described so far. The PCR-SSP method was the first used [33] and remains the most widely used [61]. The PCR-SSP methods currently in use are based on the first scheme described by Uhrberg et al. [33] to account for newly discovered loci, previously undetected alleles, and for variants affecting primer annealing. PCR-SSP is also one of the methods proposed by the International Histocompatibility Working Group NK Receptors and HLA Polymorphism [62]. Both commercial and in-house kits based on the PCR-SSP method also enable detection of the presence or absence of all 16 KIR genes but provide only limited information on common variants of KIR2DL5, KIR2DS4, and KIR3DP1. For these PCR-SSP methods, each KIR gene is amplified using at least one KIR gene-specific primer pair. In general, a positive internal control is included together with each specific KIR primer pair. A duplex [63] and multiplex PCR-SSP method [64–67] has also been described requiring less genomic DNA to provide a full KIR genotype profile. RT-PCR based on PCR-SSP is the method of choice for allotyping NK cell clones and remains largely unchanged from previous description [33]. Overall, performing KIR genotyping using a PCR-SSP method is easy and fast but is not convenient for a high number of samples, and occasionally this method fails to detect all known KIR alleles of one KIR locus. For a high number of samples, KIR genotyping can be done by PCR-SSO [68, 69] or

by reverse PCR-SSO using the Luminex platform [70, 71]. With these PCR-SSO methods, each KIR gene is detected using different probes targeting specific KIR gene polymorphism. PCR-SSO is perfectly suited for analyzing large number of samples. However, PCR-SSO methods are usually more time consuming compared to PCR-SSP. The pattern reactivity of each KIR probe must also be validated using KIR genotyped control DNAs and updated depending on the KIR gene and/or corresponding alleles identified. KIR genotypes can be further divided in terms of AA or Bx KIR genotypes [33, 72] and give information on centromeric and/or telomeric KIR gene content [46]. Even without parental KIR genotyping, KIR haplotypes can also be deduced [73]. KIR genotypes/haplotypes may serve as anthropological genetic markers [74–76] or be applied to a clinical setting such as hematopoietic stem cell transplantation (HSCT) [77, 78], organ transplantation [79], or viral infectious diseases [80].

A combination of the most up-to-date schemes may be needed for the most comprehensive analysis of the KIR gene content. However, some of the DNA-based methods for KIR genotyping described above only address the variable KIR gene content but do not detect allelic polymorphism [81]. In contrast to HLA class I genes where polymorphism is mainly located in exons 2 and 3, KIR allele polymorphism must be investigated all along the coding regions and even in intron regions as illustrated in particular for KIR3DL1 [82, 83]. Discordances between KIR genotyping and phenotyping could be observed for some KIR genes as non-expressed KIR allelic variants have been described [84]. However, allele-level typing can now be done on 14 KIR loci [85] using either PCR-SSO [86–89], PCR-SSP [84], SNP assay [90], high-resolution melting [91], and SBT methods [82, 92–97]. KIR SBT including pyrosequencing or next-generation sequencing is an emerging technology to type different KIR alleles. KIR SBT remains the method of choice to identify new KIR alleles as it enables the detection of single nucleotide polymorphisms between two KIR alleles. Different methods of high-resolution KIR typing can also be combined in order to identify all KIR alleles of one specific KIR loci without residual ambiguities [83, 98].

Within the last decade the focus has been mainly on development of KIR allele typing methods [85] as KIR allele polymorphism has been proven to impact on NK cell phenotype [99]. Control DNAs with known KIR allele repertoires such as the UCLA international KIR DNA exchange samples are often used to validate KIR genotyping. KIR allele, haplotype, and genotype frequencies are available on dedicated websites (http://www.allelefrequencies.net/) or can be collected from the last KIR anthropology component of the International Histocompatibility Working Group [74, 85].

## 1.4 KIR Polymorphisms

The KIR gene region exhibits multiple levels of polymorphic and structural diversity [31, 35, 48]. Each of these levels of polymorphism contributes to the extensive variation in KIR repertoire between individuals but also between NK cells within an individual. This diversity enables the NK cells to detect every alteration in HLA class I expression which makes them such potent effector cells within the innate immune response.

### 1.4.1 Allelic Polymorphism

In addition to KIR gene content variation as is displayed within the various haplotypes, KIRs also show an abundant level of polymorphism on the allelic level [81]. To date, 614 different KIR alleles have been identified and subsequently named by the IPD-KIR database (version 2.4.0, 15 April 2011). The IPD-KIR database provides a centralized repository for human KIR sequences and allows easy comparison between alignments of various KIRs [100]. This great number of KIR alleles means that two unrelated individuals with a similar KIR haplotype will almost always differ in the combination of KIR alleles present for each gene [81]. KIR3DL1, KIR3DL2, and KIR3DL3 seem to be the loci with most allelic variability with a total of 73, 84, and 107 alleles identified for these KIRs, respectively (http://www.ebi.ac.uk/ipd/kir/ version 2.4.0). However, the great number of alleles identified for these loci is most likely a bias caused by great interest of many research groups into unravelling more about the structure and function of these particular KIR genes. Further diversity in other KIR genes will undoubtedly be described in the future.

For many KIR genes a variation in expression levels between different alleles of the same loci has been identified. This variation in expression level was first confirmed for KIR3DL1 when Gardiner and co-workers identified KIR3DL1 alleles with high, low, or no expression on the NK cell membrane [84]. The influence of KIR3DL1 allelic polymorphism not only on expression levels but also on ligand binding, cytokine secretion, and cytolytic functions has been described [84, 99, 101, 102]. Similar influences of allelic polymorphism on expression level and function have been described for other KIR genes as well [103, 104].

### 1.4.2 KIR Expression

The receptor repertoire expressed on the NK cell membrane on the one hand must enable self-tolerance, but it should also on the other hand enable the NK cell to rapidly and specifically eliminate any unhealthy or foreign cells. The discovery that multiple KIRs are expressed on NK cells in a largely stochastic way has been fundamental in understanding the mechanism NK cells use to maintain self-tolerance. As such, KIRs are being expressed in a clonal fashion on mature NK cells, which means that not every KIR present in the genome is expressed on every NK cell within one individual [22]. The clonal expression pattern results in a large pool of NK cell clones each with their own specificity.

This broad range of functionally distinct clones makes the NK cell population as a whole perfectly adapted for rapid and sensitive detection of reduced "self" or "nonself" HLA class I molecules. Each NK cell clone maintains its acquired KIR expression repertoire even after cell division [105]. There is repertoire stability within an individual but variability in KIR expression patterns within a population [106]. All KIRs are subject to clonal expression patterns with the exception of KIR2DL4 and KIR3DL3. KIR2DL4 is ubiquitously detected on the transcriptional level by all NK cell clones, although the expression on the cell surface seems to be variable [22, 107, 108]. KIR3DL3 transcripts have been revealed to be only present at low or sometimes even undetectable levels [109, 110]. The first controlling factor influencing the KIR repertoire is of genetic origin as the KIR gene content of an individual is the sole dominant factor in dictating the KIR expression repertoire [106]. However, epigenetic mechanisms are also described that modify the KIR expression patterns. Firstly, the HLA class I repertoire has been shown to subtly adjust the relative KIR expression frequencies [99, 106]. Shilling and co-workers showed that the impact of HLA is to change the frequency of KIR-expressing cells but not the surface levels of KIR expression [106], although others have contradicted this influence of cognate HLA class I on KIR expression repertoires [111]. A second mechanism of epigenetic modulation of KIR expression is caused by the methylation state of the promoter regions of the KIR loci. The consistent demethylated state of small CpG islands in the promoter region of the expressed KIR genes as opposed to the methylated state of this region in non-expressed KIRs has been proven to play a crucial role in controlling KIR expression patterns [112–114]. This also explains how, despite high sequence similarity, KIR genes can be regulated independently.

### 1.5 KIR Ligands

The interaction between inhibitory KIRs and HLA class I is well established. Specificity of KIR2DL1, KIR2DL2, and KIR2DL3 for HLA-C was first identified in the early 1990s [115, 116]. A subdivision can be made between these three KIRs based on the HLA-C epitopes for which they are specific. A dimorphism at position 80 of the HLA-C protein divides the HLA-C alleles in two epitope groups, C1 and C2. The C1 epitope group includes all HLA-C molecules that have an asparagine at position 80, and the C2 epitopes include the HLA-C molecules that possess a lysine at this position [117]. KIR2DL1 binds to proteins of the C2 group, whereas KIR2DL2 and KIR2DL3 both bind to HLA-C proteins of the C1 group [115, 118]. In addition to the C1 specificity, interaction of KIR2DL2 and KIR2DL3 with some C2 epitopes has also been reported [119]. The affinity of the interaction of KIRs and HLA-C differs with the affinity of KIR2DL3 for C1 being

much weaker compared to the KIR2DL2–C1 interaction [119]. The specificity of KIRs for either C1 or C2 is determined by a dimorphism at position 44 in the D1 domain of the KIR protein. A mutation at this position can convert the specificity of the receptor from C1 to C2 and vice versa [120].

Other inhibitory KIRs for which the ligand has been identified are KIR3DL1, KIR3DL2, and KIR2DL4. KIR3DL1 specifically binds the Bw4 serological motif presented by many HLA-B and some HLA-A molecules [121]. Bw4 epitopes have either an isoleucine or a threonine at position 80 (80I and 80T, respectively) [117]. The Bw4-80I epitopes serve as stronger ligands for KIR3DL1 [121]. Peptide-dependent variation in binding between KIR3DL1 and Bw4 epitopes has also been reported [92]. HLA-B molecules with the Bw6 epitope have an asparagine at position 80 and do not bind to KIR3DL1. KIR3DL2 is specific for HLA-A3 and HLA-A11 allotypes. The strength of this interaction has been shown to be highly dependent on the peptide presented by the A3 and A11 allotype [122, 123]. KIR2DL4 is important in the process of placentation as it binds to trophoblast-specific HLA-G [107, 124]. Both inhibitory and activating properties have been identified for KIR2DL4 [28].

The activating KIR2DS1 receptor, as its inhibitory homologue KIR2DL1, binds C2 epitopes [125]. KIR2DS1 and KIR2DL1 are similar in their extracellular, ligand-binding domains yet KIR2DS1 binds C2 epitopes with a lower affinity. For both KIR2DL1 and KIR2DS1 the interaction with the C2 epitope is influenced by certain peptide sequence alterations [126]. KIR2DS4 is the most commonly present activating receptor and is specific for subsets of HLA-C1 and C2 epitopes and HLA-A11 [127]. The ligands for KIR2DL5, KIR3DL3, KIR2DS2, KIR2DS3, KIR2DS5, and KIR3DS1 remain to be elucidated.

### 1.6 Control of NK Cell Effector Function

The KIR gene complex segregates independently from the HLA class I complex which could potentially result in self-destructive NK cells when the inhibitory KIR does not find its cognate HLA class I ligand. Yet, NK cells are generally self-tolerant because the majority of the circulating NK cells express at least one inhibitory KIR specific for "self" HLA class I [106]. Interaction between inhibitory KIRs and HLA class I during NK cell development triggers the acquisition of functional competence which allows the mature NK cells to efficiently eliminate target cells that have downregulated or lost HLA class I expression. The process of acquisition of functional ability is referred to as "licensing" [10], "arming" [128], or "education" [129]. This also ensures that potentially autoreactive NK cells remain hyporesponsive and functionally incapable of inducing target cell killing [10, 130]. As such, the interaction with HLA class I serves as a functional tuning mechanism of randomly generated NK cell repertoires.

Apart from KIR, NK cells can also express inhibitory CD94/NKG2A heterodimers. CD94/NKG2A recognizes HLA-E which presents the peptide derived from the leader sequence of other HLA class I molecules [131]. This enables the NK cell to survey the net overall expression of total HLA class I by the target cells. The expression of CD94/NKG2A is inversely correlated with the expression of KIR and is believed to serve as a buffer to ensure functional competence of the NK cells [106, 132].

### 1.7 KIR in Hematopoietic Stem Cell Transplantation

NK cells have been the focus of many research projects. Their role in cancer surveillance was established in a large prospective study published in 2000 [133]. The vital regulatory influence of the KIR gene family on NK cell alloreactivity was demonstrated around the same time [134–136]. The potential in the curative application of NK cells in an HSCT setting is obvious with alloreactive donor NK cells eliminating residual leukemic cells in the recipient and thereby preventing relapse of the disease. The first report to show the impact of alloreactive NK cells on clinical outcome after HSCT was published by Ruggeri and co-workers in 2002 [137]. They studied the influence of KIR ligand incompatibility on the clinical outcome after HLA-haploidentical HSCT for acute myeloid leukemia (AML) or acute lymphoid leukemia (ALL). In the AML group a significant beneficial effect was seen on relapse rates, rejection, and graft-versus-host disease (GvHD) when the donor possessed alloreactive NK cell clones directed against the recipient's cells. These effects were not seen in the recipients who received a transplant from a donor who did not possess any NK cell clones with KIR ligand incompatibility in the graft-versus-host (GvH) direction. Nevertheless, subsequent publications by other research groups often did not reproduce this beneficial effect of KIR repertoire on HSCT outcome. A comprehensive overview of the contradictory findings between the various studies was reviewed by Professor Wing Leung in 2011 [138]. Comparison of the diverse results revealed some likely causes for the conflicting outcomes, and it was proposed by Leung and others that the three main causes are heterogeneity within and between study groups, the model used for prediction of NK alloreactivity, and polymorphism in KIR expression [138, 139].

The first major cause for the confounding data on the influence of KIR repertoire on transplantation outcome is heterogeneity of the study group. A lot of variation is present between various study cohorts, but T cell content of the graft and underlying disease are considered the most important factors. These two factors have both been described to influence or mask the effect that NK cell alloreactive responses exert on the clinical outcome after HSCT. Davies et al. speculated that variation in the number of T cells in the graft may alter immune reconstitution and in turn mask effects mediated by alloreactive NK cells [140]. Others then

confirmed that the alloreactive effects mediated by donor T cells can obscure the effects mediated by alloreactive NK cells [141, 142]. It was also speculated that the presence of T cells in the graft influences NK cell differentiation in vivo after haploidentical HSCT [143]. The level in which donor T cells influence, mask, or even counteract a NK cell-mediated alloreactive response will be hard to unravel.

Many publications on the influence of KIR repertoire on the clinical outcome after HSCT still include a heterogeneous cohort with regard to underlying disease. However, not all hematological diseases have similar susceptibility to NK cell-mediated alloreactivity. The most prominent influence of KIR repertoire on clinical outcome has been observed in AML patients [137, 144–146]. However, alloreactive NK cell-mediated effects have also been reported for patients suffering from ALL or chronic myeloid leukemia albeit not as prominent as in AML patients [147, 148]. Studies on large cohorts of patients suffering from the same disease type are needed to shed more light on the influence of KIR incompatibility in HSCT and the level of susceptibility of the various hematological disorders for which HSCT is performed.

The reliable prediction of the NK cell alloreactive response after HSCT has been the focus of research of many research groups, and different models have now been defined. The first model to predict NK cell alloreactivity was described by Ruggeri and co-workers in Perugia, Italy [137]. This model was based on the combination of the ligands present in the recipient and the donor and was suitably described as the ligand–ligand model. In this ligand–ligand model the assumption was made that if the ligand is present, then the cognate KIR would also be present in that individual. This means that NK cell alloreactivity in the GvH direction was predicted when HLA class I epitope groups recognized by KIR were absent in the recipient but present in the donor. No KIR genotyping was done to confirm actual presence of the KIRs.

The second NK cell alloreactivity prediction tool is known as the receptor–ligand model and was proposed by Leung and co-workers in Memphis, USA [149]. In this model the KIR repertoire of the donor is compared with the HLA ligand repertoire of the recipient. A beneficial antileukemic NK cell alloresponse is predicted when an inhibitory KIR of the donor does not find its cognate HLA ligand in the recipient. By this mismatching the generation of an inhibitory signal is prevented, and therefore donor NK cell alloreactivity towards the recipient's residual leukemic cells is assumed to be present preventing relapse of the disease. In this model the HLA repertoire of the donor nor the KIR status of the recipient is considered to affect the prediction of NK cell alloresponse.

The receptor–receptor model otherwise known as the gene–gene model was first described by Gagne and co-workers in Nantes,

France [150]. In this model it was hypothesized that there is a potential for NK cell-mediated response in the GvH direction when KIR genes that are present in the donor are absent in the recipient. On the other hand, a NK cell alloresponse in the host-versus-graft direction was predicted when the donor fails to express the KIR genes present in the recipient. The HLA repertoire of both recipient and donor was not included in this model to predict a potential NK cell alloresponse.

The last factor resulting in heterogeneity between and within study cohorts is caused by variation in the expression level of KIRs. As has been described before, variation is present in the level of expression between alleles of a single KIR gene. In many publications the assessment of KIR repertoire is only done by genotyping. However, genotyping only establishes the presence of the gene, but it does not give any further information on the allele or the subsequent expression level of the actual KIR protein on the cell membrane. The studies that are based on just KIR genotyping could therefore mistakenly assume an interaction or lack thereof between a KIR receptor and its ligand resulting in a NK cell-mediated alloresponse reflected in improved clinical outcome. In order to reliably assign an improved clinical outcome to the NK cell-mediated alloresponse, KIR phenotypic analyses should be performed. The heterogeneity in expression level between KIR alleles adds an extra level of complexity to be taken into account when comparing the various results.

The work by two research groups deserves a special mention and can be considered leading in the field as they describe large, well-defined cohorts which improve the understanding of the mechanism of action of KIR repertoire on clinical outcome after HSCT. In 2009, Cooley et al. described that donors with a B haplotype improve relapse-free survival after unrelated HSCT for patients suffering from AML [145]. In an even more extensive cohort of AML and ALL patients, they showed that for patients suffering from AML both centromeric and telomeric B motifs present in the donor contribute to relapse protection and improved survival with the presence of two B motifs in the centromeric part having the strongest independent effect. No influence of donor KIR genotype was observed in patients suffering from ALL [144]. In 2012, Hsu and co-workers reported on the influence of the combination of KIR and HLA repertoire in a cohort of 1,277 AML patients who had received HSCT from an unrelated donor. They reported that presence of KIR2DS1 in the donor provides protection against relapse in an HLA-C-dependent manner and donor KIR3DS1 was associated with reduced mortality [151].

Donor NK cells are considered good candidates to use as adoptive immunotherapy after HSCT or as a cytoreductive therapy before HSCT because they can induce a graft-versus-leukemia effect without causing GvHD. In order to maximize their

potential, the reliable prediction of their alloreactive state needs to be defined. Many retrospective reports have been published but no consensus has been achieved about the ideal HSCT setting to maximize the NK cell alloreactive effect. Concordantly, questions also still remain about how to incorporate KIR repertoire into the donor selection procedure. More large-scale studies are needed to answer the question on how to use NK cell alloreactivity to our advantage in the clinic.

## References


1. Robertson MJ, Ritz J (1990) Biology and clinical relevance of human natural killer cells. Blood 76:2421–2438
2. O'Leary JG, Goodarzi M, Drayton DL et al (2006) T cell- and B cell-independent adaptive immunity mediated by natural killer cells. Nat Immunol 7:507–516
3. Paust S, von Andrian UH (2011) Natural killer cell memory. Nat Immunol 12:500–508
4. Vivier E, Raulet DH, Moretta A et al (2011) Innate or adaptive immunity? The example of natural killer cells. Science 331:44–49
5. Parham P (2005) MHC class I molecules and KIRs in human history, health and survival. Nat Rev Immunol 5:201–214
6. Warren HS (1996) NK cell proliferation and inflammation. Immunol Cell Biol 74:473–480
7. Farag SS, Fehniger TA, Ruggeri L et al (2002) Natural killer cell receptors: new biology and insights into the graft-versus-leukemia effect. Blood 100:1935–1947
8. Karre K, Ljunggren HG, Piontek G et al (1986) Selective rejection of H-2-deficient lymphoma variants suggests alternative immune defence strategy. Nature 319: 675–678
9. Ljunggren HG, Karre K (1990) In search of the 'missing self': MHC molecules and NK cell recognition. Immunol Today 11:237–244
10. Kim S, Poursine-Laurent J, Truscott SM et al (2005) Licensing of natural killer cells by host major histocompatibility complex class I molecules. Nature 436:709–713
11. Ritz J, Schmidt RE, Michon J et al (1988) Characterization of functional surface structures on human natural killer cells. Adv Immunol 42:181–211
12. Walzer T, Jaeger S, Chaix J et al (2007) Natural killer cells: from CD3(-)NKp46(+) to post-genomics meta-analyses. Curr Opin Immunol 19:365–372
13. Lanier LL, Testi R, Bindl J et al (1989) Identity of Leu-19 (CD56) leukocyte differentiation antigen and neural cell adhesion molecule. J Exp Med 169:2233–2238
14. Yu J, Mitsui T, Wei M et al (2011) NKp46 identifies an NKT cell subset susceptible to leukemic transformation in mouse and human. J Clin Invest 121:1456–1470
15. Nagler A, Lanier LL, Cwirla S et al (1989) Comparative studies of human FcRIII-positive and negative natural killer cells. J Immunol 143:3183–3191
16. Lanier LL, Le AM, Civin CI et al (1986) The relationship of CD16 (Leu-11) and Leu-19 (NKH-1) antigen expression on human peripheral blood NK cells and cytotoxic T lymphocytes. J Immunol 136:4480–4486
17. Cooper MA, Fehniger TA, Turner SC et al (2001) Human natural killer cells: a unique innate immunoregulatory role for the CD56(bright) subset. Blood 97:3146–3151
18. Smyth MJ, Cretney E, Kelly JM et al (2005) Activation of NK cell cytotoxicity. Mol Immunol 42:501–510
19. Brown D, Trowsdale J, Allen R (2004) The LILR family: modulators of innate and adaptive immune pathways in health and disease. Tissue Antigens 64:215–225
20. Lanier LL (2005) NK cell recognition. Annu Rev Immunol 23:225–274
21. Borrego F, Masilamani M, Marusina AI et al (2006) The CD94/NKG2 family of receptors: from molecules and cells to clinical relevance. Immunol Res 35:263–278
22. Valiante NM, Uhrberg M, Shilling HG et al (1997) Functionally and structurally distinct NK cell receptor repertoires in the peripheral blood of two human donors. Immunity 7:739–751
23. Cheent K, Khakoo SI (2009) Natural killer cells: integrating diversity with function. Immunology 126:449–457
24. Raulet DH, Guerra N (2009) Oncogenic stress sensed by the immune system: role of natural killer cell receptors. Nat Rev Immunol 9:568–580

25. Trowsdale J, Barten R, Haude A et al (2001) The genomic context of natural killer receptor extended gene families. Immunol Rev 181:20–38
26. Barrow AD, Trowsdale J (2008) The extended human leukocyte receptor complex: diverse ways of modulating immune responses. Immunol Rev 224:98–123
27. Lanier LL (2009) DAP10- and DAP12-associated receptors in innate immunity. Immunol Rev 227:150–160
28. Faure M, Long EO (2002) KIR2DL4 (CD158d), an NK cell-activating receptor with inhibitory potential. J Immunol 168:6208–6214
29. Marsh SGE, Parham P, Dupont B et al (2003) Killer-cell immunoglobulin-like receptor (KIR) nomenclature report, 2002. Tissue Antigens 62:79–86
30. Vilches C, Rajalingam R, Uhrberg M et al (2000) KIR2DL5, a novel killer-cell receptor with a D0-D2 configuration of Ig-like domains. J Immunol 164:5797–5804
31. Wilson MJ, Torkar M, Haude A et al (2000) Plasticity in the organization and sequences of human KIR/ILT gene families. Proc Natl Acad Sci USA 97:4778–4783
32. Norman PJ, Stephens HA, Verity DH et al (2001) Distribution of natural killer cell immunoglobulin-like receptor sequences in three ethnic groups. Immunogenetics 52:195–205
33. Uhrberg M, Valiante NM, Shum BP et al (1997) Human diversity in killer cell inhibitory receptor genes. Immunity 7:753–763
34. Martin AM, Kulski JK, Gaudieri S et al (2004) Comparative genomic analysis, diversity and evolution of two KIR haplotypes A and B. Gene 335:121–131
35. Hsu KC, Chida S, Geraghty DE et al (2002) The killer cell immunoglobulin-like receptor (KIR) genomic region: gene-order, haplotypes and allelic polymorphism. Immunol Rev 190:40–52
36. Martin MP, Single RM, Wilson MJ et al (2008) KIR haplotypes defined by segregation analysis in 59 Centre d'Etude Polymorphisme Humain (CEPH) families. Immunogenetics 60:767–774
37. Maxwell LD, Wallace A, Middleton D et al (2002) A common KIR2DS4 deletion variant in the human that predicts a soluble KIR molecule analogous to the KIR1D molecule observed in the rhesus monkey. Tissue Antigens 60:254–258
38. Bashirova AA, Martin MP, McVicar DW et al (2006) The killer immunoglobulin-like receptor gene cluster: tuning the genome for defense. Annu Rev Genomics Hum Genet 7:277–300
39. Hiby SE, Regan L, Lo W et al (2008) Association of maternal killer-cell immunoglobulin-like receptors and parental HLA-C genotypes with recurrent miscarriage. Hum Reprod 23:972–976
40. Yawata M, Yawata N, McQueen KL et al (2002) Predominance of group A KIR haplotypes in Japanese associated with diverse NK cell repertoires of KIR expression. Immunogenetics 54:543–550
41. Toneva M, Lepage V, Lafay G et al (2001) Genomic diversity of natural killer cell receptor genes in three populations. Tissue Antigens 57:358–362
42. Yawata M, Yawata N, Abi-Rached L et al (2002) Variation within the human killer cell immunoglobulin-like receptor (KIR) gene family. Crit Rev Immunol 22:463–482
43. Gendzekhadze K, Norman PJ, Abi-Rached L et al (2009) Co-evolution of KIR2DL3 with HLA-C in a human population retaining minimal essential diversity of KIR and HLA class I ligands. Proc Natl Acad Sci USA 106:18692–18697
44. Parham P (2008) The genetic and evolutionary balances in human NK cell receptor diversity. Semin Immunol 20:311–316
45. Jiang W, Johnson C, Jayaraman J et al (2012) Copy number variation leads to considerable diversity for B but not A haplotypes of the human KIR genes encoding NK cell receptors. Genome Res 22:1845–1854
46. Pyo CW, Guethlein LA, Vu Q et al (2010) Different patterns of evolution in the centromeric and telomeric regions of group A and B haplotypes of the human killer cell Ig-like receptor locus. PLoS One 5:e15115
47. Martin MP, Bashirova A, Traherne J et al (2003) Cutting edge: expansion of the KIR locus by unequal crossing over. J Immunol 171:2192–2195
48. Uhrberg M (2005) The KIR gene family: life in the fast lane of evolution. Eur J Immunol 35:10–15
49. Norman PJ, Abi-Rached L, Gendzekhadze K et al (2009) Meiotic recombination generates rich diversity in NK cell receptor genes, alleles, and haplotypes. Genome Res 19:757–769
50. Traherne JA, Martin M, Ward R et al (2010) Mechanisms of copy number variation and hybrid gene formation in the KIR immune gene complex. Hum Mol Genet 19:737–751
51. Husain Z, Alper CA, Yunis EJ et al (2002) Complex expression of natural killer receptor genes in single natural killer cells. Immunology 106:373–380

52. Leung W, Iyengar R, Triplett B et al (2005) Comparison of killer Ig-like receptor genotyping and phenotyping for selection of allogeneic blood stem cell donors. J Immunol 174:6540–6545
53. Denis L, Gagne K, Gueglio B et al (2005) NK-KIR transcript kinetics correlate with acute graft-versus-host disease occurrence after allogeneic bone marrow transplantation. Hum Immunol 66:447–459
54. Alves LG, Rajalingam R, Canavez F (2009) A novel real-time PCR method for KIR genotyping. Tissue Antigens 73:188–191
55. Koehler RN, Walsh AM, Moqueet N et al (2009) High-throughput genotyping of KIR2DL2/L3, KIR3DL1/S1, and their HLA class I ligands using real-time PCR. Tissue Antigens 74:73–80
56. Hong HA, Loubser AS, de Assis Rosa D et al (2011) Killer-cell immunoglobulin-like receptor genotyping and HLA killer-cell immunoglobulin-like receptor-ligand identification by real-time polymerase chain reaction. Tissue Antigens 78:185–194
57. Houtchens KA, Nichols RJ, Ladner MB et al (2007) High-throughput killer cell immunoglobulin-like receptor genotyping by MALDI-TOF mass spectrometry with discovery of novel alleles. Immunogenetics 59:525–537
58. Chainonthee W, Böttcher G, Gagne K et al (2010) Improved KIR gene and HLA-C KIR ligand sequence-specific primer polymerase chain reaction genotyping using whole genome amplification. Tissue Antigens 76:135–143
59. Khan F, Liacini A, Arora E et al (2012) Assessment of fidelity and utility of the whole-genome amplification for the clinical tests offered in a histocompatibility and immunogenetics laboratory. Tissue Antigens 79:372–379
60. Ndlovu BG, Danaviah S, Moodley E et al (2012) Use of dried blood spots for the determination of genetic variation of interleukin-10, killer immunoglobulin-like receptor and HLA class I genes. Tissue Antigens 79:114–122
61. Ordóñez D, Moraru M, Gómez-Lozano N et al (2012) KIR typing by non-sequencing methods: polymerase-chain reaction with sequence-specific primers. Methods Mol Biol 882:415–430
62. Petersdorf EW, Malkki M, Hsu K et al (2013) 16th IHIW: international histocompatibility working group in hematopoietic cell transplantation. Int J Immunogenet 40:2–10
63. Ashouri E, Ghaderi A, Reed EF et al (2009) A novel duplex SSP-PCR typing method for KIR gene profiling. Tissue Antigens 74:62–67
64. Sun JY, Gaidulis L, Miller MM et al (2004) Development of a multiplex PCR-SSP method for Killer-cell immunoglobulin-like receptor genotyping. Tissue Antigens 64:462–468
65. Tajik N, Shahsavar F, Nasiri M et al (2010) Compound KIR-HLA genotype analyses in the Iranian population by a novel PCR-SSP assay. Int J Immunogenet 37:159–168
66. Kulkarni S, Martin MP, Carrington M (2010) KIR genotyping by multiplex PCR-SSP. Methods Mol Biol 612:365–375
67. Abalos AT, Eggers R, Hogan M et al (2011) Design and validation of a multiplex specific primer-directed polymerase chain reaction assay for killer-cell immunoglobulin-like receptor genetic profiling. Tissue Antigens 77:143–148
68. Crum KA, Logue SE, Curran MD et al (2000) Development of a PCR-SSOP approach capable of defining the natural killer cell inhibitory receptor (KIR) gene sequence repertoires. Tissue Antigens 56:313–326
69. Cook MA, Norman PJ, Curran MD et al (2003) A multi-laboratory characterization of the KIR genotypes of 10th International Histocompatibility Workshop cell lines. Hum Immunol 64:567–571
70. Nong T, Saito K, Blair L et al (2007) KIR genotyping by reverse sequence-specific oligonucleotide methodology. Tissue Antigens 69:92–95
71. Park HJ, Oh Y, Kang HJ et al (2011) A gene-specific primer extension and liquid bead array system for killer-cell immunoglobulin-like receptor genotyping. Tissue Antigens 77:251–256
72. Hsu KC, Liu XR, Selvakumar A et al (2002) Killer Ig-like receptor haplotype analysis by gene content: evidence for genomic diversity with a minimum of six basic framework haplotypes, each with multiple subsets. J Immunol 169:5118–5129
73. Gourraud PA, Gagne K, Bignon JD et al (2007) Preliminary analysis of a KIR haplotype estimation algorithm: a simulation study. Tissue Antigens 69(Suppl 1):96–100
74. Hollenbach JA, Meenagh A, Sleator C et al (2010) Report from the killer immunoglobulin-like receptor (KIR) anthropology component of the 15th International Histocompatibility Workshop: worldwide variation in the KIR loci and further evidence

for the co-evolution of KIR and HLA. Tissue Antigens 76:9–17

75. Sanchez-Mazas A, Fernandez-Viña M, Middleton D et al (2011) Immunogenetics as a tool in anthropological studies. Immunology 133:143–164
76. Gendzekhadze K, Norman PJ, Abi-Rached L et al (2006) High KIR diversity in Amerindians is maintained using few gene-content haplotypes. Immunogenetics 58:474–480
77. Mullighan CG, Petersdorf EW (2006) Genomic polymorphism and allogeneic hematopoietic transplantation outcome. Biol Blood Marrow Transplant 12:19–27
78. Beksaç M, Dalva K (2012) Role of killer immunoglobulin-like receptor and ligand matching in donor selection. Bone Marrow Res 2012: article ID 271695, 6 pages
79. Villard J (2011) The role of natural killer cells in human solid organ and tissue transplantation. J Innate Immun 3:395–402
80. Martin MP, Carrington M (2008) KIR locus polymorphisms: genotyping and disease association analysis. Methods Mol Biol 415:49–64
81. Shilling HG, Guethlein LA, Cheng NW et al (2002) Allelic polymorphism synergizes with variable gene content to individualize human KIR genotype. J Immunol 168:2307–2315
82. Norman PJ, Abi-Rached L, Gendzekhadze K et al (2007) Unusual selection on the KIR3DL1/S1 natural killer cell receptor in Africans. Nat Genet 39:1092–1099
83. Sun JY, Oki A, Senitzer D (2008) Alleles and intron polymorphism of KIR3DL1 shown by combination of allele group-specific primers and sequencing. Tissue Antigens 72:578–580
84. Gardiner CM, Guethlein LA, Shilling HG et al (2001) Different NK cell surface phenotypes defined by the DX9 antibody are due to KIR3DL1 gene polymorphism. J Immunol 166:2992–3001
85. Vierra-Green C, Roe D, Hou L et al (2012) Allele-level haplotype frequencies and pairwise linkage disequilibrium for 14 KIR loci in 506 European-American individuals. PLoS One 7:e47491
86. Halfpenny IA, Middleton D, Barnett YA et al (2004) Investigation of killer cell immunoglobulin-like receptor gene diversity: IV. KIR3DL1/S1. Hum Immunol 65: 602–612
87. Maxwell LD, Williams F, Gilmore P et al (2004) Investigation of killer cell immunoglobulin-like receptor gene diversity: II. KIR2DS4. Hum Immunol 65:613–621
88. Williams F, Meenagh A, Sleator C et al (2004) Investigation of killer cell immunoglobulin-like receptor gene diversity: I. KIR2DL4. Hum Immunol 65:31–38
89. Gonzalez A, Meenagh A, Sleator C et al (2008) Investigation of killer cell immunoglobulin-like receptor (KIR) gene diversity: KIR2DL2, KIR2DL5 and KIR2DS5. Tissue Antigens 72:11–20
90. Bari R, Leung M, Turner VE et al (2011) Molecular determinant-based typing of KIR alleles and KIR ligands. Clin Immunol 138: 274–281
91. Gonzalez A, McErlean C, Meenagh A et al (2009) Killer cell immunoglobulin-like receptor allele discrimination by high-resolution melting. Hum Immunol 70:858–863
92. Thananchai H, Gillespie G, Martin MP et al (2007) Cutting edge: allele-specific and peptide-dependent interactions between KIR3DL1 and HLA-A and HLA-B. J Immunol 178:33–37
93. Roberts CH, Turino C, Madrigal JA et al (2007) Enrichment of individual KIR2DL4 sequences from genomic DNA using long-template PCR and allele-specific hybridization to magnetic bead-bound oligonucleotide probes. Tissue Antigens 69:597–601
94. Roberts CH, Madrigal JA, Marsh SG (2007) Cloning and sequencing alleles of the KIR2DL4 gene from genomic DNA samples. Tissue Antigens 69:88–91
95. Du Z, Sharma SK, Spellman S et al (2008) KIR2DL5 alleles mark certain combination of activating KIR genes. Genes Immun 9: 470–480
96. Schellekens J, Tilanus MG, Rozemuller EH (2008) The elucidation of KIR2DL4 gene polymorphism. Mol Immunol 45:1900–1906
97. Hou L, Chen M, Steiner N et al (2012) Killer cell immunoglobulin-like receptors (KIR) typing by DNA sequencing. Methods Mol Biol 882:431–468
98. Witt CS, Martin A, Christiansen FT (2000) Detection of KIR2DL4 alleles by sequencing and SSCP reveals a common allele with a shortened cytoplasmic tail. Tissue Antigens 56:248–257
99. Yawata M, Yawata N, Draghi M et al (2006) Roles for HLA and KIR polymorphisms in natural killer cell repertoire selection and modulation of effector function. J Exp Med 203:633–645
100. Robinson J, Mistry K, McWilliam H et al (2010) IPD—the Immuno Polymorphism Database. Nucleic Acids Res 38:D863–D869
101. Carr WH, Pando MJ, Parham P (2005) KIR3DL1 polymorphisms that affect NK cell inhibition by HLA-Bw4 ligand. J Immunol 175:5222–5229

102. O'Connor GM, Guinan KJ, Cunningham RT et al (2007) Functional polymorphism of the KIR3DL1/S1 receptor on human NK cells. J Immunol 178:235–241
103. Kikuchi-Maki A, Yusa S, Catina TL et al (2003) KIR2DL4 is an IL-2-regulated NK cell receptor that exhibits limited expression in humans but triggers strong IFN-gamma production. J Immunol 171:3415–3425
104. Martin MP, Pascal V, Yeager M et al (2007) A mutation in KIR3DS1 that results in truncation and lack of cell surface expression. Immunogenetics 59:823–881
105. Moretta A, Tambussi G, Bottino C et al (1990) A novel surface antigen expressed by a subset of human CD3–CD16+ natural killer cells. Role in cell activation and regulation of cytolytic function. J Exp Med 171:695–714
106. Shilling HG, Young N, Guethlein LA et al (2002) Genetic control of human NK cell repertoire. J Immunol 169:239–247
107. Rajagopalan S, Long EO (1999) A human histocompatibility leukocyte antigen (HLA)-G-specific receptor expressed on all natural killer cells. J Exp Med 189:1093–1100
108. Goodridge JP, Witt CS, Christiansen FT et al (2003) KIR2DL4 (CD158d) genotype influences expression and function in NK cells. J Immunol 171:1768–1774
109. Torkar M, Norgate Z, Colonna M et al (1998) Isotypic variation of novel immunoglobulin-like transcript/killer cell inhibitory receptor loci in the leukocyte receptor complex. Eur J Immunol 28:3959–3967
110. Long EO, Barber DF, Burshtyn DN et al (2001) Inhibition of natural killer cell activation signals by killer cell immunoglobulin-like receptors (CD158). Immunol Rev 181:223–233
111. Andersson S, Fauriat C, Malmberg JA et al (2009) KIR acquisition probabilities are independent of self-HLA class I ligands and increase with cellular KIR expression. Blood 114:95–104
112. Santourlidis S, Trompeter HI, Weinhold S et al (2002) Crucial role of DNA methylation in determination of clonally distributed killer cell Ig-like receptor expression patterns in NK cells. J Immunol 169:4253–4261
113. Chan HW, Kurago ZB, Stewart CA et al (2003) DNA methylation maintains allele-specific KIR gene expression in human natural killer cells. J Exp Med 197:245–255
114. Trompeter HI, Gomez-Lozano N, Santourlidis S et al (2005) Three structurally and functionally divergent kinds of promoters regulate expression of clonally distributed killer cell Ig-like receptors (KIR), of KIR2DL4, and of KIR3DL3. J Immunol 174:4135–4143
115. Colonna M, Borsellino G, Falco M et al (1993) HLA-C is the inhibitory ligand that determines dominant resistance to lysis by NK1- and NK2-specific natural killer cells. Proc Natl Acad Sci USA 90:12000–12004
116. Moretta A, Vitale M, Bottino C et al (1993) P58 molecules as putative receptors for major histocompatibility complex (MHC) class I molecules in human natural killer (NK) cells. Anti-p58 antibodies reconstitute lysis of MHC class I-protected cells in NK clones displaying different specificities. J Exp Med 178: 597–604
117. Robinson J, Halliwell JA, McWilliam H et al (2013) The IMGT/HLA database. Nucleic Acids Res 41:D1222–D1227
118. Wagtmann N, Rajagopalan S, Winter CC et al (1995) Killer cell inhibitory receptors specific for HLA-C and HLA-B identified by direct binding and by functional transfer. Immunity 3:801–809
119. Moesta AK, Norman PJ, Yawata M et al (2008) Synergistic polymorphism at two positions distal to the ligand-binding site makes KIR2DL2 a stronger receptor for HLA-C than KIR2DL3. J Immunol 180:3969–3979
120. Winter CC, Long EO (1997) A single amino acid in the p58 killer cell inhibitory receptor controls the ability of natural killer cells to discriminate between the two groups of HLA-C allotypes. J Immunol 158:4026–4028
121. Cella M, Longo A, Ferrara GB et al (1994) NK3-specific natural killer cells are selectively inhibited by Bw4-positive HLA alleles with isoleucine 80. J Exp Med 180:1235–1242
122. Dohring C, Scheidegger D, Samaridis J et al (1996) A human killer inhibitory receptor specific for HLA-A1,2. J Immunol 156: 3098–3101
123. Hansasuta P, Dong T, Thananchai H et al (2004) Recognition of HLA-A3 and HLA-A11 by KIR3DL2 is peptide-specific. Eur J Immunol 34:1673–1679
124. Moffett-King A (2002) Natural killer cells and pregnancy. Nat Rev Immunol 2: 656–663
125. Biassoni R, Pessino A, Malaspina A et al (1997) Role of amino acid position 70 in the binding affinity of p50.1 and p58.1 receptors for HLA-Cw4 molecules. Eur J Immunol 27: 3095–3099
126. Stewart CA, Laugier-Anfossi F, Vely F et al (2005) Recognition of peptide-MHC class I complexes by activating killer immunoglobulin-like receptors. Proc Natl Acad Sci USA 102:13224–13229
127. Graef T, Moesta AK, Norman PJ et al (2009) KIR2DS4 is a product of gene conversion with KIR3DL2 that introduced specificity for

HLA-A*11 while diminishing avidity for HLA-C. J Exp Med 206:2557–2572

128. Raulet DH, Vance RE (2006) Self-tolerance of natural killer cells. Nat Rev Immunol 6:520–531
129. Anfossi N, Andre P, Guia S et al (2006) Human NK cell education by inhibitory receptors for MHC class I. Immunity 25:331–342
130. Kim S, Sunwoo JB, Yang L et al (2008) HLA alleles determine differences in human natural killer cell responsiveness and potency. Proc Natl Acad Sci USA 105:3053–3058
131. Braud VM, Allan DS, O'Callaghan CA et al (1998) HLA-E binds to natural killer cell receptors CD94/NKG2A, B and C. Nature 391:795–799
132. Fauriat C, Andersson S, Bjorklund AT et al (2008) Estimation of the size of the alloreactive NK cell repertoire: studies in individuals homozygous for the group A KIR haplotype. J Immunol 181:6010–6019
133. Imai K, Matsuyama S, Miyake S et al (2000) Natural cytotoxic activity of peripheral-blood lymphocytes and cancer incidence: an 11-year follow-up study of a general population. Lancet 356:1795–1799
134. D'Andrea A, Chang C, Franz-Bacon K et al (1995) Molecular cloning of NKB1. A natural killer cell receptor for HLA-B allotypes. J Immunol 155:2306–2310
135. Colonna M, Samaridis J (1995) Cloning of immunoglobulin-superfamily members associated with HLA-C and HLA-B recognition by human natural killer cells. Science 268:405–408
136. Wagtmann N, Biassoni R, Cantoni C et al (1995) Molecular clones of the p58 NK cell receptor reveal immunoglobulin-related molecules with diversity in both the extra- and intracellular domains. Immunity 2:439–449
137. Ruggeri L, Capanni M, Urbani E et al (2002) Effectiveness of donor natural killer cell alloreactivity in mismatched hematopoietic transplants. Science 295:2097–2100
138. Leung W (2011) Use of NK cell activity in cure by transplant. Br J Haematol 155:14–29
139. Pegram HJ, Ritchie DS, Smyth MJ et al (2011) Alloreactive natural killer cells in hematopoietic stem cell transplantation. Leuk Res 35:14–21
140. Davies SM, Ruggieri L, DeFor T et al (2002) Evaluation of KIR ligand incompatibility in mismatched unrelated donor hematopoietic transplants. Killer immunoglobulin-like receptor. Blood 100:3825–3827
141. Lowe EJ, Turner V, Handgretinger R et al (2003) T-cell alloreactivity dominates natural killer cell alloreactivity in minimally T-cell-depleted HLA-non-identical paediatric bone marrow transplantation. Br J Haematol 123:323–326
142. Bishara A, De Santis D, Witt CC et al (2004) The beneficial role of inhibitory KIR genes of HLA class I NK epitopes in haploidentically mismatched stem cell allografts may be masked by residual donor-alloreactive T cells causing GVHD. Tissue Antigens 63:204–211
143. Nguyen S, Kuentz M, Vernant JP et al (2008) Involvement of mature donor T cells in the NK cell reconstitution after haploidentical hematopoietic stem-cell transplantation. Leukemia 22:344–352
144. Cooley S, Weisdorf DJ, Guethlein LA et al (2010) Donor selection for natural killer cell receptor genes leads to superior survival after unrelated transplantation for acute myelogenous leukemia. Blood 116:2411–2419
145. Cooley S, Trachtenberg E, Bergemann TL et al (2009) Donors with group B KIR haplotypes improve relapse-free survival after unrelated hematopoietic cell transplantation for acute myelogenous leukemia. Blood 113: 726–732
146. Hsu KC, Keever-Taylor CA, Wilton A et al (2005) Improved outcome in HLA-identical sibling hematopoietic stem-cell transplantation for acute myelogenous leukemia predicted by KIR and HLA genotypes. Blood 105:4878–4884
147. Willemze R, Rodrigues CA, Labopin M et al (2009) KIR-ligand incompatibility in the graft-versus-host direction improves outcomes after umbilical cord blood transplantation for acute leukemia. Leukemia 23:492–500
148. Hsu KC, Gooley T, Malkki M et al (2006) KIR ligands and prediction of relapse after unrelated donor hematopoietic cell transplantation for hematologic malignancy. Biol Blood Marrow Transplant 12:828–836
149. Leung W, Iyengar R, Turner V et al (2004) Determinants of antileukemia effects of allogeneic NK cells. J Immunol 172: 644–650
150. Gagne K, Brizard G, Gueglio B et al (2002) Relevance of KIR gene polymorphisms in bone marrow transplantation outcome. Hum Immunol 63:271–280
151. Venstrom JM, Pittari G, Gooley TA et al (2012) HLA-C-dependent prevention of leukemia relapse by donor activating KIR2DS1. N Engl J Med 367:805–816

# Chapter 10

# Methods of Detection of Immune Reconstitution and T Regulatory Cells by Flow Cytometry

**Richard Charles Duggleby and J. Alejandro Madrigal**

## Abstract

Allogeneic hematopoietic stem cell therapy (HSCT) remains one of the few curative treatments for high-risk hematological malignancies (high-risk leukemia, myelodysplastic syndromes, advanced myeloproliferative disorders, high-risk lymphomas, and multiple myeloma) and is currently applied in more than 15,000 patients per year in Europe. Following HSCT, patients experience a period of reconstitution of the immune system, which seems to be highly dependent on conditioning, immunosuppression regimes, and the level of adverse events the patients experience. During this reconstitution period, the patient is immune compromised and susceptible to opportunistic infections and disease relapse. Consequently, a large number of clinical studies have been devoted to monitoring the recovery of the immune system following HSCT in the hopes of determining which cellular subsets are indicative of a favorable outcome. In this chapter we review the methods that have been employed to monitor the immune reconstitution and what clinical observations have been made. Of particular interest is the regulatory T cell (Treg) subset, which has been associated with tolerance and has been the subject of recent clinical trials as a possible cellular therapy for rejection reactions. Finally we will detail a proposed methodology for the flow cytometric assessment of cellular reconstitution post-HSCT.

**Key words** Hematopoietic stem cell therapy, Cellular reconstitution, B cells, NK cells, T cells, Regulatory T cells, Dendritic cells, Whole blood flow cytometry

## 1 Introduction

Since its introduction in the 1970s, allogeneic HSCT remains the only curative treatment for high-risk hematological malignancies (high-risk leukemia, myelodysplastic syndromes, advanced myeloproliferative disorders, high-risk lymphomas, and multiple myeloma) and is currently applied in more than 15,000 patients per year in Europe. While patient numbers are rapidly increasing, the treatment still carries a significant risk to the patient in the form of treatment failure and life-threatening complications. Treatment modalities and patient disease variability and background conditions necessitate a patient-tailored therapy as physicians try to respond to early indications of failure and treatment complications.

Meral Beksaç (ed.), *Bone Marrow and Stem Cell Transplantation*, Methods in Molecular Biology, vol. 1109,
DOI 10.1007/978-1-4614-9437-9_10, 

Depending on the conditioning the patient receives, patients will invariably be either completely or partially immune deficient immediately following transplantation of the stem cell graft. As a result, three main issues can occur as the immune system reconstitutes, two associated with transplant toxicity and the third related to treatment failure. The first is graft versus host disease (GvHD); with HSCT in malignant diseases, the purpose of the transplantation is to allow the reconstituting donor cells to recognize the recipient malignant cells as foreign and therefore mount an immune response that clears the malignant cells (a graft versus leukemia (GvL) response). Unfortunately while recognition of the donor as foreign seems to allow for a GvL effect, it also appears to allow for unwanted responses to tissues and immune cells to varying degrees. While there has been extensive research attempting to separate these effects, the ability to promote GvL over without GvHD remains elusive. The second is opportunistic infections; prior to full immune reconstitution, the patients lack the ability to control either preexisting or opportunistic infections, often common infections such as Epstein–Barr virus (EBV) and cytomegalovirus (CMV), with potentially fatal consequences. Finally there is relapse; while GvHD is an unwanted side effect of allogeneic HSCT, failure to mount a successful GvL response will mean failure to clear the malignant cells and results in disease relapse.

The purpose of monitoring immune reconstitution is to be able to determine which cell types are involved in these events, to both be able predict their onset and be able to influence their effect in the future. This chapter will discuss which cell subsets have been monitored in clinical studies in the past, how they were monitored, and how relevant they were to patient outcome. Also discussed will be the practical aspects of monitoring regulatory T cells (Treg). These cells, as natural immune regulators, have attracted increasing interest for their role in central and peripheral tolerance and how their reconstitution after HSCT might influence GvHD, GvL, and responses to infection. Finally a recommended method of cellular monitoring by flow cytometry is detailed, including potential practical issues that arise when analyzing patient blood.

## 1.1 Factors Affecting Immune Reconstitution

This chapter will discuss the various markers that can be used to follow immune reconstitution. However, how these markers are interpreted is highly dependent on the patient background in which the reconstitution is taking place. As HSCT therapies have become more common in patients of different ages and diseases, a number of overlaying factors have emerged that can influence the course of reconstitution. Among these are age, conditioning, and the appearance of GvHD.

*Age of the Recipient.* There have been a number of studies that have indicated an impact of age on reconstitution, in particular T cell

reconstitution, either through CD4+ cell reconstitution [1] or through quantification of T cell receptor excision circles or TRECs [2, 3]. TRECs, found in recent thymic emigrants as the result of generation of the variable region of the T cell receptor (TCR), are known to decline with age [4]. It is likely, therefore, that the underlying effect of age on reconstitution is due to its impact on the thymic-dependent pathway of T cell reconstitution; T cell reconstitution can be broken down into two main pathways, thymic-dependent and thymic-independent homeostatic reconstitution. The thymic pathway is the well-studied conventional T cell development pathway; mobilized stem cells enter a lymphocyte differentiation path whereby progenitor T cells traffic to the thymus and undergo positive and negative selection resulting in mature T cells exiting into the periphery. In homeostatic proliferation, naïve T cells expand in the lymphopenic environment following HSCT. The hypothesis is, therefore, that age will affect the thymic pathway over homeostatic proliferation. As is reviewed by Mackall et al. [5], the difference is that homeostatic proliferation might lead to deficiencies in the resulting T cell pool due to limitations in TCR repertoire.

*Immunosuppressive Therapy*. Another factor that needs to be considered is the effect of the conditioning and treatment to prevent GvHD. As reviewed by Chinen et al. [6], agents such as mycophenolate mofetil (MMF) and cyclosporin A (CSA) are designed to inhibit lymphocyte (in particular T cells) proliferation and differentiation, while antibodies such as anti-thymocyte globulin (ATG) and campath (anti-CD52) cause depletion of many cells but may favor particular subsets. All of which are likely to affect cellular reconstitution.

*GvHD*. From the start it was found that GvHD was adversely affecting reconstitution; delayed B and T cell reconstitution with reduced lymphocyte numbers and/or TRECs [7–10], with restrictions of the TCR repertoire [11]; and increased opportunistic infections [9, 12]. Animal studies suggest that GvHD causes thymic damage [13–15], which in turn would lead to poor thymic function.

*Conditioning*. Full myeloablative conditioning (MAC) is designed to remove as much of the residual disease as possible prior to transplantation. Conditioning can involve total body irradiation and chemotherapy that removes much of the recipient bone marrow and immune system. By comparison, reduced intensity conditioning (RIC) relies more on the GvL effect of the graft and involves less harsh conditioning. It has been noted that MAC regimes have a more delayed engraftment than RIC (as reviewed by Jimenez et al. ref. 16). RIC also tends to have less GvHD than MAC. In fact the reduced GvHD has such a profound effect on reconstitution

that in multivariate analysis it was found that RIC is the most important factor on the recovery of the T cell subset and TREC levels in the first few months following HSCT [16]. Thus, in this case, it is difficult to determine if the effect on reconstitution was due to the conditioning or due to reduced GvHD.

### 1.2 Monitoring Cell Subsets During HSCT

The majority of clinical studies follow a panel of cell subsets to monitor the course of the HSCT. Unfortunately, apart from a basic panel of cell types (platelets, neutrophils, and NK, T, B, and dendritic cells), there is very little consensus between centers, especially on subtypes. This is because the import of different subtypes of cells is very often dependent on the patient (disease, conditioning, and posttransplant therapy), which, as discussed above, can affect how each of these cell types reconstitutes and thereby skews the results from the "expected" reconstitution. However, in the following introduction, each of the main cell types will be reviewed for examples of how they have been assessed in the past and what clinical relevance has been observed. The subsequently suggested protocol will then reflect a "standard" panel.

#### 1.2.1 Platelets and Neutrophils

Platelets and neutrophils along with the white blood cell count are typically assessed as part of the standard, automated cellular assessment in clinical laboratories, sometimes referred to as the complete blood count (CBC). The CBC measures a number of parameters including white blood cell count and differential (numbers of neutrophils, lymphocytes, monocytes, eosinophils, and basophils). As platelets and neutrophils are some of the first populations to emerge following HSCT, they are often used as the earliest indication of engraftment. Standard indicators are levels above end points for several days. For example, Prasad et al. [17], in unrelated umbilical cord HSCT for pediatric patients with inherited metabolic disorders (no underlying GvL), used a neutrophil engraftment end point of greater or equal to $0.5 \times 10^9$ donor cells/L for 3 consecutive days and a platelet engraftment end point of $50 \times 10^9$/L or more, for 7 days. Using these end points, these pediatric patients (median age 1.5 year) had a median neutrophil engraftment of 22 days with 87 % cumulative engraftment by day 42. Meanwhile, platelets engrafted in a median of 87 days with a cumulative incidence of 71 % by day 180 [17]. As discussed above, in the 159 patients studied, underlying effects such as patient age, HLA, and seropositive status of the recipient were factors that affected time to engraftment along with more expected parameters such as CD34+ cell dose infused and colony-forming unit (CFU, a stem cell functional assay) infused. In adult recipient and donor peripheral blood HSCT (median recipient age 41, range 16–68), a study by Allan et al. [18] had a similar platelet and neutrophil engraftment end point criteria. In this study, platelet recovery was defined as three consecutive days with a platelet count of greater than $20 \times 10^9$/L. In both cases the median time to

platelet and neutrophil engraftment was 14 and 13 days, respectively. The time to engraftment also was associated with CD34+ dose infused. It can be seen from these two studies that these parameters can be wildly different in different clinical settings. However, in both studies the parameter fulfils the same basic role, as the earliest measure of engraftment, and in both cases reflected the efficacy of the transplantation by being affected by the CD34+/stem cell dose infused.

### 1.2.2 *Lymphocytes*

#### Natural Killer Cells

As one of the first lymphocyte subsets to return to normal levels post-HSCT (usually with 1–2 months), Natural killer (NK) cells have been extensively studied, as described in a recent review by Bosch et al. [19]. As part of the innate immune system, they have antimicrobial and antiviral activity as well as, importantly, antitumor/leukemic activity. It is for that reason that NK cells have attracted interest as possible therapeutic targets, with the aim to improve their reconstitution and function to combat both relapse and opportunistic infections without accompanying GVHD. In fact, it is hypothesized that by deleting mismatched allo-antigen presenting cells (NKs are activated by the absence of the correct HLA molecules; the missing self-hypotheses [20]), they might reduce GvHD. Early clinical studies tended to follow a basic definition of NK cells (Fujimaku et al. [21]), reporting that CD3–CD56+ had recovered to normal levels by 1 year, with no correlation with GvHD. More currently studies use a more detailed definition with NK cells being characterized as CD3–$CD56^{bright}CD16+/-$ or $CD3–CD56^{dim}CD16+$ with the former producing cytokines and the latter having high CTL activity (Reviewed by Cooper et al. [22]). Following these populations, Komanduri et al. found that NK reconstitution was favored in T cell-depleted environment [23]. By observing $CD56^{bright}CD16^{dim}$ and $CD56^{dim}CD16^{bright}$ populations, it has been noted that the $CD56^{bright}CD16^{dim}$ population is the most prominent reconstituting population [19, 24], although CD56–CD16+ cells can be found in significantly higher numbers than in healthy subjects [24].

Using these markers, a number of studies have linked NK reconstruction with clinical outcomes of HSCT. Porrata et al. observed in autologous HSCT that low numbers of total NK (CD56 bright and dim) cells (less than 80 cells/μL) in the first 2 weeks were associated with low overall survival (OS) and pathogen-free survival [25]. Chang et al., following $CD56^{bright}$ cells (less than 7 cells/μL in 14 days), found a similar association in haploidentical HSCT and with Transplant related mortality (TRM) [26]. Finally Baron et al., following donor chimerism of flow-sorted NKs, found that less than 50 % donor chimerism at day 14 was associated with rejection and slower establishment of complete donor chimerism led to a decrease in relapse-free survival [27]. Taken together these would seem to support the hypothesis that low NK numbers might result in increased pathogen infections and NK tolerance of

either the recipient or the donor leading to relapse. There is also association with killer cell immunoglobulin-like receptor (KIR) mismatching with their ligands but this will be dealt with comprehensively in other chapters.

*B Cells*

B cells play an important role in the adaptive immune response to microbial and viral infections, their absence during reconstitution indicating a comprised immune system. The B cell development phenotype is reviewed by Marie-Cardine et al. [28]. Briefly, the reconstitution of B cells as they differentiate from stem cells can be followed using CD19 expression. CD19+ pre-B cells differentiate from CD34+ stem cells and then into pro-B cells following immunoglobulin (Ig) heavy chain rearrangement. Light Ig chain rearrangement leads to immature B cells, which, when in the periphery, are known as transitional B cells. Pre-, pro-, and immature/transitional B cells all express CD24, CD38, and CD10. Encounters with antigens lead to either deletion (with self-antigens) or maturation into mature/naïve B cells and expression of IgM and IgD. By selecting on CD19+ cells, transitional B cells can be distinguished from mature B cells, in the peripheral blood, by $CD24^{hi}CD38^{hi}$ expression and the presence of CD10, compared to the $CD24^{int}CD38^{int}$CD10– mature phenotype [28]. As is nicely demonstrated by Sugalski et al. [29], naive B cells, memory B cells, and activated B cells can then be distinguished as CD10–CD21+CD27–, CD10–CD21+CD27+, and CD10–CD21–CD27+, respectively.

B cells take considerable time to reconstitute, with normal levels not being reached until 1–2 years [30]. Reconstitution is reminiscent of normal B cell development with naïve or immature cell predominating and very few memory B cells (defined by IgD– [30, 31]). Clinical observations include low numbers at 6 months being associated with poor outcome (death, relapse, graft failure [32]) and low numbers at 80 days with increased infection [33]. There is also evidence that both acute GvHD (aGVHD; GVHD <100 days posttransplant) and its treatment can lead to depressed B cell precursors and in turn depressed B cell numbers [34]. Fujimaki et al. also found evidence for suppressed B cell reconstitution with chronic GvHD (cGvHD; GvHD +100 days), by serum Ig levels. However, this was also associated with depressed CD4 cell reconstitution leading to the speculation that the B cell effect is a result of less T helper cell activity [21]. Taken together this would suggest that a depressed reconstitution might indicate increased risk of graft failure and infection but that underlying GvHD and effects of T cell reconstitution could be contributing factors.

T Helper/Cytotoxic Cells

T and B cells represent reconstitution of the adaptive immune response and are attributed (along with NK cells) with the majority of GvL effects; T cell-depleted grafts while having lower risk of

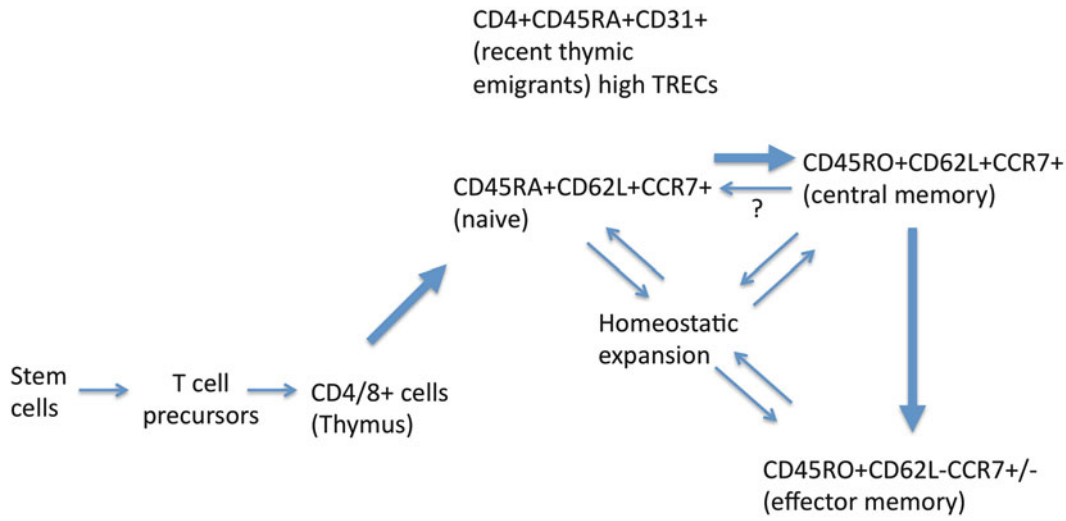


**Fig. 1** T cell phenotype during reconstitution. Hypothesis of T cell reconstitution. Shown are common T cell subtypes and their hypothetical progression through thymic reconstitution (*bold arrows*). It has been observed that in a lymphopenic environment, CD45RA+ and CD45RO+ can undergo homeostatic expansion with CD45RO+ cells predominating [112]. Finally, indicated by the *question mark*, there is evidence that reversion of the CD45RO+CD45RA– phenotype can occur to a CD45RA+ phenotype [40]

GvHD but carry a higher risk of relapse and graft failure [35–37]. Consequently, T cells are followed with the expectation that they are indications of recovery of the immune system and the source of a GvL effect. In line with this, a recent study by Bartelink et al. found that higher numbers of CD4+ T cells at earlier time points (0–90 days) were predictive of reduced patient mortality in pediatric HSCT [38].

The standard enumeration of T cells is usually through absolute counts of CD3+, CD4+, and CD8+ cells. However, the presence of the CD45RO+CD62L+ and CD62L– expressing cells indicate central and effector memory populations (as reviewed by Sallusto, Geginat, and Lanzavecchia [39] and shown in Fig. 1). The emergence of naïve CD45RA+CD62L+CCR7+ cells would indicate reconstitution, probably through the thymic-dependent pathway (Fig. 1). However, the emergence of these markers alone from the T cell pool is not conclusive. Due to the possibility of reversion of memory cells to a CD45RA+ phenotype ([40] and shown in Fig. 1), it can be argued that this phenotype alone is not sufficient to define the naïve T cell pool. As a result some studies have also included enumeration of TRECs (as discussed above) to ensure that this population is truly naïve [2, 7, 16, 41]. Since TRECs are affected by proliferation, it might be more accurate to associate their presence with recent thymic emigrants; while they often express CD45RA [2], cells with high TRECs best correlate with a CD45RA+CD31+ phenotype [42].

As reviewed by Bosch et al. [19], CD8 T cells typically take 6 months to reach normal levels with CD4 cells lagging behind at almost a year. It has also been noted that following HSCT there is a predominance of memory/effector cells, with very low numbers of naïve cells and TRECs [2, 41, 43]. This suggests that either these cells are mature cells from the graft/donor or they have been derived from homeostatic expansion of mature cells. However, high levels of T cell proliferation, such as GvHD, could be reducing the apparent naïve population (affecting both CD45RA and TRECs). In a study performed by Jimenez et al., HSCT patients on a RIC regime had lower levels of GvHD compared with patients on MAC regime [16]. In this study, there were significantly higher naïve cells and TRECs at earlier time points in the RIC patients compared to the MAC patients. Since they did not correlate with the naïve cell and TREC numbers in the graft, it can only be assumed that this apparent increase in the thymic-dependent reconstitution was through either improved thymic function or lower GvHD [16].

As discussed above, GvHD and therapies used to treat GvHD have been found to affect T cell reconstitution in a number of studies. Fujimaki et al. [21] reported that naïve cells (CD4+CD45RA+) were suppressed in chronic GVHD patients with all other subtypes unaffected and returning to normal after 1 year. In a more recent study, Komanduri el al. observed longer lymphopenia and reduced naïve cell (CD45RA+CCR7+) reconstitution in patients receiving CB as a stem cell source compared to adult donors [23]. However, the authors had to note that the CB recipients tended to have received more pre-transplant treatments and more myeloablative conditioning than the adult allo-SCT, highlighting that interpretation of the T cell reconstitution data is highly dependent on the preconditioning, GvHD, and therapy.

*Functional T Cell Recovery*

The Komanduri study of 2007 also demonstrates another important parameter that can be assessed: functional T cell recovery [23]. In the case of the Komanduri study, this was in the form of superantigen responses (streptococcal enterotoxin B, SEB) and, in seropositive recipients, a determination of both the functional response to and recovery of CMV-specific responses. CMV is one of the most common posttransplant opportunistic infections, especially since seropositive allo-SCT donors may not be available for a seropositive donor while, in the case of CB SCT, the donor will be completely naïve to CMV. Komanduri et al. assessed the recovery of CMV-seropositive recipient PBMC with CMV peptides (pp65) and seronegative recipient PBMC with the superantigen SEB. The results showed that the delayed lymphopenia that had been observed in the CB SCT patients also reflected a reduced activity to SEB and CMV peptides.

If the patients respond to pp65 peptide, then they may also respond to pp65 tetramers. This enables the CMV-specific response to be enumerated by flow cytometry. Using this technology, Gratama et al. [44] followed the reconstitution of CMV-specific responses post-HSCT in seropositive recipients with either seropositive or seronegative donors. They found that failure to recover HLA-A2-specific CD8+ T cell responses was associated with development of disease and that the number of tetramer-positive CD8 cells in the graft inversely correlated with the number of recurrent CMV infections. In this study only 1 in 5 of the seronegative donors generated a CMV-specific response. Interestingly, in the Komanduri study, despite depressed functional responses to SEB and pp65, there were significant numbers (in 50 % of recipients) of CMV-specific T cells present after CB SCT, despite the naïve nature of the CB [23].

While tetramer technology has been used to monitor the reconstitution of CMV responses with some success (see above), this methodology has some serious limitations; firstly, the dominant epitopes in the infection are required to be known and even then are likely to be restricted to specific HLA. In the case of CMV, for example, the NLV peptide (NLVPMVSTV reviewed [45]) is restricted to HLA-A*0201. Obviously this limits the patients that reconstitution can be followed in. Secondly the response only monitors CD8+ responses (class II tetramers are very rare); therefore, patients deficient in CD4 help will be missed while apparently reconstituting a specific response normally. In cases where the dominant epitopes are not well known, such as in adenovirus responses, the only real option is the more recently developed INFγ capture assay. The most widely available is that developed by Miltenyi Biotec. This conjugates anti-INFγ antibody to anti-CD45 such that IFNγ released by the cell is captured after secretion. This allows for longer stimulations than brefeldin A-treated cells for intracellular cytokine detection and allows for live isolation for adoptive therapy. Using this technology Feuchtinger et al. [46] showed that the number of adenovirus (ADV)-specific cells was significantly higher in HSCT patients that went on to clear the infection.

### Regulatory T Cells

In recent years it has become clear that regulatory T cells (Tregs) are a critical component of both central and peripheral tolerance mechanisms. This subset of T cells has been further subdivided into thymically derived Tregs (sometimes referred to as “natural” Tregs reviewed [47]) and induced forms, such as Tr1 and Th3 cells, that can be generated from non-regulatory CD4+CD25– cells [48, 49]. In humans, imbalances in this subset have been reported in an increasing list of autoimmune diseases (reviewed [50]), and a role for Tregs in controlling responses to infectious

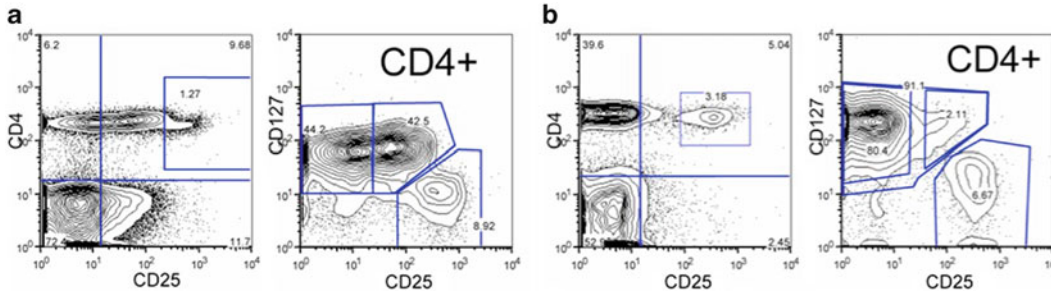


**Fig. 2** Characterization of Tregs from adult and cord mononuclear cells. PBMC (**a**) and cord blood CBMC (**b**) by first comparing CD4 and CD25 expression on lymphocytes by forward and side scatter and then CD25 and CD127 expression on CD4+ cells as described by Seddiki et al. [62]

agents has also been demonstrated [51–55]. There is even evidence that some pathogens elicit Tregs to inhibit the T cell responses mounted by the host [56, 57].

Ever since regulatory T cells (Tregs) were discovered to have a central role in peripheral tolerance, transplant researchers have speculated if these properties could be manipulated to promote graft tolerance. This is interest was heightened by the discovery of their prominent role in nature's temporary graft; pregnancy [58]. It is attractive, therefore, to speculate that Tregs could be used to promote tolerance in solid organ and allo-HSCT to ensure long-term acceptance of the graft. To date, there have been two phase I clinical trials held in HSCT, to determine the safety and feasibility of using Treg cell therapy to prevent GvHD. In these trials Tregs were either autologous to the stem cell graft [59] or third-party expanded cell lines from CB [60], and no safety issues were indicated.

Historically Tregs have been distinguished by the surface phenotype by which they were originally identified of CD4+CD25+/hi [61], examples of which are shown in Fig. 2. Later observations by Sedikki et al. [62] indicated that low surface expression of the IL-7 receptor (CD127) could separate CD25hi Tregs from CD25intermediate conventional T cells (Tcons) in PBMC (Fig. 2). The naïve state observed in CBMC results in a more distinct Treg population (Fig. 2). Unfortunately, CD25 expression is also up-regulated on activated Tcons. The only truly unique marker of Tregs so far elucidated is high and sustained expression of transcription factor FOXP3; introduction of FOXP3 expression into CD4+CD25− cells is sufficient to confer regulatory activity [63–65], although caution should be applied as lower levels of FOXP3 expression have been detected in strongly activated Tcons [66]. The harsh membrane permeabilization conditions required for detection of FOXP3 make it unsuitable for quantitative analysis and for

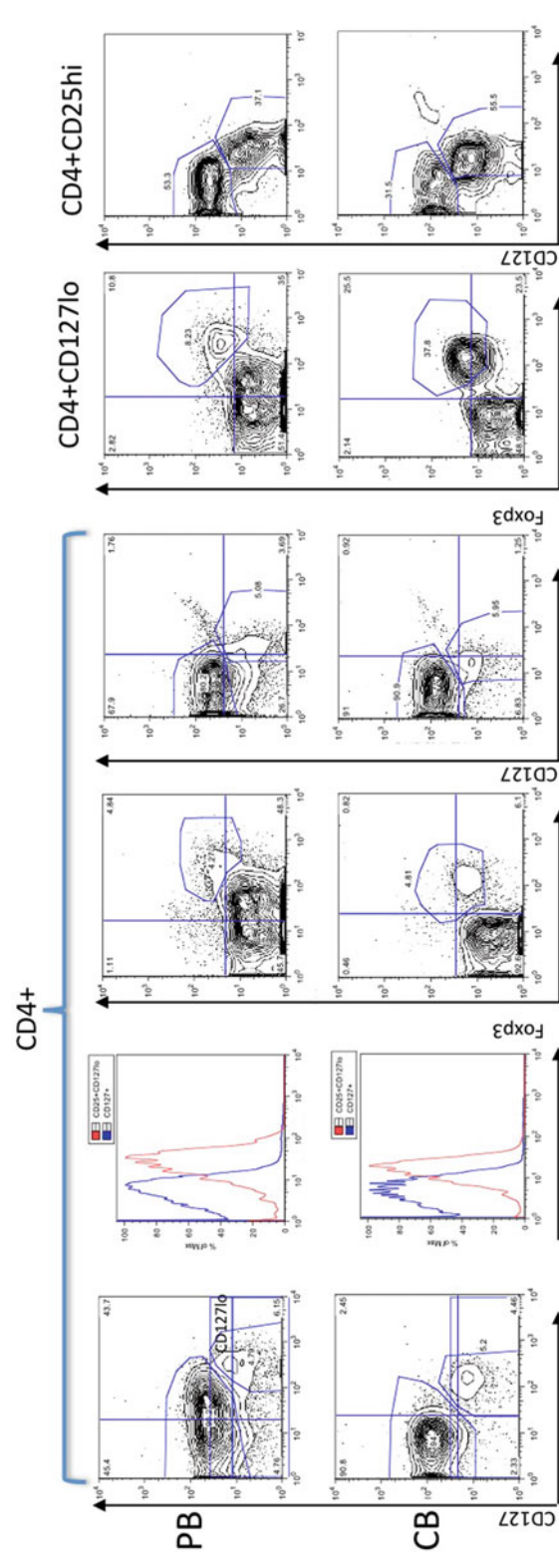


**Fig. 3** Distinguishing Tregs from Tcon in peripheral blood (PB) and umbilical cord blood (CB) using CD25, CD127, and FOXP3 expression. Shown is the CD4+ gated population characterized for CD127, CD25, and FOXP3 expression. Histograms show the FOXP3 expression of either CD25+CD127−/lo or CD127+ population gated as shown in the adjacent plots. Gating for CD4+CD127lo (CD127lo gate in first plot) or CD4+CD25hi (gate similar to that shown in Fig. 2) significantly improves definition of the FOXP3+ Treg population (last two plots)

isolation, but it remains the best marker to determine the efficacy of any surface gating strategy. As shown in the example characterizations (Fig. 3), combinations of gating on CD4, CD25, CD127, and FOXP3 can help define this relative rare population from the Tcons.

The identification of regulatory T cells as a suppressive subset of cells that appear to be integral to central and peripheral tolerance led to a great interest as to how this subset might be involved in the control of GVHD following HSCT. The hypothesis was that Tregs would naturally resist GVHD, and, therefore, low Treg numbers during reconstitution would be associated with increased GVHD. As a result a number of clinical studies have followed the involvement of Tregs in GVHD and infection. Several different studies found that the Treg content of the graft seems to be important to control GVHD [67–69]. It should be noted, however, that these observations seem to only apply in myeloablative conditioning. In fact, Wolf et al. noted that this association was lost in a parallel study performed in RIC [67]. It could therefore be speculated that the Treg content of the donor graft might be important, but only in myeloablative conditions, where residual conditioning can still affect the incoming donor cells, might the Treg load be particularly crucial.

The story as regards the reconstituting Treg populations has been less clear-cut. Some studies show a suppression of Treg numbers in aGVHD and cGVHD patients, while others show either increased numbers or no association at all. It has been noted in reviews [70] that these discrepancies might arise from differences in the methods used to identify Tregs (whether CD4+CD25+ alone are considered to be Treg or if FOXP3 assessment is employed) as mentioned above. Certainly this might be true for Clark et al.'s study in 2004 [71], who found that increased CD4+CD25+ numbers were linked to increased GVHD, and Sanchez et al. [72] who found no significant correlation between CD4+CD25+ numbers and cGVHD in the long term. However, this is not always the case; Watanabe et al. [73] showed increased CD4+CD25+FOXP3+ cells with aGVHD at day 100 post-HSCT and with cGVHD after that. By contrast Rezvani et al. [68] and Magenau et al. [74] both found that low CD4+CD25hiFOXP3+ numbers at very early time points (30 days and 14 days, respectively) could predict the onset of aGVHD. Zorn et al. [75] linked decreased FOXP3+ Tregs with cGVHD, but in the same year Meignin et al. did not detect any correlation [76]. The timing of the observations does seem to be crucial. Observations predicting aGVHD seem to be at early time points, where the differences between GVHD and non-GVHD patients seem to be greater. In the Zorn study, the

median sampling time was 19–24 months, while in the Meignin study it was 31 months. One could speculate, therefore, that early suppression of Treg numbers might indicate a predilection to GVHD, while later the Treg numbers might even be higher, in response to inflammation (but failing to control it). Recently, Kawano et al. [77] noted that telomere lengths in Tcons and Tregs were significantly shorter in patients with GVHD; however, telomerase activity (enabling the telomere to be replaced and, therefore, allowing continued cell division) was higher in Tcons compared to Tregs, as was the anti-apoptotic marker Bcl-2. This might indicate that Tregs might even be proliferating in response to GVHD and that longer term these cells are likely to die rather than be maintained.

Other observations include those by Miura et al. [78] of low FOXP3 mRNA in GVHD patients and Ngoma et al. [79], associating delayed CD4+CD25hiFOXP3+ cells and GVHD. Finally those of Mielke et al. [80] who observed that after CD25+ cell deleted donor lymphocyte infusions (after culture to activate alloreactive cells) that patients with the highest GVHD had donors with the lowest Treg numbers. Taken together these studies suggest that Treg numbers early reflect the ability to control GVHD. However, an added complication to interpretation of the peripheral Treg numbers is the possibility of active GVHD in the tissues recruiting Tregs to the tissues; Rieger et al. [81] showed that active intestinal GVHD was associated with decrease FOXP3+ cell numbers in the gastric mucosa. Ngoma et al. [79] observed a similar effect in skin biopsies, while Wu et al. [82] demonstrated increased Tregs in skin biopsies after active GVHD. Unlike in the previous study, however, there was no comparison with the CD3+CD8+ population to determine if this was proportional to inflammation (Ngoma et al. found that the Tregs/CD3+CD8+ ratio favored CD8+ cells in skin GVHD)[79].

In conclusion, following Tregs can be predictive of GVHD, especially if care is taken to distinguish between activated Tcons and Tregs, either with FOXP3+ (which can only be used to determine a proportion of the absolute CD4+CD25+ cells) or using additional surface markers such as CD62L, CD27, and CD127. Either way, it is recommended that any definition of Tregs be validated with FOXP3 labelling even if it is not used in the final study.

#### 1.2.3 DC Reconstitution

Dendritic cell involvement in HSCT has recently been extensively reviewed by Stenger et al. [83]. It is important to note that while extensive research has been performed on the pathways of DC generation, it is clear from these studies that all DC subsets can be generated from both common lymphoid and myeloid progenitors.

The majority of these progenitors are CD135+ (Flt3) with Flt3L having a central role in DC generation and GM-CSF in generating DCs from monocytes.

In immune reconstitution, two main subtypes, myeloid DCs (mDC) and plasmacytoid DCs (pDC), have been surveyed for cell numbers and phenotype resulting in associations with GVHD and patient outcome. Conventional mDC are considered to be professional antigen-presenting cells, with the mature forms expressing high levels of MHC II and co-stimulatory molecules (CD83 and CD86). By contrast pDC display lower levels of MHC and co-stimulatory molecules [84]. After activation through toll-like receptors (TLR), pDC secrete type I IFN and stimulate CD4+ and CD8+ cells [85, 86], while mDC promote Th1 and CTL responses by secreting IL-12 [83]. This has led to the idea that pDC may promote peripheral tolerance, which may have implications post-HSCT. However, it is also thought that pDC are more likely to cross-present antigens (external antigen loading onto MHC I) and promote cross-presentation in mDC, which is more likely to promote tissue rejection by CD8+ cells (reviewed [85]).

Both DC subtypes are characterized by flow cytometry as MHC II+ and lineage or lin– (lacking mature surface markers CD2, CD3, CD4, CD8, CD5, CD14, CD16, CD56, CD19, CD20, B220). They have then been subcategorized as CD11c+CD123–BDCA3 (CD141)+ or BDCA1 (CD1b/c)+ for mDC and CD11c–CD123+BDCA2 (CD303)+ for pDC [83]. Also CD304 (BDCA-4/neuropilin-1) is almost exclusively expressed by pDC, even after culture (unlike CD303), as described by Dzionek et al. [87].

In animal studies, GVHD responses are CD4+ and CD8+ dependent and require recipient DCs [88–90] and donor DCs for maximal effect [90]. However, DCs also play a crucial role in T cell-dependent GvL with recipient DC being required for a full GvL effect [90–92]. For purposes of monitoring, however, a number of clinical observations link mDC and pDC absolute numbers to GVHD and patient survival. Reddy et al. have linked low total DC after median 500 days posttransplant with low overall survival (OS), increased relapse, and increased GVHD [93]. In MAC and RIC studies, pDC have been linked with increased GVHD and pDC and mDC with increased severity of GVHD. In one study, low pDC 3 months posttransplant (RIC) was associated with severe aGVHD, decreased OS, and increased non-relapse mortality; NRM (GVHD and infections) [94]. However, another study linked high pDC at 14 months with cGVHD [95]. Waller et al. found that higher pDC in BM (Bone Marrow) grafts was linked with cGVHD and increased relapse [96], while another study using mobilized stem cells (peripheral blood) found no cor-

relation with pDC and GVHD, but there was with relapse and OS (reviewed [83]). Clearly DCs are linked to GvHD, but the story remains unclear. In early reconstitution, they are perhaps important for preserving GvL and, therefore, are likely linked with outcome. Monitoring activation status of the DCs has met with limited success; CMRF-44+ in CD11c+ (mDC) correlated with the inset and severity of aGVHD; however, other maturation markers such as CD83 and CD86 do not seem to correlate [97]. It is possible, however, that cytokine secretion of IL-10 and IL-12 might be more predictive.

Overall, therefore, the timing of pDC and mDC reconstitution might be predictive of GVHD and OS, while initial and graft DCs numbers might be important for relapse. Again though, the influence of background conditioning and GVHD prophylaxis must be considered; calcineurin inhibitors (CNI), such as CsA, suppress antigen presentation, and glucocorticoid steroids inhibit maturation, activation of DCs, and secretion of TNFα, IL-1B, and IL-12 [98–100]. Meanwhile CNI and rapamycin can both decrease the expression of co-stimulatory molecules and stimulation of allo-T cells [101, 102]. Any of these backgrounds could potentially mask any predictive markers with DCs.

### *1.3 Monitoring Immune Reconstitution*

The method detailed below is designed to be a general method for current standard practice. Consequently, this protocol has been developed around four-color flow cytometry, principally using the BD FACSCalibur. However, the method can be modified for use with a Beckman and Coulter FC500.

## 2 Materials

### *2.1 Flow Cytometric Monitoring of Immune Reconstitution*

Shown in Table 1 is a recommended assessment panel for assessing cellular reconstitution in whole blood patient samples. The panel has been optimized for use on the FACSCalibur but with modifications can be adapted for use with a Beckman and Coulter FC500 (*see* **Note 1**). Antibody concentrations are not displayed as they should be optimized by the user (*see* **Note 2**). The use of whole blood can lead to complications associated with live/partially lysed red blood cells (RBCs) affecting both analysis (*see* **Note 3**) and compensation. Consequently, Table 2 details a suggested whole blood compensation panel. The panels should then be preprepared with 50 μl/tube with a final labelling volume (when including a 50 μL blood sample) of 100 μl in a suitable flow cytometry buffer (e.g., 2 % fetal bovine serum (FBS) in phosphate buffer saline (PBS)).

**Table 1**
**Antibodies for surface and intranuclear assessment for monitoring reconstitution**

| | Target | FL1 | FL2 | FL3 | FL4 |
|---|---|---|---|---|---|
| 1 | T/NK | CD16 (BD: 3G8) | CD56 (BD: B159) | CD3 (BD: SK7) | CD45 (BD: HI30) |
| 2 | Mono/B | CD14 (ImmunoTools: MEM-15) | | CD45 (BD: HI30)[b] | CD19 (BD: HIB19) |
| 3 | Tregs | CD4 (ImmunoTools: MEM-241) | CD127 (BD: HIL-7R-M21) | CD25 (Serotec: BC96)[b] | CD3 (BD: UCHT1) |
| 3b[a] | Tregs | CD4 (ImmunoTools: MEM-241) | CD127 (BD: HIL-7R-M21) | CD25 (Serotec: BC96)[b] | FOXP3 (eBioscience: PCH101) |
| 4 | T stages | CD4 (ImmunoTools: MEM-241) | CCR7 (BD: 3D12) | CD3 (BD: SK7) | CD45RA (BD: HI100) |
| 5 | T stages | CD8 (BD: SK1) | CCR7 (BD: 3D12) | CD3 (BD: SK7) | CD45RA (BD: HI100) |
| 6 | B stages | CD24 (Serotec: SN3) | CD38 (CD: HB7) | CD4 (BD: SK3) | CD19 (BD: HIB19) |
| 7 | B stages | CD27 (BD: M-T271) | CD10 (BD: HI10a) | CD19 (R&D: 4G7-2E3) | CD21 (eBioscience: HB5) |
| 8 | RTE | CD4 (ImmunoTools: MEM-241) | CD31 (BD: WM59) | CD3 (BD: SK7) | CD45RA (BD: HI100) |
| 9 | RTE | CD8 (BD: SK1) | CD31 (BD: WM59) | CD3 (BD: SK7) | CD45RA (BD: HI100) |
| 10 | Stems | CD45 (BD: HI30) | CD38 (CD: HB7) | CD34 (BD: 8G12) | CD133 (Miltenyi Biotec: 293C3) |
| 11 | MDC | lin1 (BD: cat. 340546) | CD1c (eBioscience: L161) | HLA-DR (BD: G46-6) | CD11c (BD: B-ly6) |
| 12 | PDC | lin1 (BD: cat. 340546) | CD123 (BD: 7G3) | HLA-DR (BD: G46-6) | CD304 (Miltenyi Biotec: AD5-17 F6) |

Fluorochrome conjugates shown are fluorescein isothiocyanate (FITC) for FL1 channel, phycoerythrin (PE) for FL2 channel, peridinin-chlorophyll-protein complex (PerCP) for FL3 channel, and allophycocyanin (APC) for FL4 channel

Panel 10: Note that this a class II antibody and not the standard ISHAGE configuration for accredited CD34+ enumeration. For this either CD34-FITC or CD34-PE should be used with a class III antibody such as clone 581

[a]Note that tandem dyes are often affected by fixing. If this proves to occur, we recommend modified panel 3 of CD3-PerCP and CD25-APC and 3b of FOXP3-PerCP and CD25-APC

[b]Indicate PE-Cy5 conjugated antibodies, a tandem dye of phycoerythrin and a cyanine dye (PE-Cy5) instead of PerCP antibodies. A different compensation matrix will be required

**Table 2**
**Whole blood compensation panel**

| | FL1 | FL2 | FL3 | FL4 |
|---|---|---|---|---|
| Control 1 | CD45-FITC (BD: HI30) | – | – | CD45-APC (BD: HI30) |
| Control 2 | – | CD3-PE (BD: HIT3a) | – | CD45-APC (BD: HI30) |
| Control 3 | CD45-FITC (BD: HI30) | – | CD3-PerCP (BD: SK7) | – |
| Control 3b[a] | CD45-FITC (BD: HI30) | – | CD3-PeCy5 (BD: UCHT1) | – |
| Control 4 | – | CD3-PE (BD: HIT3a) | – | – |
| Control 5 | – | – | – | CD45-APC (BD: HI30) |
| Control 6 | – | – | – | – |

[a]Indicates alternate control 3 for Pe-Cy5 compensation matrix

## 3 Methods

### 3.1 Sampling Times

The reconstitution data described in Subheading 1 is summarized in Fig. 4. Using Fig. 4 as a guideline indicates that samples should be taken at short intervals initially ($t$=0, 14, 30, 100, and 180 days) with wider intervals later (1, 1.5, and 2 years). Full cellular recovery should be completed by 2 years. Useful data can also be obtained from the graft (*see* **Note 4**).

### 3.2 Assessments of Samples Whole Blood

1. Before performing flow analysis, a total nucleated cell count should be done for each unit under test using an automatic cell counter or Turk's solution assessment by hemocytometer.
2. Calculate the volume of blood required for $1.0\times10^6$ to $0.6\times10^6$ cells. If possible, check if the total RBC count (using an automatic cell counter) will exceed $175\times10^6$, and if so, reduce the calculated volume of blood accordingly. This is to ensure complete lysis of red cells occurs in the assay.
3. If absolute counts are being recorded, then use either TruCount (BD) tubes or equivalent. If absolute counts are not required, use a standard 5 mL round-bottomed tube.
4. Using the reverse pipetting technique, add the prescribed volume of blood. Adjust to 50 μL with flow cytometry buffer if required.

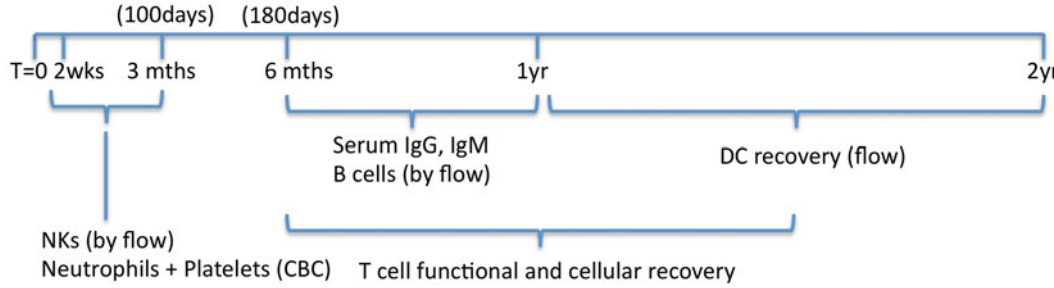


**Fig. 4** Cellular recovery time scales. Shown is a summary of the time course of reported cellular recovery as described in Subheading 1

5. Add 50 μL of the required antibody cocktail to each tube and incubate 10 min 4 °C in the dark.
6. Add 900 μL of freshly prepared BD Pharm Lyse solution. Vortex gently to mix and incubate at 15 min room temperature.
7. Once the samples have resolved (become as clear as possible), they can be acquired. Note that if they do not resolve, add more lysis buffer, noting the final total volume.
8. Acquire sample after performing a compensation setup. TruCount beads are only 6 μm. Therefore, ensure that the FSC used to exclude debris is not also excluding the beads.
9. For intranuclear labelling of FOXP3, collect the lysed cells by centrifugation at 400–500 × *g* 5 min 4 °C. Then resuspend in perm/fix buffer (eBioscience). Intranuclear labelling can then be performed following the eBioscience recommended protocol in the same manner as surface labelling of mononuclear isolated cells.

### 3.3 Absolute Count Calculation

For acquisition of beads, refer to the ISHAGE guidelines [103] or later studies, removing duplexes [104].

*Calculation*

- Bead concentration = total number of beads/volume of sample in TruCount tube.
- Volume of sample passed through flow cell = bead count/bead concentration.
- Cell concentration in sample in TruCount tube = events of interest/volume passed through flow cell.
- Cell concentration in blood sample = cell concentration in sample in TruCount tube × (volume of sample in TruCount tube/volume of blood added).

### 3.4 Compensation

Refer to Table 2, compensation panel, and *see* **Note 5**.

#### 3.4.1 Whole Blood Compensation

1. Use unlabelled control 6 to set background.
2. Take an aliquot from control 1 (FITC and APC) and an aliquot from control 5 (APC only) and combine. During acquisition, gate on CD45-APC-positive lymphocyte ($CD45^{high}SSC^{low}$) events to remove RBCs (RBC-). Adjust the background fluorescence (FL1 and FL2 voltage) on the RBC- and FL1- and FL2- negative events (the APC only added cells). Compensate FL1 to FL2 (using the double-stained cells).
3. Acquire control 2 gating on CD45-APC events (RBC-). Adjust the FL3 voltage to adjust the RBC- background. Compensate FL2 into FL1 and FL3 using CD3+ and CD3– lymphocytes.
4. Acquire control 3 gating on CD45-FITC-labelled lymphocytes to exclude RBCs. Compensate FL3 into FL2 and FL4 using CD3+ and CD3– labelling.
5. Take and aliquot of control 2 (PE and APC labelled) and mix with an aliquot of control 4 (PE only labelled). Gate on CD3+ lymphocytes and compensate FL4 into FL3.

### 3.5 Gating Cells from the Recommended Panel

Detailed below is a suggested gating protocol for analysis of the panel. A small pilot study is recommended to optimize both acquisition times (*see* **Note 6**) and controls to aid analysis (*see* **Note 7**).

*Panel 1: T Cells and NK Cells* (*T/NK*). Gate all CD45+ cells as described in the ISHAGE guidelines for the assessment of stem cells in BM, peripheral blood, and umbilical cord blood [103]. From this, a plot of CD3 against CD56 gives CD3+ CD56– T cells, CD3+CD56+ NKT cells, and CD3–CD56+ NK cells. Gating CD3– and a plot of CD56 against CD16 distinguishes CD56bright and CD56dim as shown by Takahashi et al. [105].

*Panel 2: Monocytes and B cells* (*Mono/B*). Gate all CD45+ and then CD14+ and CD19+ after gating lymphocyte-/monocyte-sized cells by forward (FSC) and side scatter (SSC). CD14+ monocytes are larger by FSC and SSC than CD19+ B cells.

*Panel 3: Regulatory T cells* (*Tregs*). Gate CD3+ and then gate CD4+CD25hiCD127lo Tregs as shown in Fig. 2. As indicated (panel 3b), CD3 can be substituted with FOXP3 (PCH101) with intranuclear staining to stain FOXP3+ cells (as shown in Fig. 3). While absolute counts can be performed from whole blood using the stated panel 3, the permeabilization and extensive washing required means that absolute counts from this alternative panel would be inaccurate. However, a surrogate FOXP3+ absolute count, using the proportion of FOXP3+ cells of the CD4+ cells, can be derived from the CD4 absolute count, as described by Meganau et al. [74].

*Panel 4 and 5: T cell stages* (*T stages*). Gate CD3+CD4+ events, then CCR7+CD45RA+ naïve cells, CCR7+CD45RA– central memory, and CCR7–CD45RA– effector memory. If CD45RA labelling does not generate a clear positive and negative population, CD45RA can be substituted for CD45RO (CD45RO+ and either CCR7+ or CCR7– for central and effector memory populations). Similar gating is performed for CD8 cells. Phenotypes are reviewed by Sallusto et al. [39] and are also summarized in Fig. 1. An example characterization of healthy cells before and after leukemic expansion is shown by Barbui et al. [106].

*Panel 6 and 7: B Cell Stages* (*B Stages*). Gating CD19+ lymphocytes (FSC and SSC then CD19+CD4–) allows for detection of transitional and mature B cells by CD24 and CD38 expression, as described in Subheading 1 and by Marie-Cardine et al. [28]. CD4 labelling is included as T cells can also express CD38. With panel 7, gating on CD19+ lymphocytes, the naïve B cell population, resting memory, and mature/activated B cells can be distinguished from a plot of CD27 and CD10 and then CD21 and CD27 (on the CD10- population). Naïve B cells are CD10–CD21+CD27–, resting memory cells are CD10–CD21+CD27+, while CD10–CD21–CD27+ represents the mature/active B cells. An example of such gating is shown by Sugalski et al. [29].

*Panel 8 and 9: Recent Thymic Emigrants* (*RTE*). Gate CD3+CD4+ cells and then CD31+CD4RA+ as described by Kimmig et al. [42]. This population represents recent thymic emigrants and also has the highest TREC content by PCR. Gate the same way for CD8+ cells (panel 9) as there is evidence that CD8+CD31+CD45RA+ cells are also thymic emigrants; however, the correlation is less in disease states [107].

*Panel 10: Stem Cells* (*Stems*). Stem cells CD34+ and CD133+ should be assessed from the CD45+ population, with CD38+ cells indicating a more mature population. Ideally, gating should refer to the ISHAGE guidelines (CD45low, lymphomono back gating to reduce nonspecific events) [103, 104].

*Panel 11, Myeloid Dendritic Cells* (*MDC*), *and Panel 12, Plasmacytoid Dendritic Cells* (*PDC*). Panel 11: gate Lin- events against FSC or SSC and then select HLA–DR+ events (also against either FSC or SSC). A plot of CD11c against CD1c should give a CD11c+CD1c+mDC population (MacDonald et al. illustrates a characterization of human peripheral blood DCs [108]). Panel 12: gate Lin- events against FSC or SSC and then HLA–DR+ in the same manner as panel 11. Myeloid and plasmacytoid DC are both CD123+, however, CD304 expression almost exclusive to pDC, even after culture (unlike CD303), as described by Dzionek et al. [87]. Consequently a plot of CD123 against CD304 should distinguish mDC from pDC.

## 4 Notes

1. *Adapting to Other Flow Cytometers.* Unless a two-laser FC500 machine, with a laser exciting in the 635 nm range is specified, then the use of the fluorochrome allophycocyanin is restricted. In these circumstances, this fluorochrome should be substituted for the tandem dye conjugate ECD (PE-Texas Red). On the FC500 the dye is detected in the FL3 channel with dyes that are detected in the FL3 on a FACSCalibur (PE-Cy5, PerCP, PE-Cy5.5) being detected in the FL4 channel on the FC500.
2. *Optimization of Labelling.* All antibody labelling should be optimized/titrated using health control PBMC and/or whole blood. For robust, repeatable identification and absolute counts, the labelling should be optimized for gating rather than for characterization, i.e., CD3, CD4, and CD8 labelling should be optimized to achieve the most defined populations, with the greatest difference between positive and negative events, even if this means higher background labelling. Whole blood and patient blood can have high background noise, especially in an inflammatory setting. Consequently, well-defined populations ensure that absolute count data is as accurate as possible and allow for minimal control samples. For a more detailed review, Maecker et al. discuss the issues associated with standardization of cellular subset analysis in clinical studies, including antibody selection and the extension of flow cytometry panels from 4 colors to 8 colors with the newer model flow cytometers [109].
3. *Use of Whole Blood.* Whole blood samples rarely lyse with complete efficiency and cord and patient samples are often separate with varying degrees of efficiency on Ficoll-Paque density gradients. The practicalities of collecting patient samples often involve comprises such that the time between collection and assessment can be less than ideal. As a result RBC contamination of both lysed and non-lysed is often a major concern during flow acquisition and analysis. RBCs are negative for all of the markers used in the panel, but where possible CD45 is included in the labelling. This allows for a gate for general leukocytes. To verify the efficacy of lysis and the gating, the CD45+ cells should be enumerated; this should correspond closely with an automatic cell counter or Turk's solution assessed total nucleated count (TNC). Additional lysis solution may be required if discrepancies occur.
4. *Sampling Times.* As described in Subheading 1, ideally the graft itself can contain useful cellular parameters. However,

ethically it is very difficult to take any more samples than is routinely assessed by the transplant center or risk affecting cell dose and, therefore, success of the graft. Transplant centers will routinely assess general cellular content CD3 and CD34 as these parameters have been found to be risk factors in the success of the graft [17, 110, 111]. The following suggested method, therefore, focuses on samples taken from the recipient.

5. *Compensation*. Ideally, if a mononuclear preparation is being used, compensation should be performed with the standard single color stains of each marker. However, with whole blood usage for absolute counts, a number of problems can arise. RBCs have their own intrinsic fluorescence and can be present in such high numbers that they obscure the background fluorescence of the leukocytes. Compensation can then be erroneously made where the MFI of the cells is compared with the MFI of unlabelled RBCs. Compensation and calibration with beads can be performed, with the advantage that machine noise is reduced. However, as indicated by the manufactures of calibration and compensation beads, final compensation should always be completed using cellular controls. Thus a whole compensation matrix has been suggested.
    - The matrix relies (on the FACSCalibur) on low spectral overlap between FL1 and FL2 channels with the FL4 channel and reduced interactions between FL1 and FL3 channels after compensation of the FL1 and FL2 channels. For the single-laser FC500, PerCP and PE-Cy5 should be used instead of the APC controls (then appear in the FL4 channel on the FC500). However, it should be noted that there is more spectral overlay.
    - It is impractical to compensate on rare events, such as CD34+ cells. Compensation, even automated, requires an average MFI for the positive population so that it can be compared with the MFI of the unlabelled population for that parameter. This often means thousands of events need to be collected for an accurate mean fluorescence. In the suggested panel, CD45 and CD3 labelling is used, but any substitute population should have equivalent MFI to the test labels.
6. *Acquisition Times*. It is always advisable to have some degree of assessment during acquisition to ensure that enough events of each subpopulation are collected. However, as described in Subheading 1 and summarized in Fig. 4, some populations will be low to nonexistent in early time points. Therefore, users must collect as many events as possible but also define the most

practical threshold of events, perhaps by performing a small pilot study.

7. *Controls.* Validation steps should determine the practicality of identifying subsets with minimal additional controls. We would suggest, however, the following additional control may help with gating.
   - Panel 1: Fluorescence-1 controls (all labels except one) to define CD3+ and CD56+ and also CD56+ and CD16+ events.
   - Panel 3b: CD4, CD127, and CD25 labelled cells (with isotype control for FOXP3) to gate FOXP3+CD127low cells.
   - Panel 6: CD19 and CD4 labelled cells to define CD24+ and CD38+ events. Note all B cells are CD24+CD38+; however, CD4+ cells are CD24low.
   - Panel 11 and 12: Fluorescence-1 controls to allow gating on the rare Lin- events. Minimum controls would be panel 11, all labels but CD11c or CD1c, and panel 12, all labels but CD123 or CD304.

## Acknowledgements

The authors would like to thank Dr Bronwen Shaw, Dr Sameer Tulpule, Damini Tewari, and Vikesh Devlia, Anthony Nolan Research Institute, London, UK, and Dr John Girdlestone and Dr Cristina Navarrete, H&I Department, NHS Blood and Transplant, Colindale, UK, for developing the panel on which Table 1 is based. The authors would also like to thank Dr Sergio Querol, Banc de Sang i Teixits, Barcelona, Spain, and medical consultant for the Anthony Nolan Cell Therapy Centre, Nottingham Trent University, Nottingham, UK, for his assistance in compiling this chapter.

## Disclosure

The authors certify that they have no affiliation with or financial involvement in any organization or entity with a direct financial interest in the subject matter or materials discussed in this manuscript.

## References


1. Mackall CL, Fleisher TA, Brown MR et al (1995) Age, thymopoiesis, and CD4+ T-lymphocyte regeneration after intensive chemotherapy. N Engl J Med 332:143–149
2. Storek J, Joseph A, Dawson MA et al (2002) Factors influencing T-lymphopoiesis after allogeneic hematopoietic cell transplantation. Transplantation 73:1154–1158
3. Eyrich M, Wollny G, Tzaribaschev N et al (2005) Onset of thymic recovery and plateau of thymic output are differentially regulated after stem cell transplantation in children. Biol Blood Marrow Transplant 11:194–205
4. Steffens CM, Al-Harthi L, Shott S et al (2000) Evaluation of thymopoiesis using T cell receptor excision circles (TRECs): differential correlation between adult and pediatric TRECs and naïve phenotypes. Clin Immunol 97:95–101
5. Mackall CL, Gress RE (1997) Thymic aging and T-cell regeneration. Immunol Rev 160: 91–102
6. Chinen J, Buckley RH (2010) Transplantation immunology: solid organ and bone marrow. J Allergy Clin Immunol 125:S324–S335
7. Weinberg K (2001) Factors affecting thymic function after allogeneic hematopoietic stem cell transplantation. Blood 97:1458–1466
8. Maury S, Mary JY, Rabian C et al (2001) Prolonged immune deficiency following allogeneic stem cell transplantation: risk factors and complications in adult patients. Br J Haematol 115:630–641
9. Lewin SR, Heller G, Zhang L et al (2002) Direct evidence for new T-cell generation by patients after either T-cell-depleted or unmodified allogeneic hematopoietic stem cell transplantations. Blood 100:2235–2242
10. Poulin JF, Sylvestre M, Champagne P et al (2003) Evidence for adequate thymic function but impaired naive T-cell survival following allogeneic hematopoietic stem cell transplantation in the absence of chronic graft-versus-host disease. Blood 102: 4600–4607
11. Fallen PR, McGreavey L, Madrigal JA et al (2003) Factors affecting reconstitution of the T cell compartment in allogeneic haematopoietic cell transplant recipients. Bone Marrow Transplant 32:1001–1014
12. Storek J, Gooley T, Witherspoon RP et al (1997) Infectious morbidity in long-term survivors of allogeneic marrow transplantation is associated with low CD4 T cell counts. Am J Hematol 54:131–138
13. Fukushi N, Arase H, Wang B et al (1990) Thymus: a direct target tissue in graft-versus-host reaction after allogeneic bone marrow transplantation that results in abrogation of induction of self-tolerance. Proc Natl Acad Sci USA 87:6301–6305
14. Holländer GA, Widmer B, Burakoff SJ (1994) Loss of normal thymic repertoire selection and persistence of autoreactive T cells in graft vs host disease. J Immunol 152:1609–1617
15. van den Brink MR, Moore E, Ferrara JL et al (2000) Graft-versus-host-disease-associated thymic damage results in the appearance of T cell clones with anti-host reactivity. Transplantation 69:446–449
16. Jiménez M, Ercilla G, Martínez C (2007) Immune reconstitution after allogeneic stem cell transplantation with reduced-intensity conditioning regimens. Leukemia 21:1628–1637
17. Prasad VK, Mendizabal A, Parikh SH et al (2008) Unrelated donor umbilical cord blood transplantation for inherited metabolic disorders in 159 pediatric patients from a single center: influence of cellular composition of the graft on transplantation outcomes. Blood 112:2979–2989
18. Allan DS, Keeney M, Howson-Jan K et al (2002) Number of viable CD34(+) cells reinfused predicts engraftment in autologous hematopoietic stem cell transplantation. Bone Marrow Transplant 29:967–972
19. Bosch M, Khan FM, Storek J (2012) Immune reconstitution after hematopoietic cell transplantation. Curr Opin Hematol 19:324–335
20. Karre K (2002) NK cells, MHC class I molecules and the missing self. Scand J Immunol 55:221–228
21. Fujimaki K, Maruta A, Yoshida M et al (2001) Immune reconstitution assessed during five years after allogeneic bone marrow transplantation. Bone Marrow Transplant 27:1275–1281
22. Cooper MA, Fehniger TA, Caligiuri MA (2001) The biology of human natural killer-cell subsets. Trends Immunol 22:633–640
23. Komanduri KV, St John LS, de Lima M et al (2007) Delayed immune reconstitution after cord blood transplantation is characterized by

impaired thymopoiesis and late memory T-cell skewing. Blood 110:4543–4551

24. De Angelis C, Mancusi A, Ruggeri L et al (2011) Expansion of CD56-negative, CD16-positive, KIR-expressing natural killer cells after T cell-depleted haploidentical hematopoietic stem cell transplantation. Acta Haematol 126:13–20
25. Porrata LF, Inwards DJ, Ansell SM et al (2008) Early lymphocyte recovery predicts superior survival after autologous stem cell transplantation in non-Hodgkin lymphoma: a prospective study. Biol Blood Marrow Transplant 14:807–816
26. Chang YJ, Zhao XY, Huang XJ (2008) Effects of the NK cell recovery on outcomes of unmanipulated haploidentical blood and marrow transplantation for patients with hematologic malignancies. Biol Blood Marrow Transplant 14:323–334
27. Baron F, Baker JE, Storb R et al (2004) Kinetics of engraftment in patients with hematologic malignancies given allogeneic hematopoietic cell transplantation after non-myeloablative conditioning. Blood 104: 2254–2262
28. Marie-Cardine A, Divay F, Dutot I et al (2008) Transitional B cells in humans: characterization and insight from B lymphocyte reconstitution after hematopoietic stem cell transplantation. Clin Immunol 127:14–25
29. Sugalski JM, Rodriguez B, Moir S et al (2010) Peripheral blood B cell subset skewing is associated with altered cell cycling and intrinsic resistance to apoptosis and reflects a state of immune activation in chronic hepatitis C virus infection. J Immunol 185:3019–3027
30. Storek J (2001) Immune reconstitution after allogeneic marrow transplantation compared with blood stem cell transplantation. Blood 97:3380–3389
31. Storek J, Witherspoon RP, Storb R (1997) Reconstitution of membrane IgD- (mIgD-) B cells after marrow transplantation lags behind the reconstitution of mIgD+ B cells. Blood 89:350–351
32. Novitzky N, Davison GM, Hale G et al (2002) Immune reconstitution at 6 months following T-cell depleted hematopoietic stem cell transplantation is predictive for treatment outcome. Transplantation 74:1551–1559
33. Storek J, Espino G, Dawson MA et al (2000) Low B-cell and monocyte counts on day 80 are associated with high infection rates between days 100 and 365 after allogeneic marrow transplantation. Blood 96: 3290–3293
34. Storek J, Wells D, Dawson MA et al (2001) Factors influencing B lymphopoiesis after allogeneic hematopoietic cell transplantation. Blood 98:489–491
35. Curtis RE, Travis LB, Rowlings PA et al (1999) Risk of lymphoproliferative disorders after bone marrow transplantation: a multi-institutional study. Blood 94:2208–2216
36. Martin PJ, Hansen JA, Buckner CD et al (1985) Effects of in vitro depletion of T cells in HLA-identical allogeneic marrow grafts. Blood 66:664–672
37. Marmont AM, Horowitz MM, Gale RP et al (1991) T-cell depletion of HLA-identical transplants in leukemia. Blood 78:2120–2130
38. Bartelink IH, Belitser SV, Knibbe CAJ et al (2013) Immune reconstitution kinetics as an early predictor for mortality using various hematopoietic stem cell sources in children. Biol Blood Marrow Transplant 19:305–313
39. Sallusto F, Geginat J, Lanzavecchia A (2004) Central memory and effector memory T cell subsets: function, generation, and maintenance. Annu Rev Immunol 22:745–763
40. Picker LJ, Treer JR, Ferguson-Darnell B et al (1993) Control of lymphocyte recirculation in man. I. Differential regulation of the peripheral lymph node homing receptor L-selectin on T cells during the virgin to memory cell transition. J Immunol 150: 1105–1121
41. Storek J, Joseph A, Espino G et al (2001) Immunity of patients surviving 20 to 30 years after allogeneic or syngeneic bone marrow transplantation. Blood 98:3505–3512
42. Kimmig S, Przybylski GK, Schmidt CA et al (2002) Two subsets of naive T helper cells with distinct T cell receptor excision circle content in human adult peripheral blood. J Exp Med 195:789–794
43. Storek J, Witherspoon RP, Storb R (1995) T cell reconstitution after bone marrow transplantation into adult patients does not resemble T cell development in early life. Bone Marrow Transplant 16:413–425
44. Gratama JW, van Esser JW, Lamers CH et al (2001) Tetramer-based quantification of cytomegalovirus (CMV)-specific CD8+ T lymphocytes in T-cell-depleted stem cell grafts and after transplantation may identify patients at risk for progressive CMV infection. Blood 98:1358–1364

45. Pastore D, Delia M, Mestice A et al (2011) Recovery of CMV-specific CD8+ T cells and Tregs after allogeneic peripheral blood stem cell transplantation. Biol Blood Marrow Transplant 17:550–557

46. Feuchtinger T, Lücke J, Hamprecht K et al (2005) Detection of adenovirus-specific T cells in children with adenovirus infection after allogeneic stem cell transplantation. Br J Haematol 128:503–509

47. Sakaguchi S (2004) Naturally arising CD4+ regulatory t cells for immunologic self-tolerance and negative control of immune responses. Annu Rev Immunol 22:531–562

48. Groux H, O'Garra A, Bigler M et al (1997) A CD4+ T-cell subset inhibits antigen-specific T-cell responses and prevents colitis. Nature 389:737–742

49. Weiner HL (2001) Induction and mechanism of action of transforming growth factor-beta-secreting Th3 regulatory cells. Immunol Rev 182:207–214

50. Dejaco C, Duftner C, Grubeck-Loebenstein B et al (2006) Imbalance of regulatory T cells in human autoimmune diseases. Immunology 117:289–300

51. Annacker O, Powrie F (2002) Homeostasis of intestinal immune regulation. Microbes Infect 4:567–574

52. Kullberg MC, Jankovic D, Gorelick PL et al (2002) Bacteria-triggered CD4(+) T regulatory cells suppress Helicobacter hepaticus-induced colitis. J Exp Med 196:505–515

53. Maloy KJ, Salaun L, Cahill R et al (2003) CD4+CD25+ T(R) cells suppress innate immune pathology through cytokine-dependent mechanisms. J Exp Med 197: 111–119

54. Hori S, Carvalho TL, Demengeot J (2002) CD25+CD4+ regulatory T cells suppress CD4+ T cell-mediated pulmonary hyperinflammation driven by Pneumocystis carinii in immunodeficient mice. Eur J Immunol 32: 1282–1291

55. Montagnoli C, Bacci A, Bozza S et al (2002) B7/CD28-dependent CD4+CD25+ regulatory T cells are essential components of the memory-protective immunity to *Candida albicans*. J Immunol 169:6298–6308

56. Aseffa A, Gumy A, Launois P et al (2002) The early IL-4 response to Leishmania major and the resulting Th2 cell maturation steering progressive disease in BALB/c mice are subject to the control of regulatory CD4+CD25+ T cells. J Immunol 169:3232–3241

57. Belkaid Y, Piccirillo CA, Mendez S et al (2002) CD4+CD25+ regulatory T cells control Leishmania major persistence and immunity. Nature 420:502–507

58. Trowsdale J, Betz AG (2006) Mother's little helpers: mechanisms of maternal-fetal tolerance. Nat Immunol 7:241–246

59. Di Ianni M, Falzetti F, Carotti A et al (2011) Tregs prevent GVHD and promote immune reconstitution in HLA-haploidentical transplantation. Blood 117:3921–3928

60. Brunstein CG, Miller JS, Cao Q et al (2011) Infusion of ex vivo expanded T regulatory cells in adults transplanted with umbilical cord blood: safety profile and detection kinetics. Blood 117:1061–1070

61. Sakaguchi S, Sakaguchi N, Asano M et al (1995) Immunologic self-tolerance maintained by activated T cells expressing IL-2 receptor alpha-chains (CD25). Breakdown of a single mechanism of self-tolerance causes various autoimmune diseases. J Immunol 155:1151–1164

62. Seddiki N, Santner-Nanan B, Martinson J et al (2006) Expression of interleukin (IL)-2 and IL-7 receptors discriminates between human regulatory and activated T cells. J Exp Med 203:1693–1700

63. Fontenot JD, Gavin MA, Rudensky AY (2003) Foxp3 programs the development and function of CD4+CD25+ regulatory T cells. Nat Immunol 4:330–336

64. Hori S, Nomura T, Sakaguchi S (2003) Control of regulatory T cell development by the transcription factor Foxp3. Science 299: 1057–1061

65. Khattri R, Cox T, Yasayko S-A et al (2003) An essential role for Scurfin in CD4+CD25+ T regulatory cells. Nat Immunol 4:337–342

66. Gavin MA, Torgerson TR, Houston E et al (2006) Single-cell analysis of normal and FOXP3-mutant human T cells: FOXP3 expression without regulatory T cell development. Proc Natl Acad Sci USA 103: 6659–6664

67. Wolf D, Wolf AM, Fong D et al (2007) Regulatory T-cells in the graft and the risk of acute graft-versus-host disease after allogeneic stem cell transplantation. Transplantation 83:1107–1113

68. Rezvani K, Mielke S, Ahmadzadeh M et al (2006) High donor FOXP3-positive regulatory T-cell (Treg) content is associated with a low risk of GVHD following HLA-matched allogeneic SCT. Blood 108:1291–1297

69. McIver Z, Melenhorst JJ, Wu C et al (2013) Donor lymphocyte count and thymic activity predict lymphocyte recovery and outcomes after matched-sibling hematopoietic stem cell transplant. Haematologica 98(3):346–352

70. Allan SE, Broady R, Gregori S et al (2008) CD4+ T-regulatory cells: toward therapy for human diseases. Immunol Rev 223:391–421

71. Clark FJ, Gregg R, Piper K et al (2004) Chronic graft-versus-host disease is associated with increased numbers of peripheral blood CD4+CD25high regulatory T cells. Blood 103:2410–2416

72. Sanchez J, Casaño J, Alvarez MA et al (2004) Kinetic of regulatory CD25high and activated CD134+ (OX40) T lymphocytes during acute and chronic graft-versus-host disease after allogeneic bone marrow transplantation. Br J Haematol 126:697–703

73. Watanabe N, Narita M, Furukawa T et al (2011) Kinetics of pDCs, mDCs, γδT cells and regulatory T cells in association with graft versus host disease after hematopoietic stem cell transplantation. Int J Lab Hematol 33: 378–390

74. Magenau JM, Qin X, Tawara I et al (2010) Frequency of CD4(+)CD25(hi)FOXP3(+) regulatory T cells has diagnostic and prognostic value as a biomarker for acute graft-versus-host-disease. Biol Blood Marrow Transplant 16:907–914

75. Zorn E, Kim HT, Lee SJ et al (2005) Reduced frequency of FOXP3+ CD4+CD25+ regulatory T cells in patients with chronic graft-versus-host disease. Blood 106:2903–2911

76. Meignin V, Peffault de Latour R, Zuber J et al (2005) Numbers of Foxp3-expressing CD4+CD25high T cells do not correlate with the establishment of long-term tolerance after allogeneic stem cell transplantation. Exp Hematol 33:894–900

77. Kawano Y, Kim HT, Matsuoka KI et al (2011) Low telomerase activity in CD4+ regulatory T cells in patients with severe chronic GVHD after hematopoietic stem cell transplantation. Blood 118:5021–5030

78. Miura Y, Thoburn CJ, Bright EC et al (2004) Association of Foxp3 regulatory gene expression with graft-versus-host disease. Blood 104:2187–2193

79. Ngoma AM, Ikeda K, Hashimoto Y et al (2012) Impaired regulatory T cell reconstitution in patients with acute graft-versus-host disease and cytomegalovirus infection after allogeneic bone marrow transplantation. Int J Hematol 95:86–94

80. Mielke S, Rezvani K, Savani BN et al (2007) Reconstitution of FOXP3. Blood 110:1689–1697

81. Rieger K, Loddenkemper C, Maul J et al (2006) Mucosal FOXP3+ regulatory T cells are numerically deficient in acute and chronic GvHD. Blood 107:1717–1723

82. Wu KN, Emmons RVB, Lisanti MP et al (2009) Foxp3-expressing T regulatory cells and mast cells in acute graft-versus-host disease of the skin. Cell Cycle 8:3593–3597

83. Stenger EO, Turnquist HR, Mapara MY et al (2012) Dendritic cells and regulation of graft-versus-host disease and graft-versus-leukemia activity. Blood 119:5088–5103

84. Wu L, Liu YJ (2007) Development of dendritic-cell lineages. Immunity 26:741–750

85. Gilliet M, Cao W, Liu YJ (2008) Plasmacytoid dendritic cells: sensing nucleic acids in viral infection and autoimmune diseases. Nat Rev Immunol 8:594–606

86. Koyama M, Hashimoto D, Aoyama K et al (2009) Plasmacytoid dendritic cells prime alloreactive T cells to mediate graft-versus-host disease as antigen-presenting cells. Blood 113:2088–2095

87. Dzionek A, Fuchs A, Schmidt P et al (2000) BDCA-2, BDCA-3, and BDCA-4: three markers for distinct subsets of dendritic cells in human peripheral blood. J Immunol 165:6037–6046

88. Shlomchik WD, Couzens MS, Tang CB et al (1999) Prevention of graft versus host disease by inactivation of host antigen-presenting cells. Science 285:412–415

89. Duffner UA, Maeda Y, Cooke KR et al (2004) Host dendritic cells alone are sufficient to initiate acute graft-versus-host disease. J Immunol 172:7393–7398

90. Matte CC, Liu J, Cormier J et al (2004) Donor APCs are required for maximal GVHD but not for GVL. Nat Med 10:987–992

91. Reddy P, Maeda Y, Liu C et al (2005) A crucial role for antigen-presenting cells and alloantigen expression in graft-versus-leukemia responses. Nat Med 11:1244–1249

92. Chakraverty R, Eom HS, Sachs J et al (2006) Host MHC class II+ antigen-presenting cells and CD4 cells are required for CD8-mediated graft-versus-leukemia responses following

delayed donor leukocyte infusions. Blood 108:2106–2113

93. Reddy V, Iturraspe JA, Tzolas AC et al (2004) Low dendritic cell count after allogeneic hematopoietic stem cell transplantation predicts relapse, death, and acute graft-versus-host disease. Blood 103:4330–4335
94. Mohty M, Blaise D, Faucher C et al (2005) Impact of plasmacytoid dendritic cells on outcome after reduced-intensity conditioning allogeneic stem cell transplantation. Leukemia 19:1–6
95. Clark FJ, Freeman L, Dzionek A et al (2003) Origin and subset distribution of peripheral blood dendritic cells in patients with chronic graft-versus-host disease. Transplantation 75: 221–225
96. Waller EK, Rosenthal H, Jones TW et al (2001) Larger numbers of CD4(bright) dendritic cells in donor bone marrow are associated with increased relapse after allogeneic bone marrow transplantation. Blood 97: 2948–2956
97. Lau J, Sartor M, Bradstock KF et al (2007) Activated circulating dendritic cells after hematopoietic stem cell transplantation predict acute graft-versus-host disease. Transplantation 83:839–846
98. Lee YR, Yang IH, Lee YH et al (2005) Cyclosporin A and tacrolimus, but not rapamycin, inhibit MHC-restricted antigen presentation pathways in dendritic cells. Blood 105:3951–3955
99. Piemonti L, Monti P, Allavena P et al (1999) Glucocorticoids affect human dendritic cell differentiation and maturation. J Immunol 162:6473–6481
100. Lee YH, Lee YR, Im S et al (2007) Calcineurin inhibitors block MHC-restricted antigen presentation in vivo. J Immunol 179: 5711–5716
101. Turnquist HR, Raimondi G, Zahorchak AF et al (2007) Rapamycin-conditioned dendritic cells are poor stimulators of allogeneic CD4+ T cells, but enrich for antigen-specific Foxp3+ T regulatory cells and promote organ transplant tolerance. J Immunol 178:7018–7031
102. Szabo G, Gavala C, Mandrekar P (2001) Tacrolimus and cyclosporine A inhibit allostimulatory capacity and cytokine production of human myeloid dendritic cells. J investig med 49(5):442–449
103. Sutherland DR, Anderson L, Keeney M et al (1996) The ISHAGE guidelines for CD34+ cell determination by flow cytometry. International Society of Hematotherapy and Graft Engineering. J Hematother 5:213–226
104. Sutherland DR, Nayyar R, Acton E et al (2009) Comparison of two single-platform ISHAGE-based CD34 enumeration protocols on BD FACSCalibur and FACSCanto flow cytometers. Cytotherapy 11:595–605
105. Takahashi E, Kuranaga N, Satoh K et al (2007) Induction of CD16+ CD56bright NK cells with antitumour cytotoxicity not only from CD16- CD56bright NK cells but also from CD16- CD56dim NK cells. Scand J Immunol 65:126–138
106. Barbui AM, Borleri G, Conti E et al (2006) Clinical grade expansion of CD45RA, CD45RO, and CD62L-positive T-cell lines from HLA-compatible donors: high cytotoxic potential against AML and ALL cells. Exp Hematol 34:475–485
107. Tanaskovic S, Fernandez S, Price P et al (2010) CD31 (PECAM-1) is a marker of recent thymic emigrants among CD4+ T-cells, but not CD8+ T-cells or gammadelta T-cells, in HIV patients responding to ART. Immunol Cell Biol 88:321–327
108. MacDonald KPA, Munster DJ, Clark GJ et al (2002) Characterization of human blood dendritic cell subsets. Blood 100:4512–4520
109. Maecker HT, McCoy JP, Nussenblatt R (2012) Standardizing immunophenotyping for the Human Immunology Project. Nat Rev Immunol 12:191–200
110. Pulsipher MA, Chitphakdithai P, Logan BR et al (2009) Donor, recipient, and transplant characteristics as risk factors after unrelated donor PBSC transplantation: beneficial effects of higher CD34+ cell dose. Blood 114: 2606–2616
111. Wagner JE, Barker JN, DeFor TE et al (2002) Transplantation of unrelated donor umbilical cord blood in 102 patients with malignant and nonmalignant diseases: influence of CD34 cell dose and HLA disparity on treatment-related mortality and survival. Blood 100:1611–1618
112. Haynes B, Hale L, Weinhold K et al (1999) Analysis of the adult thymus in reconstitution of T lymphocytes in HIV-1 infection. J Clin Invest 103:921

# Chapter 11

# Molecular Methods Used for Detection of Minimal Residual Disease Following Hematopoietic Stem Cell Transplantation in Myeloid Disorders

**Ahmet H. Elmaagacli**

## Abstract

The monitoring of minimal residual disease (MRD) in patients with acute or chronic myeloid disorders is performed routinely after allogeneic or autologous transplantation. The detection of MRD helps to identify patients who are at high risk for leukemic relapse after transplantation. The most commonly used techniques for MRD detection are qualitative and quantitative PCR methods, fluorescence in situ hybridization (FISH), fluorescence-activated cell sorting (FACS), and cytogenetic analysis, which are often performed complementary in order to assess more precisely MRD. Here we describe the most used sensitive real-time RT-PCR methods for chronic and acute myeloid disorders. Besides protocols for real-time RT-PCR and multiplex RT-PCR procedures for the most common fusion-gene transcripts in acute and chronic myeloid disorders, methods for detections of disease-specific genetic mutated alterations, as NPM1 and FLT3 gene length mutations, and aberrantly expressed genes, as WT1 gene transcripts, are described in detail for daily use.

**Key words** MRD, Transplant, Real-time RT-PCR, Myeloid disorders, Fusion transcripts, FLT3 length mutations, WT1

## 1 Introduction

Outcome after transplant has improved mainly due to improvements in supportive care, conditioning regimens, graft-versus-host-disease (GVHD) treatment, and prophylaxis schedules during the last years, while the rate of relapse of the underlying malignant disease after transplant remained essentially unchanged. Early and accurate detection of minimal residual disease (MRD) after transplant enables to counter most effectively an impending hematological relapse by inducing a graft-versus-leukemia effect with donor lymphocyte infusion, for example [1–4]. The majority of transplant indications nowadays represent acute leukemia for which new disease-specific markers have been detected recently, which could be detected often by use of quantitative polymerase chain

Meral Beksaç (ed.), *Bone Marrow and Stem Cell Transplantation*, Methods in Molecular Biology, vol. 1109,
DOI 10.1007/978-1-4614-9437-9_11, © Springer Science+Business Media New York 2014

**Table 1**
**Most common MRD marker in chronic and myeloid leukemia**

| Disease | Type of marker | Chromosomal changes | Molecular changes |
|---|---|---|---|
| CML, AML, ALL | Chromosomal aberration | Translocation (9;22) | BCR-ABL (fusion gene) |
| AML | Chromosomal aberration | Translocation (8;21) | AML1-ETO (fusion gene) |
| AML | Chromosomal aberration | Translocation (15;17) | PML-RARA (fusion gene) |
| AML | Chromosomal aberration | Inversion (16) | CBFβ-MYH11 (fusion gene) |
| AML | Chromosomal aberration | Translocation 11q23 | MLL |
| AML | Length mutation of FLT3 Gene | – | FLT3-LM |
| AML, ALL, CML | Aberrantly over-expressed Wilms tumor 1gene | – | WT-1 |
| AML | NPM1 | Mutations | |
| AML | CEBPA | Mutations | |
| AML | IDH1, IDH2 | Mutations | |
| AML | KRAS | Mutations | |
| AML | NRAS | Mutations | |
| AML | DNMT3A | Mutations | |
| AML | FLT3 TKD | Mutations | |

reaction (PCR) (Table 1) [5–9]. Indeed, quantitative real-time RT-PCR methods are able to predict a clinical relapse more reliable by monitoring the kinetics of increasing MRD than qualitative methods alone [10]. Nevertheless, qualitative PCR methods and other techniques as fluorescence in situ hybridization (FISH), fluorescence-activated cell sorting (FACS), and cytogenetic analysis are further pillars of MRD detection in hematology [11–13]. However, they should not be regarded as competitive methods to PCR but moreover as complementing techniques in the detection and assessment of MRD. Targets for MRD detection by PCR are fusion-gene transcripts, breakpoint regions around molecular rearrangements, and aberrantly expressed genes. Table 1 shows the frequently expressed fusion genes and mutations in acute and chronic myeloid leukemia.

Real-time RT-PCR measures the mRNA expression level of a target gene relative to one or more other reference genes. The used RNA per sample or cell may vary greatly in each real-time RT-PCR due to the quality of the sample, the time from obtaining the sample to RNA preparation, and many other factors. Also, the cDNA yield may vary additionally due to variation in enzyme activities or inhibitors in the sample. To normalize these quality variations, each target mRNA should be quantified in relation to the expression of the so-called housekeeping genes which are expressed at similar levels in all different cell types [14]. Commonly, two different real-time RT-PCR methods are performed routinely based on the real-time RT-PCR method using hybridization probes. One real-time PCR method is based on the TaqMan™ technology using TaqMan™ probes and the other one on the LightCycler® method using hybridization probes.

The TaqMan™ probe has a 5′ fluorescent reporter dye, which is quenched by a 3′ quencher dye through Förster-type energy transfer (FRET). After hybridization to the template, the fluorogenic TaqMan™ probes will be hydrolyzed during PCR by the 5′ secondary structure-dependent nuclease activity of the Taq DNA polymerase [15]. After hydrolysis the release of the reporter signal caused an increase in fluorescence intensity that was proportional to the accumulation of the PCR product. The LightCycler® method uses two hybridization probes which hybridize at the template closely together with a distance of only 1–5 bases. The first probe is fluorescent labeled at the 3′ and the second probe at the 5′ site. Only after specific hybridization of both probes together to the template a fluorescent signal is released in proportion to the accumulated PCR product.

Both systems then generate a real-time amplification plot based upon the normalized (background) fluorescent signal. Subsequently a threshold cycle is determined, i.e., the fractional cycle number at which the amount of amplified target reached a fixed threshold. This threshold is defined in general as 3–10 times the standard deviation of the background fluorescent signal. When plotting the fluorescent signal versus the cycle number, the higher the initial copy number is, the earlier the signal appeared out of the defined threshold line. The “crossing points” are used to create a standard curve by plotting known concentration of serial dilutions of a control mRNA versus the “crossing points.” The target mRNA expression in patient samples can be related to a standard curve of a control RNA (plasmid or leukemic cell line with the specific target fusion gene) with the same level of expression or in numbers of the copies of the target gene. In the following, the most commonly used qualitative and quantitative PCR methods for acute and chronic myeloid disorders are described in detail.

## 2 Materials

### 2.1 Equipments

1. LightCycler® device (Roche Diagnostics, Mannheim, Germany) (*see* **Note 1**).
2. ABI Prism Genetic Analyzer 310 including Genemapper v.3.10 software (Applied Biosystems, Darmstadt, Germany).
3. Capillaries for LightCycler® device (Roche Diagnostics).
4. Cooling centrifuge for 2 mL Eppendorf tubes (17,500 × *g*) (Eppendorf, Hamburg).
5. Agarose gel electrophoresis apparatus (Bio-Rad).
6. UV Light Hofer Scientific Instruments (San Francisco).
7. Spectrometer Lambda Bio for RNA/DNA measurement (Applied Biosystems).
8. MagNA Pure™ Compact (Roche Diagnostics, Mannheim, Germany).

### 2.2 Reagents

#### 2.2.1 RNA Isolation

1. RNeasy® Mini Kit (Qiagen, Hilden, Germany).
2. Erythrocyte-lysis buffer (Qiagen, Hilden).
3. RLT-buffer (Qiagen, Hilden).

#### 2.2.2 DNA Isolation

MagNA Pure™ compact nucleic acid isolation kit I (Roche Diagnostics).

#### 2.2.3 Reverse Transcription

Ultrapure deoxynucleosidetriphosphate (dNTP)—set 100 mM (Pharmacia, Uppsala, Sweden); add 20 μL of each of the four different dNTP:

dATP, dCTP, dGTP, and dTTP—80.0 μL.

Add aqua bidest—1,520 μL.

M-MLV reverse transcriptase 200 U/μL (Gibco Life Technologies, Eggenstein).

rRNAsin ribonuclease inhibitor 40 U/μL (Promega AG, Heidelberg).

Pd (N)6 random hexamer 10 pM/μL (Pharmacia, Uppsala, Sweden).

#### 2.2.4 RT-PCR and PCR

1. Oligonucleotide primers (Invitrogen).
2. AmpliTaq DNA polymerase 5 U/μL (Applied Biosystems).
3. AmpliTaq Gold polymerase 5 U/μL (Applied Biosystems).
4. PCR buffer includes $MgCl_2$ 25 mM solution (Applied Biosystems).
5. SeaKem® LE agarose (FMC Bioproducts, Rockland, Maine).

*2.2.5 Real-Time PCR*

1. TaqMan™ and hybridization probes (TIBMOL, Berlin, Germany).

   TaqMan™ probes are labeled at the 5′-site with a reporter signal using FAM-6-fluorescence marker and at the 3′-site with a quencher-signal using TAMRA (Applied Biosystems, Darmstadt).

   The hybridization probe is labeled at the 3′-site with fluorescein. The anchor probe is labeled at the 5′-site with Red640 and at the 3′-site with phosphate (TIP MOLBIOL).
2. Oligonucleotide primers (Invitrogen).
3. 20 μL Capillaries (Roche Diagnostics).
4. SuperScript II RT-PCR kit includes:

   $MgSO_4$, Platinum Taq®, 2× reaction mix (Invitrogen).

   Bovine serum albumin (Roche Diagnostics).

   RNAsin (Promega).

   AmpErase uracil-*N*-glycosylase (UNG) 1 U (μL) (Roche Diagnostics).

   dUTP 25 μM in 250 μL 100 mM (Roche, Diagnostics).

*2.2.6 FLT3 Length Mutations*

FAM fluorescent-labeled primer (Applied Biosystems).

High-fidelity master mix (Roche Diagnostics).

Rox 500 internal standard (Applied Biochemicals).

*2.2.7 Cell Lines as Controls for Quantitative PCR*

The following cell lines can be used: K-562, chronic myeloid leukemia in myeloid blast crisis; Kasumi-1, acute myeloid leukemia (FAB M2 with t(8;21)); MV4-11, acute monocytic leukemia FAB M5 with t(4;11)(q21;q23); and NB-4, acute promyelocytic leukemia (FAB M3) with t(15;17), ME-1 with inv(16) AML (all purchased from DSMZ, Braunschweig, Germany). The cells can be grown in RPMI 1640 medium (Invitrogen, Heidelberg, Germany) supplemented with 10 % fetal bovine serum. All cells were maintained in a humidified 37 °C incubator with 5 % $CO_2$ (*see* **Note 2**).

## 3 Methods

***3.1 Preparation of the Samples and RNA Isolation Using the RNeasy® Mini Kit***

All samples should be collected in EDTA tubes. The first step prepares the samples:

- Use 3–5 mL of blood or bone marrow sample and add erythrocyte-lysis buffer up to a total volume of 50 mL.
- Place at room temperature for 10 min for erythrocyte lysis.
- Centrifuge at 390 RCF for 10 min at room temperature.
- Discard the supernatant and refill up to 25 mL.

– Centrifuge at 390 RCF for 10 min at room temperature again.
– According to the size of the obtained pellet, add 350 μL to 2 mL of RLT-buffer.
– Store at –20 °C until needed.

The RNA isolation using the RNeasy® Mini Kit should be performed according to Qiagen's recommendation including the use of QIAshredder (*see* **Note 3**).

### 3.2 cDNA Synthesis

Prepare the following mixture:

– Add 8 μL of RNA (2 μg) to 2 μL of Pd (N)6 random hexamers (10 pM/μL) on ice.
– Incubate the mixture at 70 °C for 10 min and then on ice for at least 1 min.
– Prepare reaction master mix:

| 40 μL total volume | 1× (in μL) |
|---|---|
| 10× PCR buffer | 5 |
| dNTP | 8 |
| M-MLV-RT | 0.025 |
| RNAsin | 0.25 |
| $H_2O$ | 27 |

– Mix gently and add 10 μL of RNA and Pd(N)6 random hexamer mixture.
– Incubate the tubes at 37 °C for 60 min, heat inactivate at 95 °C for 5 min, and then chill in ice. Store at –20 °C until use for real-time PCR (*see* **Note 4**).

### 3.3 Real-Time RT-PCR Protocols

#### 3.3.1 Real-Time RT-PCR Protocol for BCR-ABL Transcripts

Detects a2b2 and a2b3 BCR-ABL transcripts (not e1a2).

Primers:

bcr-abl forward: 5′-ACG TTC CTG ATC TCC TCT GA-3′, length: 20.

bcr-abl reverse: 5′-AGA TGC TAC TGG CCG CTG AA-3′, length: 20.

Hybridization probes:

Anchor probe bcr-abl UP: 5′-GCA GAG TGG AGG GAG AAC ATC CGG GAG CAG CAG AA-x (x = 3′ fluorescein), length: 35.

Sensor probe bcr-abl DOWN: 5′-LC Red 640-AAG TGT TTC AGA AGC TTC TCC CTG AC-p (p = 3′ phosphat), length: 26.

LightCycler conditions: bcr-abl

| | Temperature | Incubation time |
|---|---|---|
| Reverse transcription | 55 °C | 20 min |
| Initial denaturation | 95 °C | 30 s |
| Denaturation | 95 °C | 1 s |
| Annealing | 56 °C | 15 s |
| Extension | 72 °C | 18 s |
| Cooling | 4 °C | 1 min |
| 50 cycles | | |

Prepare the following master mix for 1×:

| 12 µL total volume | 1× |
|---|---|
| 2× reaction mix | 4.8 |
| 50 mM $MgSO_4$ | 0.675 |
| 20 mg/mL BSA | 0.3 |
| Primer FOR 10 pmol | 0.12 approx.[a] |
| Primer REV 10 pmol | 0.12 approx.[a] |
| Probe UP 4 pmol | 0.24 approx.[a] |
| Probe Down 8 pmol | 0.48 approx.[a] |
| SuperScript Platinum Taq | 0.3 |
| RNAsin | 0.168 |
| dUTP (1:20 freshly prepared) | 0.24 |
| UNG | 0.6 |
| RNA 1,000 ng | 4 |
| Mix | 8 |

[a]May vary in volume

Controls (all in duplicate):

Positive control: RNA of the K562 cell line.
Dilution: 100, 10, 1, and 0.1 ng.
Negative control: water (*see* **Note 5**).

### *3.3.2 Real-Time RT-PCR Protocol for AML1/ETO Transcripts*

Detects AML1-ETO transcripts that have only one breakpoint locus.

Primers:

AML M2 A1: 5′-AGC CAT GAA GAA CCA GG-3′, length: 17.
AML M2 E1: 5′-AGG CTG TAG GAG AAT GG-3′, length: 17.

Hybridization probes:

Anchor probe AML-M2 UP: 5′-ACA ATG CCA GAC TCA CCT GTG GAT GTG AAG ACG C-x; (x = 3′ fluorescein), length: 34.

Sensor probe AML-M2 DOWN: 5′-LC Red 640-ATC TAG GCT GAC TCC TCC AAC AAT g-p; (p = 3′ phosphat), length: 25.

LightCycler conditions—AML M2 RNA:

| | Temperature | Incubation time |
|---|---|---|
| Reverse transcription | 95 °C | 20 min |
| Initial denaturation | 95 °C | 30 s |
| Denaturation | 95 °C | 1 s |
| Annealing | 52 °C | 15 s |
| Extension | 72 °C | 18 s |
| Cooling | 4 °C | 1 min |
| 45 cycles | | |

Prepare the following master mix (mix for 1×):

| 20 μL total volume | 1× (in μL) |
|---|---|
| 2× reaction mix | 10 |
| 50 mM $MgSO_4$ | 1.0 |
| 20 mg/mL BSA | 0.5 |
| Primer FOR 10 pmol | 0.25 approx.[a] |
| Primer REV 10 pmol | 0.25 approx.[a] |
| Probe UP 4 pmol | 0.4 approx.[a] |
| Probe Down 8 pmol | 0.8 approx.[a] |
| SuperScript Platinum Taq | 0.5 |
| RNAsin | 0.28 |
| RNA | 6 |
| UNG | 14 |
| dUTP (1:20 freshly prepared) | |
| Mix | 14 |

[a]May vary in volume

Controls (all in duplicate):

Positive control: RNA of the Kasumi-1 cell line.

Dilution: 100, 10, 1, and 0.1 ng.

*Negative control*: *water* (*see* **Note 6**).

### 3.3.3 Real-Time RT-PCR for CBFβ-MYH11 Transcripts

Detects transcripts A, B, C, D, E, and F.

Primers:

Forward: 5′-GCAGGCAAGGTATATTTGAAGG-3′, length: 22.

Reverse A: 5′-CTCTTCTCCTCATTCTGCTC-3′, length: 20.

Reverse B: 5′-TTGAGCATTTTGTTGGTCCG-3′, length: 20.

Reverse C: 5′-CTTCCAGAGCTTCCACGGT-3′, length: 19.

Reverse D: 5′-TCCCTGTGACGCTCTCAACT-3′, length: 20.

Reverse E: 5′-GGCCAGGTCTGCGTTCTCT-3′, length: 19.

Reverse F: 5′-TCCTCTTCTCCTCATTCTGCTC-3′, length: 22.

Hybridization probes:

Anchor probe CBFB UP: GGCTCGCTCCTCATCAAACTCCA-x (x = 3′ fluorescein), length: 23.

Sensor probe CBFB DOWN: 5′-LC Red 640-ACAGCCCATACCA TCCAGTCTTTGG (p = 3′ phosphat), length: 25.

PCR conditions for CBFβ:

| | Temperature | Incubation time |
|---|---|---|
| Reverse transcription | 55 °C | 20 min |
| Initial denaturation | 95 °C | 30 s |
| Denaturation | 95 °C | 10 s |
| Annealing | 64 °C | 10 s |
| Extension | 72 °C | 26 s |
| Cooling | 4 °C | 1 min |
| 45 cycles | | |

Prepare the following master mix for 1×:

| 20 µL total volume | 1× (in µL) |
|---|---|
| 2× reaction mix | 4.8 |
| 50 mM $MgSO_4$ | 0.675 |
| 20 mg/mL BSA | 0.3 |
| Primer FOR | 50 pmol |
| Primer REV | 50 pmol |
| Probe UP | 25 pmol |
| Probe Down | 25 pmol |
| LC FastStart DNA master hybridization probes | 2 µL |
| $MgCl_2$ | 4 mM |
| cDNA | 2 µL |
| Mix | |

Controls (all in duplicate):

Positive control: RNA of the ME-1 cell line.

Dilution: 100, 10, 1, and 0.1 ng.

Negative control: water (*see* **Note 7**).

### *3.3.4 Real-Time RT-PCR for PML-RARA Transcripts*

Detects S and L transcripts.

Primers:

AML-M3-L-forward: 5′-GTC TTC CTG CCC AAC AGC AAC C-3′, length: 22.

AML-M3-S-forward: 5′-AGC TCT TGC ATC ACC CAG GGG A-3′, length: 22.

AML-M3-reverse: 5′-CTC ACA GGC GCT GAC CCC ATA GT-3′, length: 23.

Hybridization probes:

AML-M3-UP: 5′-TGA AGA GAT AGT GCC CAG CCC TCC CTC-x (x = 3′ fluorescein), length: 27.

AML-M3-DOWN: 5′-LC Red 640-CCA CCC CCT CTA CCC CGC ATC TAC A-p (p = 3′ phosphat), length: 25.

PCR conditions for PML-RARA:

| | Temperature | Incubation time |
|---|---|---|
| Reverse transcription | 55 °C | 20 min |
| Initial denaturation | 95 °C | 30 s |
| Denaturation | 95 °C | 10 s |
| Annealing | 60 °C | 10 s |
| Extension | 72 °C | 30 s |
| Cooling | 4 °C | 1 min |
| 45 cycles | | |

Prepare the following master mix for 1×:

| 20 µL total volume | 1× (in µL) |
|---|---|
| 2× reaction mix | 10 |
| 50 mM $MgSO_4$ | 0.16 |
| 20 mg/mL BSA | 0.5 |
| Primer L FOR 20 pmol | 0.094 (approx.[a]) |
| Primer S FOR 20 pmol | 0.076 (approx.[a]) |
| Primer REV 20 pmol | 0.078 (approx.[a]) |

(continued)

(continued)

| | |
|---|---|
| Probe UP 10 pmol | 0.5 (approx.[a]) |
| Probe Down 10 pmol | 0.5 (approx.[a]) |
| SuperScript Platinum Taq | 0.5 |
| RNAsin | 0.28 |
| dUTP | 0.2 |
| UNG | 0.5 |
| Aqua bidest | 0.6 |
| RNA | 6 |
| Master mix | 16 |

[a]May vary in volume

Controls (all in duplicate):

Positive control: RNA of the NB-4 cell line.

Dilution: 100, 10, 1, and 0.1 ng.

Negative control: water (*see* **Note 8**).

### *3.3.5 Real-Time PCR for GAPDH as Housekeeping Gene*

Primers:

GAPDH forward: 5′-TTC ACC ACC ATG GAG AAG GCT-3′, length: 21.

GAPDH reverse: 5′-ATG GCA TGG ACT GTG GTC ATG-3′, length: 21.

Hybridization probes:

Anchor probe GAPDH UP: 5′-ATC ATC AGC AAT GCC TCC TGC ACC ACC AAC TGC T-x; (x = 3′ fluorescein), length: 34.

Sensor probe GAPDH DOWN: 5′-LC Red 640-AGC ACC CCT GGC CAA GGT CAT CCA T-p; (p = 3′ phosphat), length: 25.

PCR conditions for GAPDH:

| | Temperature | Incubation time |
|---|---|---|
| Reverse transcription | 55 °C | 20 min |
| Initial denaturation | 95 °C | 30 s |
| Denaturation | 95 °C | 1 s |
| Annealing | 56 °C | 15 s |
| Extension | 72 °C | 18 s |
| Cooling | 4 °C | 1 min |
| 50 cycles | | |

Prepare the following master mix for 1×:

| 12 µL total volume | 1× in µL |
|---|---|
| 2× reaction mix | 4.8 |
| 50 mM $MgSO_4$ | 0.675 |
| 20 mg/mL BSA | 0.3 |
| Primer FOR 10 pmol | 0.12 (approx.[a]) |
| Primer REV 10 pmol | 0.12 (approx.[a]) |
| Probe UP 4 pmol | 0.24 (approx.[a]) |
| Sonde Down 8 pmol | 0.48 (approx.[a]) |
| SuperScript Platinum Taq | 0.3 |
| RNAsin | 0.168 |
| dUTP | 0.24 |
| UNG | 0.6 |
| RNA | 4 |
| Master mix | 8 |

[a]May vary in volume

Controls (all in duplicate):

Positive control: RNA of the K562 cell line.

Dilution: 100, 10, 1, and 0.1 ng.

Negative control: water (*see* **Note 9**).

### *3.3.6 Real-Time RT-PCR Protocol for WT1*

Detects: aberrantly over-expressed panleukemic marker WT 1 in acute leukemia.

Primers:

WT 1 forward: 5′-CGC TAT TCG CAA TCA GGG TTA C-3′, length: 22.

WT 1 reverse: 5′-ATG GGA TCC TCA TGC TTG AAT G-3′, length: 22.

TaqMan™ probe:

WT 1 probe: 6 FAM-CGG TCA CCT TCG ACG GGA CGC xT-pH, length: 22.

LightCycler conditions for WT1:

| | Temperature | Incubation time |
|---|---|---|
| Reverse transcription | 55 °C | 20 min |
| Initial denaturation | 95 °C | 30 s |
| Denaturation | 95 °C | 1 s |

(continued)

(continued)

| | Temperature | Incubation time |
|---|---|---|
| Annealing | 56 °C | 15 s |
| Extension | 72 °C | 18 s |
| Cooling | 4 °C | 1 min |
| 45 cycles | | |

Prepare the following master mix for 1×:

| 12 µL total volume | 1× (in µL) |
|---|---|
| 2× reaction mix | 4.8 |
| 50 mM $MgSO_4$ | 0.675 |
| UNG | 0.6 |
| SuperScript | 0.3 |
| 20 mg/mL BSA | 0.3 |
| dUTP | 0.24 |
| TaqMan™ probe | 0.24 approx.[a] |
| RNAsin | 0.168 |
| Primer FOR 20 pmol | 0.08 approx.[a] |
| Primer REV 20 pmol | 0.08 approx.[a] |
| RNA | 4 |
| Mix | 7.5 |

[a]May vary in volume

Controls (all in duplicate):

Positive control: RNA of the K562 cell line.

Dilution: 100, 10, 1, and 0.1 ng.

Negative control: water (*see* **Note 10**).

### *3.3.7 FLT3 Length Mutations Detection by RT-PCR*

Detects in up to 30 % of all acute myeloid leukemia.

Primers:

FLT3 R5: 5′-TGTCGAGCAGTACTCTAAACATG-3′, length: 23.

FLT3 12R: 5′-CTTTCAGCATTTTGACGGCAACC-3′, length: 23.

PCR program—FLT3-RT-PCR:

| Initial denaturation | 94 °C | 2 min | |
|---|---|---|---|
| Denaturation | 94 °C | 30 s | |
| Annealing | 56 °C | 1 min | 35 cycles |

(continued)

(continued)

| | | |
|---|---|---|
| Extension | 72 °C | 2 min |
| Final extension | 72 °C | 10 min |
| Cooling | 4 °C | |

Prepare the following master mix for 1×:

| 50 µL total volume | 1× (in µL) |
|---|---|
| 25 µL total volume | 1× (in µL) |
| Water | 15.46 |
| DNTP | 4.0 |
| 10× PE buffer | 2.5 |
| Primer 1 | 10 pmol |
| Primer 2 | 10 pmol |
| PE Taq | 0.4 |
| cDNA | 2 µL |
| Mix | 22.5 µL |

1× high-fidelity master mix: 25

| | | |
|---|---|---|
| FLT3-5R | 10 pmol | 0.08 approx.[a] |
| FLT3-12R | 10 pmol | 0.08 approx.[a] |

[a]May vary in volume

Results

The wild type has 456 bp, whereas the peaks (one or more) of length mutations can be detected >456 bp.

### 3.3.8 FLT3 Length Mutation Detection by Using a Genetic Analyzer

Detects in up to 30 % of all acute myeloid leukemia.

Primers:

FLT3 11F: 5′-6-FAM-GCAATTTAGGTATGAAAGCCAGC-3′, length: 23.

FLT3 12R: 5′-CTTCAGCATTTTGACGGCAACC-3′, length: 22.

PCR program—FLT3-A:

| Initial denaturation | 94 °C | 2 min | |
|---|---|---|---|
| Denaturation | 94 °C | 30 s | |
| Annealing | 60 °C | 1 min | 30 cycles |
| Extension | 72 °C | 1.15 min | |
| Final extension | 68 °C | 45 min | |
| Cooling | 4 °C | | |

Prepare the following master mix for 1×:

| 50 µL total volume | 1× (in µL) |
|---|---|
| 1× high-fidelity master mix | 25 |
| FLT3-11 Fam 15 pmol | 0.75 approx.[a] |
| FLT3-12 R 15 pmol | 0.07 approx.[a] |
| Aqua bidest | 19.18 |
| 100 ng DNA | |
| Master mix | 45 |

[a]May vary in volume

ABI Prism Genetic Analyzer 310 conditions:

| Polymer | POP 4 | Injection time in | 1 s |
|---|---|---|---|
| Capillary | 47 cm | Injection | 10.0 kV |
| Dye set | DS 30 (Matrix) | Run | 15.0 kV |
| Filter set | D (GS STR POP 4-1 mL) | Run | 55 ° C |
| Size STD | SSTD 500 Rox FLT3 | Run (time) | 66 min |

### *3.3.9 Preparation of Samples*

Mix 1 µL of PCR product with 8.5 µL aqua bidest and 0.5 µL ROX500 internal size standard.

1 µL PCR product.

8.5 µL aqua bidest.

0.5 µL SSTD Rox 500.

Prepare denaturation of the samples:

| 95 °C | 3 min |
|---|---|
| 4 °C | 3 min |

### Results

Data can be analyzed with the ABI Prism Genetic Analyzer 310 including Genemapper v.3.10 software. The wild type has 329 bp, whereas the peaks (one or more) of length mutations can be detected >329 bp. For controls the cell line MV4-11 can be used which shows peaks at 359 bp (*see* **Note 11**).

### *3.3.10 NPM1 Mutation Detection by Real-Time RT-PCR*

Primers:

NPM1 forward: 5′-GAAGAATTGCTTCCGGATGACT-3′, length: 22.

NPM1-A reverse: 5′-CTTCCTCCACTGCCAGACAGA-3′, length: 21.

NPM1-B reverse: 5′-TTCCTCCACTGCCATGCAG-3′, length: 19.

TaqMan™ probe:

NPM1 probe: 5′-FAM-ACCAAgAggCTATTCAA x-3′, length: 17.

PCR conditions for NPM1-A:

| | Temperature | Incubation time |
|---|---|---|
| Reverse transcription | 55 °C | 20 min |
| Initial denaturation | 95 °C | 10 min |
| Denaturation | 95 °C | 15 s |
| Annealing and extension | 62 °C | 1 min |
| Cooling | 4 °C | 1 min |
| 50 cycles | | |

For NPM1-B annealing and extension, the temperature is 59 °C instead of 62 °C.

Prepare the following master mix for 1×:

| 12 μL total volume | 1× (in μL) |
|---|---|
| 2× reaction mix | 4.8 |
| 50 mM $MgSO_4$ | 0.675 |
| UNG | 0.6 |
| SuperScript | 0.3 |
| 20 mg/mL BSA | 0.3 |
| dUTP | 0.24 |
| TaqMan™ probe | 0.24 approx.[a] |
| RNAsin | 0.168 |
| Primer FOR 20 pmol | 0.08 approx.[a] |
| Primer REV 20 pmol | 0.08 approx.[a] |
| RNA | 4 |
| Mix | 7.5 |

[a]May vary in volume

Controls (all in duplicate):

For NPM1-A mutations NPM1 forward and NPM1-A reverse primer and TaqMan™ probe NPM1 are used; for NPM1-B mutations NPM1 forward and NPM1-B reverse primer and TaqMan™ probe are used.

Positive control: RNA of the Kasumi-1 cell line.

Dilution: 100, 10, 1, and 0.1 ng.

Negative control: water (*see* **Note 12**).

### 3.3.11 Multiplex Nested Qualitative RT-PCR for 11Q23 Chromosomal Aberrations [t(6;11), t(9;11), and t(11;19)]

Detects MLL/AF4, MLL/AF6, MLL/AF9, and MLL/ENL transcripts.

Primers:

P1: 5′-CCT GAA TCC AAA CAG GCC ACC ACT-3′, length: 24.
P2: 5′-CTT CCA GGA AGT CAA GCA AGC AGG-3′, length: 24.
P3: 5′-GTC ACT GAG CTG AAG GTC GTC TTC G-3′, length: 25.
P4: 5′-AGC ATG GAT GAC GTT CCT TGC TGA g-3′, length: 25.
P5: 5′-TCC AAT TCA GTT GTA CAA CTA GAG G-3′, length: 25.
P6: 5′-CCA ATC TTC TTT CTC CGC TGA CAT G-3′, length: 25.
P7: 5′-TCT GAT TTG CTT TGC TTT ATT GGA C-3′, length: 25.
P8: 5′-CGT GAT GTA GGG GTG AAG AAG CAG-3′, length: 24.
P9: 5′-CCA CGA AGT GCT GGA TGT CAC AT-3′, length: 23.
P10: 5′-CGG ACA AAC ACC ATC CAG TCG TG-3′, length: 23.

First step: cDNA synthesis (*see* Subheading 3.2).
Nested PCR:

| Program | 11Q23 1. Step | Program | 11Q23 2. Step | |
|---|---|---|---|---|
| 94 °C | 1.00 min | 94 °C | 1.00 min | |
| 60 °C | 2.00 min 35× | 60 °C | 2.00 min | 25× |
| 74 °C | 2.00 min | 74 °C | 2.00 min | |
| 4 °C | ∞ | 4 °C | ∞ | |

Prepare the following master mix for 1× (1. Step):

| 50 µL total volume | 1× (in µL) |
|---|---|
| Water | 30.92 |
| dNTP | 8.0 |
| 10× PE buffer | 5.0 |
| Primer 1 | 10 pmol |
| Primer 3 | 10 pmol |
| Primer 5 | 10 pmol |
| Primer 7 | 10 pmol |
| Primer 9 | 10 pmol |
| PE Taq | 0.4 |
| cDNA | 5 µL |
| Mix | 45 µL |

Master mix for 2. PCR (2. Step):

| 50 µL volume | 1× (in µL) |
|---|---|
| Aqua bidest | 30.9 |
| dNTP | 8.0 |
| 10× PE buffer | 5.0 |
| Primer 2 | 10 pmol |
| Primer 4 | 10 pmol |
| Primer 6 | 10 pmol |
| Primer 8 | 10 pmol |
| Primer 10 | 10 pmol |
| PE Taq | 0.4 |
| cDNA | 5 µL |
| Mix | 45 µL |

Controls: cDNA of cell line MV4-11. Agarose gel electrophoresis 2 % (*see* **Note 13**).

## 4 Notes

1. All quantitative PCR protocols here are designed for use of a LightCycler™ device.
2. For positive controls RNA of a specific cell line was used. The use of plasmid as control is also possible but is associated with a little bit more crossover decontaminations.
3. In order to avoid carry-over decontamination, the recommendations of Kwok and Higuchi should be considered strictly [16]. RNA or DNA isolation should be performed at different places. Use positive-displacement pipettes to avoid inaccuracies in pipetting.
4. Reverse transcription of mRNA to cDNA should be done with random hexamers (not with oligo-dT). Most of the above-shown real-time RT-PCR protocols do not have a separate cDNA-synthesis step here.
5. This is a one-step real-time RT-PCR using mRNA as a template [5]. The master mix contains only 4.8 µL instead of 6 µL of a 2× reaction mix in 12 µL total PCR volume, which is absolutely sufficient.
   It is of importance to know that results of real-time PCR for one sample can vary between laboratories and even between individuals, which perform the test as shown in internal laboratory quality assurance tests [17]. All standard dilutions and patient's

samples should be tested in duplicate. For quantification, the average value of both duplicates should be used. Samples that had a more than a hundredfold difference for both housekeeping gene values should be excluded from further analysis. Samples negative for the housekeeping gene but positive for the target gene should be excluded from quantification. A negative assay requires the absence of the target PCR product as well as no amplification of the "blank" sample and a positive amplification of the positive control but a successful housekeeping gene PCR amplification. The expression of the target gene is given as the quotient of the target gene and housekeeping gene. The housekeeping gene should also be related to a standard curve derived from a serial dilution of plasmids or RNA of a target-specific leukemic cell line into water.

6. UNG is added in the reaction to prevent the re-amplification of carry-over PCR products by removing any uracil incorporated into amplicons. Please *see* also refs. 18–20.
7. Please note that template is cDNA for this real-time PCR here. There are six different CBFβ-MYH11 transcripts commonly found in AML with inv(16). Type A is most commonly found up to 80 %. Further, the control cell line ME-1 does express only type A. For each subtype a separate PCR must be performed using the specific reverse primer and the common forward primer. The use of SYBR® Green instead of hybridization probes is not recommended due to the high risk of contamination, which can shut down every laboratory for a longer period of time. Please *see* also refs. 19–25.
8. This real-time RT-PCR is again a single-step PCR using RNA as template. It detects the fusion transcripts S and L of PML-RARA in a single run, but not the variant type. Please *see* also refs. 12, 21, 26.
9. As housekeeping genes GAPDH, G6PDH, Abelson (ABL), beta-2-microglobulin (B2M), and beta-glucuronidase (GUS) are most commonly used. To avoid pseudogenes and maintain a stability in the level of expression of mRNA in each cell, B2M, ABL, and beta-glucuronidase were recently recommended by the Europe Against Cancer (EAC) program [14]. Nevertheless, most laboratories continue to use GAPDH as their housekeeping genes [10]. For quantification please *see* also **Note 1** above.
10. The use of WT1 as an MRD marker is still discussed controversially and should only be used if no other specific MRD marker is available. This real-time RT-PCR uses a TaqMan™ probe. K562 can be used as a control cell line. Please *see* also refs. 27–30.

11. Use only the high-fidelity master mix kit (from Roche Diagnostics) for PCR when subsequently a genetic analyzer is used. Results showing more than a single PCR product of 329 bp indicate that a FLT3 mutation is detected. Please *see* also refs. 30–32.
12. Detect mutations A and B which consist 90 % of mutations of the nucleophosmin (NPM1) gene in AML by a real-time PCR assay with a common forward primer and probe and two different mutation-specific reverse primers.
13. This is a very robust nested multiplex RT-PCR, which uses cDNA as template and detects the most common MLL rearrangement genes: MLL/AF4, MLL/AF6, MLL/AF9, and MLL/ENL. Please *see* also ref. 33.

## References


1. Elmaagacli AH, Becks HW, Beelen DW et al (1995) Detection of minimal residual disease and persistence of host-type hematopoiesis: a study in 28 patients after sex-mismatched, non T-cell-depleted allogeneic bone marrow transplantation for Philadelphia-chromosome positive chronic myelogenous leukemia. Bone Marrow Transplant 16:823–829
2. Mackinnon S, Barnett L, Heller G, O'Reilly RJ (1994) Minimal residual disease is more common in patients who have mixed T-cell chimerism after bone marrow transplantation for chronic myelogenous leukemia. Blood 83:3409–3416
3. Kolb H, Mittermüller J, Clemm C et al (1990) Donor leukocyte transfusions for treatment of recurrent chronic myelogenous leukemia in marrow transplant patients. Blood 76:2462–2465
4. Elmaagacli AH, Beelen DW, Opalka B, Seeber S, Schaefer UW (1999) The risk of residual molecular and cytogenetic disease in patients with Philadelphia-chromosome positive first chronic phase chronic myelogenous leukemia is reduced after transplantation of allogeneic peripheral blood stem cells compared to bone marrow. Blood 94:384–389
5. Kiyoi H, Naoe T, Yokota S et al (1997) Internal tandem duplication of FLT3 associated with leukocytosis in acute promyelocytic leukemia. Leukemia Study Group of the Ministry of Health and Welfare (Kohseisho). Leukemia 11:1447–1452
6. Gorello P, Cazzaniga G, Alberti F et al (2006) Quantitative assessment of minimal residual disease in acute myeloid leukemia carrying nucleophosmin (NPM1) gene mutations. Leukemia 20:1103–1108
7. Marcucci G, Haferlach T, Döhner H (2011) Molecular genetics of adult acute myeloid leukemia: prognostic and therapeutic implications. J Clin Oncol 29:475–486
8. Kumar CC (2011) Genetic abnormalities and challenges in the treatment of acute myeloid leukemia. Genes Cancer 2:95–107
9. Sanders MA, Valk PJM (2013) The evolving molecular genetic landscape in acute myeloid leukaemia. Curr Opin Hematol 20:79–85
10. Elmaagacli AH, Freis A, Hahn M et al (2001) Estimate the relapse stage in chronic myeloid leukaemia patients after allogeneic stem cell transplantation by the amount of BCR-ABL fusion transcripts detected using a new real-time polymerase chain reaction method. Br J Haematol 113:1072–1075
11. Reading CL, Estey EH, Huh YO et al (1996) Expression of unusual immunophenotype combinations in acute myelogenous leukemia. Blood 81:3083–3090
12. Macedo A, San Miguel JF, Vidriales MB et al (1996) Phenotypic changes in acute myeloid leukaemia: implications on the detection of minimal residual disease. J Clin Pathol 49:15–18
13. Bernell P, Arvidsson I, Jacobsson B, Hast R (1996) Fluorescence in situ hybridization in combination with morphology detects minimal residual disease in remission and heralds relapse in acute leukaemia. Br J Haematol 95:666–672
14. Weisser M, Haferlach T, Schoch C et al (2003) The use of housekeeping genes for real-time PCR based quantification of fusion gene transcripts in AML. Leukemia 17:2474–2486
15. Holland PM, Abramson RD, Watson R, Gelfand DH (1991) Detection of specific

polymerase chain reaction product utilizing the 5′–3′ exonuclease activity of Thermus aquaticus DNA polymerase. Proc Natl Acad Sci USA 88:7276–7280
16. Kwok S, Higuchi R (1989) Avoiding false positives with PCR. Nature 339:237–238
17. Burmeister T, Maurer J, Aivado M et al (2000) Quality assurance in RT-PCR-based BCR/ABL diagnostics—results of an interlaboratory test and a standardization approach. Leukemia 14:1850–1856
18. Schnittger S, Weiser M, Schoch C et al (2003) New score predicting for prognosis in PML-RARA+, AML1-ETO+, or CBFB-MYH11+ acute myeloid leukemia based on quantification of fusion transcripts. Blood 102:2746–2755
19. Krauter J, Wattjes MP, Nagel S et al (1999) Real-time RT-PCR for the detection and quantification of AML1/MTG fusion transcripts in t(8;21)-positive AML patients. Br J Haematol 107:80–85
20. Elmaagacli AH, Beelen DW, Kroll M et al (1997) Detection of AML1/ETO fusion transcripts in patients with t(8;21) acute myeloid leukemia after allogeneic bone marrow transplantation or peripheral blood progenitor cell transplantation. Blood 90:3230–3231
21. Guerrasio A, Pilatrino C, De Micheli D et al (2002) Assessment of minimal residual disease (MRD) in CHFbeta/MYH11-positive acute myeloid leukemias by qualitative and quantitative RT-PCR amplification of fusion transcripts. Leukemia 16:1176–1181
22. Krauter J, Hoellge W, Wattjes MP et al (2001) Detection and quantification of CBFB/MYH11 fusion transcripts in patients with inv(16)-positive acute myeloblastic leukaemia by real-time RT-PCR. Genes Chromosomes Cancer 30:342–348
23. Marcucci G, Caliguri MA, Dohner H et al (2001) Quantification of CBFbeta/MYH11 fusion transcript by real time RT-PCR in patients with INV(16) AML. Leukemia 15:1072–1080
24. Buonamici S, Ottaviani E, Testoni N et al (2002) Real-time quantification of minimal residual disease in inv (16)-positive acute myeloid leukaemia may indicate risk for clinical relapse and may identify patients in a curable state. Blood 99:443–449
25. Elmaagacli AH, Beelen DW, Kroll M, Trzensky S, Stein C, Schaefer UW (1998) Detection of CBFB/MYH11 fusion transcripts in patients with inv(16) AML after allogeneic bone marrow or peripheral blood progenitor cell transplantation. Bone Marrow Transplant 21: 159–166
26. Gallagher RE, Yeap BY, Bi W et al (2003) Quantitative real-time RT-PCR analysis of PML-RARA alpha mRNA in acute promyelocytic leukaemia: Assessment of prognostic significance in adult patients from intergroup protocol 0129. Blood 101:2521–2528
27. Ogawa H, Tamaki H, Ikegame K et al (2003) The usefulness of monitoring WT1 gene transcripts for the prediction and management of relapse following allogeneic stem cell transplantation in acute type leukaemia. Blood 101:1698–1704
28. Cilloni D, Gottardi E, Fava M et al (2003) Usefulness of quantitative assessment of the WT1 gene transcript as a marker for minimal residual disease detection. Blood 102:773–774
29. Elmaagacli AH, Beelen DW, Trenschel R, Schaefer UW (2000) The detection of wt-1 transcripts is not associated with an increased leukemic relapse rate in patients with acute leukemia after allogeneic bone marrow or peripheral blood stem cell transplantation. Bone Marrow Transplant 25:91–96
30. Vaughn CP, Elenitoba-Johnson KSJ (2004) High-resolution melting analysis for detection of internal tandem duplications. J Mol Diagn 6:211–216
31. Schnittger S, Schoch C, Dugas M et al (2002) Analysis of FLT3 length mutations in 1003 patients with acute myeloid leukemia: correlation to cytogenetics, FAB subtype, and prognosis in the AMLCG study and usefulness as a marker for the detection of minimal residual disease. Blood 100:59–66
32. Yokota S, Kiyoi H, Nakao M et al (1997) Internal tandem duplications of the FLT3 gene is preferentially seen in acute myeloid leukemia and myelodysplastic syndrome among various hematological malignancies. A study on a large series of patients and cell lines. Leukemia 11:1605–1609
33. Repp R, Borkhardt A, Haupt E et al (1995) Detection of four different 11q23 chromosomal abnormalities by multiplex-PCR and fluorescent-based automatic DNA-fragment analysis. Leukemia 9:210–216

# Chapter 12

# Molecular Methods for Detection of Minimal Residual Disease Following Transplantation in Lymphoid and Plasma Cell Disorders

**Paolo Corradini and Cristiana Carniti**

## Abstract

Relapse represents the main cause of treatment failure after stem cell transplantation (SCT). Thus, monitoring of minimal residual disease (MRD) in allografted patients allows an early detection of recurrence and a subsequent intervention prior to clinically detectable relapse. MRD assessment by polymerase chain reaction-based methods is currently part of the routine clinical management of patients with chronic myeloid leukemia after allo-SCT. It is also recognized that it is a useful prognostic tool in several mature lymphoid and plasma cell disorders such as chronic lymphocytic leukemia, follicular lymphoma, mantle cell lymphoma, and multiple myeloma. In some of these entities, clinical trials employing MRD as a decision-making tool are currently ongoing and will define whether sensitive MRD detection allows for earlier therapeutic intervention to improve the outcome of SCT. We here discuss the methods of MRD evaluation in lymphoid and plasma cell disorders following transplantation with the ultimate aim of providing critical information for the setup of molecular approaches to detect MRD.

**Key words** Minimal residual disease, Stem cell transplantation, Polymerase chain reaction, Lymphoid malignancies, Multiple myeloma

## 1 Introduction

During the last decade, a large number of studies have shown that detection of very low numbers of malignant cells, that is, detection of minimal residual disease (MRD), significantly correlates with clinical outcome in many hematologic malignancies. The sensitive quantification of MRD after treatment has been suggested as an alternative means to predict response duration and overall survival [1]. The highest sensitivity and specificity can be achieved by molecular monitoring of tumor- or patient-specific markers measured by polymerase chain reaction (PCR)-based techniques. Allogeneic stem cell transplant (allo-stem cell transplantation (SCT)) is an effective therapeutic option for many hematological disorders including follicular lymphoma (FL), chronic lymphocytic

Meral Beksaç (ed.), *Bone Marrow and Stem Cell Transplantation*, Methods in Molecular Biology, vol. 1109,
DOI 10.1007/978-1-4614-9437-9_12, 

leukemia (CLL), Hodgkin's disease (HD), mantle cell lymphomas (MCL), and multiple myeloma (MM) [2–4]. Outcome of patients with clinical relapse after transplantation generally remains poor, but intervention prior to florid relapse might improve the outcome. Therefore detection of MRD is commonly used after allo-SCT in order to closely monitor patients.

In the setting of MRD, along with the established qualitative PCR-based methods that allow the amplification of a tumor-specific molecular marker, which ideally consists of a DNA sequence that is always detectable in tumor cells and always absent in normal cells, a number of quantitative and semiquantitative PCR strategies have been investigated to assess the tumor burden. Among them, real-time quantitative PCR is a recently introduced technique which allows the determination of residual tumor, overcoming most of the limitations associated with quantitative or semiquantitative PCR. The main advantages associated with real-time PCR method are the following: (1) the measurement of target DNA copy number is made in the PCR tube as the reaction proceeds without the need for post-PCR sample processing; (2) it greatly reduces the occurrence of false-positive results by adding the specificity of a probe to the one of primers; and (3) it has a relatively wide dynamic range, allowing the accurate quantification of samples over a wide range of tumor contamination with a sensitivity of $10^{-4}$–$10^{-6}$.

A paradigm for the importance of minimal molecular disease and prediction of relapse after allo-SCT is CML. Here, it is now well established that the detection of the chimeric *BCR–ABL* mRNA transcript by reverse-transcriptase polymerase chain reaction (RT-PCR) is a powerful predictor of subsequent relapse [5]. The use of quantitative PCR has greatly increased the clinical value of monitoring MRD.

The clinical impact of MRD detection in different lymphomas is not identical and depends on the markers. The majority of lymphoid and plasma cell malignancies are characterized by a clonal rearranged immunoglobulin heavy chain (IgH) DNA sequence [6]. This is a *clonotypic* sequence because it is present in all the members of the tumor clone. In normal lymphocytes, clones of cells with different IgH sequences coexist, reflecting the normal development of polyclonal B-cells in response to antigen. In lymphoid and plasma cell malignancies, clonotypic cells greatly outnumber normal polyclonal B-cells, and therefore the clonotypic sequence is the most frequently occurring Ig sequence, greatly exceeding the frequency of any normal Ig sequence. The clonotypic sequence can be isolated from tumor samples by PCR using consensus primers that amplify the entire repertoire of Ig sequences [6]. In follicular lymphomas and mantle cell lymphomas the clonotypic IgH sequence can be isolated, but these tumors are also characterized by the presence of specific translocation that might serve as markers for MRD monitoring.

CLL is the most common adult leukemia. Despite improvements in treatment responses using multiagent therapy, CLL remains incurable with available immunochemotherapy regimens [7]. Patients with relapsed CLL and those with high-risk features at presentation, such as 17p deletions or unmutated IGH regions, are generally referred for allo-SCT [8]. Fifty percent of CLL patients undergoing allo-SCT experience long-term disease-free survival (DFS) and may be cured. Nevertheless, 50 % of patients will experience disease recurrence [8]. Quantification of CLL MRD has prognostic value because achievement of MRD negativity 1 year after allo-SCT is associated with long-term DFS [1]. Furthermore, strategies for treating post-allo-SCT relapse, including additional chemotherapy, donor lymphocyte infusions, and cell vaccines, may be more effective when CLL progression is detected with low tumor burden. The utility of MRD assessment in CLL has been studied in several clinical contexts, but most reports have focused on MRD following hematopoietic cell transplantation because only allo-SCT achieves long-term remissions in high-risk CLL. PCR quantification of clonal IgH sequences was developed >20 years ago [9], and after demonstration that this technique has single-cell sensitivity, allele-specific oligonucleotide-PCR (ASO-PCR) was developed for MRD quantification [10]. There is evidence that even qualitative MRD methods can provide prognostic information [1]. However, as the superior prognostic significance using certain MRD levels or even MRD kinetics [11] has been shown, MRD quantification nowadays is clearly preferable and ASO IgH RQ-PCR is generally considered the more sensitive quantitative technique.

In multiple myeloma MRD can be detected by PCR using patient-specific primers derived from the rearrangement of IgH genes. It could be shown that durable PCR negativity after allografting had a cumulative risk of relapse at 5 years of 0 %, in comparison to 33 % for PCR-mixed patients and 100 % for patients who never achieved PCR negativity [4].

In FL, allo-SCT should be considered in high-risk populations early in the disease process as well as in the setting of relapsed disease. Monitoring of MRD can be an important tool for early intervention with drugs, cyclosporine withdrawal, or donor lymphocyte infusions [2, 12]. In this setting only the major breakpoint region (MBR) and minor clustering region (mcr) breakpoints have been currently exploited as targets for MRD detection. Thus, only a subset of patients ranging from 50 to 65 % can be assessed using this approach [13]. However, there are no technical reasons precluding development of novel MRD PCR assays that could also detect “minor” BCL-2 breakpoints such as the minor cluster region breakpoint. This would allow the development of a more extensive PCR screening platform and the identification of a tumor marker in the majority of patients with FL.

Patients with relapsed or refractory MCL following conventional intensive chemotherapy or auto-SCT have limited therapeutic options. Allogeneic transplant using myeloablative regimens was initially studied as a potentially curative approach for these patients. Fludarabine-based reduced intensity conditioning (RIC) regimens have gained precedence over myeloablative regimens in the last decade. The chromosomal translocation t(11;14)(q13;q32) represents a chromosomal aberration that is pathogenetically related to MCL development and is a stable molecular marker for this lymphoma entity [14]. However, the main disadvantage of chromosomal translocations as MRD markers is that they are restricted to those cases with a PCR-detectable translocation. While the translocation t(11;14)(q13;q32) is detectable in 80–90 % of MCL by fluorescence in situ hybridization (FISH) or chromosome banding analysis [15], PCR is able to detect the translocation in only 25–40 %. The most broadly applicable marker for MRD studies, the IgH gene rearrangement, can also be applied to MCL [16]. Analysis of MRD by consensus PCR demonstrated evidence of a graft-versus-lymphoma effect in four of seven patients. PCR monitoring of MRD will be extremely helpful to evaluate efficiency of this treatment approach and will allow programmed infusion of donor lymphocytes depending on MRD status. In contrast to FL, where a proportion of patients remain in continuous clinical CR despite continuous presence of PCR-detectable MRD, data in MCL demonstrate that reappearance of MRD after allo-SCT is associated with clinical relapse [17] and patients have an adverse prognosis [17]. Sequential MRD monitoring is therefore a powerful predictor for treatment outcome in MCL and allows targeted treatment.

This chapter focuses on the methods used to determine the molecular markers characteristics of lymphoid malignancies and multiple myeloma and on the methods for MRD monitoring.

## 2 Materials

### 2.1 Mononuclear Cell Isolation

1. Dulbecco's phosphate-buffered saline (D-PBS) without calcium and magnesium.
2. Ficoll separating solution (density 1.077 g/mL).
3. Live/dead staining solution for the counting (e.g., Trypan Blue).

### 2.2 Genomic DNA Extraction

1. DNAzol reagent (Invitrogen, Carlsbad, California, USA).
2. Ethanol 100 % stored at –20 °C.
3. Ethanol 70 % stored at –20 °C.
4. Sterile water or 8 mM NaOH or 0.1× TE buffer.

### 2.3 Qualitative PCR

1. dNTP mix (dATP, dCTp, dGTP, and dTTP) (various companies such as Bio-Rad, Invitrogen, and Sigma supply suitable dNTP sets) (*see* **Note 1**).
2. 10× Buffer Taq DNA polymerase (*see* **Note 2**).
3. 25 mM $MgCl_2$ solution.
4. Any commercially available thermostable DNA polymerase, for example, *Taq* DNA Polymerase, native (Invitrogen, cat. no. 18038-042) 5 Units/μL (*see* **Note 3**).
5. Forward and reverse primers (10 pmol/μL) (Tables 1 and 2).
6. Sterile water or DNase/RNase-free water.
7. 1–3 % (wt./vol) agarose gel (depending on the size of PCR product to be analyzed).
8. Low-melting-point (LMP) agarose.
9. 12 % polyacrylamide gel (19:1 acrylamide:bisacrylamide).
10. Ethidium bromide (10 mg/mL) (*see* **Note 4**) or fluorescent nucleic acid gel stain (e.g., Lonza GelStar™ Gel Stain 10,000×).
11. Loading buffer (convenient 10× sample buffer stock consists of 50 % glycerol, 0.25 % bromophenol blue, and 0.25 % xylene cyanol FF in 1× Tris–acetate–EDTA (TAE) buffer (40 mM Tris (pH 7.6), 20 mM acetic acid, and 1 mM EDTA)).
12. Buffer 10× Tris–boric acid–EDTA (TBE) (89 mM Tris (pH 7.6), 89 mM boric acid, 2 mM EDTA).
13. Double-stranded DNA molecular weight markers.
14. Single-step enzymatic cleanup of PCR products that eliminates unincorporated primers and dNTPs (e.g., USB ExoSAP-IT reagent, US Biochemicals, Cleveland, OH).
15. Any one-step cloning strategy for the direct insertion of a PCR product into a plasmid vector.
16. *E. coli* competent cells suitable for transformation.
17. S.O.C. medium (2 % tryptone, 0.5 % yeast extract, 10 mM NaCl, 2.5 mM KCl, 10 mM $MgCl_2$, 10 mM MgSO4, 20 mM glucose).
18. LB plates containing antibiotics (50 μg/mL kanamycin or 100 μg/mL ampicillin) and 40 mg/mL X-gaL in dimethylformamide (DMF).
19. Any kit for plasmid purification of cloned inserts from *E. coli*.

Reagent stocks for the PCR reaction and molecular weight marker are stored at –80 °C. Reagent aliquots are stored at –20 °C; molecular weight marker and loading buffer aliquots are stored at 4 °C.

**Table 1**
**Primers for immunoglobulin heavy chain gene VDJ rearrangement amplification**

| | | |
|---|---|---|
| **Forward primers** | | |
| *FR1 region-derived primers* | | |
| VH/FS | VH1/FS | 5′-CAGGTGCAGCTGGTGCA(C/G)(A/T)CTG-3′ |
| | VH2/FS | 5′-CAG(A/G)TCACCTTGAAGGAGTCTG-3′ |
| | VH3/FS | 5′-CAGGTGCAGCTGGTG(G/C)AGTC(C/T)G-3′ |
| | VH4a/FS | 5′-CAG(C/G)TGCAGCTGCAGGAGTC(C/G)G-3′ |
| | VH4b/FS | 5′-CAGGTGCAGCTACA(A/G)CAGTGGG-3′ |
| | VH5/FS | 5′-GAGGTGCAGCTG(G/T)TGCAGTCTG-3′ |
| | VH6/FS | 5′-CAGGTACAGCTGCAGCAGTCAG-3′ |
| VH/D | VH1/D | 5′-CCTCAGTGAAGGTCTCCTGCAAGG-3′ |
| | VH2/D | 5′-TCCTGCGCTGGTGAAAGCCACACA-3′ |
| | VH3/D | 5′-GGTCCCTGAGACTCTTCCTGTGCA-3′ |
| | VH4a/D | 5′-TCGGAGACCCTGTCCCTCACCTGCA-3′ |
| | VH4b/D | 5′-CGCTGTCTCTGGTTACTCCATCAG-3′ |
| | VH5/D | 5′-GAAAAAGCCCGGGGAGTCTCTGAA-3′ |
| | VH6/D | 5′-CCTGTGCCATCTCCGGGGACAGTG-3′ |
| *Leader region-derived primers* | | |
| VH/LS | VH1/LS | 5′-CTCACCATGGACTGGACCTGGAG-3′ |
| | VH2/LS | 5′-ATGGACATACTTTGTTCCACGCTC-3′ |
| | VH3/LS | 5′-CCATGGAGTTTGGGCTGAGCTGG-3′ |
| | VH4/LS | 5′-ACATGAAACA(C/T)CGTGGTTCTTCC-3′ |
| | VH5/LS | 5′-ATGGGGTCAACCGCCATCCTCG-3′ |
| | VH6/LS | 5′-ATGTCTGTCTCCTTCCTCATCTTC-3′ |
| | VH7/LS | 5′-TTCTTGGTGGCAGCAGCCACA-3′ |
| VH/L | VH1/L | 5′-CCATGGACTGGACCTGGAGG-3′ |
| | VH2/L | 5′-ATGGACATACTTTGTTCCAC-3′ |
| | VH3/L | 5′-CCATGGAGTTTGGGCTGAGC-3′ |
| | VH4/L | 5′-ATGAAACACCTGTGGTTCTT-3′ |
| | VH5/L | 5′-ATGGGGTCAACCGCCATCCT-3′ |
| | VH6/L | 5′-ATGTCTGTCTCCTTCCTCAT-3′ |
| *FR3 region-derived primers* | | |
| FR3.3 | FR3.3 | 5′-ACACGGC(C/T)(G/C)TGTATTACTGT-3′ |
| **Reverse primers** | | |
| *FR1 and leader VH families* | | |
| | JHD | 5′-ACCTGAGGAGACGGTGACCAGGGT-3′ |
| FR3.3 | JH3.3 | 5′-GTGACCAGGGT(A/G/C/T) CCTTGGCCCCAG-3′ |

**Table 2**
**Primers for minimal residual disease analysis of Bcl-2 MBR/mcr and Bcl-1 by qualitative PCR**

| | |
|---|---|
| *Forward primers* | |
| Bcl-2 MBR first PCR | MBR-2 5′-CAGCCTTGAAACATTGATGG-3′ |
| Bcl-2 MBR second PCR | MBR-3 5′-ATGGTGGTTTGACCTTTAG-3′ |
| Bcl-2 mcr first PCR | mcr-2 5′-CGTGCTGGTACCACTCCTG-3′ |
| Bcl-2 mcr second PCR | mcr-3.1 5′-CCTGGCTTCCTTCCCTCTG-3′ |
| Bcl-1 first PCR | P2 5′-GAAGGACTTGTGGGTTGC-3′ |
| Bcl-1 second PCR | P4 5′-GCTGCTGTACACATCGGT-3′ |
| *Reverse primers* | |
| First PCR JH3 | 5′-ACCTGAGGAGACGGTGACC-3′ |
| Second PCR JH4 | 5′-ACCAGGGTCCCTTGGCCCCA-3′ |

*MBR* major breakpoint cluster region, *mcr* minor cluster region

### 2.4 Sequencing of PCR Products

1. Single-step enzymatic cleanup of PCR reagent (such as ExoSAP-IT, US Biochemicals, Cleveland, OH).
2. Reagents for automated fluorescent cycle sequencing such as a Big Dye terminator kit (Applied Biosystems, Foster City, CA).

### 2.5 Programs and Databases for IgH Sequence Analysis and Primer Design

1. IMGT, the international ImMunoGeneTics information system (http://imgt.cines.fr:8104/).
2. IMGT/V-QUEST Ig sequence alignment program (http://imgt.cines.fr:8104/textes/vquest/).
3. V BASE database of human Ig variable region genes (www.mrc-cpe.cam.ac.uk/).
4. DNAPLOT Ig sequence alignment program (http://www.mrc-cpe.cam.ac.uk/DNAPLOT.php?menu=901).
5. DNA analysis program such as Genetool 2.0 (BioTools, Edmonton, Alberta, Canada).
6. Primer design program such as Primer3 (www.frodo.wi.mit.edu/cgi-bin/primer3/primer3_www.cgi) and OligoCalc (http://www.basic.northwestern.edu/biotools/oligocalc.html).
7. Primer analysis such as Primer Blast (http://www.ncbi.nlm.nih.gov/tools/primer-blast/).

### 2.6 Quantitative PCR

1. TaqMan® Universal PCR Master Mix (Applied Biosystems, Warrington, UK).
2. Forward and reverse primers (10 pmol/μL or according to the optimization procedure described in Applied Biosystems Instrument Manual) (Table 4).
3. TaqMan probe (15 pmol/μL or according to the optimization procedure described in Applied Biosystems Instrument Manual).
4. Sterile water or DNase/RNase-free water.

Reagent stocks are stored at –80 °C. Reagent aliquots are stored at –20 °C. TaqMan probes are stored in the dark. TaqMan universal master mix is stored at 4 °C.

### 2.7 Instruments

1. Spectrophotometer.
2. Thermal cycler for qualitative PCR.
3. DNA electrophoresis apparatus and power supply.
4. Electrophoresis imaging system.
5. Any genetic analyzer for sequencing or service dedicated.
6. General devices for cloning (42 °C water bath, 37 °C shaking and non-shaking incubator, electroporator, hood, general microbiological supplies such as plates, spreaders). Cloning should be performed in a separate area to avoid contamination.
7. Real-time quantitative PCR system (any device is suitable; we use an Applied Biosystems 7900HT Fast Real-Time PCR System from Life Technologies, but we have also used an older non-laser-based instrument with comparable results).

## 3 Methods

### 3.1 Mononuclear Cell Isolation

1. Dilute peripheral blood or bone marrow samples with 1× DPBS (dilution factor 1:1 for peripheral blood and from 1:2 to 1:5 for bone marrow) (*see* **Notes 5**–**7**).
2. Add 4 mL of Ficoll separating reagent to a 15 mL tube for a sample volume ≤10 mL or add 10 mL of Ficoll solution to a 50 mL tube for a sample volume ≥10 mL (the proportion between Ficoll and blood should be 1/3 and 2/3, respectively).
3. Gently overlay diluted blood on top of Ficoll solution (*see* **Note 8**).
4. Centrifuge at 500 × *g* for 40 min, 20 °C, in a swinging-bucket rotor without brake (*see* **Note 9**).
5. Carefully remove the mononuclear cells from the Ficoll/plasma interphase with a 10 mL shorty pipette, and collect them into a new 50 mL conical tube.

6. Add DPBS to 50 mL and centrifuge at 300 × *g* for 10 min at 20 °C; repeat twice (*see* **Note 10**).
7. Remove supernatant, and resuspend the pellet in 10 or 20 mL 1× DPBS (according to the pellet).
8. Count the cells in a counting chamber (1/2 or 1/5 in Trypan Blue), and separate the cells according to the aliquots that you want to either extract or freeze.
9. Collect the cells in a 1.5 mL sterile plastic microcentrifuge tube.
10. Spin the tube in a microcentrifuge at 10,000 × *g* for 1 min.
11. Remove supernatant and store at –80 °C.

### 3.2 DNA Extraction

1. Add 1 mL of DNAzol (Invitrogen) to $10 \times 10^6$ frozen cells, and gently resuspend the pellet (*see* **Notes 11** and **12**).
2. Centrifuge at 10,000 × *g* for 10 min at RT.
3. Collect the supernatant in a new tube; do not remove the sediment.
4. Add 0.5 mL (for 1 mL of DNAzol) of 100 % ethanol and mix gently by inversion.
5. Remove the DNA precipitate by spooling with a pipette tip, and collect it into another tube.
6. Wash with 500 μL of 70 % ethanol twice.
7. Remove the DNA precipitate from ethanol and collect into a new 1.5 mL sterile plastic microcentrifuge tube.
8. Air-dry the DNA by storing open the tube for 5–15 min at RT.
9. Dissolve the DNA in sterile water or 8 mM NaOH (60–130 μL based on the precipitate dimensions).
10. Store the sample at 4 °C.
11. Check the DNA quality and quantity by means of a UV spectrophotometer (the A260:A280 ratio should be ~1.8 [range 1.7–2]) (*see* **Note 13**).

### 3.3 Qualitative PCR

#### 3.3.1 Biospecimen to Be Analyzed

As discussed, DNA can be extracted from peripheral blood (PB) cells, from bone marrow aspirate cells, or from embedded tissues depending on the disease for which we need to look for the tumor-associated VDJ rearrangement. In details for CLL, given the high leukocyte count in most CLL patients, PB, which is easy to obtain, is generally the preferred source of cells for the analysis. In cases with a low peripheral leukemic burden, other compartments such as bone marrow (BM) and lymph node may be used. For multiple myeloma, CD138+ malignant plasma cells (*see* **Note 14**) from BM aspirates represent the ideal starting material for the analysis. For

follicular lymphomas and mantle cell lymphomas, DNA might be extracted from BM aspirates in case of bone marrow involvement, but the best source would be an affected lymph node.

### 3.3.2 IgH Rearrangement

IgH rearrangement is an early event in B-lymphocyte ontogenesis, and it can be used as a molecular marker of the tumor clone in the vast majority of B-cell malignancies (Fig. 1). Three gene segments are present in the rearranged IgH genes, namely, the variable (V), diversity (D), and joining (J) regions. During B-lymphoid differentiation, the D segment joins J segment, and the resulting D–J segment joins one V region sequence producing a VDJ complex [18]. Diversity of antigen recognition is generated by the existence of many distinct V, D, and J segments with the potential to form the VDJ unit: 123–129 V segments (seven different families based on sequence homology), 27 D segments, and 9 J segments [18]. Sequence variability at the VDJ junctions [18] and somatic hypermutation [18] further contribute to the diversity. The VDJ region is subdivided into the VH leader region, encoding a conserved signal peptide sequence; three hypervariable complementarity-determining regions (CDRs) that are involved in antigen recognition; and four conserved framework regions (FRs) that maintain structural integrity of the molecule (Fig. 1).

The most hypervariable region produced by this phenomenon is the third complementarity-determining region (CDR3), which can be considered a unique marker for a given B-cell clone [18]. The strategy for amplifying the IgH VDJ region is to use primers specific for conserved sequences in the VH leader, FR, and con-

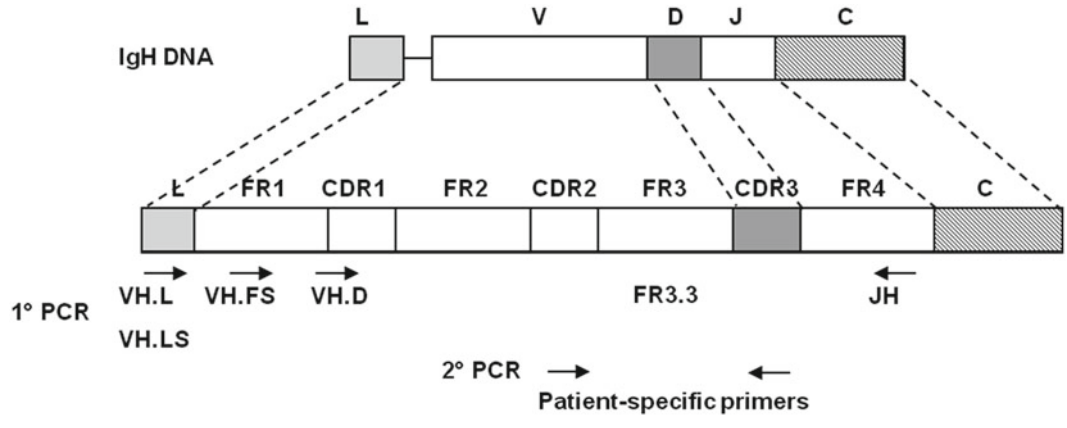


**Fig. 1** Schematic representation of the strategy used to analyze the immunoglobulin heavy chain (IgH) gene rearrangement. IgH gene leader (*L*), variable (*V*), diversity (*D*), and joining (*J*) regions are indicated. *Arrows* indicate the position of primer pairs used for PCR amplification of VDJ segment (1° PCR) and for patient-specific nested or seminested PCR (second PCR)

stant JH regions [19]. Positive PCR products are resolved by gel electrophoresis and directly sequenced and aligned with known IgH sequences in repositories such as IMGT. Patient-specific IgH primers can therefore be designed based on this alignment, which highlights the regions of the clonotypic sequence that differentiate it from the database IgH sequences. To obtain the best specificity, two patient-specific primers are designed for each clonotypic sequence: a sense primer specific for CDR2 and an antisense primer specific for CDR3. These primers can be used for nested-PCR amplification of the tumor-specific IgH rearrangement, thus allowing MRD detection with high sensitivity and specificity [20].

### PCR Protocol for the Identification of Patient-Specific (Clonotypic) IgH Sequences with VH FR1 and Leader Forward Primers

The FR1-based PCR strategies are frequently employed in IgH clonality testing and show a rather high detection rate, especially the widely used multiplex FR1 PCR of the BIOMED-2 consortium [21]. We prefer a more comprehensive approach to identify the tumor-associated IgH sequence that includes a leader-based strategy next to an FR1-based method. This standard PCR protocol uses four distinct primer sets that provide the best coverage of the VDJ region.

The PCR reaction must include a no-template control sample with each VH primer to exclude any possible contamination (*see* **Note 15**). DNA or cDNA is amplified using the four sets of forward consensus primers together with a JH region antisense primer. Nucleotide sequences of primers used in PCR experiments are listed in Table 1.

For each primer pair, set up a reaction (*see* Table 3 for representative scheme of PCR setup) in a 0.2-mL thin-walled PCR tube on ice as follows:

**Table 3**
**Representative qualitative PCR protocol**

| | Initial concentration | Final concentration | Final volume/ 50 µL reaction |
|---|---|---|---|
| PCR buffer | 10× | 1× | 5 µL |
| $MgCl_2$ | 25 mM | 1.5–2 mM | 3–5 µL |
| Template DNA | | | *X*µL |
| dNTP mix | 2 mM | 200 µM | 5 µL |
| Forward primer | 10 µM | 200 µM | 1 µL |
| Reverse primer | 10 µM | 200 µM | 1 µL |
| DNA polymerase | 5 U/µL | 1 U/50 µL | 0.25 µL |
| $dH_2O$ | | | Up to 50 µL |

1. Add 10 μM of each VH consensus forward primer to each tube (*see* **Note 16**).
2. Aliquot PCR reaction mix in each tube.
3. Add 0.5–1 μg of DNA sample in each tube except the no-template control sample.
4. Amplification profile:

   *First step*: 94 °C 1 min.
   *Second step x 35 cycles*: 94 °C 30 s; 62 °C 30 s; 72 °C 30 s.
   *Third step*: 72 °C 7 min (*see* **Note 3**).
5. Run 10 μL of PCR product (with 1 μL of loading buffer) and 10 μL of molecular weight marker (with 1 μL of loading buffer) on a 2 % agarose gel stained with ethidium bromide (0.5 μg/mL) or fluorescent nucleic acid gel stain (e.g., Lonza GelStar™ Gel Stain 10,000×) in TBE 1× and visualize under UV. Expected size: VH/FS and VH/D → 350–400 bp; VH/LS and VH/L → 500–550 bp.

### Identification of the IgH VDJ Rearrangement with VH FR3-Derived Forward Primer

Where negative results with the FR1 and consensus PCR strategy are obtained, an FR3 strategy might be considered as an alternative (Table 1), although it should be noted that the resulting IGHV gene sequences are shorter. The PCR reaction must include a "no-template" control sample to exclude any possible contamination.

1. Reaction mix (× number of samples + 1): dNTPs 0.2 mM 5 μL; 10× buffer Taq DNA polymerase 5 μL; 20 mM $MgCl_2$ 5 μL; FR3.3 (10 pmol/μL) 1 μL; JH3.3 (10 pmol/μL) 1 μL (*see* Table 1 for primer sequences); Taq DNA polymerase 0.2 μL; and sterile water to a final volume of 50 μL (*see* Table 3 for representative scheme of PCR setup).
2. Aliquot PCR reaction mix in each 0.2-mL thin-walled PCR tube.
3. Add 0.5–1 μg of DNA sample in each tube out of no-template control sample.
4. Amplification profile:

   *First step*: 94 °C 1 min.
   *Second step x 35 cycles*: 94 °C 30 s; 55 °C 30 s; 72 °C 30 s.
   *Third step*: 72 °C 7 min (*see* **Note 3**).
5. Run 5 μL of PCR product (with 1 μL of loading buffer) and 5 μL of molecular weight marker (with 1 μL of loading buffer) on 12 % polyacrylamide gel (19:1 acrylamide:bisacrylamide) in 1× TAE buffer. Stain gel in ethidium bromide (0.5 μg/mL) to visualize bands. Expected size: ≤120 bp.

### Preparation of PCR Products for Sequencing

When a distinct, clear PCR product is obtained from the previous steps, this will be subjected to sequencing. Clonal amplifications give sharp band of the appropriate size that can be directly sequenced after enzymatic removal of unincorporated primers and

nucleotides which can interfere with downstream sequencing reactions using USB ExoSAP-IT reagent as follows:

1. Mix 5 μL of a post-PCR reaction product with 2 μL of ExoSAP-IT reagent for a combined 7 μL reaction volume (*see* **Note 17**).
2. Incubate at 37 °C for 15 min to degrade the remaining primers and nucleotides.
3. Incubate at 80 °C for 15 min to inactivate ExoSAP-IT reagent.

If necessary, PCR products can be electrophoresed through a 0.8 % LMP agarose gel, excised, and purified using QIAquick gel extraction kits (Qiagen). Direct sequencing of amplified DNAs can be performed using automated sequencing. The sequencing process can be started using either the consensus primer (JHD) or the forward FR1 or leader primer to generate a complete sequence.

### Design of Patient-Specific Primers

For the analysis of the immunoglobulin (Ig) rearranged nucleotide sequences, align the obtained sequence at http://www.imgt.org. IMGT/V-QUEST identifies the V, D, and J genes and alleles by alignment with the germline Ig gene and allele sequences of the IMGT reference directory; hypervariable regions CDR2 and CDR3 should be identified as the junctions including N-insert (*see* **Note 18**), from which patient-specific primers can be designed for the nested PCR approach used in MRD monitoring.

If FR3-derived forward primer has been used, the length of the DNA sequence allows only the design of a patient-specific forward primer within the CDR3 region for a seminested PCR to be performed with JH-derived consensus primer as reverse primer (Fig. 1).

These ASO primers are usually 18–20 bp long with a melting temperature of approximately 60 °C (*see* **Note 19**). For primer design, several software are available (*see* **Note 20**). This is a very critical step. The most critical primer for PCR specificity is the CDR3-derived antisense primer. This primer should be chosen in the most hypervariable area of the patient sequence. The forward 5′ primer is less critical. In order to determine the optimal PCR conditions that allow the amplification of a single, discrete PCR product, the so-called Oligotest should be performed. The optimal primer and $MgCl_2$ concentrations should be determined (usually 1 μL of 10–20 pmol/μL primers and 5 μL of 15–25 mM $MgCl_2$, respectively) together with the right annealing temperature (*see* **Note 21**); the right annealing temperature is based on the melting temperature ($T_m$) estimations. It is necessary to estimate $T_m$ to design an effective thermal cycling program (*see* **Note 22**).

### Minimal Residual Disease Monitoring Using Nested ASO-PCR

Once the tumor-specific IgH rearrangement has been identified and characterized and the primers for its analysis have been generated, MRD monitoring can be performed on PB or BM samples. The PCR reaction must include the following:

- A patient positive sample as a positive control (ideally the patient sample at diagnosis that has been used to generate the patient-specific primers).
- Healthy individuals' DNA (polyclonal DNA) as a negative sample to assess the specificity.
- A "no-template" control sample to exclude possible contaminations.

*First PCR amplification*

The first PCR amplification is performed as described in Subheading 3.3.2.1 using only the specific IgH forward primer that is able to amplify the tumor-associated rearrangement we are studying.

*Second PCR amplification*

1. Reaction mix (× *n* samples + 1): dNTPs 2 mM 5 μL; 10× buffer Taq DNA polymerase (TaqGold DNA Polymerase is recommended, Applied Biosystems, Warrington, UK) 5 μL; $MgCl_2$ (the most appropriate concentration of $MgCl_2$ determined during the "Oligotest") 5 μL; AmpliTaq Gold (Applied Biosystems, Warrington, UK) 0.2 μL; patient-specific forward primer (as defined by "Oligotest") 1 μL; patient-specific reverse primer (as defined by "Oligotest") 1 μL; sterile water for a final volume of 50 μL (*see* Table 3 for representative scheme of PCR setup).
2. Aliquot PCR reaction mix in each tube.
3. Add 1 μL of first-PCR product (*see* **Note 23**).
4. Amplification profile: As defined by "Oligotest."
5. Run 10 μL of PCR product (with 1 μL of loading buffer) and 10 μL of molecular weight marker (with 1 μL of loading buffer) on a 2 % agarose gel stained with ethidium bromide (0.5 μg/mL) in TBE 1× or fluorescent nucleic acid gel stain (e.g., Lonza GelStar™ Gel Stain 10,000×) in TBE 1× and visualize under UV (*see* **Note 24**). If the expected size is below 100–120 bp run 5 μL of PCR product and 5 μL of molecular weight marker on 12 % polyacrylamide gel (19:1 acrylamide:bisacrylamide) in TAE 1×.

All the patient samples that are available for MRD studies are amplified in triplicate; this allows the detection of tumor cells that are just at the limit of assay sensitivity (*see* **Note 24**).

### 3.3.3 Bcl-2/IgH Rearrangement

Follicular lymphoma is characterized by the translocation t(14;18)(q32;q21), in which the bcl-2 proto-oncogene, located on chromosome 18, is juxtaposed to the IgH locus on chromosome 14 [22]. This rearrangement is detectable in up to 85 % of FCL patients and in 25 % of diffuse large-cell lymphomas. The translocation occurs most frequently in two molecular sites: the

major breakpoint cluster region (MBR); a restriction fragment of 2.8 kb, within the 3′ untranslated region of the bcl-2 gene (70 % of patients) [23]; and the minor cluster region (mcr), located 20 kb downstream (10–15 % of patients) [24]. The clustering of the breakpoints at these two main regions and the availability of consensus IgH joining regions make this an ideal PCR target for the detection of lymphoma cells. Since there is a sequence diversity at the site of the breakpoint, the PCR product length, assessed by gel electrophoresis, dictates the specificity for a specific patient.

The PCR reactions described below are used to identify the molecular marker as well as for MRD analysis. PCR reaction must include:

- A bcl-2/IgH positive sample to assess the sensitivity.
- Healthy individuals' DNA (polyclonal DNA) as a negative sample to assess the specificity.
- A "no-template" control sample to exclude contamination.

### Bcl-2 MBR Nested PCR

IgH/Bcl2 rearrangements cluster to specific Bcl2 breakpoint regions, with the majority of cases occurring in the MBR. The PCR protocol to analyze the presence of this rearrangement is as follows:

*First PCR amplification*

1. Reaction mix (× *n* samples + 1): dNTPs 2 mM 5 μL; 10× buffer Taq polymerase 5 μL; 20 mM $MgCl_2$ 5 μL; MBR-2 (10 pmol/μL) 1 μL; JH3 (10 pmol/μL) 1 μL (*see* Table 2 for primer sequences); Taq polymerase (0.2 μL); and sterile water for a final volume of 50 μL (*see* Table 3 for representative scheme of PCR setup).
2. Aliquot PCR reaction mix in each tube.
3. Add 0.5–1 μg of DNA sample in each tube except in the "no-template" control sample.
4. Amplification profile:

   *First step*: 94 °C 3 min; 55 °C 1 min; 72 °C 1 min.
   *Second step x 30 cycles*: 94 °C 1 min; 55 °C 1 min; 72 °C 1 min.
   *Third step*: 72 °C 7 min (*see* **Note 3**).

*Second PCR amplification*

1. Reaction mix (× *n* samples + 1): dNTPs 2 mM 5 μL; 10× DNA polymerase buffer 5 μL; 20 mM $MgCl_2$ 5 μL; MBR-3 (10 pmol/μL) 1 μL; JH4 (10 pmol/μL) 1 μL (*see* Table 2 for primer sequences); Taq DNA polymerase 0.2 μL; and sterile water for a final volume of 50 μL (*see* Table 3 for representative scheme of PCR setup).

2. Aliquot PCR reaction mix in each tube.
3. Add 5 μL of first-PCR product (*see* **Note 16**).
4. Amplification profile:

   *First step*: 94 °C 3 min; 58 °C 1 min; 72 °C 1 min.
   *Second step x 30 cycles*: 94 °C 1 min; 58 °C 1 min; 72 °C 1 min.
   *Third step*: 72 °C 7 min (*see* **Note 3**).
5. Run 10 μL of PCR product (with 1 μL of loading buffer) and 10 μL of molecular weight marker (with 1 μL of loading buffer) on a 2 % agarose gel stained with ethidium bromide (0.5 μg/mL) or fluorescent nucleic acid gel stain (e.g., Lonza GelStar™ Gel Stain 10,000×) in TBE 1× and visualize under UV. Expected size: bcl-2 MBR→130 ± 50–80 bp. All patient samples available for MRD studies are amplified in triplicate; this allows the detection of tumor cells that are just at the limit of assay sensitivity (*see* **Note 24**).

Bcl-2 mcr Nested PCR

In addition to the breakpoint located in the MBR the mcr should be analyzed as follows:

*First PCR amplification*

1. Reaction mix (× *n* samples + 1): dNTPs 2 mM 5 μL; 10× buffer Taq DNA polymerase 5 μL; 20 mM $MgCl_2$ 5 μL; mcr-2 (10 pmol/μL) 1 μL; JH3 (10 pmol/μL) 1 μL (*see* Table 2 for primer sequences); Taq DNA polymerase 0.2 μL; and sterile water for a final volume of 50 μL.
2. Aliquot PCR reaction mix in each tube.
3. Add 0.5–1 μg of DNA sample in each tube except the no-template control sample.
4. Amplification profile:

   *First step*: 94 °C 3 min; 58 °C 1 min; 72 °C 1 min.
   *Second step x 30 cycles*: 94 °C 1 min; 58 °C 1 min; 72 °C 1 min.
   *Third step*: 72 °C 10 min (*see* **Note 3**).

*Second PCR amplification*

1. Reaction mix (× *n* samples + 1): dNTPs 2 mM 5 μL; 10× buffer Taq polymerase 5 μL; 20 mM $MgCl_2$ 5 μL; mcr-3.1 (10 pmol/μL) 1 μL; JH4 (1 pmol/μL) 1 μL (*see* Table 2 for primer sequences); Taq DNA polymerase 0.2 μL; and sterile water for a final volume of 50 μL (*see* Table 3 for representative scheme of PCR setup).
2. Aliquot PCR reaction mix in each tube.
3. Add 5 μL of first-PCR product (*see* **Note 23**).
4. Amplification profile:

*First step*: 94 °C 3 min; 60 °C 1 min; 72 °C 1 min.
*Second step x 30 cycles*: 94 °C 1 min; 60 °C 1 min; 72 °C 1 min.
*Third step*: 72 °C 10 min (*see* **Note 3**).

5. Run 10 μL of PCR product (with 1 μL of loading buffer) and 10 μL of molecular weight marker (with 1 μL of loading buffer) on a 2 % agarose gel stained with ethidium bromide (0.5 μg/mL) or fluorescent nucleic acid gel stain (e.g., Lonza GelStar™ Gel Stain 10,000×) in TBE 1× and visualize under UV. Expected size: bcl-2 mcr → 550–600 ± 50–80 bp. All patient samples available for MRD studies are amplified in triplicate; this allows the detection of tumor cells that are just at the limit of assay sensitivity (*see* **Note 24**).

### 3.3.4 Bcl-1/IgH Rearrangement

MCL is characterized by the t(11;14)(q13;q32) translocation, in which the bcl-1 gene on chromosome 11 is juxtaposed to the IgH locus on chromosome 14; the t(11;14) is detected by cytogenetic or Southern blot analysis in the vast majority of MCL patients (70–100 %) [14]. Breakpoints on chromosome 11 have been found dispersed over more than 100 kb of genomic DNA; the major translocation cluster (MTC) contains approximately 30–50 % of these translocations, and it is a suitable target for PCR amplification. Because of this large breakpoint area less than 30 % of MCL patients have a rearrangement that is detectable by PCR.

The PCR reactions described below are used to identify the molecular marker as well as for MRD analysis (*see* **Note 7**). They must include:

- A bcl-1/IgH MTC positive sample to assess the sensitivity.
- Healthy individuals' DNA (polyclonal DNA) as a negative sample to assess the specificity.
- A no-template control sample to exclude any possible contamination.

#### Bcl-1/IgH MTC Nested PCR

*First PCR amplification*

1. Reaction mix (× *n* samples + 1): dNTPs 2 mM 5 μL; 10× buffer Taq DNA polymerase 5 μL; 15 mM $MgCl_2$ 5 μL; P2 (10 pmol/μL) 1 μL; JH3 (10 pmol/μL) 1 μL (*see* Table 2 for primer sequences); Taq DNA polymerase 0.2 μL; and sterile water for a final volume of 50 μL.
2. Aliquot PCR reaction mix in each tube.
3. Add 0.5–1 μg of DNA sample in each tube out of no-template control sample.
4. Amplification profile:

   *First step x 33 cycles*: 94 °C 1 min; 58 °C 30 s; 72 °C 30 s.
   *Second step*: 72 °C 7 min (*see* **Note 3**).

*Second PCR amplification*

1. Reaction mix (× *n* samples + 1): dNTPs 2 mM 5 μL; 10× Buffer Taq polymerase (Applied Biosystems, Warrington, UK) 5 μL; 15 mM $MgCl_2$ 5 μL; P4 (10 pmol/μL) 1 μL; JH3 (10 pmol/μL) 1 μL (*see* Table 2 for primer sequences); Taq DNA polymerase 0.2 μL; and sterile water for a final volume of 50 μL (*see* Table 3 for representative scheme of PCR setup).
2. Aliquot PCR reaction mix in each tube.
3. Add 2 μL of first-PCR product (*see* **Note 23**).
4. Amplification profile:

   *First step x 30 cycles*: 94 °C 1 min; 58 °C 30 s; 72 °C 30 s.
   *Second step*: 72 °C 7 min (*see* **Note 3**).
5. Run 10 μL of PCR product (with 1 μL of loading buffer) and 10 μL of molecular weight marker (with 1 μL of loading buffer) on a 2 % agarose gel stained with ethidium bromide (0.5 μg/mL) or fluorescent nucleic acid gel stain (e.g., Lonza GelStar™ Gel Stain 10,000×) in TBE 1× and visualize under UV. Expected size: 250–350 bp. All patient samples available for MRD studies are amplified in triplicate; this allows the detection of tumor cells that are just at the limit of assay sensitivity (*see* **Note 24**).

### 3.4 Real-Time Quantitative PCR

Currently, most clinical trials for lymphoid and myeloid malignancies tend to include MRD detection by real-time quantitative PCR (RQ-PCR) [1, 25–27]. It is still a matter of debate whether older qualitative approaches based on nested PCR should be considered to be obsolete or if they might still have a role together with RQ-PCR. Nested PCR is probably more sensitive as higher amounts of DNA can be tested in each reaction and it is less expensive [20]. On the other hand, RQ-PCR has the advantage not only of being able to quantify the amount of residual tumor cells but also of ensuring a lower risk of contamination, so it is definitely more suitable for standardization programs.

As for qualitative PCR-based analysis, several targets are available for MRD detection in lymphoid and plasma cell malignancies. The two main MRD-PCR target categories are (1) rearrangements of Ig and/or TCR genes and (2) breakpoint fusion regions of chromosome aberrations and fusion gene transcripts. RQ-PCR-based MRD detection using tumor-specific primers derived from the IgH variable region is an established disease-monitoring tool with high predictive value in MCL and MM. It is highly sensitive and has been standardized in the context of international cooperative groups such as the European Scientific Foundation for Laboratory Hemato-oncology (ESLHO).

Although different equipment and techniques can be utilized for real-time PCR-based quantitative MRD monitoring [28], here

we present in detail the most common strategy. This strategy utilizes a hydrolysis probe approach on a high-throughput instrument for absolute quantification of the tumor genomes (number). The hydrolysis probe approach is based on the 5′ exo-nuclease activity of the Taq polymerase and requires the synthesis of three oligonucleotides: one forward primer, one reverse primer, and one probe. The probe is labelled at the 5′ end with reporter fluorochrome (e.g., 6-carboxyfluorescein [6-FAM]) and at the 3′ end with a quencher fluorochrome (e.g., 6-carboxy-tetramethylrhodamine [TAMRA]). This oligonucleotide is designed to be inside the amplicon between the two primers in order to be cleaved by the Taq polymerase 5′ exo-nuclease activity during the amplification. As a result of this cleavage reporter fluorochrome is separated from quencher and the fluorescence can be detected by the instrument. Specific PCR product quantity can thus be detected as the reaction proceeds (*see* **Note 25**).

In lymphomas with chromosomal translocations as tumor markers, consensus primers and probes, suitable for a large number of patients, can be used to target the specific translocation [29]. A TaqMan system (primer pair and fluorogenic probe) for quantification of the bcl-2-MBR rearrangement is detailed in Table 4.

When the molecular marker is based on the IgH gene rearrangement, the target gene is unique for each patient; thus, the TaqMan system should be designed on each IgH sequence. For this purpose different strategies have been proposed. In the "ASO probe approach" the probe is positioned in the CDR3 region of the IgH gene rearrangement, and therefore it is specific for each patient, while the forward and reverse primer are designed in VH and JH germline sequences, respectively. Since patient-specific probes are expensive and time consuming, assays based on a limited

**Table 4**
**Primers and probes for real-time polymerase chain reaction**

| | |
|---|---|
| *BCL-2 MBR* | |
| Forward primer | 5′-CTATGGTGGTTTGACCTTTAGAGAG-3′ |
| Reverse primer | 5′-ACCTGAGGAGACGGTGACC-3′ |
| Probe | 5′-FAM-CTGTTTCAACACAGACCCACCCAGAC-TAMRA-3′ |
| *GAPDH* | |
| Forward primer | 5′-CAAAGCTGGTGTGGGAGG-3′ |
| Reverse primer | 5′-CTCCTGGAAGATGGTGATGG-3′ |
| Probe | 5′-VIC-CAAGCTTCCCGTTCTCAGCC-TAMRA-3′ |

*MBR* major breakpoint cluster region, *GAPDH* glyceraldehyde-3-phosphate dehydrogenase

number of probes designed within FR3 region have been developed [30]. In this case (called the ASO primer approach), the specificity is given by forward and reverse primers, which are located in the VH and CDR3 segments, respectively. As an alternative, the forward primer can be positioned in the CDR3 region and the reverse primer and probe within the JH segment. The ASO primer approach has the advantage that it is much cheaper as no patient-specific probes need to be ordered. For the guidelines to be followed for the design of the ASO primer, refer to Subheading 3.3.2.4. Consensus probes are not a fixed panel, and different authors suggest their own panel [29]. Consensus probes allow the amplification of a large proportion of IgH sequences [29]. These probes can easily tolerate one and often two mismatches, provided that the first 5′ base is homologous. Historically, probes were preferentially chosen from the reverse strand, but now both sense and antisense probes are used as required. Additional probes might be designed if required. For primer and probe design, several software are available (e.g., Primer Express®, Applied Biosystems, Warrington, UK). The following parameters should however be always satisfied: probe melting temperature 10 °C higher than the primers, primer melting temperature between 58 and 60 °C, amplicon size between 50 and 150 bp, no 5′ G residue, and no more than three consecutive G residues.

#### *3.4.1 Assessing the Sensitivity and Specificity of RQ-PCR*

In order to determine the sensitivity of the RQ-PCR assay and the specificity of a designed ASO primer or probe, serial dilutions of the diagnostic sample should be used. Like in all other PCR analyses, appropriate negative and positive controls should be used in RQ-PCR analysis. Negative controls generally include "no-template" controls (e.g., water), "no-amplification" controls (no *Taq* polymerase added), and negative controls for the PCR target (DNA without the PCR target). Perform the experiments as follows:

1. Obtain the cells (either BM or PB cells depending on the type of disease as discussed in Subheading 3.3.1), extract the DNA, quantify, and store if necessary as described in Subheadings 3.1 and 3.2. To generate the standard curve, dilute the diagnostic DNA sample into a pool of DNA from 5 to 10 samples of normal PB mononuclear cells.
2. Perform an RQ-PCR reaction using the $10^{-1}$–$10^{-5}$ dilutions in duplicate as well as the normal control DNA in triplicate and water as a negative control in duplicate (300 ng DNA are used per well) 1. Reaction mix (per number of samples +1): TaqMan Universal PCR Master Mix (Applied Biosystems, Warrington, UK) 12.5 μL; 1 μL of each primer (10 pmol/μL); 1 μL of probe (15 pmol/μL) (*see* Table 4 for primer and probe sequences); and sterile water to a final volume of 25 μL (*see* Table 5 for representative scheme of RQ-PCR setup).

**Table 5**
**Representative quantitative PCR protocol**

| | Initial concentration | Final concentration | Final volume/25 μL reaction |
|---|---|---|---|
| PCR Universal Master Mix | 2× | 1× | 12.5 μL |
| Template DNA | 30 ng/μL | 300 ng | 10 μL |
| Forward primer | 10 μM | 10 μM | 1 μL |
| Reverse primer | 10 μM | 10 μM | 1 μL |
| Probe | 15 μM | 2.4 μM | 0.16 μL |
| $dH_2O$ | | | Up to 25 μL |

3. Aliquot PCR reaction mix in each tube.
4. Add 300 ng in 10 μL of DNA sample in each tube except the no-template control sample.
5. Amplification profile:

   *First step*: 50 °C 2 min.
   *Second step*: 95 °C 10 min.
   *Third step* (*for 42 cycles*): 95 °C 15 s; 60 °C 1 min.
6. Analyze the RQ-PCR data using appropriate software.
7. The threshold of the RQ-PCR assay should always be set in the region of exponential amplification across all amplification plots. This region is depicted in the log view of amplification plots as the portion of the curve that is linear. Often the threshold automatically determined by the instrument software can be used. However, if the threshold appears to be positioned outside the linear part of the amplification curves, adjustments may be made [26].
8. Construct the standard curve by plotting the logarithmic value of the dilution series against the cycle threshold ($C_T$) obtained. If tenfold dilutions are used, the slope of the standard curve should be −3.3 (−3.0, −3.9) with a correlation coefficient >0.98. In order to normalize patient samples for DNA quality and quantity, a control gene must be included in every real-time PCR analysis. The glyceraldehyde-3-phosphate dehydrogenase (GAPDH) is often used as reference standard (*see* Table 4), but other genes, such as β-actin, β-globin, Abelson, RNase P, albumin genes, can be chosen as well.

*3.4.2 MRD Analysis During Follow-Up*

Obtain the cells (either BM or PB cells depending on the type of disease as discussed in Subheading 3.3.1), extract the DNA, quantify, and store if necessary as described in Subheadings 3.1 and

3.2. Be sure to extract enough DNA to perform all MRD RQ-PCR analysis of the IgH targets or chromosomal translocations as well as the RQ-PCR analysis of the control gene necessary to normalize samples for DNA quality and quantity. These reactions must be performed using exactly the same DNA sample in identical reaction volumes and using identical amounts.

For each MRD-PCR target, analyze the dilution series ($10^{-1}$–$10^{-5}$; as in Subheading 3.5.1) of the diagnostic DNA (30 ng/μL) in duplicate, the follow-up samples (30 ng/μL) in triplicate, normal control DNA in triplicate, and no template as a negative control in triplicate.

RQ-PCR is conducted as follows:

1. Reaction mix (× *n* samples + 1): TaqMan Universal PCR Master Mix (Applied Biosystems, Warrington, UK) 12.5 μL; 1 μL of each primer (10 pmol/μL); 1 μL of probe (15 pmol/μL) (*see* Table 4 for primer and probe sequences); and sterile water to a final volume of 25 μL (*see* Table 5 for representative scheme of RQ-PCR setup).
2. Aliquot PCR reaction mix in each tube.
3. Add 300 ng in 10 μL of DNA sample in each tube except the no-template control sample.
4. Amplification profile:

   *First step*: 50 °C 2 min.
   *Second step*: 95 °C 10 min.
   *Third step* (*for 42 cycles*): 95 °C 15 s; 60 °C 1 min.
5. Analyze the RQ-PCR data using appropriate software.
6. The threshold of the RQ-PCR assay should always be set in the region of exponential amplification across all amplification plots. This region is depicted in the log view of amplification plots as the portion of the curve that is linear. Often the threshold automatically determined by the instrument software can be used. However, if the threshold appears to be positioned outside the linear part of (some of) the amplification curves, adjustments may be made [26]. The MRD value is calculated as the mean of triplicates of target gene divided by the mean of triplicates of GAPDH as control gene. For defining the sensitivity, several criteria (including reproducibility of the measurement, the difference between specific and nonspecific amplification, slope and correlation coefficient of the standard curve) should be taken into account as clearly outlined by van der Velden [28]. Calculation of MRD levels is based on comparative $C_T$ analysis between follow-up samples and standards in ASO and GAPDH PCRs. MRD values were specified in relation to target copy number in the diagnostic sample and according to the 2007 guidelines of the European Study Group on MRD detection in ALL [28].

### 3.5 Next-Generation Sequencing for (MRD) Detection Using the Immunoglobulin Heavy Chain Variable Region

Recently, novel protocols to monitor MRD based on deep sequencing have been proposed [31, 32]. IgH-based next-generation sequencing (NGS) allows to identify clonal rearrangements in diagnostic samples and enables their tracking during therapy. The assay was shown to be precise, quantitative, and sensitive when applied to patients with B-lineage acute lymphoblastic leukemia (ALL) and CLL (this assay allows monitoring of all rearrangement regardless of their prevalence at diagnosis, thus providing an interesting tool to the study of clonal evolution which is particularly relevant in multiple myeloma). The wide applicability of this approach using consensus primers without the need for any patient customization is a significant development and will increase the availability of MRD quantification in patients with B-cell malignancies undergoing SCT.

## 4 Notes

1. A 2 mM stock of dNTPs (dATP, dCTp, dGTP, and dTTP) in $ddH_2O$ is used. We find that this more dilute stock offers greater control, as minor variations in pipetting 10 mM dNTP stock can affect the final dNTP concentration, which in turn can influence the free $Mg^{2+}$ concentration and the fidelity of the reaction.
2. Most commercially available thermostable DNA polymerases include a 10× PCR buffer, usually containing minor variations of 100 mM Tris–HCl, 500 mM KCl, pH 8.4–9.0. However, users should be aware that different companies may employ different solvent formulations, which can in turn affect stringency and specificity.
3. Most commercially available thermostable DNA polymerases are suitable. In case a hot start enzyme is used, a first step (94 °C 10 min) is required in each amplification reaction in order to activate the enzyme; this is recommended as it minimizes the binding of primers to each other or at nonhomologous locations in the target DNA.
4. Ethidium bromide is a known mutagen and suspected carcinogen. When handling, gloves should be worn at all times, and appropriate care should be taken to avoid skin contact. Avoid adding ethidium bromide to very hot agarose in order to limit exposure to toxic vapors: cool hot agarose to 60 °C in a water bath with constant stirring, and then add ethidium bromide.
5. Ficoll solution and DPBS should be at room temperature. Use of whole lysed cell material is not recommended because inhibitors of PCR amplification such as hemoglobin are present.

6. Preparation of blood with EDTA is best to isolate DNA and RNA (heparin makes complexes with DNA). However, in our experience, the use of heparin tubes is a realistic option, implying that heparinized PB and BM samples that are collected for flow cytometric or cytogenetic evaluation can also be used for PCR evaluation as well.
7. The more diluted the blood sample, the better the purity of the mononuclear cells after separation.
8. The blood must remain on top of the Ficoll solution. Do not mix.
9. This would prevent mixing of the two phases resulting in a poor-quality cell isolation.
10. For removal of platelets resuspend the cell pellet in 50 mL DPBS and centrifuge at $200 \times g$ for 15 min at 20 °C. Most platelets will remain in the supernatant upon centrifugation at $200 \times g$.
11. For DNA extraction other methods can be used, like phenol/chloroform DNA precipitation that provides the same DNA quality and quantity, but it is more time consuming. One should be aware that phenol–chloroform-based extraction methods generally give rise to high-molecular-weight DNA which is hard to pipet in a reproducible way. Several other methods have been proposed such as commercial kits for DNA extraction. The use of kits offers a low risk of manipulation, and they are faster than conventional protocols, but the amount of DNA recovered from the commercial kits is highly variable (Loffler et al. 1997). DNA precipitation by means of DNA-binding columns (e.g., Nucleospin®, BD Biosciences, France) is particularly useful when less than $5 \times 10^6$ cells are available although very recently a standardized protocol for DNA isolation from low cell numbers down to 1,000 cells has been proposed for chimerism studies [33]. cDNA can also be used as a template. cDNA sample preparation requires RNA isolation followed by reverse transcription; the acid guanidinium method or commercially available reagents such as Trizol (Invitrogen) are both adequate for RNA isolation, and reverse transcriptase kits such as Superscript III (Invitrogen) are sufficient for cDNA generation, with the methodology performed as directed by the manufacturer's protocols.
12. Archival paraffin-embedded BM or lymph node slides that had been prepared for diagnosis may serve as a source of DNA for PCR-based MRD detection. In case of paraffin-embedded tissues, the following protocol can be used:
    - Cut 30 μm sections of formalin-fixed paraffin samples into Eppendorf tubes, add 1 mL of xylene to two sections, and incubate at 37 °C in water bath for 15 min.

- Spin down for 3 min at 10,000 × *g*.
- Discard the supernatant, and resuspend the pellet with 1 mL of xylene, repeating all the steps described above.
- Add 1 mL of 100 % ethanol, mix, and incubate at RT for 15 min.
- Spin for 5 min at 10,000 × *g*, and discard the supernatant.
- Allow the pellet to dry on air.
- Resuspend the dried pellet in proteinase K buffer (50 mM Tris pH 8, 1 mM EDTA, 0.5 % Tween 20), and add 0.4 mg/mL proteinase K.
- Incubate at 55 °C overnight; repeat the above digestion steps until the tissue is fully dissolved.
- Add an equal volume of buffer-saturated phenol, and mix by inversion.
- Spin for at least 5 min at 10,000 × *g* in microcentrifuge, and then transfer the aqueous layer to a new tube.
- Add an equal volume of phenol:chloroform:isoamyl alcohol (25:24:1), shake gently, incubate for 10 min at RT, and then spin down for 5 min at 10,000 × *g*.
- Collect the supernatant into new Eppendorf tubes and precipitate with 2 volumes of 100 % ethanol and 1/10 volume of 3 M Na acetate pH 8.2.
- Spin for 10 min at 10,000 × *g*.
- Wash the pellet with 70 % ethanol and spin for 10 min at 10,000 × *g*; discard the supernatant.
- Air-dry the pellet and dissolve in 25 μL of water or TE buffer before quantitation.

13. For small quantities of DNA, measurement using a Nanodrop spectrophotometer is preferred. The Nanodrop is a cuvette-free spectrophotometer. It uses just 1 μL of sample and is accurate from 5 up to 3,000 ng/μL. Although spectrophotometry is most commonly used, it can be unreliable and inaccurate. Fluorometric quantitation generates more accurate and precise results across a lower concentration range than those obtained by UV absorbance measurements. Due to this accuracy and precision, fluorescent quantitation of nucleic acids is recommended in the MIQE (Minimal Information for Publication of Quantitative Real-Time PCR Experiments) Guidelines [34].
14. CD138 is expressed on normal and malignant human plasma cells and commonly used as a universal marker for their identification and isolation. The isolation of highly pure $CD138^{+}$ plasma cells from the bone marrow blood of multiple myeloma patients can be obtained using immunomagnetic separation procedures such as the one developed by Miltenyi Biotec as

described in http://www.miltenyibiotec.com/download/protocols_cellsep_special_en/1400/SP_Isolation_of_CD138_plasma_cells.pdf.

15. The PCR mix is set up in the "PCR area," and, in order to avoid contamination, DNA is added on a different bench and with dedicated instruments (use always sterilized aerosol-resistant tips); PCR machines and PCR products are located in the "post-PCR area"; for nested PCR, first-PCR product amplification is added in this room.
16. Tubes combining each of the forward primer (derived from the FR1 region and the Leader region, Table 1) and the reverse primer (JHD, Table 1) must be set up. Given the high number of tubes, it is recommended to perform the amplification reaction using first the VH/FS forward primers followed by the VH/LS primers and then set up a new experiment with the remaining primers to avoid contaminations and confusion. In order to limit the number of PCR tubes per locus, multiplexing of PCR primers can be used as proposed by the BIOMED-2 consortium [21].
17. When treating PCR product volumes greater than 5 μL, simply increase the amount of ExoSAP-IT reagent proportionally.
18. When the sequence quality does not allow a complete reading of CDR regions, the PCR product can be cloned with TA cloning kit. Plasmid DNAs are isolated by miniprep, and, after restriction enzyme analysis, those containing the insert are sequenced (the IgH rearrangement of the tumor clone is found if at least 60 % of 15–20 sequenced plasmid DNAs have the same insert).
19. Avoid primers that can fold and anneal against themselves or with other copies of themselves or with the reverse primer; avoid more than three adjacent G or C.
20. These software for the design of appropriate primers include Primer3: WWW primer tool (available for use as an online tool http://frodo.wi.mit.edu/primer3/input.htm and freely available for download), a very powerful PCR primer design program permitting one considerable control over the nature of the primers, including size of product desired, primer size and Tm range, and presence/absence of a 3′-GC clamp or Primer-BLAST developed at NCBI to help users make primers that are specific to the input PCR template. It uses Primer3 to design PCR primers and then submits them to BLAST search against user-selected database. The blast results are then automatically analyzed to avoid primer pairs that can cause amplification of targets other than the input template.
21. The primers should allow the generation of a very distinct band. Unfortunately especially with CLL samples, the presence

of an unmutated IgH sequence gives problems in generating primers that satisfy this requirement. The generation of multiple products is often caused by poor melting temperature ($T_m$) estimations and improper annealing conditions, in response to which many different methods have been suggested to increase the specificity of the reaction, ranging from the addition of additives to the reaction mix (e.g., DMSO, formamide, betaine, and others) to variations in salt concentration and altering the annealing temperature. In our experience, touchdown (TD) PCR offers a simple and rapid means to optimize PCRs, increasing specificity, sensitivity, and yield, without the need for lengthy optimizations and/or redesigning of primers. The key principle in TD-PCR is to employ successively lower annealing temperatures, beginning first with an annealing temperature above the projected $T_m$ and then transitioning to a lower, more permissive temperature over the course of 10–15 cycles. This protocol also has the potential to largely overcome the problems associated with high annealing temperatures required for some primer–template combinations and is particularly useful for difficult-to-amplify templates. The only inherent limitation of the technique is that it is not suitable for quantitative assessment of target concentration by real-time PCR approaches.

22. A useful online tool for $T_m$ calculation and oligonucleotide properties is OligoCalc (http://www.basic.northwestern.edu/biotools/oligocalc.html), which offers basic, salt-adjusted, and nearest-neighbor $T_m$ estimations. However, despite the utility of OligoCalc, users should be aware that it still suffers from the limitations inherent in $T_m$ estimations mentioned previously. Regardless of the method used, it is important to calculate $T_m$ in the same manner every time to achieve consistent results.
23. To avoid contamination during the nested-PCR reactions, use dedicate instruments (pipette and tips); keep each tube capped except when adding each respective first-PCR product; start adding PCR product from negative samples, patient sample, and, at the end, positive control sample (it is advisable to respect this order in all the PCR amplifications).
24. In order to avoid false-negative results, all the MRD-negative samples must be tested with PCR amplification of a gene located on a chromosome not frequently involved in the malignancy, e.g., β-actin.
25. Other probe formats can also be used [28]. The use of nonspecific dyes, such as SYBR Green I, should be avoided since this limits the sensitivity.

## References


1. Farina L, Carniti C, Dodero A et al (2009) Qualitative and quantitative polymerase chain reaction monitoring of minimal residual disease in relapsed chronic lymphocytic leukemia: early assessment can predict long-term outcome after reduced intensity allogeneic transplantation. Haematologica 94:654–662
2. Corradini P, Ladetto M, Zallio F et al (2004) Long-term follow-up of indolent lymphoma patients treated with high-dose sequential chemotherapy and autografting: evidence that durable molecular and clinical remission frequently can be attained only in follicular subtypes. J Clin Oncol 22:1460–1468
3. Corradini P, Tarella C, Olivieri A et al (2002) Reduced-intensity conditioning followed by allografting of hematopoietic cells can produce clinical and molecular remissions in patients with poor-risk hematologic malignancies. Blood 99:75–82
4. Corradini P, Cavo M, Lokhorst H et al (2003) Molecular remission after myeloablative allogeneic stem cell transplantation predicts a better relapse-free survival in patients with multiple myeloma. Blood 102:1927–1929
5. Román J, Alvarez MA, Torrea A (2000) Molecular basis for therapeutic decisions in chronic myeloid leukemia patients after allogeneic bone marrow transplantation. Haematologica 85:1072–1082
6. Inghirami G, Szabolcs MJ, Yee HT et al (1993) Detection of immunoglobulin gene rearrangement of B cell non-Hodgkin's lymphomas and leukemias in fresh, unfixed and formalin-fixed, paraffin-embedded tissue by polymerase chain reaction. Lab Invest 68:746–757
7. Hallek M (2009) Review state-of-the-art treatment of chronic lymphocytic leukemia. Hematology (Am Soc Hematol Educ Program) 440–449
8. Hallek M, Cheson BD, Catovsky D et al (2008) Guidelines for the diagnosis and treatment of chronic lymphocytic leukemia: a report from the International Workshop on Chronic Lymphocytic Leukemia updating the National Cancer Institute-Working Group 1996 guidelines. Blood 111:5446–5456
9. Brisco MJ, Tan LW, Orsborn AM (1990) Development of a highly sensitive assay, based on the polymerase chain reaction, for rare B-lymphocyte clones in a polyclonal population. Br J Haematol 75:163–167
10. Böttcher S, Ritgen M, Dreger P et al (2011) Allogeneic stem cell transplantation for chronic lymphocytic leukemia: lessons to be learned from minimal residual disease studies. Blood Rev 25:91–96
11. Moreno C, Villamor N, Colomer D et al (2006) Clinical significance of minimal residual disease, as assessed by different techniques, after stem cell transplantation for chronic lymphocytic leukemia. Blood 107:4563–4569
12. Schmitt C, Grundt A, Buchholtz C et al (2006) One single dose of rituximab added to a standard regimen of CHOP in primary treatment of follicular lymphoma appears to result in a high clearance rate from circulating bcl-2/IgH positive cells: is the end of molecular monitoring near? Leuk Res 30:1563–1568
13. Yunis JJ, Oken MM, Kaplan ME et al (1982) Distinctive chromosomal abnormalities in histologic subtypes of non-Hodgkin's lymphoma. N Engl J Med 307:1231–1236
14. Tsujimoto Y, Yunis J, Onorato-Showe L et al (1984) Molecular cloning of the chromosomal breakpoint of B-cell lymphomas and leukemias with the t(11;14) chromosome translocation. Science 224:1403–1406
15. Siebert R, Matthiesen P, Harder S et al (1998) Application of interphase cytogenetics for the detection of t(11;14)(q13;q32) in mantle cell lymphomas. Ann Oncol 9:519–526
16. Kurokawa T, Kinoshita T, Murate T et al (1997) Complementarity determining region-III is a useful molecular marker for the evaluation of minimal residual disease in mantle cell lymphoma. Br J Haematol 98:408–412
17. Pott C (2011) Minimal residual disease detection in mantle cell lymphoma: technical aspects and clinical relevance. Semin Hematol 48:172–184
18. Tonegawa S (1983) Somatic generation of antibody diversity. Nature 302:575–581
19. Deane M, McCarthy KP, Wiedemann LM et al (1991) An improved method for detection of B-lymphoid clonality by polymerase chain reaction. Leukemia 5:726–730
20. Voena C, Ladetto M, Astolfi M et al (1997) A novel nested-PCR strategy for detection of rearranged immunoglobulin heavy chain genes in B-cell tumours. Leukemia 11:1793–1798
21. Van Dongen JJ, Langerak AW, Brüggemann M et al (2003) Design and standardization of PCR primers and protocols for detection of

clonal immunoglobulin and T-cell receptor gene recombinations in suspect lymphoproliferations: report of the BIOMED-2 Concerted Action BMH4-CT98-3936. Leukemia 17:2257–2317

22. Tsujimoto Y, Finger LR, Yunis J et al (1984) Cloning of the chromosome breakpoint of neoplastic B cells with the t(14;18) chromosome translocation. Science 226:1097–1099
23. Cleary ML, Sklar J (1985) Nucleotide sequence of a t(14;18) chromosomal breakpoint in follicular lymphoma and demonstration of a breakpoint-cluster region near a transcriptionally active locus on chromosome 18. Proc Natl Acad Sci USA 82:7439–7443
24. Cleary ML, Galili N, Sklar J (1986) Detection of a second t(14;18) breakpoint cluster region in human follicular lymphomas. J Exp Med 164:315–320
25. Ladetto M, De Marco F, Benedetti F et al (2008) Prospective, multicenter randomized GITMO/IIL trial comparing intensive (R-HDS) versus conventional (CHOP-R) chemoimmunotherapy in high-risk follicular lymphoma at diagnosis: the superior disease control of R-HDS does not translate into an overall survival advantage. Blood 111:4004–4013
26. Pott C, Hoster E, Delfau-Larue MH et al (2010) Molecular remission is an independent predictor of clinical outcome in patients with mantle cell lymphoma after combined immunochemotherapy: a European MCL intergroup study. Blood 115:3215–3223
27. Putkonen M, Kairisto V, Juvonen V et al (2010) Depth of response assessed by quantitative ASO-PCR predicts the outcome after stem cell transplantation in multiple myeloma. Eur J Haematol 85:416–423
28. Van der Velden VHJ, Hochhaus A, Cazzaniga G et al (2003) Detection of minimal residual disease in hematologic malignancies by real-time quantitative PCR: principles, approaches, and laboratory aspects. Leukemia 17: 1013–1034
29. Luthra R, McBride JA, Cabanillas F et al (1998) Novel 5′ exonuclease-based real-time PCR assay for the detection of t(14;18) (q32;q21)in patients with follicular lymphoma. Am J Pathol 153:63–68
30. Donovan JW, Ladetto M, Zou G et al (2000) Immunoglobulin heavy-chain consensus probes for real-time PCR quantification of residual disease in acute lymphoblastic leukemia. Blood 95:2651–2658
31. Faham M, Zheng J, Moorhead M et al (2012) Deep-sequencing approach for minimal residual disease detection in acute lymphoblastic leukemia. Blood 120:5173–5180
32. Logan AC, Gao H, Wang C, Sahaf B et al (2011) High-throughput VDJ sequencing for quantification of minimal residual disease in chronic lymphocytic leukemia and immune reconstitution assessment. Proc Natl Acad Sci USA 108:21194–21199
33. Van der Burg M, Kreyenberg H, Willasch A et al (2011) Standardization of DNA isolation from low cell numbers for chimerism analysis by PCR of short tandem repeats. Leukemia 25:1467–1470
34. Bustin SA, Benes V, Garson JA et al (2009) The MIQE guidelines: minimum information for publication of quantitative real-time PCR experiments. Clin Chem 55:611–622

# Chapter 13

# Molecular Methods for Detection of Invasive Fungal Infections and Mycobacteria and Their Clinical Significance in Hematopoietic Stem Cell Transplantation

**Pinar Yurdakul and Sule Colakoglu**

## Abstract

Infection remains an important source of morbidity and mortality in patients who undergo hematopoietic stem cell transplantation (HSCT). In the immune reconstitution period after transplantation, HSCT recipients are most likely to have bacterial or fungal infections. Invasive fungal infections (IFIs) and mycobacterial infections (MBIs) are among the complications of HSCT, with high morbidity and mortality rates. Early diagnosis of both is crucial in order to manipulate the disease and to avoid fulminant outcomes. This chapter reviews the current knowledge on the molecular diagnosis of IFIs and MBIs in HSCT recipients, describing two different polymerase chain reaction (PCR)-based methods, one commercial (qPCR, Roche) and one *in-house IS*6110-based protocol.

**Key words** Hematopoietic stem cell transplantation, Aspergillosis, Candidiasis, Mycobacteria, Tuberculosis, Nucleic acid amplification tests, qPCR, *IS*6110

## 1 Introduction

Infections are the most important cause of morbidity and mortality in patients undergoing hematopoietic stem cell transplantation (HSCT). Invasive fungal infections (IFIs) and mycobacterial infections (MBIs) are amongst important complications of HSCT, developing more commonly in allogeneic than in autologous HSCT recipients [1–4].

Invasive aspergillosis (most commonly *Aspergillus fumigatus*) is the most common cause of IFIs in HSCT patients, followed by invasive candidiasis (IC) (most commonly *Candida glabrata*). *Zygomycete* group is also found increasingly, among others. The risk of having IFIs in HSCT hosts can be 3.4 % or higher under certain circumstances [1–4].

Meral Beksaç (ed.), *Bone Marrow and Stem Cell Transplantation*, Methods in Molecular Biology, vol. 1109,
DOI 10.1007/978-1-4614-9437-9_13, 

*Mycobacterium tuberculosis* complex[1] (MTC) or nontuberculous mycobacteria (NTM)[2] are commonly responsible for MBIs, generally occurring as late complications in HSCT patients [5–10]. The incidence of MBI including NTM among HSCT recipients was reported to range between 0.6 and 8.7 % with increasing number of reported cases [5, 7, 10–13].

### 1.1 IFIs in HSCT

IFIs are of the major causes of morbidity and mortality after HSCT. The high mortality rates associated with documented IFIs are mainly attributed to difficulty of diagnosis retarding the initiation of treatment. In 1980s, candida infections mainly caused by *Candida albicans* (*C. albicans*) were recognized as common during early post-HSCT. The introduction of fluconazole (FLCZ) prophylaxis has reduced the overall attack rate of IC and also caused a shift to FLCZ-resistant *C. glabrata* and *C. krusei*. Mold infections, caused especially by *Aspergillus* spp., have been increasingly encountered, and other molds including *Zygomycetes*, *Fusarium* spp., and *Scedosporium* spp. have emerged during late 1990s [14–17].

### 1.2 Clinical Diagnosis of IFIs

Early diagnosis of infection and early initiation of therapy are crucial for controlling the progress of this infection and reduce mortality. Therefore, all diagnostic approaches primarily aim at an early confirmation of the infection. A consensus group of the European Organization for Research and Treatment of Cancer/Invasive Fungal Infections Cooperative Group (EORTC) and the National Institute of Allergy and Infectious Diseases Mycoses Study Group (MSG) published standard definitions for clinical and epidemiological research on IFIs that develop in patients with cancer and HSCT. The definitions retain the classification of "proven," "probable," and "possible" IFI. A definite diagnosis of proven IFI requires histological and/or cultural evidence, from tissue biopsies or normally sterile body fluid. However, these criteria may not be applicable at early stages of infection. The decision to start antifungal therapy in HSCT patients is mostly based on clinical criteria such as antibiotic-refractory fever and/or pulmonary symptoms with detection of pulmonary infiltrates by chest X-ray and/or computed tomography (CT). The current methods for diagnosing IFIs include assessment of clinical signs and symptoms, mycological examination by microscopy, and cultural as well as non-cultural techniques, such as antigen tests and molecular methods, imaging techniques, endoscopic methods, and cytology and/or histological examination of biopsy material [4, 18, 19].

[1] *M. tuberculosis*, *M. africanum*, *M. microti*, *M. canetti*, and *M. bovis* including bacillus Calmette–Guerin (BCG) group.

[2] Most commonly encountered species in HSCT: *M. fortuitum*, *M. chelonae*, *M. abscessus*, and *M. avium* complex; for more detailed information on NTM, *see* ref. 6.

### 1.3 Molecular Diagnosis of IFIs by Nucleic Acid Amplification Techniques

The introduction of molecular methods into clinical laboratory has led to significant advances in the diagnosis of infectious diseases, including those caused by fungi [19]. These methods were expected to overcome the low sensitivity and specificity of conventional phenotypic tests to provide early diagnosis, leading to earlier adapted antimicrobial treatment, with potential reduction in mortality and morbidity rates [20].

Nucleic acid amplification techniques (NAATs) are the most often used molecular methods for detecting pathogenic fungi. Until recently, there has been no standardized or clinically validated method for most fungi. As a consequence, each investigator has developed his/her own method, and the lack of standardized methods has made it difficult to evaluate the utility of these techniques for routine use. Since the molecular diagnosis of fungi is neither a standardized nor a widely available diagnostic tool, it is still not included in the guidelines for diagnosis of IFIs in hematology and oncology [4, 18, 20].

In recent years, quantitative real-time polymerase chain reaction (PCR) (qPCR) technologies have become the method of choice in molecular diagnosis of IFI. Unfortunately, there is no consensus on other aspects, including DNA extraction technique, genetic targets, and specific amplification chemistry. Depending on the target gene, molecular assays (from blood and bronchoalveolar lavage [BAL]) demonstrate high specificity (81–100 %) [21, 22]. The sensitivity of the assays has been highly variable (0–100 %) [23, 24] because of several factors, including type of disease, choice of clinical sample type, DNA extraction method, format of PCR, PCR target gene, study design, and size of population studied [20, 25, 26].

Molecular studies for detecting fungal DNA have focused mainly on two approaches: (1) detection of genus-specific single-copy genes or (2) detection of multiple-copy genes identifiable in almost all fungal species. Amplification of a gene with several hundred copies improves PCR assay sensitivity compared to that of tests amplifying single-copy genes. Most PCR assays, the so-called panfungal PCR, have targeted the multicopy rRNA (18S rRNA or 28S rRNA genes) or mitochondrial genes, followed by hybridization with species-specific probes, hybridization to a DNA microarray, or direct nucleic acid sequencing [4, 20].

The main advantage of a panfungal strategy is that the strategy tolerates changes in the spectrum of emerging molds and yeasts. The potential disadvantage of panfungal assays is an increased risk of detecting non-relevant DNA, since there are numerous mold species in the environment, as well as various enzymes and reagents used in the laboratory tests. Also, panfungal assays would not be able to amplify all the putative pathogenic fungi with similar yields. The challenge seems even more sound in cases with mixed fungal infections. In such cases, only the most prevalent DNA may be detected, not always the most relevant one in terms of tissue damage or treatment [20].

When the etiological agents being targeted are limited, more specific primers and probes can be used. This can improve assay sensitivity and allow direct species-level identification without additional steps, therefore potentially improving the speed of diagnosis and therapeutic decision making. However, it is often difficult to avoid cross-reactivity of the primer and probe sequences when examining closely related species. Restricting amplification to a limited set of fungi also presents the obvious risk of missing other species that may be less commonly involved in fungal disease pathogenesis [20].

As with every PCR assay designed to detect a low load of a given microorganism among a huge number of human cells, all PCR parameters must be optimized to obtain a positive result with the highest sensitivity possible. By doing this, however, one might increase the risk of false-positive results, usually by contamination either with previously amplified products or with environmental microorganisms [20].

The small amount of fungal DNA in clinical specimens has led several teams to develop *nested PCR* formats for *Aspergillus* and *Candida* [23, 27–30]. Nested PCR consists of a first round of amplification with one set of primers and a second round of amplification run using primers that hybridize within the first amplicon. The main drawback of this method is the need for adding reagents between two PCR runs. This step dramatically increases the risk of carryover amplicon contamination. Therefore, most clinical laboratories have avoided using nested PCR techniques, because of high rates of contamination, with well-documented false-positive results in the fields of virology and bacteriology [20].

Although initial studies frequently used end point PCR, *qPCR* has been dominant in most recent PCR-based diagnostic studies of fungal infections [21, 22, 31–36]. This technology combines nucleic acid target amplification using standard PCR chemistry and detection using fluorescent probes (e.g., 5′ nuclease, molecular beacons, and fluorescent resonance energy transfer (FRET) hybridization probes) in a simultaneous, single-well reaction [19, 25]. Molecular testing utilizing qPCR technology offers several advantages over conventional PCR methods. First of all, qPCR testing has demonstrated equivalent sensitivity and specificity with that of conventional PCR testing. Secondly, qPCR testing decreases the turnaround time by eliminating the necessity to perform post-amplification processing and detection. qPCR can rapidly identify species- and nonspecific products with melting curve analysis when dsDNA-binding dyes (such as SYBR green) are used. Third, to control PCR inhibition, the multiplex PCR can be made with internal amplification control [20]. Fourth, by combining target amplification and detection in single, closed-reaction vessels, qPCR testing reduces the possibility for contamination with "carryover" amplified product and environmental fungi. Finally, qPCR assays (e.g., Light Cycler™,

TaqMan™) can provide quantitative results in predicting clinical progression in transplant patients, differentiating colonization and disease, and monitoring the efficacy of antifungal therapy. This format is also useful to rapidly compare different protocols with respect to parameters such as the clinical specimen, DNA extraction methods, and primer and probe designs and indirectly constitutes an initial step toward standardization [4, 19, 20].

Several limitations of qPCR testing should also be considered, although this method has routinely been used in the diagnosis of fungal infections. First, the high sensitivity of qPCR assays may allow for the detection of fungi (e.g., *Aspergillus* spp., *Candida* spp.) that are colonizing or causing a subclinical infection. Second, the false-positive results can be observed because of contamination with environmental fungi, previously amplified PCR products, or cross-reactivity of PCR primers and probes with non-targeted fungi, other organisms, or human DNA [15, 20, 37]. Fungal spores are ubiquitous in the air and environment. Precautions should be taken during specimen collection, processing, and testing to reduce the potential for contamination events. Negative controls can be used, and standard laboratory precautions should be applied, including using laminar-flow biosafety cabinets for reaction setup, enforcement of unidirectional workflow patterns (pre- to post-PCR), physically separating laboratories for pre- and post-PCR analysis, and using aerosol-resistant pipette tips. The qPCR format is currently often associated with the use of uracyl-N-glycosylase (UNG) enzyme and dUTP instead of dTTP in the PCR master mix to destroy amplicons prior to PCR. Using environmental fungal DNA-free reagents and hot-start procedures using heat-activated polymerase also improve specificity of the assay [19, 20, 25]. Finally, growth in culture is still required if antifungal susceptibility testing is to be performed. Several studies have evaluated the ability of real-time PCR assays to detect fungal resistance markers using culture isolates and clinical specimens, and this approach may represent a promising alternative in the future [19].

*Nucleic acid sequence-based amplification (NASBA)* was developed as a diagnostic method to detect target mRNA in an isothermal amplification process. Unlike PCR to detect DNA, the detection of mRNA means that the presence of viable fungal organisms and highly expressed genes can be used to assess the viability of the infecting fungal organisms following antifungal therapy. Also, an isothermal process could have less chance of contamination than the PCR process using thermal cycling [37].

### 1.4 Molecular Species-Level Identification of Fungi

Identification of fungal species has traditionally relied on macroscopic colony characteristics, microscopic morphology, and other phenotypic features. Unfortunately, culture may be required for several days, or even weeks, for the development of specific phenotypic characteristics. In some cases, hyphae remain sterile or develop

atypical morphology, impeding morphology. Therefore, rapid nucleic acid-based methods that identify species are now being developed to supplement or replace phenotypic identification [20].

The most successful molecular identification methods rely on a PCR amplification of informative gene fragments followed by *sequencing* [20]. The clinical utility of sequencing has been demonstrated for the identification of medically important yeasts by several studies. But it has not been as extensively evaluated for the identification of filamentous fungi (e.g., *Aspergillus* spp.) [19]. The targets most commonly used for sequencing of fungi are the ITS1 and ITS2 regions between the 18S and 28S ribosomal subunits and an ~600 base-pair (bp) region of the D1–D2 region of the 25–28S large ribosomal subunit. As new molecular platforms have been developed sequencing of selected genes has become an easy way to obtain reliable and highly specific data. However, there are unresolved questions regarding the nature and the number of sequences needed for definitive identification. Furthermore, these methods remain too time consuming to be efficient for large-scale studies. In addition, continuously changing fungal taxonomy, limitations of the currently available fungal sequence libraries, and lack of a consensus agreement on the percent identity score needed to identify specimens to the genus or the species level make fungal identification using sequence analysis somewhat less robust at the present time than bacterial identification using this technique. Investigation of selected genes is clearly important for identification, but it may also be used in other ways. For instance, sequencing of selected genes involved in metabolic pathways can be used to help explain the resistance profiles of yeasts or molds to antifungal agents [19, 20].

The recently described technology, *pyrosequencing*, represents a rapid (~1 min/bp), less expensive (~$1/sample for reagent costs) alternative to the use of conventional sequencing technology (i.e., the Maxam–Gilbert chemical cleavage method and the Sanger chain-terminator method) for the identification of fungi and evaluation of antifungal susceptibility [19].

Because of such vulnerability to misidentification, several authors have developed other means to identify fungi without sequencing or in addition to sequencing. These methods include detection of amplicons in a colorimetric enzyme immunoassay format or in situ hybridization techniques to identify organisms in histological sections. Some methods are already commercially available, such as the peptide nucleic acid probes used with fluorescent in situ hybridization. Others are still under experimental study, such as Fourier transform-infrared microspectroscopy and ionization mass spectrometry [20].

Future studies will likely be directed at adapting existing technologies, including *Luminex microbead hybridization technology* (Luminex Corporation, Austin, Texas), *microarray-based methods*,

and *matrix-assisted laser desorption ionization-time of flight (MALDI-TOF) mass spectrometry (MS)*, to further enhance the speed, throughput, and accuracy of fungal diagnostic testing [20].

### 1.5 Clinical Significance of Molecular Detection of Invasive Pulmonary Aspergillosis

Invasive aspergillosis (IA) is a common cause of infection-related mortality in HSCT recipients. The incidence of IA after HSCT varies between 5, 4, and 11.2 % [16, 38, 39]. The diagnosis of IA still represents a challenge today, with some studies reporting less than half of cases diagnosed antemortem. IA has to be considered in differential diagnosis in the presence of antibiotic-resistant fever along with infiltrates on the chest X-ray. The current diagnosis is mainly based on the use of different methods, including radiology (especially high-resolution CT), histopathology and culture from clinical specimens, the rapid diagnostic techniques (e.g. serum galactomannan by enzyme immunosorbent assay [GM-EIA] (1→3)-β-D-glucan assay or NAATs) enabling early detection of the infection [14, 37, 39–42].

The clinical utility of molecular methods in the setting of invasive aspergillosis has been hampered by several unresolved issues. Most studies using qPCR have shown very little *Aspergillus* DNA even in full-blown invasive disease. Therefore, the prognostic significance of the quantity of DNA detected and qualitative test reproducibility may be poor, simply because of the random distribution of targeted molecules in the clinical specimen tested. If a single positive result obtained at the beginning of an infection represents a true positive result, the antifungal therapy given in this stage can improve the outcome. In contrast, if a single positive PCR test represents a false-positive result, the patient can be given unnecessary treatment. Fungi are ubiquitous in the environment, so a PCR method is even more likely to yield products that are the result of exogenous contamination. Fungemia may be intermittent, possibly because of hepatic clearance of fungal elements, so it is not surprising that some patients were not consistently PCR positive. Additionally, a single positive PCR result under antifungal therapy may indicate a worse prognosis, potentially reflecting breakthrough infection or a limited response to therapy. Thus, it has generally been agreed that testing serial samples by PCR enhances sensitivity, just as antigen testing. Several authors have shown that PCR assay specificity is improved if two consecutive positive PCR results are required to establish a diagnosis. However, waiting for additional samples to improve the predictive value of a PCR test might reduce its relevance for clinical decision making [20].

Interpretation of negative PCR results is also no easier. Given the high negative predictive value of PCR seen in nearly all trials, negative results could be used to rule out invasive aspergillosis in HSCT patients [27, 29, 42–45]. However, it is almost impossible to rule out an IFI by PCR due to the fact that there are many

causes of PCR inhibition and false-negative results. Therefore, the use of negative PCR results to exclude patients from antifungal therapy may be risky, especially when other signs or symptoms suggestive of invasive aspergillosis are present. As a result, it remains unclear whether PCR-based screening or PCR-based early antifungal treatment is clinically effective or reduces cost of care [20].

Ideally, PCR results should be interpreted together with the results of other tests whose performance characteristics are already well established, such as antigen detection. Previous studies in the literature supported that simultaneous application of galactomannan and PCR assays increases the sensitivity and negative predictive value of diagnosis in cases of aspergillosis. If implemented together, PCR and antigen testing can be performed simultaneously on the same blood samples from recipients of allogeneic HSCT collected twice a week at the onset of fever and neutropenia, the same schedule as is already common practice for galactomannan screening in hematological wards. Another possibility is to perform PCR testing only on initial antigen-positive samples, to improve specificity of antigen test, reducing the need to wait for a second sample to confirm the first positive result. PCR can also complement HRCT findings or histological findings when culture has not been performed or was inhibited by empirical antifungal treatment. Diagnostic strategies can also include tissue, cerebrospinal fluid (CSF) samples, and effusions. All diagnostic strategies utilizing NAATs should be validated using studies of targeted populations of immunocompromised patients [4, 20, 29, 32, 34, 36, 43, 46].

### 1.6 Clinical Significance of Molecular Detection of IC

*Candida* spp. are found as normal flora members on digestive and vaginal mucosa. When intestinal colonization increases, yeast cells or yeast DNA may circulate in peripheral blood without indicating disease. In contrast to invasive aspergillosis, in which the etiological agent is dominated by *A. fumigatus*, there are a wide variety of *Candida* spp. which can be recovered from clinical samples. Identification beyond the genus level is important for therapeutic decision making, since antifungal drug susceptibility differs among many common yeast species [20].

Blood culture is the gold standard test in the diagnosis of IC and can produce a positive result in 24–48 h. However, the sensitivity of blood cultures for the diagnosis of candidemia is estimated to be as low as 50 % [47]. In addition, 1–2 days are required for isolation and phenotype-based identification from cultures [48]. Studies showed that a delay of 12–48 h in appropriate antifungal therapy is associated with significantly increased mortality [49].

A number of molecular methods, such as peptide nucleic acid fluorescent in situ hybridization (PNA FISH; AdvanDx, Woburn, MA) [50] and PCR-based assays [51, 52], have been developed to enable rapid identification of fungi directly from blood cultures. However, these methods rely on the sensitivity of the blood culture

systems used. Efforts to facilitate the earlier diagnosis of fungemia, more recently qPCR formats [19, 53–55], DNA microarray chips, and luminex technology [48, 56–58], have been developed. Although these tests are highly sensitive, the clinical utility of these platforms is limited by the lack of standardization and high setup costs. Other amplification formats have been used to detect resistance to antifungal drugs, such as NAATs [59].

Avni et al. reviewed studies assessing the diagnostic accuracy of direct PCR on blood samples for IC. They underlined the fact that PCR of whole blood samples targeting panfungal genes (a ribosomal DNA sequence between 18S and 5.8S) has higher sensitivity for the diagnosis of IC than conventional blood cultures, with a specificity of 90 %, which is acceptable for clinical practice. The assay should have an in vitro sensitivity of at least 10 colony-forming units (cfu)/mL to give consistently positive results [49].

A theoretical advantage of PCR is its fast turnaround times than conventional methods [60]. Blood cultures can produce positive results mostly in 24–48 h in IC, and the results can be obtained by PCR-based method mostly on the same day. However, this time to result highly depends on how samples are batched and how often PCR reaction runs. Moreover, identification to the species level does not directly assess the sensitivity of a specific yeast strain to antifungal drugs, since variations can occur within a given species. Therefore, PCR assays cannot currently replace phenotypic minimum inhibitory concentration (MIC)-based testing. It is also difficult to conclude if higher positive rates of PCR represent increased sensitivity compared to that of blood culture or whether the results reflect false-positive results [20]. Most DNA extraction kits recommend 200 μL as the starting volume of sample for DNA purification from blood. This volume must be compared with that of a typical blood culture, 10 mL. Increasing the starting volume of blood increases the concentration of PCR inhibitors [61]. From a technical point of view, it seems difficult to compete with blood cultures when the aim is to detect living yeast. Currently, PCR for the diagnosis of IC may be useful as an adjunct but is clearly not a substitute for blood culture [20].

### 1.7 MTC Infections in HSCT

Immunosuppressed patients are at a higher risk for reactivation of latent MBI and developing progressive active disease due to the underlying comorbidities and immune-suppressive condition of the HSCT host [9]. The mycobacterial disease could follow unusual patterns, disseminate, and lead to mortal outcomes in vulnerable HSCT patients [10, 62–65].

Tuberculosis (TB) is not a common infectious disease among HSCT recipients [66]. The rate of TB reported after HSCT is ten times less than after solid organ transplantation, still 10–40 times higher than that in the healthy population [6, 63]. The incidence of TB in allogeneic HSCT has been reported to

range between 0.1 and 16 % showing variations between endemic/non-endemic populations [62, 63, 67, 68]. Although the reported incidences are not very high and response to treatment is generally well, the mortality rates due to TB are considerable, varying between 16 and 50 % [63, 67, 68]. Different studies report that umbilical cord blood transplantation recipients might have a higher risk for rapidly progressing disseminated TB, and higher mortality rates have been reported than transplantation recipients having another stem cell source [64, 69, 70]. With *M. tuberculosis* infection, pneumonia is most common, while extrapulmonary diseases, such as catheter-related bloodstream infections, soft tissue infections, and bone and joint infections, are more common manifestations of NTM infections, although increased risk of dissemination has been described with *Mycobacterium tuberculosis* (*M. tuberculosis*) affected by the type and duration of the immune deficiency [6, 62, 63, 65, 67, 68, 70].

### 1.8 NTM Infections in HSCT

NTM are considered as important opportunistic pathogens predominating in HSCT recipients particularly in regions where TB incidence is low [71]. The estimated incidence of NTM infection has been reported to range between 0.4 and 9.7 %, 50–600 times that in the general population, with higher rates in allogeneic HSCT patients [6, 71–74]. The most frequently isolated NTM species (45 %) are among rapidly growing mycobacteria,[3] their most common manifestation being venous catheter-related infections, accounting for 37 % of cases. *M. avium* complex and *M. haemophilum* are other common pathogens associated with pulmonary, cutaneous, or disseminated disease [6, 71, 75].

NTM infections are relatively uncommon complications of HSCT, but once detected the management relies upon reduction of immunosuppression along with implications of antimycobacterial drugs. Moreover, the interactions of antimycobacterials with immunosuppressive drugs make the rapid differential diagnosis more of an important issue between NTM group of mycobacteria among HSCT recipients [71, 74].

### 1.9 Clinical Diagnosis of MBI

The lack of an established assessment criteria and the nonspecific clinical and radiological manifestations of MBI in HSCT patients make the definitive diagnosis a challenging issue [62, 65]. Conventional diagnosis of pulmonary TB is based on sputum smear microscopy and mycobacterial culturing/susceptibility methods interpreted in light of clinical symptoms and chest radiography [75–79]. The sensitivity of smear microscopy ranges between 50 and 80 % [79] and unsatisfactory particularly in sputum negative pulmonary TB, as seen with children and immunocompromised

[3] Predominantly *M. fortuitum*, *M. abscessus*, and *M. chelonae*.

hosts [78]. Moreover, a positive smear may not be distinctive; positivity relates both to MTC and NTM group of microorganisms. Turnaround times for culture are long, and even the improved liquid-based systems do not yield satisfactory *M. tuberculosis* recovery results in the expected short period of time, causing serious delays in patient management.

Early diagnosis of TB is of paramount significance both because of the serious nature of the disease and high mortality rates in HSCT recipients [62]. In addition to that, the course, treatment options, and outcome of infections due to MTC and NTM are different; thus, it is very important to rapidly determine the mycobacterial etiology and apply appropriate prophylaxis and/or treatment measures [5, 9, 62, 63].

Official diagnostic criteria described by American Thoracic Society (ATS) in detail is to be met for the definitive diagnosis of NTM [80]. For pulmonary NTM infections, diagnosis based on radiological and clinical signs is inadequate given the presence of diverse clinical presentations [6, 73]. Microbiological culture- and species-level identification is essential both for the therapeutic decision and the exclusion of an environmental contamination [80]. For extrapulmonary disease, due to the fact that catheter-related infections are dominant in HSCT, blood can be used and diagnosis is generally based on routine microbiological blood culture results [71, 73]. Generally, NTM detection from blood, other sterile body fluids, or tissues is considered clinically significant particularly in immunodeficient HSCT host [6].

### 1.10 Molecular Diagnosis of MBI by NAATs

NAATs for the detection of TB and other mycobacterial diseases have become commonly used tests in industrialized countries because of their great advantage of speed compared to culture [81]. NAATs are the most promising rapid tests currently recommended by CDC and WHO (under certain testing and interpretation algorithms) for reducing the time to detection of TB disease to a few h/days [78, 79, 82, 83]. Both *in-house* and commercial NAATs are available for the early diagnosis of TB and molecular drug susceptibility testing for anti-*M. tuberculosis* drugs from clinical specimens, differentiation of MTC and NTM, and species-level identification of mycobacteria.

#### 1.10.1 In-House NAATs

A plethora of *in-house* NAATs have been developed, used, and evaluated for the diagnosis of TB in smear-positive and -negative, respiratory and non-respiratory specimens [84–89]. PCR is the base amplification technique of most NAATs to amplify various DNA sequences in *M. tuberculosis* genome. Many DNA sequences have been targets of *in-house* NAATs, most commonly amplified target being *IS*6110 insertion sequence. 16S and 23S rRNA; 65 kDa protein (*hsp*); genes encoding MTP40, MPB64, and MPB70 antigen; *mtp* genomic fragment; *IS*986 insertion sequence;

resistance-associated genes such as *rpoB* and *gyrB*; and other targets have also been used [86–88, 90–93].

The reported overall sensitivity and specificity of *in-house* NAATs were reported to be 96 and 81 %, respectively, for smear-positive respiratory specimens [87]. The diagnostic accuracies for smear-negative respiratory specimens were highly variable: sensitivity ranged from 9 to 100 % and specificity from 25 to 100 % [86].

*In-house* NAATs have been widely implemented on patients with extrapulmonary TB, using different clinical specimens. Takahashi et al. have reviewed the sensitivity and specificity estimates for TB meningitis of *in-house* assays for TB diagnosis on CSF. The sensitivities ranged between 31 and 100 %, and specificities ranged between 66 and 100 % for *in-house* NAATs [88]. Cheng et al. and Chakravorty et al. have indicated encouraging diagnostic value estimates for the diagnosis of TB pleuritis with a sensitivity range of 66.7–83 % and a specificity range of 75–100 % [89, 94]. Molecular diagnosis of bloodstream infections due to the dissemination of *M. tuberculosis* or an NTM infection has also been performed using blood as the specimen [95, 96].

The overall diagnostic accuracy of commercial NAATs was found to be higher than that of *in-house* assays for TB meningitis, pleuritis, and lymphadenitis [92, 97, 98]. Almost all meta-analyses conducted so far indicated considerable discrepancies between sensitivity and specificity estimates for the *in-house* molecular tests [79, 89, 91, 93, 97, 98]. The specificity yields of all NAATs were higher than their sensitivities, justifying their use for confirming diagnosis but limiting their clinical value for the exclusion of mycobacterial disease.

The clinical implications of *in-house* assays for the diagnosis of pulmonary and extrapulmonary TB are debatable due to the high heterogeneity in accuracy estimates limiting their clinical value [91]. The quality of the reference test, specimen type, presence of inhibitors (leading to false-negative results and thus decreased sensitivity), cross contamination (leading to false positivity and thus decreased specificity), amplification target/using multiple target copies, and PCR format (nested, multiplex, or real-time PCR) are among the parameters affecting sensitivity and specificity of the *in-house* assays [86–89, 99].

The use of commercial NAATs may not be possible in most low-income/high-TB-burden settings; thus, many laboratories continue using relatively inexpensive *in-house* approaches. *In-house* NAATs are recommended to be used in light of a sound clinical and radiological suspicion with strict quality control measures [86, 87].

#### 1.10.2 Commercial NAATs

Automated commercial systems also do use PCR-based amplification with varying target sequences for the detection of MTC in clinical specimens. They utilize standardized protocols and reagents for all steps of sample processing, amplification, and detection [79, 100]

overcoming many drawbacks of *in-house* NAATs, such as false positivity and false negativity. There are many different commercial NAATs available for rapid diagnosis of MTC in clinical specimens. The literature claims that commercial NAATs, particularly the US Food and Drug Administration (FDA)-approved tests, show perfect performances with smear-positive pulmonary samples [77, 79, 101]. None of the commercial systems have been FDA approved to be used with extrapulmonary specimens; still, reliable and faster diagnosis of extrapulmonary TB by commercial NAATs is also reviewed elsewhere [92, 97, 98, 102, 103].

Of the numerous commercial molecular assays developed and evaluated, Gen-Probe Amplified Mycobacterium tuberculosis Test (AMTD, Gen-Probe, San Diego, California) and Roche's Amplicor Mycobacterium Tuberculosis (MTB) System (Amplicor, Roche Molecular Systems, Branchburg, NJ) are two tests that have been widely used and have been approved by FDA. Roche Amplicor MTB System is only approved to be used with smear-positive respiratory specimens, while the new-generation AMTD system, E-AMTD test is also approved for smear-negative respiratory specimens as well as positives [77, 79, 104].

*COBAS Amplicor MTB Test* is a PCR-amplified qualitative test targeting the 584 bp region of the 16S rRNA gene of mycobacteria. The reported overall sensitivity of FDA cleared Cobas Amplicor MTB Test for respiratory specimens range between 83 and 96.7 %. The sensitivity estimates for smear-positive pulmonary specimens were 90–100 % and for smear-negative cases, 50–96.7 %. When extrapulmonary specimens or mixture of pulmonary and extrapulmonary specimens were tested simultaneously, the estimated sensitivities were 27.3 and 85 %, respectively [100, 101, 104, 105].

*E-AMTD* assay is a transcription-mediated amplification (TMA)-based system. The amplification takes place at isothermal conditions at 42 °C, targeting the mycobacterial rRNA [79, 104, 105]. As with COBAS Amplicor MTB Test, the diagnostic accuracy of E-AMTD is higher in smear-positive pulmonary TB. The sensitivity of the test for respiratory specimens was reported to be between 91.7 and 100 % and 65.5 and 92.9 % for smear-positive and -negative pulmonary specimens, respectively [100, 104, 105]. Inclusion of extrapulmonary specimens changed the range of overall sensitivity rates to 74.3 and 100 % (smear-positive specimens 88–100 % and smear-negative specimens 63.6–100 % [105]). Absence of an internal control is the main drawback of the E-AMTD system. Parsons et al. have reviewed results of three separate studies on the diagnostic efficacy of E-AMTD test on TB meningitis suspects, the sensitivity and specificity ranging between 83 and 93.8 % and 97 and 100 %, respectively [101].

Another currently available commercial system is the *BD ProbeTec Energy Transfer (ET) system* (Becton Dickinson, Sparks, MD) which is an isothermal amplification system using strand displacement

amplification (SDA) targeting *IS*6110 repetitive sequence along with 16S rRNA [79, 100, 105]. The differences in sensitivity measures between smear-positive pulmonary specimens and smear-negative extrapulmonary specimens were claimed to be less significant for BD ProbeTec ET than the other commercial NAATs tested. Reported sensitivities in the literature ranged from 89 to 100 % for smear-positive cases and 33.3–85.7 % for smear-negative cases [79, 100, 105]. Overall specificity was ranging from 98.9 to 100 % [105]. The sensitivity and specificity of the BD ProbeTec ET system were assessed on extrapulmonary specimens in a recent study. Overall sensitivities and specificities were 82.7 and 99 %, respectively, when tested on consecutive extrapulmonary samples (including CSF, gastric aspirates, urine, sterile body fluids, fine needle aspirates, biopsies, and stool). The diagnostic accuracy of the BD ProbeTec ET system was found high enough to be used with extrapulmonary specimens [103].

*Loop-Mediated Isothermal Amplification* (LAMP; Eiken Chemical Company, Japan) is the novel commercial technology that has been developed to be used in low-income/high-TB-burden settings. The system uses multiple primers to increase specificity, and the amplification takes place in isothermal conditions [81, 106]. The sensitivity of LAMP in smear-positive sputum specimens was 97.7 %, and the sensitivity in smear-negative specimens was 48.8 % as noted by Boehme et al. [81]. The specificity of LAMP assay was published to be 99 % [77, 79, 93], and in the recent review by Neonakis et al., LAMP test has been proven to be a highly specific and sensitive, easy-to-use, and cost-effective system that could be implemented in low resource settings for the rapid detection of MTC from clinical specimens [106].

The pooled specificity and sensitivity estimates of seven different commercial assays for both smear-positive and -negative respiratory specimens were evaluated in a large meta-analysis overlooking 125 studies by Ling et al. The pooled sensitivity and specificity of these tests were 85 and 97 %, respectively [107]. Specificity was more consistent than the sensitivity, sensitivity results being heterogenous, mainly on smear-negative specimens [87, 100]. Commercial NAATs can be useful for establishing TB diagnosis in smear-positive disease along with conventional microbiology and clinical suspicion.

The diagnostic accuracies of commercial NAATs for the diagnosis of TB meningitis, TB pleuritis, and TB lymphadenitis were evaluated in three separate meta-analyses, using CSF, pleural fluid, lymph node-aspirated tissue material as the specimens, respectively. High specificities but lower and inconsistent sensitivities were reported. The sensitivity estimates for E-AMTD test were superior when compared to COBAS Amplicor Test on extrapulmonary specimens. Commercial NAATs might have a potential role in confirming TB meningitis, pleuritis, and lymphadenitis, whereas the tests were not dependable for ruling out the diseases due to the low sensitivity [92, 97, 98].

### 1.11 Molecular Drug Susceptibility Testing Along with MTC Diagnosis

The increase in multidrug-resistant (MDR)[4] strains and the emergence of extensively drug-resistant (XDR)[5] strains jeopardize global TB control and treatment outcomes in every population prone to TB [78, 108]. The recent progress in understanding the mechanisms underlying *M. tuberculosis* drug resistance has shed light to the advances in determining gene regions responsible for resistance by NAATs. Mutations in an 81-bp RIF resistance-determining region (RRDR) of the rpoB gene are responsible for RIF resistance in approximately 95 % of the RIF resistant strains [77, 79, 109]. *rpoB* being a hot spot gene strongly correlated with RIF resistance, and because monoresistance to RIF is rare, determining RIF resistance by the amplification of *rpoB* gene also gives a strong indication of MDR TB.

*In-house* PCR and real-time PCR assays with molecular beacons or FRET have been used successfully to detect drug-resistant TB strains, targeting many different resistance-associated gene regions [9, 90, 93, 109].

Currently two commercial assays are available for the simultaneous detection of resistance by the time of TB diagnosis, namely, Line Probe Assays (LIPAs) and the GeneXpert MTB/RIF system.

LIPAs are DNA strip-based tests which amplify the mycobacterial target region with PCR and use reverse hybridization for the detection of common mutations that are associated with resistance [77, 79, 93, 110, 111].

*Inno-Lipa RIF.TB Test* (Innogenetics, Zwijndrecht, Belgium) and *Genotype MTBDR* and *Genotype MTBDRplus* (Hain Lifesciences GmBH, Nehren, Germany) assays are two most commonly used LIPAs that simultaneously detect *M. tuberculosis* and the presence of RIF resistance both from culture and clinical samples by multiplex PCR followed by reverse hybridization. Morgan and colleagues evaluated the results of 14 different studies to assess the diagnostic accuracy of InnoLipaRIF.TB assay. When tested on various clinical specimens, the sensitivity was found to range between 80 and 100 %, with a 100 % specificity. Inno-Lipa RIF.TB is a highly sensitive tool for the detection of *M. tuberculosis* and RIF-resistant MTC from clinical isolates with lower diagnostic sensitivity on clinical specimens [79, 110–112].

Crudu et al. have evaluated the diagnostic accuracy of Genotype MTBDR*plus* reporting an overall sensitivity and specificity of 87.6 and 99.2 %, respectively [112]. The combined sensitivity and specificity in the subgroup of smear-negative samples were detected to be 79.8 and 99.2 %, respectively. The MTBDR*plus* assay is a rapid and highly sensitive test for the detection of *M. tuberculosis* strains

[4] *M. tuberculosis* strains which are resistant to at least rifampicin and isoniazid.
[5] *M. tuberculosis* strains which are resistant to any fluoroquinolone and one of the three injectable aminoglycosides (capreomycin, kanamycin, and amikacin) in addition to rifampicin and isoniazid.

from smear-positive and -negative clinical specimens as well as informing about their RIF and INH resistance status [110, 111].

Based on scientific evidence and expert opinion, both LIPAs were endorsed by WHO for rapid screening of patients with a high risk of MDR-TB [113]. The main disadvantages of LIPAs are their labor-intensive nature, needing experienced staff/laboratory setting, and the lower sensitivity estimates when tested on smear-negative clinical specimens [109, 112].

*The GeneXpert MTB/RIF test (Cepheid, USA)* is a very promising molecular diagnostic test introduced in 2010, combining TB diagnosis with simultaneous detection of resistance to RIF directly from clinical samples. The test, endorsed by WHO in 2010, is claimed to be the "game changer" of molecular diagnosis of *M. tuberculosis* and drug resistance detection, approaching the standards of a point-of-care (POC)[6] test [104, 109, 114, 115].

The GeneXpert MTB/RIF uses real-time PCR technology having a fully automated cartridge system, the only manual step being the addition of buffer on the sputum (or the clinical specimen to be used), which makes the assay suitable and user friendly. The system utilizes molecular beacons and hemi-nested PCR to detect *M. tuberculosis*-specific DNA sequences and *rpoB* region for the detection of RIF resistance [109, 114]. The GeneXpert test can rapidly identify the presence of *M. tuberculosis* simultaneously with RIF resistance from clinical specimens, regardless of the smear status. The test has high efficacy not only for the diagnosis of pulmonary TB from respiratory samples but also from extrapulmonary samples [102].

In an analytical validation study conducted by Helb et al., the reported sensitivity of the GeneXpert MTB/RIF for the detection of *M. tuberculosis* from smear-positive isolates was 100 %, and detection of smear-negative isolates was between 71.2 and 84.6 %, ranging due to the gold standard used. The specificity of the assay was 100 %. The sensitivity and specificity of RIF resistance detection was also 100 and 100 %, respectively [116]. Boehme et al. also had encouraging results regarding the clinical performance of the assay. An overall sensitivity of 97 % was reported in their study. A single direct test identified more than 98 % of all smear-positive TB cases and about 72.5 % of all smear-negative culture-positive cases with 99.2 % overall specificity. The RIF resistance detection sensitivity and specificity were also as high as 97.6 and 98.1 %, respectively. The addition of a second or a third test on smear-negative specimens increased the diagnostic sensitivity and specificity to 85.1 and 90.2 %, respectively [117].

[6] POC tests are diagnostic tests that do not require laboratory facilities or specialist training and that can be used where care is provided within a clinic or in the community.

The overall sensitivity and specificity of the GeneXpert MTB/RIF assay were also quite high when tested on non-respiratory samples as indicated by Lawn et al. [102]. Although higher for smear-positive specimens and for pulmonary TB, still high sensitivities were detected with CSF, tissue samples, gastric aspirates, and pus and fine needle aspirates (85.7, 75, 78.7, and 88.3 %, respectively). The lowest sensitivity was found with pleural fluid (44.4 %) and other body fluids [114]. Overall sensitivities suggest that the GeneXpert MTB/RIF assay may be a routine part of extrapulmonary TB detection tool.

The GeneXpert MTB/RIF test overcomes many limitations of most other NAATs such as complexity, manual steps of specimen preparation, risk of cross contamination, and inhibitors. The assay system is simple to use, total hands-on time being 5–15 min, and the results which could be interpreted easily are obtained almost in 2 h without the need of batch testing [102, 104, 116, 117]. The GeneXpert is by far the best currently available molecular NAAT for TB diagnosis and is proven to be superior to other molecular tests when used with smear-negative specimens [118].

### 1.12 Molecular Differentiation of MTC and NTM/Species-Level Identification

Rapid and reliable diagnosis of an NTM infection in a TB-suspected patient would likely have an impact on treatment choice and other patient management measures, particularly in NTM high-risk populations/situations such as HSCT. Rapid exclusion of patients with NTM- and species-level identification depends on molecular testing [74].

The first step for the differential diagnosis of pulmonary NTM infections would be to rule out pulmonary TB in smear-positive cases or to rule in pulmonary TB in TB-suspected smear-negative cases. As for this purpose, all the aforementioned NAATs may have implications and value for the exclusion of an NTM infection, either by confirming MTC or by ruling out MTC and directing suspicion to NTM infection [87, 100, 103]. After the exclusion of a likely MTC disease by NAATs, species identification for the most appropriate choice of antimicrobial can be done with various molecular methods, with *in-house* PCR-based species-specific target detection methods or gene probe-based LIPAs [119, 120]. PCR-, PCR-RFLP-, and PCR-gene sequencing- as well as PCR gene probe-based detection of several mycobacteria-specific targets such as 16S rRNA, *hsp*65, internal transcribed spacers (ITS), *rec*A, *dna*J and *rpo*B, and *IS*1245 are performed for mycobacterial species-level typing. Species-level identification and susceptibility testing of clinically significant NTM are recommended where possible [6, 9, 73, 74, 80].

For species identification from clinical respiratory specimens, *in-house* multiplex and real-time PCR assays, liquid–solid microarrays, and broad-range PCR followed by spoligotyping, pyrosequencing, and genotyping can be applied with sequencing being the gold standard method [6, 9, 80].

### 1.13 Clinical Significance of Molecular Detection of MBI in HSCT

The low incidence and the diagnostic difficulties of MBIs may lead to an underestimation of the frequency of these infections in HSCT, which are often not considered in the differential diagnosis [65]. Nonetheless, comorbid infections and severe immune suppression after HSCT may lead to poor prognosis and fatal outcomes of MBIs in HSCT recipients. NAATs are promising tests which may provide infection data in advance and help in implementing the appropriate precautions.

A plethora of reviews and meta-analysis in the literature have evaluated the diagnostic accuracies of molecular methods for rapid diagnosis of MBIs. For *in-house* tests, variations and inconsistency in diagnostic accuracy results are more profound mainly because of the different protocols used and high yields of false negativity and false positivity due to the lack of a standardized quality control. Their sensitivity estimates were generally more variable and lower than specificities, decrease in sensitivity being more significant in smear-negative and extrapulmonary forms of TB [86, 87, 91]. On the contrary, commercial NAATs have proven to be more reliable with more comparable diagnostic accuracies than those of *in-house* assays. Sensitivity was generally optimal for smear-positive pulmonary specimens and lower for the negatives for most of the commercial NAATs evaluated so far [86, 87, 91, 92, 97, 100, 101, 103, 107]. General accuracies of commercial NAATs for the detection of MTC as well as resistance were considerably higher in pulmonary specimens than nonpulmonary specimens in general [100, 101, 105, 117]. None of the NAATs are FDA approved for the detection of extrapulmonary specimens. Having limited roles as stand-alone tests, it is still valuable to adjunct those tests in the diagnosis of TB meningitis, pleuritis, pericardial TB, and other conditions in which yield of other tests is low and where there is a high risk of progressing active TB [79, 89, 92, 97, 104].

Both commercial NAATs and *in-house* NAATs are helpful for confirming pulmonary TB in smear-positive patients along with clinical suspicion (particularly in TB endemic regions). If the opportunistic infections are of concern, a negative commercial or a highly controlled (inhibitor free) *in-house* NAAT can drive diagnosis toward NTM pulmonary disease with smear positivity. In the case of smear negativity or extrapulmonary TB suspicion, a negative commercial or an *in-house* NAAT cannot eliminate TB due to the low sensitivity yields of the tests. But, the high specificity of a commercial assay might rule in TB interpreted with clinical data also in some of the smear-negative specimens [86, 87, 91].

As pointed out by WHO and CDC, determining drug resistance patterns at the time of established diagnosis carries importance. Although there are only a few MDR cases reported in HSCT patients [121], in a life or death situation such as the case with HSCT, the drug susceptibility results should also be determined as soon as *M. tuberculosis* is detected, particularly in places where the

disease is endemic and MDR is common. There are currently two commercial systems that could rapidly detect RIF resistance along with rapid diagnosis, which are LIPAs and GeneXpert System, both of which are endorsed and recommended by WHO [113, 115]. If the cost is not a matter of concern, commercial NAATs, particularly LIPAs and GeneXpert MTB/RIF, are the molecular tests holding great promise for rapid TB diagnosis and detection of resistance in seriously ill adults and children who undergo HSCT.

Due to the sensitivity issues of most NAATs discussed, they cannot be used alone for ruling in TB. But in combination with clinical suspicion and conventional tests, they can still be implemented for the efficient and fast management of active *M. tuberculosis* infection in HSCT. Both *in-house* assays with strict quality measures and commercial tests can complement HSCT findings and help to direct the early and effective onset of therapy. All tests do amplify nonviable or dead mycobacteria, so they should not be implemented in patients on treatment and are still not reliable for monitoring treatment outcomes and prognosis [79].

## 2 Materials

### 2.1 qPCR for Molecular Diagnosis of IFIs

The following protocol is from LightMix® for the detection of fungi (Roche Diagnostics) by qPCR. PCR conditions do not differ from standard qPCR conditions.

#### 2.1.1 Sample

Optimization of the choice of clinical sample and the appropriate fraction to be tested can impact diagnostic performance. For the diagnosis of IC, blood is the sample of choice. The optimal specimen (e.g., BAL, blood) is still not resolved for the diagnosis of invasive aspergillosis. Several authors have pointed to high sensitivity and specificity of molecular methods when applied to BAL specimens [43, 122] (*see* **Note 1**). On the other hand, numerous studies in the literature have investigated the applicability of blood or serum samples for the diagnosis of invasive aspergillosis [4, 20, 25, 36, 40, 43] (*see* **Notes 2** and **3**).

There is also no consensus on the optimal blood fraction to be used (whole blood or serum) from which to isolate fungal DNA [20, 36, 48] (*see* **Notes 4–6**).

#### 2.1.2 DNA Extraction

Suboptimal DNA extraction is one of the main reasons of obtaining false-negative results. The European Aspergillus PCR Initiative (EAPCRI) reported that PCR results are dependent on the extraction protocol rather than the PCR amplification [4, 43] (*see* **Note 7**).

Both commercial kits and *in-house* methods can be used for fungal DNA extraction [29, 31, 33–36, 44, 123] (*see* **Note 8**). Optimal DNA extraction from fungi could be performed via

manual methods such as boiling with Tris–EDTA and phenol–chloroform extraction and by commercial kits (e.g., MagNA Pure LC System [Roche Diagnostics], QIAamp DNA Mini kit [Qiagen], ZR Fungal/Bacterial DNA MiniPrep [Zymo Research]). In this chapter ZR Fungal/Bacterial DNA MiniPrep kit is described for the extraction of fungal DNA from clinical specimens. Materials needed for the extraction are:

1. ZR Fungal/Bacterial DNA MiniPrep™ kit.
2. Heat block.
3. Vortex mixer.
4. Microcentrifuge.
5. Sterile 1.5 mL screwed microcentrifuge vials.
6. Sterile 1.5 mL microcentrifuge vials.
7. Cell disruptor/pulverizer (recommended).
8. Automatic pipettes (1,000, 200, and 10 μL) and sterile filter tips.
9. 96–100 % ethanol.

#### 2.1.3 Primers

A pan-fungi-specific primer set is used that binds to a highly conserved region of the 750 bp long fragment of the fungal 18S rRNA gene. All primers were synthesized by TIB MOLBIOL (Berlin, Germany).

#### 2.1.4 PCR Reaction

PCR conditions do not differ from standard qPCR conditions. Materials needed for PCR reaction are:

1. Template DNA.
2. LightCycler®FastStart DNA Master HybProbe.
3. LightCycler®Instrument 2.0.

Lyophilized reagents are stable for at least 3 months after shipment when stored protected from light at room temperature (18–25 °C). Do not freeze lyophilized reagents. Dissolved reagents are stable for at least 5 days when stored protected from light and refrigerated (4 °C).

### 2.2 IS6110 PCR for Molecular Diagnosis of MBIs

#### 2.2.1 Sample

For the detection of pulmonary MBI, sputum is the most common specimen used. Induced sputum, BAL, and nasopharyngeal aspirates (NPA) can also be used. For children and adults who are not able to produce sputum, gastric lavage is the alternative specimen to be taken as the respiratory sample (*see* **Note 9**). If extrapulmonary disease is suspected due to MTC or NTM, then the specimen of choice would be either blood or body fluids, namely, CSF, urine, lymph node aspirates, pleural fluid, and tissue materials among others [6, 9, 88, 89] (*see* **Note 10**).

#### 2.2.2 Sample Processing: Decontamination/Inhibitor Removal

The isolation of high-quality inhibitor-free DNA/RNA extraction is of paramount importance, affecting the sensitivity of the NAATs. Inhibitor removal from clinical samples, sputum, fluids, and tissues considerably increases sensitivity [94]. Sputum, bronchial, gastric aspirates, and urine need decontamination among others [9]. The most commonly used homogenization and decontamination method is *N*-acetyl L-cysteine (NALC)–NAOH method, described by Kent et al., also known as CDC method [124] (*see* **Note 11**). A novel specimen processing technology (universal sample processing, USP) developed by Chakravorty et al. has proven to work better with PCR, both for pulmonary and extrapulmonary specimens [95] (*see* **Note 12**). For USP method:

1. USP solution consisting of:
   4–6 M guanidinium hydrochloride (GuHCl).
   50 mM Tris–Cl, pH 7.5.
   25 mM EDTA, 0.5 % Sarkosyl.
   0.1–0.2 M mercaptoethanol.
2. Phosphate-buffered saline pH 6.8 and/or sterile $H_2O$.
3. Centrifuge is used.

USP solution both results in reduced rate of contamination compared to the CDC method and is the only available specimen processing method that could guarantee the isolation of optimum quality DNA for PCR. The sediment obtained after USP processing could be used for smear microscopy, culture, and NAATs after resuspension [94, 95] (*see* **Note 13**).

#### 2.2.3 DNA Extraction

Due to the unique structure of the cell wall of mycobacteria, the nucleic acid extraction may sometimes be challenging. The abundance of lipids and polysaccharides can interfere with DNA isolation; thus, the extraction method carries importance. Optimal DNA extraction from mycobacteria could be performed via manual methods such as boiling with Tris–EDTA (TE) buffer, phenol–chloroform extraction, CETAB, or sodium dodecyl sulfate (SDS)–Triton X extraction and by commercial kits (e.g., kits by Roche, Qiagen [84, 125, 126]) (*see* **Note 8**).

In this chapter QIAGEN QIAamp DNA Mini/Blood Mini kit is described for the extraction of mycobacterial DNA.

Materials needed for DNA extraction are:

1. QIAGEN QIAamp DNA Mini/Blood Mini kit.
2. Heat block.
3. Vortex mixer.
4. Microcentrifuge.
5. Sterile 1.5 mL screwed microcentrifuge vials.

6. Sterile 1.5 mL microcentrifuge vials.
7. Automatic pipettes (1,000, 200, and 10 μL) and sterile filter tips.
8. 96–100 % ethanol.

#### 2.2.4 Primers

Depending on the target gene sequence chosen to be amplified different primers can be used. An unrelated gene should be included as the internal PCR control. For the current *IS*6110-PCR described here, the specific oligonucleotide and the internal control sequences are as follows:

1. *IS*6110 insertion sequence-specific primers: TB-1 forward 5′ CCT GCG AGC GTA GGC GTC GG 3′ and TB-2 reverse 5′ CTC GTC CAG CGC CGC TTC GG 3′ [127].
2. Internal control gene (beta globin) primers: BetaGLF forward 5′ CAA CTT CAT CCA CGT TCA CC 3′ and BetaGLR reverse 5′ GAA GAG CCA AGG ACA GGT AC 3′ [128].

#### 2.2.5 PCR Reaction

PCR reaction is similar to any conventional PCR scheme. Materials needed for PCR reaction are the following:

1. For PCR reaction: Primers (each 20 pM/μL), $H_2O$, PCR buffer, $Mg^{+2}$ (25 mM), dNTP (each 0.2 nM), *Taq* DNA Polymerase (5 U/μL) and template DNA (3 μL).
2. A thermal cycler.
3. 10× TBE buffer (1 L, pH:8: 108 g Tris base, 55 g boric acid, and 14.8 g EDTA are dissolved in $ddH_2O$, and the volume is adjusted to 1 L).
4. 0.5× TBE buffer: 50 mL of 10× TBE buffer is diluted with $ddH_2O$ to 1 L.
5. 2 % (w/v) agarose.
6. Ethidium bromide solution.
7. Electrophoresis tank.
8. Ultraviolet transilluminator.

### 2.3 Quality Control

Strict quality control is required for both *in-house* and commercial NAATs. Negative (extraction) controls as well as positive (internal) inhibition controls should be used in each run. Most commercial NAATs do have internal controls and standardized PCR conditions/procedures (E-AMTD does not possess an internal control) resulting in more consistent sensitivity and specificity with less false positivity/negativity [79, 110]. For *in-house* NAATs, assay performance is highly affected by false-positive and false-negative results [86, 87]. False positivity due to cross contamination may account for low specificity of a given NAAT. DNA purification utilizing dUTP/UNG with NAATs limits the contamination rate with higher

specificity but sometimes at the expense of sensitivity [86, 89]. Real-time PCR minimizes the risk of carryover contamination and thus increases the specificity for *in-house* assays.

The presence of inhibitors that would interfere with the amplification process can lead to false negativity leading to sensitivity issues; thus, optimal inhibitor removal is essential [86, 87]. Particularly when extrapulmonary specimens are used, suboptimal nucleic acid extraction method is an important factor for getting false-negative results, mainly because of the abundant presence of inhibitors [89].

## 3 Methods

### 3.1 qPCR

#### 3.1.1 DNA Extraction

Fungal DNA extraction can be performed from respiratory specimens (such as BAL), blood, body fluids, and tissue samples (fresh) by the ZR Fungal/Bacterial DNA MiniPrep Kit, according to the manufacturer's instructions.

#### 3.1.2 PCR Reaction

Briefly, parameter-specific reagents, standard row (quantification), and reaction mix are prepared according to the manufacturer's instructions.

1. In a cooled reaction tube, prepare 15 μL PCR reaction mix (for a single reaction) using 2 μL FastStart mix, 4 μL reagent mix, 1.6 μL 25 mM $Mg^{2+}$ solution, and 7.4 μL water.
2. Mix the reaction tube gently.
3. Spin down the tube.
4. Transfer the PCR reaction mix to a LightCycler® capillary.
5. Add 5 μL sample or standard to each capillary to give a final reaction volume of 20 μL.

Fungal DNA is amplified under the following conditions: program 1 (denaturation of sample and activation of the enzyme) for 10 min at 95 °C; then program 2 (PCR amplification of the target DNA) for 5 s at 95 °C, 5 s at 55 °C, 5 s at 55 °C, and 20 s at 72 °C for 45 cycles; then program 3 (melting curve of the fungal DNA-derived PCR product) for 20 s 95 °C and 20 s 40 °C for one cycle; and then program 4 (cooling the instrument) for 30 s at 40 °C.

#### 3.1.3 Interpretation

Data analysis is done using LightCycler®Instrument 2.0. A fragment of the fungi genome, amplified with specific primers, is detected with probes labeled LightCycler®Red 640 (detected in channel 640). The PCR product is identified by running a melting curve with a specific melting point (Tm) of 65.5–67.5 °C (concentration dependent) in channel 640.

### 3.2 IS6110 PCR

#### 3.2.1 Starting Material

The USP method involves homogenization and decontamination of clinical specimens by treatment with USP solution (described in Subheading 2.2.2).

1. Add USP solution on the specimen (1.5–2 volumes).
2. Vortex for about 30–40 s (or hand shake for 1–2 min).
3. Incubate the homogenate at room temperature for 5–10 min.
4. After incubation, add 10–15 mL sterile water or 68 mM PBS and mix well.
5. Centrifuge the sample at 5,000–6,000 × *g* for 10–15 min at room temperature.
6. Discard the supernatant.
7. Use the sediment for PCR.

The USP protocol described here is mainly for the processing of sputum samples, for blood, tissue and fluids, protocols are also detailed [94, 95].

#### 3.2.2 DNA Extraction

Mycobacterial DNA extraction can be performed from sputum, blood, body fluids, and tissue samples (embedded in paraffin or fresh) by the QIAGEN QIAamp DNA Mini/Blood Mini Kit, according to the manufacturer's instructions with minor modification. The step where proteinase K is heat inactivated at 56 °C in the procedure (which is after lysis and digestion of the specimen) is recommended to be done by boiling the samples for 20 min or leaving the samples at 95 °C in the heat block for another 20 min. This modification would increase the mycobacterial DNA yield because heat is the best way for extracting DNA from mycobacteria (Personal communication, Prof. Dr. Tanil Kocagoz).

#### 3.2.3 PCR Reaction

Briefly, a 25 μL of PCR reaction is set up containing 1 μL (20 pM/μL) of each primer including internal beta globin primers, 11.4 μL $H_2O$, 2.6 μL PCR buffer, 2.8 μL $Mg^{+2}$ (25 mM), 1 μL dNTP (each 0.2 nM), 0.13 μL *Taq* DNA Polymerase (5 U/μL), and 3 μL of template DNA (*see* **Note 14**).

The thermal cycling parameters are as follows: initial denaturation for 3 min at 94 °C followed by 45 cycles, each cycle being 30 s at 94 °C, 45 s at 58 °C, and 45 s at 72 °C, and a final extension step of 3 min at 72 °C.

#### 3.2.4 Interpretation

The *IS*6110-specific PCR product is 123 bp, and beta globin amplicon is 268 bp. PCR products can be detected on 2 % agarose gel followed by ethidium bromide staining and visualized under ultraviolet light. At least one negative control should be amplified in each run by replacing the template DNA with water (*see* **Note 15**).

## 4 Notes

1. There are several drawbacks when BAL fluid is used for the diagnosis of invasive aspergillosis. BAL is usually performed at a late stage of clinical disease, when the patient already has pneumonia or prolonged fever of unknown origin. It can be difficult to distinguish true infection from colonization and environmental contamination. False-positive results have been reported with BAL fluid. The quantity of BAL varies depending on localization of the lesions and alveolar permeability. Therefore, PCR results cannot be assigned to a reliable denominator. Serial BAL sampling is generally impractical and therefore cannot be used effectively to monitor therapeutic response. Based on these uncertainties, some authors have emphasized the limited clinical predictive value of positive PCR results from respiratory specimens.
2. Blood samples are easily obtained for repeated testing and can be used for detection of infection prior to clinically evident disease than BAL. As environmental contamination of blood specimens is minimal, the presence of fungal DNA in blood would appear to have a higher positive predictive value than the same result in respiratory specimens.
3. BAL fluids have a higher burden of organisms, and testing BAL samples achieves higher sensitivity and specificity rates than testing blood samples. The values of diagnostic performance for blood and BAL fluid are scattered in a similar range (55–100 %), and therefore further investigation is warranted to determine the true potential of each sample type with highly optimized assays.
4. Although whole blood contains both free and cell-associated fungal DNA, free fungal DNA is removed during the process of red blood cell lysis and the removal of PCR inhibitors.
5. DNA extraction from serum is simpler and shorter than DNA extraction from whole blood. Automated methods can be used, providing standardization and quality control measures. Also, it allows the use of a single sample for galactomannan ELISA, β-D-glucan, and PCR analysis, thereby providing a great convenience for screening of high-risk patients.
6. The clinically relevant biological target circulating in blood has not been precisely determined. Therefore, a multicenter comparison of whole blood PCR (targeting fungal cell-associated DNA) and serum PCR (targeting free circulating DNA) is required to determine the optimal specimen for PCR testing.

7. EAPCRI recommends the use of ≥3 mL EDTA blood specimens, a red and white cell lysis step, bead beating to lyse the fungal elements, use of negative and positive extraction controls and an internal control, and use of DNA elution volumes smaller than 100 μL.
8. Please refer to specific literature for the comparison of several extraction methods for different types of specimens [29, 31, 35, 36, 44, 88, 95, 96, 123, 128].
9. The sensitivity of the NAATs for the diagnosis of MBIs largely depends on the choice of clinical specimen, volume, and eligibility and pretreatment procedures, especially for extrapulmonary and smear-negative specimens [9, 86]. The diagnostic yield of *in-house* NAATs was found to be better with BAL specimens and NPA and suboptimal with gastric lavage particularly in smear-negative specimens [86, 87, 89]. On the contrary, with GeneXpert higher sensitivity results were noted with many specimens [102].
10. Generally, NTM detection from blood, other sterile body fluids, or tissues is considered to be clinically significant. The clinical relevance of recovering NTM from blood cultures drawn through catheters should be interpreted cautiously because of possible environmental contamination with asymptomatic colonization at the site of an indwelling line. Features in the clinical history (e.g., extensive immunosuppressive therapy, prolonged fever, and embolic events) may aid in clinical differentiation between infection and contamination.
11. Most *in-house* NAATs work well with homogenized and decontaminated specimens [6, 80]. For commercial NAATs, pretreatment procedures generally are not provided by the manufacturer; some might work better with decontaminated specimens, and sometimes harsh decontamination procedures would result in unwanted sensitivity issues [107]. Unprocessed specimens can be used with LAMP assay [106]. Unprocessed sputum or processed sediment regardless of the smear status could directly be loaded onto the GeneXpert machine, but it is recommended that the body fluids are concentrated by centrifugation [114].
12. Particularly for those with paucibacillary disease as seen with children and extrapulmonary forms, mycobacteria from different body fluids can be more effectively detected by PCR using USP method. USP method is claimed to identify patients with TB and other MBIs in a variety of settings [85, 94, 95]. NAAT performance is also very much affected by mycobacterial burden in the sample. Low bacilli load or uneven distribution particularly in sterile body fluids and smear-negative specimens leads to sampling bias and false negativity both for *in-house* and commercial NAATs [79, 110]. USP method is proven to overcome unequal distribution of bacilli [94, 95].

13. Examination of smears from clinical specimens and concomitant culturing/susceptibility testing are recommended by CDC and WHO along with NAATs. Although the most commonly used method for acid fast staining is Ziehl–Neelsen or Kinyoun methods, fluorochrome and auramine-rhodamine staining are superior for clinical specimens [6, 9, 80]. For detailed information about the media used to cultivate mycobacteria, incubation conditions, and susceptibility testing please refer to refs. 9, 129.
14. Mg levels need to be optimized depending on the conditions and the enzyme of choice.
15. The use of *IS*6110 target and nested PCR seem to have better diagnostic accuracies, but contamination is a matter of concern while performing nested PCR [87, 91].

## References


1. Babady NE, Miranda E, Gilhuley KA (2011) Evaluation of Luminex xTAG fungal analyte-specific reagents for rapid identification of clinically relevant fungi. J Clin Microbiol 49: 3777–3782
2. Srinivasan A, Wang C, Srivastava DK et al (2013) Timeline, epidemiology, and risk factors for bacterial, fungal, and viral infections in children and adolescents after allogeneic hematopoietic stem cell transplantation. Biol Blood Marrow Transplant 19:94–101
3. Kontoyiannis DP, Marr KA, Park BJ et al (2010) Prospective surveillance for invasive fungal infections in hematopoietic stem cell transplant recipients, 2001-2006: overview of the Transplant-Associated Infection Surveillance Network (TRANSNET) Database. Clin Infect Dis 50:1091–1100
4. Ruhnke M, Bohme A, Buchheidt D et al (2012) Diagnosis of invasive fungal infections in hematology and oncology – guidelines from the Infectious Diseases Working Party in Haematology and Oncology of the German Society for Haematology and Oncology (AGIHO). Ann Oncol 23:823–833
5. Cordonnier C, Martino R, Trabasso P et al (2004) Mycobacterial infection: a difficult and late diagnosis in stem cell transplant recipients. Clin Infect Dis Infect Dis Soc Am 38:1229–1236
6. Warren NG, Woods GL (2009) Mycobacteria. In: Hayden RT, Carrol KC, Tang YW et al (eds) Diagnostic microbiology of the immunocompromised host. ASM Press, New Hampshire, MA, pp 253–268
7. Muñoz A, Gonzalez-Vicent M, Badell I et al (2011) Mycobacterial diseases in pediatric hematopoietic SCT recipients. Bone Marrow Transplant 46:766–768
8. Kumar D, Humar A (2011) The AST handbook of transplant infections. Wiley-Blackwell, Oxford
9. Procop GW, Roberts GD (2011) Laboratory diagnosis and susceptibility testing. In: Schlossberg D (ed) Tuberculosis and nontuberculous mycobacterial infections, 6th edn. ASM Press, New Hampshire, MA, pp 66–74
10. Al-Anazi KA, Al-Jasser AM, Evans DAP (2007) Infections caused by mycobacterium tuberculosis in patients with hematological disorders and in recipients of hematopoietic stem cell transplant, a twelve year retrospective study. Ann Clin Microbiol Antimicrob 6:16
11. Arslan O, Gürman G, Dilek I et al (1998) Incidence of tuberculosis after bone marrow transplantation in a single center from Turkey. Haematologia 29:59–62
12. Ip MS, Yuen KY, Chiu EK et al (1995) Pulmonary infections in bone marrow transplantation: the Hong Kong experience. Respir Int Rev Thorac Dis 62:80–83
13. Martino R, Martínez C, Brunet S et al (1996) Tuberculosis in bone marrow transplant recipients: report of two cases and review of the literature. Bone Marrow Transplant 18:809–812
14. Asano-Mori Y (2010) Fungal infections after hematopoietic stem cell transplantation. Int J Hematol 91:576–587
15. Georgiadou SP, Kontoyiannis DP (2012) Concurrent lung infections in patients with

hematological malignancies and invasive pulmonary aspergillosis: how firm is the Aspergillus diagnosis? J Infect 65:262–268

16. Salmeron G, Porcher R, Bergeron A et al (2012) Persistent poor long-term prognosis of allogeneic hematopoietic stem cell transplant recipients surviving invasive aspergillosis. Haematologica 97:1357–1363
17. Maschmeyer G (2011) Invasive fungal disease: better survival through early diagnosis and therapeutic intervention. Expert Rev Anti Infect Ther 9:279–281
18. De Pauw B, Walsh TJ, Donnelly JP et al (2008) Revised definitions of invasive fungal disease from the European Organization for Research and Treatment of Cancer/Invasive Fungal Infections Cooperative Group and the National Institute of Allergy and Infectious Diseases Mycoses Study Group (EORTC/MSG) Consensus Group. Clin Infect Dis 46: 1813–1821
19. Wengenack NL, Binnicker MJ (2009) Fungal molecular diagnostics. Clin Chest Med 30: 391–408
20. Bretagne S (2011) Molecular detection and characterization of fungal pathogens. In: Persing DH, Tenover FC, Tang Y-W et al (eds) Molecular microbiology: diagnostic principles and practices. American Society for Microbiology, New Hampshire, MA, pp 655–667
21. Cesaro S, Stenghele C, Calore E et al (2008) Assessment of the light cycler PCR assay for diagnosis of invasive aspergillosis in paediatric patients with onco-haematological diseases. Mycoses 51:497–504
22. Sanguinetti M, Posteraro B, Pagano L et al (2003) Comparison of real-time PCR, conventional PCR, and galactomannan antigen detection by enzyme-linked immunosorbent assay using bronchoalveolar lavage fluid samples from hematology patients for diagnosis of invasive pulmonary aspergillosis. J Clin Microbiol 41:3922–3925
23. Buess M, Cathomas G, Halter J et al (2012) Aspergillus-PCR in bronchoalveolar lavage for detection of invasive pulmonary aspergillosis in immunocompromised patients. BMC Infect Dis 12:237
24. Suarez F, Lortholary O, Buland S et al (2008) Detection of circulating Aspergillus fumigatus DNA by real-time PCR assay of large serum volumes improves early diagnosis of invasive aspergillosis in high-risk adult patients under hematologic surveillance. J Clin Microbiol 46: 3772–3777
25. Khot PD, Fredricks DN (2009) PCR-based diagnosis of human fungal infections. Expert Rev Anti Infect Ther 7:1201–1221
26. Mengoli C, Cruciani M, Barnes RA et al (2009) Use of PCR for diagnosis of invasive aspergillosis: systematic review and meta-analysis. Lancet Infect Dis 9:89–96
27. Williamson EC, Leeming JP, Palmer HM et al (2000) Diagnosis of invasive aspergillosis in bone marrow transplant recipients by polymerase chain reaction. Br J Haematol 108: 132–139
28. Buchheidt D, Baust C, Skladny H et al (2001) Detection of Aspergillus species in blood and bronchoalveolar lavage samples from immunocompromised patients by means of 2-step polymerase chain reaction: clinical results. Clin Infect Dis 33:428–435
29. Halliday C, Hoile R, Sorrell T et al (2006) Role of prospective screening of blood for invasive aspergillosis by polymerase chain reaction in febrile neutropenic recipients of haematopoietic stem cell transplants and patients with acute leukaemia. Br J Haematol 132:478–486
30. Badiee P, Alborzi A, Karimi M et al (2012) Diagnostic potential of nested PCR, galactomannan EIA, and beta-D-glucan for invasive aspergillosis in pediatric patients. J Infect Dev Ctries 6:352–357
31. Spiess B, Buchheidt D, Baust C et al (2003) Development of a LightCycler PCR assay for detection and quantification of *Aspergillus fumigatus* DNA in clinical samples from neutropenic patients. J Clin Microbiol 41:1811–1818
32. Musher B, Fredricks D, Leisenring W et al (2004) Aspergillus galactomannan enzyme immunoassay and quantitative PCR for diagnosis of invasive aspergillosis with bronchoalveolar lavage fluid. J Clin Microbiol 42: 5517–5522
33. Buchheidt D, Hummel M, Schleiermacher D et al (2004) Prospective clinical evaluation of a LightCycler-mediated polymerase chain reaction assay, a nested-PCR assay and a galactomannan enzyme-linked immunosorbent assay for detection of invasive aspergillosis in neutropenic cancer patients and haematological stem cell transplant recipients. Br J Haematol 125:196–202
34. Kawazu M, Kanda Y, Nannya Y et al (2004) Prospective comparison of the diagnostic potential of real-time PCR, double-sandwich enzyme-linked immunosorbent assay for galactomannan, and a (1→3)-beta-D-glucan test in weekly screening for invasive aspergillosis in patients with hematological disorders. J Clin Microbiol 42:2733–2741
35. White PL, Linton CJ, Perry MD et al (2006) The evolution and evaluation of a whole blood polymerase chain reaction assay for the detection of invasive aspergillosis in hematology

patients in a routine clinical setting. Clin Infect Dis 42:479–486

36. White PL, Mengoli C, Bretagne S et al (2011) Evaluation of Aspergillus PCR protocols for testing serum specimens. J Clin Microbiol 49:3842–3848
37. Kim SH, Park C, Kwon EY et al (2012) Real-time nucleic acid sequence-based amplification to predict the clinical outcome of invasive aspergillosis. J Korean Med Sci 27:10–15
38. Kurosawa M, Yonezumi M, Hashino S et al (2012) Epidemiology and treatment outcome of invasive fungal infections in patients with hematological malignancies. Int J Hematol 96:748–757
39. Reichenberger F, Habicht J, Matt P et al (1999) Diagnostic yield of bronchoscopy in histologically proven invasive pulmonary aspergillosis. Bone Marrow Transplant 24:1195–1199
40. Tuon FF (2007) A systematic literature review on the diagnosis of invasive aspergillosis using polymerase chain reaction (PCR) from bronchoalveolar lavage clinical samples. Rev Iberoam Micol 24:89–94
41. Jones ME, Fox AJ, Barnes AJ et al (1998) PCR-ELISA for the early diagnosis of invasive pulmonary aspergillus infection in neutropenic patients. J Clin Pathol 51:652–656
42. Hebart H, Loffler J, Reitze H et al (2000) Prospective screening by a panfungal polymerase chain reaction assay in patients at risk for fungal infections: implications for the management of febrile neutropenia. Br J Haematol 111:635–640
43. Avni T, Levy I, Sprecher H et al (2012) Diagnostic accuracy of PCR alone compared to galactomannan in bronchoalveolar lavage fluid for diagnosis of invasive pulmonary aspergillosis: a systematic review. J Clin Microbiol 50:3652–3658
44. Hebart H, Loffler J, Meisner C et al (2000) Early detection of aspergillus infection after allogeneic stem cell transplantation by polymerase chain reaction screening. J Infect Dis 181:1713–1719
45. Cuenca-Estrella M, Meije Y, Diaz-Pedroche C et al (2009) Value of serial quantification of fungal DNA by a real-time PCR-based technique for early diagnosis of invasive Aspergillosis in patients with febrile neutropenia. J Clin Microbiol 47:379–384
46. Florent M, Katsahian S, Vekhoff A et al (2006) Prospective evaluation of a polymerase chain reaction-ELISA targeted to *Aspergillus fumigatus* and *Aspergillus flavus* for the early diagnosis of invasive aspergillosis in patients with hematological malignancies. J Infect Dis 193:741–747
47. Meyer MH, Letscher-Bru V, Jaulhac B et al (2004) Comparison of mycosis IC/F and plus aerobic/F media for diagnosis of fungemia by the bactec 9240 system. J Clin Microbiol 42:773–777
48. Lau A, Halliday C, Chen SC et al (2010) Comparison of whole blood, serum, and plasma for early detection of candidemia by multiplex-tandem PCR. J Clin Microbiol 48:811–816
49. Avni T, Leibovici L, Paul M (2011) PCR diagnosis of invasive candidiasis: systematic review and meta-analysis. J Clin Microbiol 49:665–670
50. Shepard JR, Addison RM, Alexander BD et al (2008) Multicenter evaluation of the *Candida albicans/Candida glabrata* peptide nucleic acid fluorescent in situ hybridization method for simultaneous dual-color identification of *C. albicans* and *C. glabrata* directly from blood culture bottles. J Clin Microbiol 46:50–55
51. Lau A, Sorrell TC, Lee O et al (2008) Colony multiplex-tandem PCR for rapid, accurate identification of fungal cultures. J Clin Microbiol 46:4058–4060
52. Metwally L, Hogg G, Coyle PV et al (2007) Rapid differentiation between fluconazole-sensitive and -resistant species of Candida directly from positive blood-culture bottles by real-time PCR. J Med Microbiol 56:964–970
53. Dunyach C, Bertout S, Phelipeau C et al (2008) Detection and identification of *Candida* spp. in human serum by LightCycler real-time polymerase chain reaction. Diagn Microbiol Infect Dis 60:263–271
54. Innings A, Ullberg M, Johansson A et al (2007) Multiplex real-time PCR targeting the RNase P RNA gene for detection and identification of *Candida* species in blood. J Clin Microbiol 45:874–880
55. White PL, Shetty A, Barnes RA (2003) Detection of seven *Candida* species using the Light-Cycler system. J Med Microbiol 52:229–238
56. Spiess B, Seifarth W, Hummel M et al (2007) DNA microarray-based detection and identification of fungal pathogens in clinical samples from neutropenic patients. J Clin Microbiol 45:3743–3753
57. Westh H, Lisby G, Breysse F et al (2009) Multiplex real-time PCR and blood culture for identification of bloodstream pathogens in patients with suspected sepsis. Clin Microbiol Infect 15:544–551
58. Mallus F, Martis S, Serra C et al (2013) Usefulness of capillary electrophoresis-based

multiplex PCR assay for species-specific identification of *Candida* spp. J Microbiol Methods 92:150–152

59. Loeffler J, Dorn C, Hebart H et al (2003) Development and evaluation of the nuclisens basic kit NASBA for the detection of RNA from *Candida* species frequently resistant to antifungal drugs. Diagn Microbiol Infect Dis 45:217–220
60. Morrell M, Fraser VJ, Kollef MH (2005) Delaying the empiric treatment of candida bloodstream infection until positive blood culture results are obtained: a potential risk factor for hospital mortality. Antimicrob Agents Chemother 49:3640–3645
61. Klingspor L, Jalal S (2006) Molecular detection and identification of *Candida* and *Aspergillus* spp. from clinical samples using real-time PCR. Clin Microbiol Infect 12:745–753
62. Erdstein AA, Daas P, Bradstock KF et al (2004) Tuberculosis in allogeneic stem cell transplant recipients: still a problem in the 21st century. Transplant Infect Dis J Transplant Soc 6:142–146
63. de la Cámara R, Martino R, Granados E et al (2000) Tuberculosis after hematopoietic stem cell transplantation: incidence, clinical characteristics and outcome. Spanish Group on Infectious Complications in Hematopoietic Transplantation. Bone Marrow Transplant 26:291–298
64. Maeda T, Kusumi E, Kami M et al (2005) Disseminated tuberculosis following reduced-intensity cord blood transplantation for adult patients with hematological diseases. Bone Marrow Transplant 35:91–97
65. Biral E, Faraci M, Lanino E et al (2012) Mycobacterium tuberculosis pneumonia and bacteremia after allogeneic hematopoietic stem cell transplant: report of an instructive pediatric case. New Microbiol 35:353–357
66. Gea-Banacloche J, Masur H, Arns da Cuhna C et al (2009) Guidelines for preventing infectious complications among hematopoietic cell transplantation recipients: a global perspective. In: Tomblyn M, Chiller T, Einsele H et al (eds) Biology of blood and marrow transplantation: journal of the American Society for Blood and Marrow Transplantation, pp 37–45
67. Akan H, Arslan O, Akan OA (2006) Tuberculosis in stem cell transplant patients. J Hospit Infect 62:421–426
68. Russo RL, Dulley FL, Suganuma L et al (2010) Tuberculosis in hematopoietic stem cell transplant patients: case report and review of the literature. Int J Infect Dis IJID Int Soc Infect Dis 14:187–191
69. De Assis RA, Kerbauy FR, Rodrigues M et al (2009) Mycobacterium tuberculosis infection: a rare late complication after cord blood hematopoietic SCT. Bone Marrow Transplant 43:667–668
70. Shima T, Yoshimoto G, Miyamoto T et al (2009) Disseminated tuberculosis following second unrelated cord blood transplantation for acute myelogenous leukemia. Transplant Infect Dis J Transplant Soc 11:75–77
71. Doucette K, Fishman JA (2004) Nontuberculous mycobacterial infection in hematopoietic stem cell and solid organ transplant recipients. Clin Infect Dis Infect Dis Soc Am 38:1428–1439
72. Weinstock DM, Feinstein MB, Sepkowitz KA et al (2003) High rates of infection and colonization by nontuberculous mycobacteria after allogeneic hematopoietic stem cell transplantation. Bone Marrow Transplant 31:1015–1021
73. Gaviria JM, Garcia PJ, Garrido SM et al (2000) Nontuberculous mycobacterial infections in hematopoietic stem cell transplant recipients: characteristics of respiratory and catheter-related infections. Biol Blood Marrow Transplant 6:361–369
74. Razonable RR (2009) Nontuberculous mycobacterial infections after transplantation: a diversity of pathogens and clinical syndromes. Transplant Infect Dis J Transplant Soc 11:191–194
75. Nicholson O, Feja K, LaRussa P et al (2006) Nontuberculous mycobacterial infections in pediatric hematopoietic stem cell transplant recipients: case report and review of the literature. Pediatr Infect Dis J 25:263–267
76. WHO (2012) Global tuberculosis report 2012. World Health Organization
77. Nyendak MR, Lewinsohn DA, Lewinsohn DM (2009) New diagnostic methods for tuberculosis. Curr Opin Infect Dis 22:174–182
78. Lawn SD, Zumla AI (2011) Tuberculosis. Lancet 378:57–72
79. Forbes B (2011) Molecular detection and characterization of Mycobacterium tuberculosis. In: Persing DH, Tenover FC, Tang Y-W et al (eds) Molecular microbiology: diagnostic principles and practices. American Society for Microbiology, New Hampshire, MA, pp 415–436
80. Griffith DE, Aksamit T, Brown-Elliott BA et al (2007) An official ATS/IDSA statement: diagnosis, treatment, and prevention of nontuberculous mycobacterial diseases. Am J Respir Crit Care Med 175:367–416
81. Boehme CC, Nabeta P, Henostroza G et al (2007) Operational feasibility of using loop-mediated isothermal amplification for diagnosis of pulmonary tuberculosis in microscopy centers of developing countries. J Clin Microbiol 45:1936–1940

82. CDC Laboratories (2011) CDC|TB| report of an expert consultation on the uses of nucleic acid amplification tests for the diagnosis of tuberculosis. http://www.cdc.gov/tb/publications/guidelines/amplification_tests/default.htm. Accessed 14 Jan 2013
83. WHO (2008) WHO library cataloguing-in-publication data: new laboratory diagnostic tools for tuberculosis control. http://www.finddiagnostics.org/resource-centre/reports_brochures/laboratory-diagnostic-tools-tuberculosis-control.html. Accessed 15 Jan 2013
84. Kocagöz T, Yilmaz E, Ozkara S et al (1993) Detection of *Mycobacterium tuberculosis* in sputum samples by polymerase chain reaction using a simplified procedure. J Clin Microbiol 31:1435–1438
85. Chakravorty S, Pathak D, Dudeja M et al (2006) PCR amplification of shorter fragments from the devR (Rv3133c) gene significantly increases the sensitivity of tuberculosis diagnosis. FEMS Microbiol Lett 257:306–311
86. Sarmiento OL, Weigle KA, Alexander J et al (2003) Assessment by meta-analysis of PCR for diagnosis of smear-negative pulmonary tuberculosis. J Clin Microbiol 41:3233–3240
87. Greco S, Rulli M, Girardi E et al (2009) Diagnostic accuracy of in-house PCR for pulmonary tuberculosis in smear-positive patients: meta-analysis and metaregression. J Clin Microbiol 47:569–576
88. Takahashi T, Tamura M, Takasu T (2012) The PCR-based diagnosis of central nervous system tuberculosis: up to date. Tuberculosis Res Treat 2012:831292
89. Cheng VCC, Yew WW, Yuen KY (2005) Molecular diagnostics in tuberculosis. Eur J Clin Microbiol Infect Dis Eur Soc Clin Microbiol 24:711–720
90. Pfyffer GE (1999) Nucleic acid amplification for mycobacterial diagnosis. J Infect 39:21–26
91. Flores LL, Pai M, Colford JM Jr et al (2005) In-house nucleic acid amplification tests for the detection of Mycobacterium tuberculosis in sputum specimens: meta-analysis and meta-regression. BMC Microbiol 5:55
92. Daley P, Thomas S, Pai M (2007) Nucleic acid amplification tests for the diagnosis of tuberculous lymphadenitis: a systematic review. Int J Tuberculosis Lung Dis J Int Union Tuberculosis Lung Dis 11:1166–1176
93. Palomino JC (2009) Molecular detection, identification and drug resistance detection in Mycobacterium tuberculosis. FEMS Immunol Med Microbiol 56:103–111
94. Chakravorty S, Sen MK, Tyagi JS (2005) Diagnosis of extrapulmonary tuberculosis by smear, culture, and PCR using universal sample processing technology. J Clin Microbiol 43:4357–4362
95. Chakravorty S, Tyagi JS (2005) Novel multipurpose methodology for detection of mycobacteria in pulmonary and extrapulmonary specimens by smear microscopy, culture, and PCR. J Clin Microbiol 43:2697–2702
96. Kumar M, Sharma S, Ram AB et al (2010) Efficient mycobacterial DNA extraction from clinical samples for early diagnosis of tuberculosis. Int J Tuberculosis Lung Dis J Int Union Tuberculosis Lung Dis 14:847–851
97. Pai M, Flores LL, Hubbard A et al (2004) Nucleic acid amplification tests in the diagnosis of tuberculous pleuritis: a systematic review and meta-analysis. BMC Infect Dis 4:6
98. Pai M, Flores LL, Pai N et al (2003) Diagnostic accuracy of nucleic acid amplification tests for tuberculous meningitis: a systematic review and meta-analysis. Lancet Infect Dis 3:633–643
99. Pai M, Ling DI (2008) Rapid diagnosis of extrapulmonary tuberculosis using nucleic acid amplification tests: what is the evidence? Future Microbiol 3:1–4
100. Greco S, Girardi E, Navarra A et al (2006) Current evidence on diagnostic accuracy of commercially based nucleic acid amplification tests for the diagnosis of pulmonary tuberculosis. Thorax 61:783–790
101. Parsons LM, Somoskövi A, Gutierrez C et al (2011) Laboratory diagnosis of tuberculosis in resource-poor countries: challenges and opportunities. Clin Microbiol Rev 24:314–350
102. Lawn SD, Zumla AI (2012) Diagnosis of extrapulmonary tuberculosis using the Xpert(®) MTB/RIF assay. Expert Rev Anti Infect Ther 10:631–635
103. Piersimoni C, Bornigia S, Gherardi G (2012) Performance of a commercial nucleic acid amplification test with extrapulmonary specimens for the diagnosis of tuberculosis. Eur J Clin Microbiol Infect Dis Eur Soc Clin Microbiol 31:287–293
104. Ginocchio CC (2011) Strengths and weaknesses of FDA-approved/cleared diagnostic devices for the molecular detection of respiratory pathogens. Clin Infect Dis Infect Dis Soc Am 52(Suppl 4):S312–S325
105. Piersimoni C, Scarparo C (2003) Relevance of commercial amplification methods for direct detection of Mycobacterium tuberculosis complex in clinical samples. J Clin Microbiol 41:5355–5365
106. Neonakis IK, Spandidos DA, Petinaki E (2011) Use of loop-mediated isothermal amplification of DNA for the rapid detection

of Mycobacterium tuberculosis in clinical specimens. Eur J Clin Microbiol Infect Dis Eur Soc Clin Microbiol 30:937–942

107. Ling DI, Flores LL, Riley LW et al (2008) Commercial nucleic-acid amplification tests for diagnosis of pulmonary tuberculosis in respiratory specimens: meta-analysis and meta-regression. PLoS One 3:e1536
108. WHO (2010) WHO | Multidrug and extensively drug-resistant TB (M/XDR-TB): 2010 global report on surveillance and response. http://www.who.int/tb/publications/2010/978924599191/en/index.html. Accessed 15 Jan 2013
109. O'Grady J, Maeurer M, Mwaba P et al (2011) New and improved diagnostics for detection of drug-resistant pulmonary tuberculosis. Curr Opin Pulmonary Med 17:134–141
110. Ling DI, Zwerling AA, Pai M (2008) GenoType MTBDR assays for the diagnosis of multidrug-resistant tuberculosis: a meta-analysis. Eur Respir J Eur Soc Clin Respir Physiol 32:1165–1174
111. Morgan M, Kalantri S, Flores L et al (2005) A commercial line probe assay for the rapid detection of rifampicin resistance in Mycobacterium tuberculosis: a systematic review and meta-analysis. BMC Infect Dis 5:62
112. Crudu V, Stratan E, Romancenco E et al (2012) First evaluation of an improved assay for molecular genetic detection of tuberculosis as well as rifampin and isoniazid resistances. J Clin Microbiol 50:1264–1269
113. WHO (2008) Molecular line probe assays for rapid screening of patients at risk of multidrug-resistant tuberculosis (MDR-TB). www.who.int/tb/features_archive/policy_statement.pdf. Accessed 15 Jan 2013
114. Lawn SD, Nicol MP (2011) Xpert® MTB/RIF assay: development, evaluation and implementation of a new rapid molecular diagnostic for tuberculosis and rifampicin resistance. Future Microbiol 6:1067–1082
115. WHO (2010) Roadmap for rolling out Xpert MTB/RIF for rapid diagnosis of TB and MDR-TB. http://www.who.int/tb/laboratory/roadmap_xpert_mtb-rif.pdf. Accessed 15 Jan 2013
116. Helb D, Jones M, Story E et al (2010) Rapid detection of Mycobacterium tuberculosis and rifampin resistance by use of on-demand, near-patient technology. J Clin Microbiol 48: 229–237
117. Boehme CC, Nicol MP, Nabeta P et al (2011) Feasibility, diagnostic accuracy, and effectiveness of decentralised use of the Xpert MTB/RIF test for diagnosis of tuberculosis and multidrug resistance: a multicentre implementation study. Lancet 377:1495–1505
118. Scott LE, McCarthy K, Gous N et al (2011) Comparison of Xpert MTB/RIF with other nucleic acid technologies for diagnosing pulmonary tuberculosis in a high HIV prevalence setting: a prospective study. PLoS medicine 8:e1001061
119. Williams KJ, Ling CL, Jenkins C et al (2007) A paradigm for the molecular identification of Mycobacterium species in a routine diagnostic laboratory. J Med Microbiol 56:598–602
120. Slany M, Pavlik I (2012) Molecular detection of nontuberculous mycobacteria: advantages and limits of a broad-range sequencing approach. J Mol Microbiol Biotechnol 22: 268–276
121. Altclas J, Lescano A, Salgueira C et al (2005) Multidrug-resistant tuberculosis in bone marrow transplant recipient. Transplant Infect Dis J Transplant Soc 7:45–46
122. Hummel M, Spiess B, Roder J et al (2009) Detection of *Aspergillus* DNA by a nested PCR assay is able to improve the diagnosis of invasive aspergillosis in paediatric patients. J Med Microbiol 58:1291–1297
123. Scotter JM, Chambers ST (2005) Comparison of galactomannan detection, PCR-enzyme-linked immunosorbent assay, and real-time PCR for diagnosis of invasive aspergillosis in a neutropenic rat model and effect of caspofungin acetate. Clin Diagn Lab Immunol 12: 1322–1327
124. Kent P, Kubica G (1985) Public health microbiology: a guide for the level III laboratory. Centers for Disease Control, Atlanta, GA
125. Belisle JT, Mahafey SB, Preston J (2008) Isolation of *Mycobacterium* species genomic DNA. In: Parish T, Brown AC (eds) Mycobacteria protocols. Humana Press, Totowa, NJ, pp 1–13
126. Khan IUH, Yadav JS (2004) Development of a single-tube, cell lysis-based, genus-specific PCR method for rapid identification of mycobacteria: optimization of cell lysis, PCR primers and conditions, and restriction pattern analysis. J Clin Microbiol 42:453–457
127. Eisenach KD, Cave MD, Bates JH et al (1990) Polymerase chain reaction amplification of a repetitive DNA sequence specific for Mycobacterium tuberculosis. J Infect Dis 161:977–981
128. Schewe C, Goldmann T, Grosser M et al (2005) Inter-laboratory validation of PCR-based detection of *Mycobacterium tuberculosis* in formalin-fixed, paraffin-embedded tissues. Virchows Archiv Int J Pathol 447:573–585
129. Standards NCCL, Woods GL (2000) Susceptibility testing mycobacteria, nocardia, and other aerobic actinomycetes. Tentative standard. NCCLS

# Chapter 14

# Post-transplant Monitoring of Chimerism by Lineage-Specific Analysis

**Sandra Preuner and Thomas Lion**

## Abstract

Molecular surveillance of hematopoietic chimerism is an important part of the routine diagnostic program in patients after allogeneic stem cell transplantation. Chimerism testing permits early prediction and documentation of successful engraftment and facilitates early risk assessment of impending graft rejection. In patients transplanted for treatment of malignant hematologic disorders, monitoring of chimerism can provide an early indication of incipient disease relapse. The investigation of chimerism has therefore become an indispensable tool for the management of patients during the post-transplant period. Increasing use of reduced-intensity conditioning, which is associated with prolonged duration of mixed hematopoietic chimerism, has further increased the clinical importance of chimerism analysis. At present, the most commonly used technical approach to the investigation of chimerism is microsatellite analysis by polymerase chain reaction. The investigation of chimerism within specific leukocyte subsets isolated from peripheral blood or bone marrow samples by flow sorting- or magnetic bead-based techniques provides more specific information on processes underlying the dynamics of donor/recipient chimerism. Moreover, cell subset-specific analysis permits the assessment of impending complications at a significantly higher sensitivity, thus providing a basis for earlier treatment decisions.

**Key words** Chimerism, Microsatellites, Leukocyte subsets, Flow sorting, Graft rejection, Relapse

## 1 Introduction

Investigation of donor- and recipient-derived hemopoiesis (chimerism) by molecular techniques facilitates the monitoring of engraftment kinetics in patients after allogeneic stem cell transplantation (allo-HSCT). The increasing employment of reduced-intensity conditioning (RIC) regimens and cord blood transplants, which require very careful surveillance of the graft, has further reinforced the clinical importance of chimerism testing. The analysis of chimerism in peripheral blood (PB) during the immediate post-transplant period permits early assessment of successful engraftment or graft failure [1, 2]. The risk of graft rejection is particularly high in patients transplanted with T-cell-depleted grafts, and the surveillance of NK- and T-cell chimerism can provide timely indication of

Meral Beksaç (ed.), *Bone Marrow and Stem Cell Transplantation*, Methods in Molecular Biology, vol. 1109,
DOI 10.1007/978-1-4614-9437-9_14, 

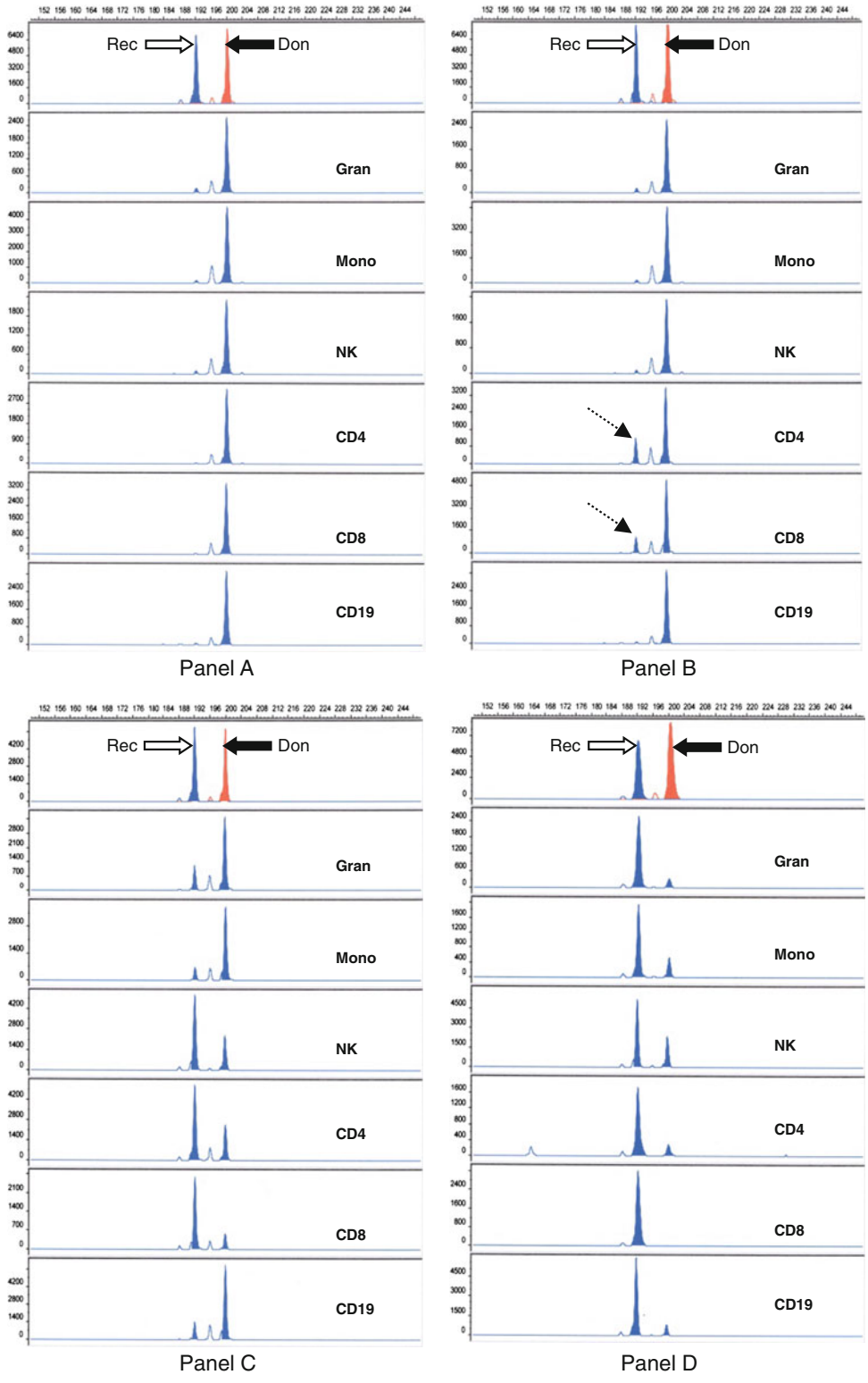


**Fig. 1** Detection of impending graft rejection by lineage-specific chimerism analysis. The *panels A–D* represent sequential time points of lineage-specific chimerism testing in a patient who ultimately rejected the allograft. *Panel A* reveals the presence of virtually pure donor chimerism in all leukocyte subsets analyzed, at the level

impending allograft rejection [3–7]. In patients undergoing allogeneic stem cell transplantation for the treatment of leukemia, impending disease recurrence can be indicated by an increasing proportion of recipient-derived cells [4, 8, 9]. Polymerase chain reaction (PCR)-based chimerism assays analyzing highly polymorphic microsatellite (short tandem repeat) markers permit the detection of residual autologous cells with a sensitivity of about 1 % [10–15]. When investigating chimerism in total leukocyte preparations from PB, this level of sensitivity may not be sufficient to allow early assessment of impending complications. It is possible to overcome this problem by investigating chimerism in specific leukocyte subsets of interest isolated by flow sorting or by immunomagnetic bead separation. Since residual recipient-derived cells can be detected within the individual leukocyte fractions with similar sensitivity, it is possible to identify and monitor minor autologous populations that escape detection in total PB leukocyte samples. The overall sensitivity of chimerism assays achievable by investigating specifically enriched leukocyte subsets is in a range of 0.1–0.01 % [4], i.e., one to two logs higher than analysis of total leukocyte preparations.

### *1.1 Risk Assessment of Graft Rejection by the Monitoring of Chimerism Within Specific Lymphocyte Subsets*

Patients who receive RIC reveal persisting leukocytes of recipient genotype more commonly than patients after myeloablative conditioning. The higher incidence of mixed or recipient chimerism may be attributable both to cells of myeloid and lymphoid lineages [3]. In patients who receive T-cell-depleted grafts, there is a strong correlation with the presence of mixed or recipient chimerism within T-cells (CD3+) and NK-cells (CD56+). Detection of mixed chimerism within lymphocyte populations is associated with an increased risk of late rejection [3, 4]. In most instances, serial analysis reveals a persistently high or an increasing recipient-specific allelic pattern prior to overt graft rejection [3, 4, 8] (Fig. 1). The correlation between the observation of mixed or recipient chimerism and graft rejection was shown to be higher for NK-cells than

**Fig. 1** (continued) of sensitivity achievable by the technique used (*see* **Notes 6**, **9**, **18**). In *panel B*, mixed chimerism appears in CD4 and CD8 lymphocyte subsets (*dotted arrows*), while (nearly) complete donor chimerism is present in all other populations tested. *Panel C* reveals the predominance of autologous cells within the CD4, CD8, and NK cell subsets, and all other fractions show a small proportion of recipient-derived cells. This constellation is highly suggestive of imminent graft rejection. Finally, *panel D* documents autologous recovery in all cell populations, with minor proportions of residual donor cells in some fractions. Don: donor-specific allele, indicated by *black arrow*; Rec: recipient-specific allele, indicated by *white arrow*. In this example, both donor and recipient are homozygous for the marker selected and thus display only one allele, respectively. *Gran* granulocytes, *Mono* monocytes, *NK* natural killer cells, *CD4* helper T-lymphocytes, *CD8* suppressor T-lymphocytes, *CD19* B-lymphocytes

for T-helper (CD3+/CD4+) or T-suppressor (CD3+/CD8+) cells [3]. Patients displaying recipient chimerism in CD56+ cells between days +14 and +35 appear to have an extremely high risk of graft rejection. By contrast, virtually all patients who experience late graft rejection show pure donor genotype within the myeloid (CD14+ and CD15+) cell compartment during the same period [3]. Hence, the observation of recipient chimerism within the CD56+ and CD3+ cell subsets is highly predictive for the occurrence of late graft rejection. These findings underscore the importance of cell subset analysis in post-transplant chimerism testing because timely diagnosis of impending graft rejection is crucial for effective therapeutic intervention. In a recent study, the predictive potential of early leukocyte subset-specific chimerism for graft loss has been investigated in children undergoing allo-HSCT for treatment of malignant and nonmalignant diseases after reduced-intensity or myeloablative conditioning. Monitoring of lineage-specific chimerism was performed at first appearance of leukocyte counts amenable to cell sorting. The first chimerism analysis of T- and NK-cells performed at a median of 20 days after HSCT identified three different risk groups which were independent from the conditioning regimen: recipient chimerism (RC) levels in T-cells below 50 % indicated a very low risk of rejection (1.4 %), while high levels of RC (>90 %) both in T- and NK-cells were associated with graft loss in the majority of patients (90 %) despite therapeutic interventions. Recipient chimerism >50 % in T-cells and ≤90 % in NK-cells defined an intermediate-risk group in which timely immunotherapy frequently prevented rejection. Early assessment of T- and NK-cell chimerism can therefore be instrumental in the risk assessment and therapeutic management of imminent graft rejection [7].

### *1.2 Detection of Imminent Relapse by Serial Analysis of Leukemia Lineage-Specific Chimerism*

In most instances, surveillance of residual or reappearing leukemic cells after allo-HSCT is performed by leukemia- or clone-specific markers. In instances in which specific markers are not available, the exploitation of chimerism testing may be instrumental for the assessment of impending relapse. Investigation of the entire leukocyte fractions from PB has been shown to reveal reappearance of autologous cells (mixed chimerism) before the diagnosis of relapse [8], thus providing a basis for timely initiation of treatment, which may include the reduction or the withdrawal of immunosuppressive therapy or the administration of donor lymphocyte infusions (DLI). In several instances, however, analysis of chimerism within total leukocytes may not show any changes indicative of impending relapse [1, 4]. Owing to its higher sensitivity, investigation of specific leukocyte subsets derived from PB or bone marrow (BM) has a greater potential of revealing informative changes in patients who later experience hematologic relapse. These patients can reveal persistence or reappearance of autologous allelic patterns within cell

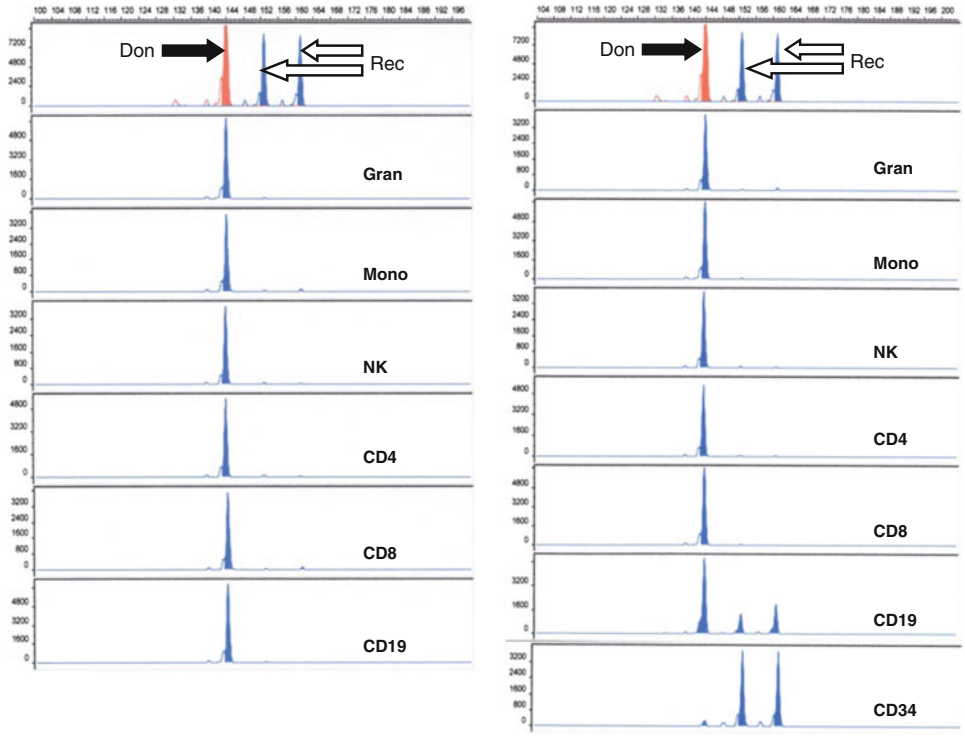


**Fig. 2** Detection of incipient relapse by lineage-specific chimerism analysis. In this example, surveillance of residual disease after allogeneic stem cell transplantation is shown for a patient with B-cell precursor acute lymphocytic leukemia. The immunophenotype of the original leukemic clone revealed co-expression of CD34 and CD19. Residual or reappearing leukemic cells are therefore expected to occur within these leukocyte fractions. The *panels A* and *B* show the investigation of different leukocyte subsets isolated by flow sorting from peripheral blood at two sequential time points. *Panel A* reveals the presence of complete donor chimerism in all leukocyte subsets analyzed, at the level of sensitivity achievable by the technique used. In *panel B*, the CD19-positive cell fraction shows mixed chimerism, indicating the reappearance of autologous cells. The CD34-positive cell population, which was not detectable at the previous time point of chimerism analysis (*panel A*), consists of recipient-derived cells. This finding is highly suggestive of reappearance of the leukemic clone. At this time point, the size of the leukemic clone may be well below the detection level of chimerism testing within total white blood cells. In instances in which a leukemia- or a clone-specific marker is available (e.g., translocation-associated gene rearrangement, immunoglobulin- or T-cell receptor rearrangement), the finding can be controlled by an independent technique. In cases in which no other informative marker is available, lineage-specific chimerism testing is the most sensitive approach to early detection of impending relapse. Don: donor-specific allele, indicated by *black arrow*; Rec: recipient-specific alleles, indicated by *white arrow*. In this example, the donor is homozygous for the marker selected and thus displays only one allele, while the recipient is heterozygous. *Gran* granulocytes, *Mono* monocytes, *NK* natural killer cells, *CD4* helper T-lymphocytes, *CD8* suppressor T-lymphocytes, *CD19* B-lymphocytes, *CD34* hematopoietic stem cells

populations expected to harbor leukemic cells, if present (Fig. 2). These cell populations can be specifically enriched for chimerism testing by targeting the original immunophenotype of the leukemic clone. The stem cell marker CD34 is commonly expressed by

the leukemic cells in combination with lineage-specific markers. For example, the leukemic clone in B-cell precursor acute lymphocytic leukemias is generally characterized by co-expression of CD34 and CD19. The cell populations expressing these markers can therefore be specifically targeted for the assessment of residual disease by monitoring the presence and the kinetics of recipient chimerism (Fig. 2). Occasionally, however, the only observation made before hematologic relapse is lineage-specific chimerism kinetics suggestive of graft rejection [4]. This observation may be attributable to the loss of the graft-versus-leukemia effect associated with rejection of the allograft.

### 1.3 Technical Aspects

Current methodological approaches to chimerism analysis are rather diverse. Despite the introduction of single-nucleotide polymorphism (SNP) and insertion/deletion (Indel) polymorphism analysis by real-time PCR for the investigation of chimerism several years ago [16–18], DNA microsatellites, also referred to as short tandem repeats (STRs), have remained the most commonly used source of polymorphic markers for quantitative assessment of donor/recipient hemopoiesis after allo-HCST. In the sex-mismatched transplant setting, fluorescence in situ hybridization (FISH) analysis of the X and Y chromosomes in interphase nuclei has been used for many years and is still regarded as a highly accurate technique for quantitative investigation of chimerism [19]. Technical approaches that can be employed regardless of the gender constellation are commonly based on molecular methods including primarily the PCR. Techniques based on PCR amplification of polymorphic DNA sequences facilitating unequivocal distinction and quantitative assessment of recipient- and donor-derived cells have been the preferred approach to chimerism testing at most centers. Amplification of STR markers by PCR coupled with fluorescence detection of the donor/recipient alleles using capillary electrophoresis has been a widely used approach to the monitoring of hematopoietic chimerism [20]. The main advantages of automated fluorescence-based detection of STR markers over the use of conventional gel electrophoresis include greater precision and easier performance of quantitative analysis, reduced manual handling of PCR products, and higher sensitivity.

### 1.4 Criteria for Optimal Selection of STR Markers for Chimerism Analysis

The accuracy and reliability of quantitative chimerism analysis in post-transplant samples are greatly affected by factors such as the homozygosity/heterozygosity of STR alleles, shared alleles between donor and recipient, and positional relationship between alleles. The *EuroChimerism (EUC)* consortium, an international collaborative group (see below), has therefore established criteria facilitating selection of STR markers eligible for quantitative chimerism testing. The EUC group has

developed a common descriptive nomenclature for allelic configurations termed the *Recipient-Shared-Donor* (RSD) code with the aim to facilitate rapid identification of STR markers displaying optimal allelic constellations for accurate and reproducible chimerism analysis [21].

### 1.5 Use of Multiplex Versus Singleplex PCR Assays for Chimerism Analysis

Multiplex PCR assays are commonly used for initial recipient/donor genotyping to select one or more informative STR markers for the subsequent monitoring of chimerism. Moreover, investigation of post-transplant peripheral blood samples with multiple STR markers may improve the reproducibility and accuracy of quantitative chimerism analysis. The accuracy of quantitative chimerism assays can be increased by testing each sample with more than one marker and calculating mean values [22]. Some investigators therefore perform clinical testing of chimerism with commercial multiplex kits facilitating co-amplification of several microsatellite markers in a single PCR [22]. However, the indicated advantages may be counterbalanced by increased costs of consumables and lower sensitivity resulting from the high number of different fragments amplified in the same reaction. Most diagnostic centers therefore rely on the use of singleplex PCR for sensitive assessment and quantitative monitoring of chimerism [23].

### 1.6 Chimerism Analysis of Specific Cell Lineages Versus Testing of Total Leukocytes

PCR-based chimerism tests analyzing highly polymorphic STR markers mostly permit the detection of residual autologous cells with a sensitivity limit in the range of 1 %. When investigating chimerism in total leukocyte preparations from PB, this level of sensitivity may not be sufficient to facilitate timely assessment of impending complications. This problem can be overcome by investigating chimerism in specific leukocyte subsets of interest isolated by flow sorting or by immunomagnetic bead separation. Since residual recipient-derived cells can be detected within the individual leukocyte fractions with similar sensitivity, it is possible to identify and monitor minor autologous populations that would escape detection in total PB leukocyte samples. Investigation of individual leukocyte fractions not only provides more specific information but also permits the assessment of impending complications at a significantly higher sensitivity [4], thus providing a basis for earlier treatment decisions.

### 1.7 Heterogeneity of Current Methods and Approaches to Standardization

The methods for STR-PCR analysis of chimerism performed in most diagnostic laboratories are based on various in-house assays. The heterogeneity of technical approaches and the diversity of STR markers used render the comparison of results generated at different centers difficult. Attempts have therefore been made to introduce a commercially available platform for chimerism testing (http://www.biotype.de) or to exploit existing commercial microsatellite kits designed for forensic purposes which, however,

**Table 1**
**EUC markers, primer sequences, fluorescence labels, and primer concentrations in singleplex reactions**

| Marker | | Sequence (5′–3′) | Fluorescence label | Primer conc. (nM) for singleplex reactions |
|---|---|---|---|---|
| D2S1360 | Fw | ctgcattaaaacattcgaaaccaa | JOE | 80 |
| | Rev | gcagcagattgtgggacttctcag | | 80 |
| D7S1517 | Fw | agcctgatcattaccaggt | JOE | 160 |
| | Rev | gtttctattggggccatcttgc | | 160 |
| D8S1132 | Fw | tctctctctccctctctctttcgag | TMR | 80 |
| | Rev | gtttgccatcttcttacctctgttggtc | | 80 |
| D9S1118 | Fw | caggatattatgtgatggaatcc | FL | 320 |
| | Rev | gatctcttctctctctctttctccc | | 80 |
| D10S2325 | Fw | tatggtgaccttaagcagccatg | JOE | 80 |
| | Rev | gtgtcttagctgagagatcacgcagtgc | | 80 |
| D11S554 | Fw | ggtatgcagagcaagactgtc | FL | 80 |
| | Rev | gtttcaccttcatcctaaggcagc | | 80 |
| D12S1064 | Fw | actactccaaggttccagcc | TMR | 160 |
| | Rev | actgttatctctcttgtggtag | | 160 |
| D12S391 | Fw | atcaacaggatcaatggatgcat | FL | 160 |
| | Rev | gggcttttagacctggactgag | | 160 |
| D17S1290 | Fw | ccaacagagcaagactgtc | FL | 80 |
| | Rev | gtttgaaacagttaaatggccaaag | | 80 |
| D19S253 | Fw | atagacagacagacggactg | FL | 160 |
| | Rev | gtttgggagtggagattacccct | | 160 |
| MYCL1 | Fw | aaccgtagcctggcgagact | FL | 160 |
| | Rev | gtttccttttaagctgcaacaaatttc | | 160 |
| P450CYP19 | Fw | gttccacataatgaagcacaatc | FL | 240 |
| | Rev | gtttaatcgcctgagtcctggga | | 240 |
| SE-33 | Fw | aatctgggcgacaagagtga | FL | 160 |
| | Rev | acatctcccctaccgctata | | 160 |

*Fw* forward, *Rw* reverse; the acronyms JOE, TMR, and FL designate green, yellow, and blue fluorescence dyes, respectively

are not optimally suited for chimerism testing [21]. To address the urgent need for a standardized technology specifically adapted to the requirements of quantitative chimerism analysis, 12 leading centers from 10 European countries have established the *EUC* consortium to perform a collaborative study supported by the European Commission within the 5th Framework Program. The primary goal of the consortium was to establish a standardized approach to quantitative chimerism testing, with the aim to facilitate harmonization of chimerism diagnostics between European centers and to provide a basis for appropriate quality control. Following extensive analysis of a large set of STR loci, the *EUC* marker panel was established. The panel comprises 13 STR markers selected to optimally meet the specific requirements of quantitative chimerism analysis (Table 1). Based on highly stringent selection criteria [21], the EUC panel provides multiple informative markers in any transplant setting. The *EUC* assay provides standardized STR-PCR tests permitting detection of donor- or recipient-derived cells with a sensitivity limit of 0.8–1.6 %. Moreover, the assay facilitates accurate and reproducible quantification of donor and recipient hematopoietic cells [23]. The EUC assay may serve as a tool for the harmonization of post-transplant monitoring between diagnostic laboratories. Its implementation in the clinical monitoring of chimerism could help eliminate the problems of heterogeneity in the currently used technical approaches and could greatly improve the comparability of data and the exchange of information between centers.

## 2 Materials

### 2.1 Purification of DNA

#### 2.1.1 DNA Extraction from Peripheral Blood or Bone Marrow

*Hardware*

1. Spectrophotometer.
2. Benchtop centrifuge.
3. Thermomixer.
4. Vortex mixer.

*Reagents*

1. Qiagen DNA Blood Mini Kit (Qiagen, Hilden, Germany).
2. Ethanol.

#### 2.1.2 DNA Extraction from Nails

Variant A: Phenol–chloroform extraction.

*Hardware*

1. Benchtop centrifuge.
2. Thermomixer.
3. Vortex mixer.

*Reagents*

1. Washing solution: 0.5 % SDS and 0.5 M NaOH.
2. $dH_2O$ (DNAase free).
3. Extraction buffer: 1× TBE, 1.4 % SDS, 0.14 M NaCl, 0.28 M dithiothreitol (DTT), and 68 μg/mL proteinase K.
4. Phenol/Chloroform/Isoamylalcohol (AppliChem, Darmstadt, Germany).
5. Chloroform/Isoamylalcohol 25:1 (AppliChem).
6. 3 M Na-Acetate, pH 5.2 (Sigma-Aldrich, St. Louis, USA).
7. Ethanol.
8. Ethanol 70 %.

Variant B: Tissue and Hair Extraction Kit with the DNA IQ™ System; Promega.

*Hardware*

1. Benchtop centrifuge.
2. Thermomixer.
3. Vortex mixer.
4. MagneSphere® Technology Magnetic Separation Stand (Promega, Madison, WI, USA).

*Reagents*

1. Tissue and Hair Extraction Kit (Promega).
2. DNA IQ™ System (Promega).
3. Nuclease-free water.
4. Ethanol.
5. Isopropyl alcohol.

Variant C: PrepFiler® Forensic DNA Extraction Kit, Life Technologies.

*Hardware*

1. Benchtop centrifuge.
2. Thermomixer.
3. Vortex mixer.
4. Magnetic separation stand.

*Reagents*

1. PrepFiler Forensic DNA Extraction Kit (Life Technologies, Carlsbad, CA).
2. Isopropyl alcohol.
3. Ethanol.
4. 1 M DTT.

#### 2.1.3 DNA Extraction from Cell Subsets Isolated by Flow Sorting

*Hardware*

1. Benchtop centrifuge.
2. Thermomixer.
3. Vortex mixer.

*Reagents*

1. Qiagen DNA Blood Mini Kit (Qiagen, Hilden, Germany).
2. Ethanol.

### 2.2 STR-PCR and Capillary Electrophoresis with Fluorescence-Assisted Detection

*Hardware*

1. PCR cycler (e.g., GeneAmp® PCR system 2400 or 9600; Applied Biosystems (ABI), Foster City, USA).
2. Benchtop centrifuge.
3. Vortex mixer.
4. Capillary electrophoresis instrument (e.g., ABI 310/ABI 3100-Avant, ABI 3130 Genetic Analyzer, ABI).

*Reagents and solutions*

1. Genomic DNA.
2. Amplitaq Gold® DNA Polymerase Buffer II (10×, ABI).
3. 25 mM $MgCl_2$ (ABI).
4. dNTPs (Promega).
5. STR-locus-specific primers (forward or reverse primer labelled with a fluorescence dye (FL, JOE, or TMR) (see Tables 1 and 2).
6. Amplitaq Gold® DNA Polymerase (ABI).
7. Hi-Di™ Formamide (ABI).
8. Internal Lane Standard (ILS) 600 (Promega).

Consumables for capillary electrophoresis on the ABI310/ABI 3100-Avant/ABI 3130 Genetic Analyzer:

1. Running buffer as specified by the manufacturer for the instrument used (ABI).
2. Pop-4® Polymer for the 310 Genetic Analyzer, Pop-4® Polymers for the 3100/3100-Avant Genetic Analyzer, or POP-7 Polymer for 3130/3130 XL Genetic Analyzers (ABI).
3. 310 Genetic Analyzer Capillary 47 cm (36 cm WTR) or 3130/3100-Avant Genetic Analyzer Capillary Array 36 cm (ABI).

**Table 2**
**EUC multiplex panels**

| | Concentrations (nM) | FL | JOE | TMR |
|---|---|---|---|---|
| Group 1 | | | | |
| D9S1118 | [a] | 92–128 | | |
| MYCL1 | 240 | 156–225 | | |
| D7S1517 | 200 | | 164–212 | |
| D11S554 | 400 | | | 166–246 |
| D8S1132 | 400 | | | 347–379 |
| Group 2 | | | | |
| D10S2325 | 360 | 163–213 | | |
| D12S391 | 480 | 220–269 | | |
| P450CYP19 | 800 | 304–454 | | |
| D2S1360 | 800 | | 213–253 | |

The abbreviations FL (blue), JOE (green), and TMR (yellow) indicate the fluorescent dyes used for labelling of the forward or the reverse primer. The numbers below the fluorescent dyes show the respective range of PCR product lengths. The most informative STR marker SE33 could not be included in the multiplex panels for technical reasons. Hence, if desired or required for initial genotyping, this marker has to be tested in a separate singleplex reaction (*see* Table 2)
[a]D9S1118 asymmetric PCR: fw primer 320 nM and rev primer 80 nM

## 3 Methods

### *3.1 Purification of DNA*

#### *3.1.1 DNA Extraction from Peripheral Blood or Bone Marrow (See **Note 1**)*

- Use Qiagen DNA Blood Mini Kit according to the manufacturer's recommendations.
- Quantify DNA yield by spectrophotometry.
- Use 10 ng of DNA as template in individual PCR reactions.

#### *3.1.2 DNA Extraction from Nails (See **Note 2**)*

Variant A: Phenol–chloroform extraction method:

- Collect nail clippings from one to ten fingers (or toes).
- Place the nail sample in a 1.5 mL Eppendorf tube.
- Add an appropriate amount of washing solution, and cover the nails.
- Vortex briefly.
- Pulse spin (Eppendorf centrifuge, maximum speed).
- Aspirate washing solution.
- Add ~1 mL $dH_2O$.

- Vortex briefly.
- Pulse spin.
- Aspirate $dH_2O$.
- Repeat last four steps.
- Add 600 µL extraction buffer.
- Incubate sample at 56 °C overnight (or over the weekend, if convenient).
- Upon complete (or partial) digestion of the nails, extract the DNA using standard phenol/chloroform extraction and ethanol precipitation.

Variant B: Tissue and Hair Extraction Kit with DNA IQ™ System; Promega.

The kits are applied according to the manufacturer's recommendations.

Variant C: PrepFiler® Forensic DNA Extraction Kit, Life Technologies.

The kit is used according to the manufacturer's recommendations.

*3.1.3 DNA Extraction from Flow-Sorted Cell Subsets (See **Note 3**)*

- Resuspend flow-sorted cells with 200 µL PBS.
- Add 20 µL protease.
- Add 200 µL AL buffer.
- Vortex for 15 s.
- Incubate at 70 °C for 30 min.
- Pulse spin.
- Add 210 µL ethanol.
- Vortex briefly.
- Pulse spin.
- Apply the solution to the spin column.
- Centrifuge and wash sample according to the standard Qiagen protocol.
- Collect DNA with 130 µL of elution buffer (*see* **Note 4**).

### *3.2 STR-PCR and Capillary Electrophoresis with Fluorescence-Assisted Detection for Chimerism Analysis (See Note 5)*

Set up both PCR reactions (group 1 and group 2) in a total volume of 50 µL as follows:

dNTPs 800 µM.

$MgCl_2$ 2 mM.

AmpliTaq Gold® 5 U.

10× PCR buffer II (ABI).

10 ng genomic DNA of each recipient and donor.

*3.2.1 Multiplex Analysis for the Selection of Informative Maker(s) (See **Notes 11, 15–18**)*

For primer concentrations see Table 2.

The amplification program is identical to that recommended for the PP16® kit on different instruments.

### 3.2.2 Singleplex Analysis for Post-transplant Monitoring of Chimerism

Set up the PCR reaction in a total volume of 25 µL as follows:

dNTPs 400 µM.

$MgCl_2$ 2 mM.

AmpliTaq Gold® 1 U.

10× PCR buffer II (AB).

18.6 µL DNA extracted from flow-sorted cell subsets (*see* **Note 6**).

For primer concentrations see Table 1.

The amplification program is identical to that recommended for the PP16® kit on different instruments, using 22 cycles during the second phase of amplification being the only difference (*see* **Note 7**).

- Prepare PCR products for loading onto the capillary electrophoresis apparatus by setting up the following mixture:

  24 µL HiDi Formamide.

  1 µL ILS 600.

  1.0 µL PCR product.
- Denature the mixture by incubation at 95 °C for 2 min and cool to 4 °C.
- Load the samples to ABI 310/3100-Avant/3130 Genetic Analyzer according to the manufacturer's recommendations.
- Adjust the electrophoresis time ("run time") according to the length of the analyzed PCR products (*see* **Note 8**).
- To obtain max. peak heights but not "off-scale" peaks choose the appropriate injection time and voltage (*see* **Note 9**).
- Apply the GeneScan/GeneMapper software (supplied with ABI310/3100/3130 apparatus) to analyze the results.
- Use the height (or area) of individual peaks to calculate donor/recipient chimerism by employing the formulas indicated below (*see* **Note 10**).

Commonly encountered problems and recommended measures are outlined in **Notes 11–18**.

Microsatellites for initial genotyping and selection of markers for the follow-up of chimerism are described in Table 2 and **Notes 11**, **15–18**.

## 4 Notes

1. Capillary electrophoresis-based PCR product analysis is sensitive to variations in DNA template quality. It is necessary therefore to use isolation protocols yielding high-quality DNA in

order to obtain reproducible results and satisfactory sensitivity. DNA isolation kits (e.g., from Qiagen) have proven to be adequate for this application.

2. Initial genotyping for the detection of informative STR loci is usually performed using PB from the recipient and PB or BM from the donor. In some instances, no cell material is available from the allograft recipient before transplantation. To identify an appropriate genetic marker for the monitoring of chimerism, assessment of the patient's genotype is necessary, but PB can no longer be used due to the presence of donor cells. We have tested cell material from different sources to identify patient-specific genetic fingerprints. Epithelial cells derived from the oral mucosa or from the skin may contain donor leukocytes. In fact, buccal swabs were demonstrated to contain granulocytes of donor origin already during the first days after SCT, before they were detected in PB [24] (and own unpublished observations). The same applies to cells isolated from urinary sediment. Hair provides a reliable source of endogenous DNA but may not be available in patients after several courses of chemotherapy. Nail clippings were found to be an ideal source of patient DNA in this setting. They are readily available in all patients, and sufficient quantities of good-quality DNA adequate for PCR genotyping can be obtained.
3. The amount of cells within individual fractions isolated by flow sorting ranges mostly between 2,000 and 10,000 but may occasionally be as low as a few hundred. A technique permitting efficient DNA extraction from small cell numbers is therefore required. We try to obtain 4,000 cells per cell fraction in order to have sufficient amounts of DNA for PCR analysis. The use of a modified protocol for the Qiagen DNA Blood Mini Kit provides very pure DNA, and the yields are sufficient for subsequent PCR.
4. The volume of elution buffer should be kept low in order to provide DNA concentrations adequate for subsequent PCR analysis. The eluate can be re-applied to the spin column in order to increase the DNA yield. Alternatively, if the yields do not provide sufficient amounts of DNA for PCR analysis, addition of a carrier to the cell lysate prior to application to the spin column may be warranted.
5. The employment of capillary electrophoresis instruments requires less hands-on time than the formerly used conventional gel electrophoresis due to the automated loading and electrophoresis of samples as well as the measurement of fluorescence signals. However, the capacity of devices with a single capillary and an average electrophoresis time of 20–30 min per sample may be a limiting factor for sample throughput.

The efficiency can be improved by loading PCR products of different chimerism assays onto the capillary and analyzing all fragments in the same run. This can be done when primers for amplification of various microsatellite loci are labelled with different dyes, thus permitting easy identification of the products after electrophoresis [22]. These considerations are of relevance at major diagnostic centers, where high sample throughput is required, and the implementation of instruments with multiple capillaries permitting simultaneous analysis of several samples is preferable.

6. The amount of template DNA in the PCR reactions can play a role in the achievable sensitivity of the assay. Most investigators use 50–100 ng of template (corresponding to about $7.5 \times 10^3$–$15 \times 10^3$ diploid human cells), a quantity readily available when analyzing chimerism within the entire white blood cell population. In such instances, it is feasible to reproducibly detect residual recipient cell subsets in the range of 1 % (i.e., about 100 cells). This level of sensitivity may not be readily achievable, however, when specific white blood cell fractions isolated by flow sorting or by magnetic bead separation are investigated. In these instances, only small cell numbers are available for DNA isolation yielding no more than 1–30 ng of DNA (corresponding to about $1.5 \times 10^2$–$4.5 \times 10^3$ cells). Although 1 % sensitivity (equivalent to detecting about 45 cells or less) can be reached even in this experimental setting, it is more common to achieve sensitivities around 3–5 %. Despite the slightly decreased sensitivity of assays using low cell numbers as starting material, the overall sensitivity in detecting minor autologous cell fractions within specifically enriched leukocyte populations is generally one to two logs higher than chimerism analysis in whole white blood cell preparations. However, our experience within the EUC study indicated that the reproducibility of chimerism results is higher when using 10 ng template DNA as compared to 1 ng.
7. Split peaks: Several DNA polymerases can catalyze the addition of a single nucleotide (usually adenosine) to the 3′ends of double-stranded PCR amplicons. This non-template addition leads to the generation of PCR products that are one base pair longer than the actual target sequence. In order to avoid the occurrence of split peaks that are one base apart due to inefficient nucleotide addition, a terminal cycling step at 60 °C for 30 min is included in the PCR profile. This step provides the polymerase with extra time to complete nucleotide addition to all double-stranded PCR products, thus usually preventing formation of split peaks.

8. A run time of 20 min is sufficient for the separation of PCR products up to ~400 bp in length. For analysis of longer PCR products, the run time has to be extended.
9. The injection parameters need to be adjusted according to the yield of the PCR reaction and generally range between 5- and 15-s injection time and 1–6 kV. Usually, samples are analyzed using different parameters in order to achieve optimal sensitivity. Because the lower limit of specific signal detection considering the noise level is around 50 rfu, the peak height of the dominant alleles should be around 5,000 rfu. This permits the detection of subdominant alleles at a sensitivity level of about 1 %. Quantitative assessment is possible only if the detected peaks are not off-scale. Off-scale peaks are very high peaks (saturated signals), recognized and indicated by the software. They are either displayed as double peaks (tip of the peak is bent down) or indicated by a colored bar.
10. For quantitative analysis of donor and recipient alleles, both peak height and peak area can be used. The formula used for calculating the degree of (most commonly recipient) chimerism is based on the quotient between recipient and donor allele peak heights or areas. The mode of quantitative analysis may differ between individual centers [20]. Some investigators select only one unique allele from each recipient and donor for the calculation. Like many others, we include all unique recipient and donor alleles in the calculation, while shared alleles are excluded [25]. The general formula used is

    $$\text{Percentage of recipient cells} = 100 \times (A+B) : (A+B) + (C+D).$$

    The letters A and B represent the peak heights or areas of recipient alleles and the letters C and D those of donor alleles.
11. The so-called stutter peaks resulting from polymerase slippage during the amplification of microsatellite loci typically migrate at a distance of one repeat unit in front of the parent allele and may interfere with specific allelic peaks. This problem must be accounted for by judicious marker selection. As a general rule, informative donor and recipient alleles must be separated by at least two repeat units to prevent interference with stutter peaks. Occasionally, a second stutter allele, located at a distance of two repeat units from the main peak, may be present. If the second stutter is of relevant height, i.e., more than 1 % of the main peak, another marker should be selected for chimerism analysis. The problem of second stutter peaks can be avoided by selecting a marker that provides donor and recipient peaks separated by more than two repeat units. In general, tetra- and pentanucleotide repeat markers (i.e., microsatellite loci displaying a repeat motif of four and five nucleotides in length,

respectively) yield less prominent stutter peaks and are therefore preferred over di- and trinucleotide repeat markers (i.e., microsatellite loci displaying a repeat motif of two or three nucleotides in length).

12. In certain instances, the so-called bleed-through signals [26] may be observed, which may affect the interpretation of results. When using very high injection parameters, the standard (red) may result in signals visible in analyses of green-labelled PCR products. The same phenomenon may occur in multiplex PCR reactions combining primers labelled by different dyes or in the presence of extremely high signals where false (bleed-through) signals may be observed in different color windows.
13. The occurrence of dye-associated nonspecific peaks [27] is a problem peculiar to the fluorescence-based technology discussed. Apparently, the fluorescent dyes FAM, HEX, and NED may give rise to formation of multiple template-independent peaks at positions characteristic for each dye. The peaks can be relatively high and migrate in a range similar to that of many microsatellite markers. The signals may therefore interfere with specific microsatellite peaks and thus compromise the analysis of chimerism. There is currently no clear explanation for this phenomenon. If this problem is observed, a feasible approach to its elimination is having primers for each microsatellite locus labelled with different fluorescent dyes and selecting a primer/dye combination that does not show any interference between the specific alleles of the marker used and the dye-associated peak positions.
14. In addition to the occurrence of nonspecific peaks, as indicated above, other problems may lead to the appearance of extra signals. Conversely, the problem of faint or absent peaks may also occur. Some of the common causes and possible measures are listed below:

Extra signals and background signals

| Possible cause | Recommended measure |
|---|---|
| Contamination with extraneous DNA | Use appropriate precautions and controls (aerosol-resistant pipette tips, separation of pre- and post-PCR areas) |
| DNA input too high | Decrease the amount of template DNA or reduce the number of PCR cycles |
| Sample not completely denatured | Heat sample to 93 °C for 3 min before capillary electrophoresis |
| Insufficient DNA quality | Prevent samples from DNA degradation |

Faint or no signals

| Possible cause | Recommended measure |
|---|---|
| Impure DNA—presence of inhibitors | Test different extraction methods combined with purification of DNA through a spin column |
| Insufficient template DNA | Increase the amount of DNA template |
| Primer concentration too low | Increase primer concentration |
| Incorrect PCR program | Check the PCR program |
| Wrong $MgCl_2$ concentration | Test different concentrations of $MgCl_2$ |

15. If highly polymorphic microsatellite loci are used, only a limited number need to be tested in order to reveal one or more informative markers in virtually any donor/recipient constellation. In matched sibling and haploidentical transplants, more markers are generally required in order to differentiate between donor and recipient cells as compared to the unrelated setting. The screening panels used at most centers include 6–15 microsatellite markers. Genotyping by multiplex reactions established within the EUC study including 4–5 selected EUC markers [23] was demonstrated to provide at least one STR marker optimally suited for quantitative chimerism analysis in any related or unrelated donor/recipient setting.
16. Criteria for the selection of optimal informative markers have been proposed by the EUC consortium: the minimum requirements for an eligible allelic constellation include the presence of at least one unique donor and recipient allele and a distance between informative alleles corresponding to at least two tandem repeat units [21].
17. Due to preferential amplification of short fragments during PCR cycling, minor recipient cell populations may be detected with greater sensitivity if the informative recipient alleles are shorter in length than any donor allele. Although microsatellite markers usually show relatively small differences in length between alleles, amplification efficiencies may nevertheless differ significantly and therefore have an impact on the sensitivity of the assays.
18. The reported average sensitivity in detecting minor (in most instances recipient-derived) cell populations using different microsatellite markers ranges from 1 to 5 %. The sensitivity may to a large extent depend on the size (i.e., amplicon length) of the informative recipient allele(s), the allelic constellation, and the number of alleles co-amplified. In practice, however, some markers from the panels used at individual centers tend to provide higher sensitivity than others and are therefore used preferentially.

## References


1. Dubovsky J, Daxberger H, Fritsch G, Printz D, Peters C, Matthes S et al (1999) Kinetics of chimerism during the early post-transplant period in pediatric patients with malignant and non-malignant hematologic disorders: implications for timely detection of engraftment, graft failure and rejection. Leukemia 13:2060–2069
2. Pérez-Simón JA, Caballero D, Lopez-Pérez R, Mateos G, Canizo C, Vazquez L et al (2002) Chimerism and minimal residual disease monitoring after reduced intensity conditioning (RIC) allogeneic transplantation. Leukemia 16:1423–1431
3. Matthes-Martin S, Lion T, Haas OA, Frommlet F, Daxberger H, Konig M et al (2003) Lineage-specific chimaerism after stem cell transplantation in children following reduced intensity conditioning: potential predictive value of NK-cell chimaerism for late graft rejection. Leukemia 17:1934–1942
4. Lion T, Daxberger H, Dubovsky J, Filipcik P, Fritsch G, Printz D et al (2001) Analysis of chimerism within specific leukocyte subsets for detection of residual or recurrent leukemia in pediatric patients after allogeneic stem cell transplantation. Leukemia 15:307–310
5. Liesveld JL, Rothberg PG (2008) Mixed chimerism in SCT: conflict or peaceful coexistence? Bone Marrow Transplant 42:297–310
6. Lawler M, McCann SR, Marsh JC, Ljungman P, Hows J, Vandenberghe E, Severe Aplastic Anaemia Working Party of the European Blood and Marrow Transplant Group et al (2009) Serial chimerism analyses indicate that mixed haemopoietic chimerism influences the probability of graft rejection and disease recurrence following allogeneic stem cell transplantation (SCT) for severe aplastic anaemia (SAA): indication for routine assessment of chimerism post SCT for SAA. Br J Haematol 144:933–945
7. Breuer S, Preuner S, Fritsch G, Daxberger H, Koenig M, Poetschger U et al (2012) Early recipient chimerism testing in the T- and NK-cell lineages for risk assessment of graft rejection in pediatric patients undergoing allogeneic stem cell transplantation. Leukemia 26:509–519
8. Bader P, Kreyenberg H, Hoelle W, Dueckers G, Handgretinger R, Lang P et al (2004) Increasing mixed chimerism is an important prognostic factor for unfavorable outcome in children with acute lymphoblastic leukemia after allogeneic stem-cell transplantation: possible role for pre-emptive immunotherapy? J Clin Oncol 22:1696–1705
9. Bader P, Kreyenberg H, Hoelle W, Dueckers G, Kremens B, Dilloo D et al (2004) Increasing mixed chimerism defines a high-risk group of childhood acute myelogenous leukemia patients after allogeneic stem cell transplantation where pre-emptive immunotherapy may be effective. Bone Marrow Transplant 33:815–821
10. Chalandon Y, Vischer S, Helg C, Chapuis B, Roosnek E (2003) Quantitative analysis of chimerism after allogeneic stem cell transplantation by PCR amplification of microsatellite markers and capillary electrophoresis with fluorescence detection: the Geneva experience. Leukemia 17:228–231
11. Schraml E, Daxberger H, Watzinger F, Lion T (2003) Quantitative analysis of chimerism after allogeneic stem cell transplantation by PCR amplification of microsatellite markers and capillary electrophoresis with fluorescence detection: the Vienna experience. Leukemia 17:224–227
12. Kreyenberg H, Holle W, Mohrle S, Niethammer D, Bader P (2003) Quantitative analysis of chimerism after allogeneic stem cell transplantation by PCR amplification of microsatellite markers and capillary electrophoresis with fluorescence detection: the Tuebingen experience. Leukemia 17:237–240
13. Acquaviva C, Duval M, Mirebeau D, Bertin R, Cave H (2003) Quantitative analysis of chimerism after allogeneic stem cell transplantation by PCR amplification of microsatellite markers and capillary electrophoresis with fluorescence detection: the Paris-Robert Debre experience. Leukemia 17:241–246
14. Hancock JP, Goulden NJ, Oakhill A, Steward CG (2003) Quantitative analysis of chimerism after allogeneic bone marrow transplantation using immunomagnetic selection and fluorescent microsatellite PCR. Leukemia 17:247–251
15. Koehl U, Beck O, Esser R, Seifried E, Klingebiel T, Schwabe D, Seidl C (2003) Quantitative analysis of chimerism after allogeneic stem cell transplantation by PCR amplification of microsatellite markers and capillary electrophoresis with fluorescence detection: the Frankfurt experience. Leukemia 17:232–236

16. Maas F, Schaap N, Kolen S, Zoetbrood A, Buno I, Dolstra H et al (2003) Quantification of donor and recipient hemopoietic cells by real-time PCR of single nucleotide polymorphisms. Leukemia 17:621–629
17. Fredriksson M, Barbany G, Liljedahl U, Hermanson M, Kataja M, Syvänen AC (2004) Assessing hematopoietic chimerism after allogeneic stem cell transplantation by multiplexed SNP genotyping using microarrays and quantitative analysis of SNP alleles. Leukemia 18:255–266
18. Jimenez-Velasco A, Barrios M, Roman-Gomez J, Navarro G, Buno I, Castillejo JA et al (2005) Reliable quantification of hematopoietic chimerism after allogeneic transplantation for acute leukemia using amplification by real-time PCR of null alleles and insertion/deletion polymorphisms. Leukemia 19:336–343
19. Najfeld V, Burnett W, Vlachos A, Scigliano E, Isola L, Fruchtman S (1997) Interphase FISH analysis of sex-mismatched BMT utilizing dual color XY probes. Bone Marrow Transplant 19:829–834
20. Lion T (2003) Summary: reports on quantitative analysis of chimerism after allogeneic stem cell transplantation by PCR amplification of microsatellite markers and capillary electrophoresis with fluorescence detection. Leukemia 17:252–254
21. Watzinger F, Lion T, Steward C (2006) The RSD code: proposal for a nomenclature of allelic configurations in SRT-PCR-based chimerism testing after allogeneic stem cell transplantation. Leukemia 20:1448–1452
22. Thiede C, Bornhäuser U, Brendel C, Leo R, Daxberger H, Mohr B et al (2001) Sequential monitoring of chimerism and detection of minimal residual disease after allogeneic blood stem transplantation (BSCT) using multiplex PCR amplification of short tandem repeat-markers. Leukemia 15:293–302
23. Lion T, Watzinger F, Preuner S, Kreyenberg H, Tilanus M, de Weger R et al (2012) The EuroChimerism concept for a standardized approach to chimerism analysis after allogeneic stem cell transplantation. Leukemia 26: 1821–1828
24. Thiede C, Prange-Krex G, Freiberg-Richter J, Bornhauser M, Ehninger G (2000) Buccal swabs but not mouthwash samples can be used to obtain pretransplant DNA fingerprints from recipients of allogeneic bone marrow transplants. Bone Marrow Transplant 25:575–577
25. Thiede C, Lion T (2001) Quantitative analysis of chimerism after allogeneic stem cell transplantation using multiplex PCR amplification of short tandem repeat markers and fluorescence detection. Leukemia 15:303–306
26. Moretti TR, Baumstark AL, Defenbaugh DA, Keys KM, Smerick JB, Budowle B (2001) Validation of short tandem repeats (STRs) for forensic usage: performance testing of fluorescent multiplex STR systems and analysis of authentic and simulated forensic samples. J Forensic Sci 46:647–660
27. Schraml E, Lion T (2003) Interference of dye-associated fluorescence signals with quantitative analysis of chimerism by capillary electrophoresis. Leukemia 17:221–223

# Chapter 15

# Urinary Proteomics Employing Capillary Electrophoresis Coupled to Mass Spectrometry in the Monitoring of Patients After Stem Cell Transplantation

**Eva M. Weissinger, William Mullen, and Amaya Albalat**

## Abstract

Complex biological samples hold significant information on the health status and development of disease. Approximately 22,000 human genes give rise to more than 400,000 proteins as functional entities (Anderson and Anderson, Electrophoresis 19:1853–1861, 1998). Thus, the proteome provides a much richer source of information than the genome for describing the state of health or disease of humans. The composition of body fluids comprises a rich source of information on changes of protein and peptide expression. Here we describe the application of capillary electrophoresis (CE) coupled online to an electrospray-ionization time-of-flight mass spectrometer (ESI-TOF-MS) to analyze human urine for the identification of biomarkers specific for complications after allogeneic hematopoietic stem cell transplantation (Kaiser et al. Blood 104:340–349, 2004; Weissinger et al. Blood 109:5511–5519, 2007). In addition, we describe methods for the sequencing of native proteins/peptides, necessary for the identification of possible new therapeutic targets.

**Key words** Proteomics, Hematopoietic stem cell transplantation, Capillary electrophoresis, Mass spectrometry, Polypeptide, Clinical diagnosis

## 1 Introduction

Application of proteome analysis towards clinical questions has developed into a growing field. Several different technologies have been applied, and a plethora of specimen types has been investigated. While the apparently obvious choice of an appropriate specimen at first sight seemed to be plasma or serum, urine has received growing attention, mostly due to the fact that it can be easily collected and also due to its stability [4].

The current mostly used technological approaches are 2D gel electrophoresis, followed by mass spectrometry (MS) of tryptically digested proteins or liquid chromatography (LC)-based approaches coupled to MS for initial discovery aiming at higher molecular mass proteins. When examining the lower molecular

Meral Beksaç (ed.), *Bone Marrow and Stem Cell Transplantation*, Methods in Molecular Biology, vol. 1109,
DOI 10.1007/978-1-4614-9437-9_15, 

proteome/peptidome, LC or capillary electrophoresis (CE) coupled to MS are most widely used [5]. Of these CE demonstrated several advantages in direct comparison [6].

Depending on the approach, the proposed biomarkers are subsequently either assessed (aiming at validation) using the same platform as in the discovery studies (mostly applicable to CE-MS) or transferred onto a different platform that allows targeted assessment and higher throughput [7]. In most cases, these platforms are immunological type assays. Recently, the use of mass spectrometry-based multiple reaction monitoring (MRM)-type approaches has been advocated [8]. While these assays have the advantage of not requiring specific agents (like antibodies), their applicability in a true clinical setting still has to be demonstrated.

CE-MS has been developed as a routine platform for the analysis of urinary peptides [9, 10]. It has been employed for the comparable analysis of over 20,000 urine samples, including >2,000 samples from patients after allogeneic hematopoietic stem cell transplantation (HSCT) [11, 12]. HSCT currently represents the only permanent cure for many patients with hematological malignancies or marrow dysfunction syndromes. Complications after HSCT, such as concurrent infection in the time of aplasia, reactivation of viruses such as cytomegalovirus (CMV), or development of immunological complications such as graft-versus-host disease (GvHD), limit the application of HSCT.

Here we describe the application of CE-MS for the analysis of urine from patients after allogeneic HSCT, aiming at early detection of GvHD [3]. This approach is currently already employed in a clinical intervention study and hence represents an example for clinical decision making based on proteome analysis. We describe the methods employed for urine sample preparation, MS analysis, and data evaluation. Further, we describe the methods used for sequencing of the naturally occurring peptides that are employed as biomarkers.

CE-MS is a powerful tool allowing fast and reliable analysis of peptides from complex biological samples, such as urine [13], plasma [14], cerebrospinal fluid [15], dialysis fluid [16], or tissue culture supernatant [17]. Information on >1,000 peptides can be obtained from an ~1-h analysis, and the platform has been extensively characterized [18]. Although these peptides and proteins can serve as excellent biomarkers for diagnostic purposes, their potential physiological role remains unknown as long as their identity defined by their amino acid sequence is not determined. The identification of the defined biomarkers presents some unique challenges. The biomarkers cannot be easily isolated; the sequence analysis has to be performed from a complex mixture, and potential biomarkers are frequently post-translationally modified [5]. For this purpose, two principal approaches have been employed: direct interfacing of CE with MS/MS instruments, or employing LC-MS/MS, and calculating the CE migration time based on the peptide sequence [19].

## 2 Materials

### 2.1 Preparation of Urine

1. Urine samples are collected cold, immediately frozen, and stored at −20 °C.
2. Buffer for sample dilution: 2 M Urea, 100 mM NaCl, 0.0125 % $NH_4OH$ containing 0.01 % SDS.
3. Elution buffer: 0.01 % $NH_4OH$ in HPLC-grade water (pH 10.5–11.5).
4. Centrisart ultrafilter tubes 20 kD, 0.62 $cm^2$ tubes (Sartorius Stedim Limited, UK).
5. PD-10 desalting columns (GE Healthcare Biosciences AB, Bedford, USA).
6. BCA protein quantification kit (Uptima, Interchim, Montluçon, France).
7. Lyophilization Christ Speed-Vac RVC 2-18/Alpha 1-2 (Christ, Osterode am Harz, Germany).

### 2.2 Proteomic Profiling Using CE-MS

1. Capillary Electrophoresis P/ACE MDQ system (Beckman Coulter, Fullerton, USA).
2. Capillary: 90 cm, 50 μm I.D. fused silica capillary (New Objective, Woburn, USA).
3. Conditioning of new capillaries: 1 M NaOH in HPLC-grade water.
4. $NH_4OH$ solution: 2 % solution of $NH_4OH$ in HPLC-grade water.
5. CE-running buffer: 20 % (v/v) ACN and 0.95 % formic acid.
6. Sheath liquid: 30 % (v/v) iso-propanol (Sigma-Aldrich, Germany) and 0.4 % (v/v) formic acid in HPLC-grade water.
7. ESI-TOF sprayer-kit (Agilent Technologies, Palo Alto, CA, USA).
8. Micro-TOF-MS (ESI-TOF; Bruker Daltonik, Bremen, Germany).
9. Single-syringe infusion pump (Cole-Parmer Instrument Company, USA).
10. Hamilton syringe 500 μL (Hamilton Company, USA).
11. Software: Mosaiques Visu: for peak detection (biomosaiques software, Hannover, Germany).
12. MosaCluster: SVM-based program for grouping according to multiple parameters (biomosaiques software, Hannover, Germany).

### 2.3 Sequencing of Peptides

1. Dionex Ultimate 3000 RSLS nano flow system (Dionex, Camberly, UK).
2. Nano trap column: Dionex 0.1 × 20 mm 5 μm C18 (Dionex, Camberly, UK).
3. Nano column: Acclaim PepMap C18 nano column 75 μm × 50 cm, 2 μm 100 Å (Dionex, Camberly, UK).
4. Proxeon nano spray ESI source (Thermo Fisher, Hemel, UK).
5. Orbitrap Velos FTMS mass spectrometer (Thermo Fisher, Hemel, UK).

## 3 Methods

The methods described below outline (1) the sample preparation; (2) the CE-MS analysis; (3) data processing, analysis to evaluate the CE-MS data for clinical application and identify specific biomarkers, and development of high-dimensional classifiers for different diseases or complications; and (4) sequencing of possible biomarkers.

### 3.1 Sample

Body fluids are complex mixtures of molecules with a wide range of polarity, hydrophobicity, and size. When analyzing complex biological samples, major concerns are loss of analytes during the sample preparation as well as reproducibility of the data generated. Ideally, a crude unprocessed sample should be analyzed. This would avoid all artifacts, losses, or biases arising from sample preparation. However, this is impossible, and compromises have to be made, also due to the respective technology used. In CE-MS analysis of urine, salts, lipids, and large molecules, e.g., albumin, immunoglobulin, and others, have to be removed, since these molecules will interfere with the detection of smaller, less abundant proteins and peptides.

#### 3.1.1 Collection and Storage of the Samples

Urine samples were obtained from patients at different time points before and after HSCT, starting prior to conditioning and weekly thereafter for the time on the transplantation ward. The samples are typically taken as the second spot urine, voiding the first urine of the day, as also suggested by the recommendations for urinary proteomics [20]. Proper handling of the samples is of outmost importance; the urine should be aliquoted, frozen immediately after collection, and stored at −20 °C until analysis (*see* **Note 1**).

#### 3.1.2 Sample Preparation

1. Defrost urine samples at room temperature and mix gently by inversion.
2. While samples are thawing, mix them with PMSF (saturated solution in ethanol) in a ratio of 1/1,000 (v/v).

3. Thaw a 0.7 mL aliquot of urine immediately before use and dilute with 0.7 mL of urea buffer (2 M urea, 100 mM NaCl, 0.0125 % $NH_4OH$ containing 0.01 % SDS).
4. In order to remove high-molecular-weight polypeptides, filter samples using Centrisart ultracentrifugation filter devices (20 kDa molecular weight cutoff; Sartorius, Goettingen, Germany) at 3,000 × *g* until 1.1 mL of filtrate was obtained.
5. Subsequently, desalt the filtrate using a PD-10 column (GE Healthcare, Sweden) equilibrated in 0.01 % $NH_4OH$ in HPLC-grade water.
6. Finally lyophilize samples, and store the samples at 4 °C. Shortly before CE-MS analysis, resuspend all lyophilisates in HPLC-grade water to a final protein concentration of 2 μg/μL checked by BCA assay (Interchim, Montlucon, France) (*see* **Note 2**).

### 3.2 CE-MS Analysis of the Samples

The samples are transferred to appropriate vials and stored in the CE-auto sampler section at 5 °C. For capillary electrophoresis a P/ACE MDQ (Beckman Coulter, Fullerton, USA) system is used equipped with a 90 cm, 50 μm inner diameter, bare-fused silica capillary. The use of coated capillaries, at present, appears not to be beneficial (*see* **Note 3**).

#### 3.2.1 Capillary Electrophoresis

1. Rinse the capillary with running buffer for 3 min prior to sample injection.
2. Inject the sample for 99 s with 2 psi, resulting in the injection of ~250 nL of sample.
3. Perform separation with +25 kV at the injection side, and set the capillary temperature to 35 °C for the entire length of the capillary up to the ESI interface.
4. After each run, rinse the capillary, with deionized water (50 psi) for 1 min followed by a washing step with $NH_4OH$ solution (50 psi) for 3 min, followed by a flushing step with deionized water (50 psi) for 3 min. The CE-MS setup is depicted in Fig. 1.

#### 3.2.2 CE-MS Interface and Analysis

The MS analysis is performed in positive electrospray mode with an ESI-TOF sprayer-kit (Agilent technologies, Palo Alto, CA, USA) using a Micro-TOF-MS (Bruker Daltonik, Bremen, Germany). The ESI sprayer is grounded and the ion spray interface potential is set between –3,700 and –4,100 V. The sheath liquid is applied coaxially, consisting of 30 % (v/v) iso-propanol (Sigma-Aldrich) and 0.4 % (v/v) formic acid in HPLC-grade water, at a flow rate of 0.02 mL/h. These conditions result in a detection limit of about 1 fmol of different standard peptides. MS spectra are accumulated every 3 s, over a *m/z* range from 400 to 2,500 or 3,000 for about 45–60 min.

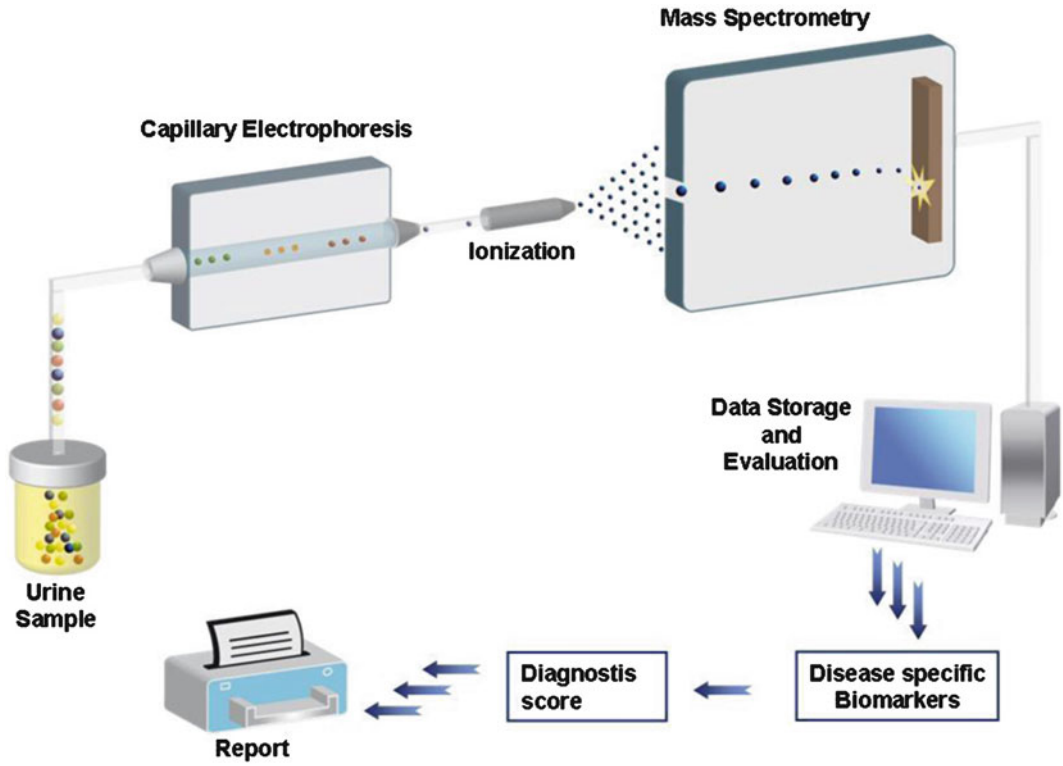


**Fig. 1** Online coupling of CE-MS and setup for data processing. A schematic drawing of the online coupling of CE-MS is shown here. After preparation the sample is separated in the CE and sprayed directly into the MS, where the *m/z* and the signal intensity are scored. The data processing and identification of the pattern take place, and all data are stored in the database. Reprinted with permission from ref. 35

### *3.3 Data Processing and Statistical Analysis*

#### *3.3.1 Data Processing: Peak Annotation*

Mass spectral ion peaks representing identical molecules at different charge states were deconvoluted into single masses using Mosaiques Visu software [22]. Mosaiques Visu employs a probabilistic clustering algorithm and uses both isotopic distribution as well as conjugated masses for charge-state determination of polypeptides. In a first analysis, the software identifies all peaks within each single spectrum. This usually results in more than 100,000 peaks from a single sample. Since true analytes must appear in several, e.g., at least three, successive spectra, signals from individual peptides present in consecutive spectra are collected, evaluated with respect to charge state, and combined. This reduces the list to 3,000–7,000 "CE/MS" peaks. These data are termed "peak list" of an individual sample. Signals have to meet certain criteria, like the following: (1) the signal intensity must be greater than the threshold (usually $S/N > 4$); (2) peaks must be multiply charged; and (3) peak width must be below the threshold of 2 min. Signals not conforming with the abovementioned criteria are removed. In the next step peaks representing identical molecules with different charge states are identified and combined, and all *m/z* signals are

deconvoluted into mass. The data are condensed to a list of features, defined by migration time and mass and signal intensity as a measure for relative abundance for each individual peptide, generally between 1,000 and 2,500 individual peptides per sample.

#### 3.3.2 Data Normalization

Both CE migration time and ion signal intensity show variability, mostly due to different amounts of salt and peptides in the sample. To allow comparison and search for conformity and differences between several samples, data have to be normalized as described in detail [21]. Reference signals from 1,770 urinary polypeptides are used for CE time calibration by local regression. For normalization of analytical and urine dilution variances, MS signal intensities are normalized relative to 29 "housekeeping" peptides generally present with high frequency in all urine samples and with small relative standard deviation. For calibration, local linear regression is performed. Precise TOF-MS data are calibrated using 80 accurately characterized reference masses (mass deviation <0.5 ppm) by FT-ICR-MS applying linear regression. The obtained peak lists characterize each polypeptide by its molecular mass (Da), calibrated CE migration time (min), and normalized signal intensity. All detected peptides are deposited, matched, and annotated in a Microsoft SQL database allowing further statistical analysis (Fig. 2). Intra- and inter-assay variability are ascertained by repeated analysis of one sample and by analysis of samples obtained at different time points from the same patient under comparable conditions, respectively, and have been described in detail [18, 23].

#### 3.3.3 Identification of Potential Biomarkers

In the discovery phase, the natural logarithm-transformed signal amplitude of the individual urinary peptides is compared between patients and controls, using the Wilcoxon rank sum test. This nonparametric test has been found to be well suitable for skewed proteomic data [24]. We tested the null hypothesis that patients and controls have the same continuous distribution of signal amplitude of CE-MS urinary polypeptide profile. The signal amplitude represents the calibrated counts (intensity) recorded by the mass spectrometry device. Statistical adjustment for multiple testing is performed by applying Benjamini–Hochberg [25], controlling the false discovery rate at a level of 0.05. Hence urinary peptides discriminating between cases and controls, serving as potential biomarkers, are identified based on statistical evaluation.

### 3.4 Establishment of a High-Dimensional Classifier

As no single biomarker that can ideally separate cases and controls could be identified, several biomarkers are ideally combined into a classifier. Several different approaches of combining biomarkers have been investigated [24]. In general multidimensional classifiers consistently outperformed linear combinations. Of the high-dimensional classifiers, support vector machines (SVM) are generally among the highest scoring, and hence they are routinely employed. SVM perform

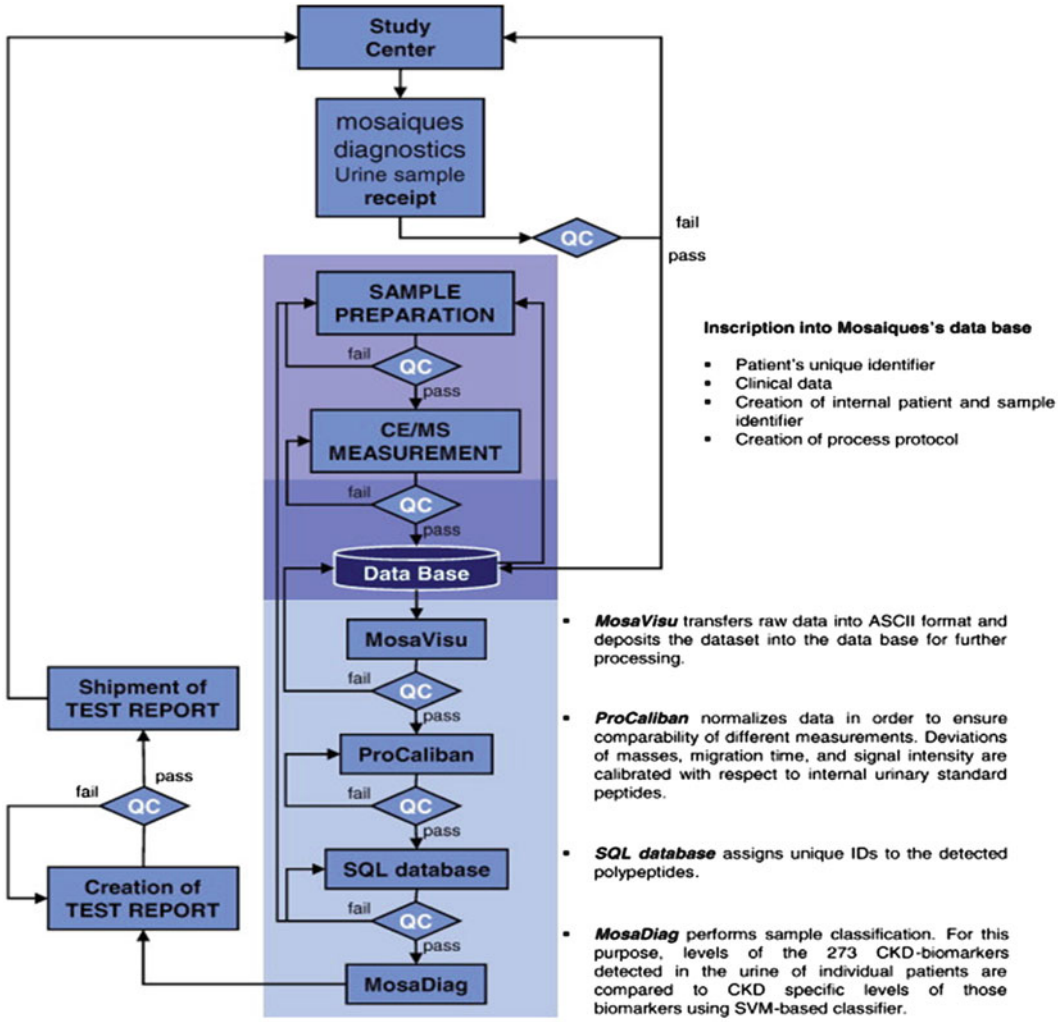


**Fig. 2** Graphic depiction of the information flow and quality control step in analysis and data processing. Reprinted with permission from ref. 18

classification by constructing an $N$-dimensional hyperplane that optimally separates subjects (e.g., case and controls, see Fig. 3) into two categories. A set of features that describes a subject i (i.e., a row built by $N$ intensities of the biomarkers) is called a *vector* and denoted here by $x_i$.

The aim of SVM classification is to find the optimal hyperplane that separates clusters of vectors in such a way that case subjects are on one side of the plane and controls are on the other side. The vectors near the hyperplane are called *support vectors*. If the two classes are separable, the simplest way to distinguish either group would be a flat ($N$–1)-dimensional plane embedded in the $N$-dimensional space. In reality, the points in the case/control study are separated by a nonlinear region. Instead of trying to fit

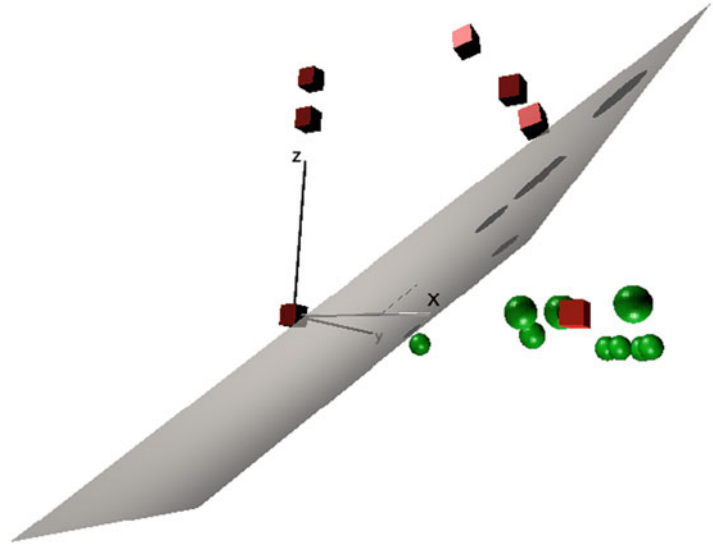


**Fig. 3** Graphic depiction of separation in an SVM-based classifier. The position of each patient (*red* cubes) and control (*green* spheres) is defined by the log-transformed amplitude of three biomarkers, X, Y, and Z, which define the unique position in this 3-dimensioanl space. Subsequently, a (3-1) 2-dimensional plane is introduced that separates the two groups in the best possible way. Classifiers based on *N* biomarkers (hence dimensions) and an *N*–1-dimensional separating hyperplane cannot be graphically depicted but can well be mathematically defined

nonlinear curves to the data, SVM handles this by using a *kernel function* to map the data into a different space, where a hyperplane can be found to do the separation. MosaCluster uses Gaussian basis radial functions for transforming the data into a higher dimensional space to make the separation possible. Ideally SVM classification should produce a hyperplane that completely separates the subjects into two non-overlapping groups. However, in reality perfect separation is often impossible. Hence misclassification and some flexibility in the separating hyperplane are allowed, defined as cost for misclassification $C$ and flexibility, $\gamma$, creating a *soft margin* that permits some misclassifications. Increasing the value of $C$ increases the cost of misclassifying points and forces the algorithm to adapt the model to a higher extent to the training dataset. However, a highly adapted model may not generalize well in independent datasets, a phenomenon called *over-fitting*.

The accuracy of an SVM model is largely dependent on the selection of the model parameters $C$ and $\gamma$ (Fig. 3). Grid searches are employed to identify best possible parameter combinations of $C$ and $\gamma$ in the training set, employing cross-validation. Based on these parameters every new subject is assigned an SVM score that depends on the Euclidian distance of the dataset to the ($N$-1)-dimensional maximal margin hyperplane (absolute value of the normal vector) and the direction of the vector.

### 3.5 Assessing the Performance of the Proteomics-Based Classifier

As a result of possible bias, but also over-fitting of high-dimensional classifiers, it is mandatory that the results are verified or validated in an independent test set, prior to clinical application [7, 24, 26, 27]. In the test set, researchers blinded to the clinical condition of the study participants measured the cluster polypeptides. After breaking the code, we calculated sensitivity and specificity based on tabulating the number of *correctly classified* samples in the test set, using receiver operating characteristic (ROC) plots. The area under the ROC curve (AUC) provides a single measure of overall accuracy that is independent of any particular threshold [20].

### 3.6 Mass Spectrometry for Polypeptide Identification

Sequencing of biomarkers is not necessary for diagnostic application of proteomic patterns but is essential for further investigation of pathophysiology of different diseases and for the search for therapeutic targets. The "bottom-up" approach (2D gel electrophoresis and multidimensional protein identification technology) of analytical protein mass spectrometry utilizes an initial treatment with a protease (usually trypsin) for protein identification to break proteins into relatively small peptides of which the $m/z$ can be accurately determined by mass spectrometry. This so-called peptide mass fingerprinting allows reliable identification (see for example [28]). In biomarker discovery experiments a different approach has become popular: a "top-down" approach, in which polypeptides are delivered to the mass spectrometer without prior trypsinization. Depending on the mass accuracy of the mass spectrometer used, peptides and small proteins up to 10–20 kDa can be sequenced [29]. This approach requires very high accuracy and resolution to avoid false-positive identifications. Ion traps or any other low-resolution instruments are generally not recommended for this approach (see also required mass accuracy, below).

To identify biomarker candidates associated with complications in HSCT, selected ions (peptides) were sequenced using CE-MS/MS or LC-MS/MS analysis, as described in detail [23]. MS/MS experiments were performed on a CE instrument under identical conditions as described above, using a Micro-TOFQ-MS (Bruker Daltonik, Bremen, Germany) or using an Ultimate 3000 nano-flow system (Dionex/LC Packings, USA) connected to an LTQ Orbitrap hybrid mass spectrometer (Thermo Fisher Scientific, Germany) equipped with a nano-electrospray ion source. The mass spectrometer was operated in a data-dependent mode to automatically switch between MS and MS/MS acquisition. Survey full-scan MS spectra (from $m/z$ 300–2,000) were acquired in the Orbitrap. Ions were sequentially isolated for fragmentation. All resultant MS/MS data were searched against the IPI human non-redundant database using the Open Mass Spectrometry Search Algorithm (OMSSA, http://pubchem.ncbi.nlm.nih.gov/omssa), with an e-value cutoff of 0.01. Accepted deviations in the parent ion mass were 10 ppm and 0.05 Da for the fragment ions. For further

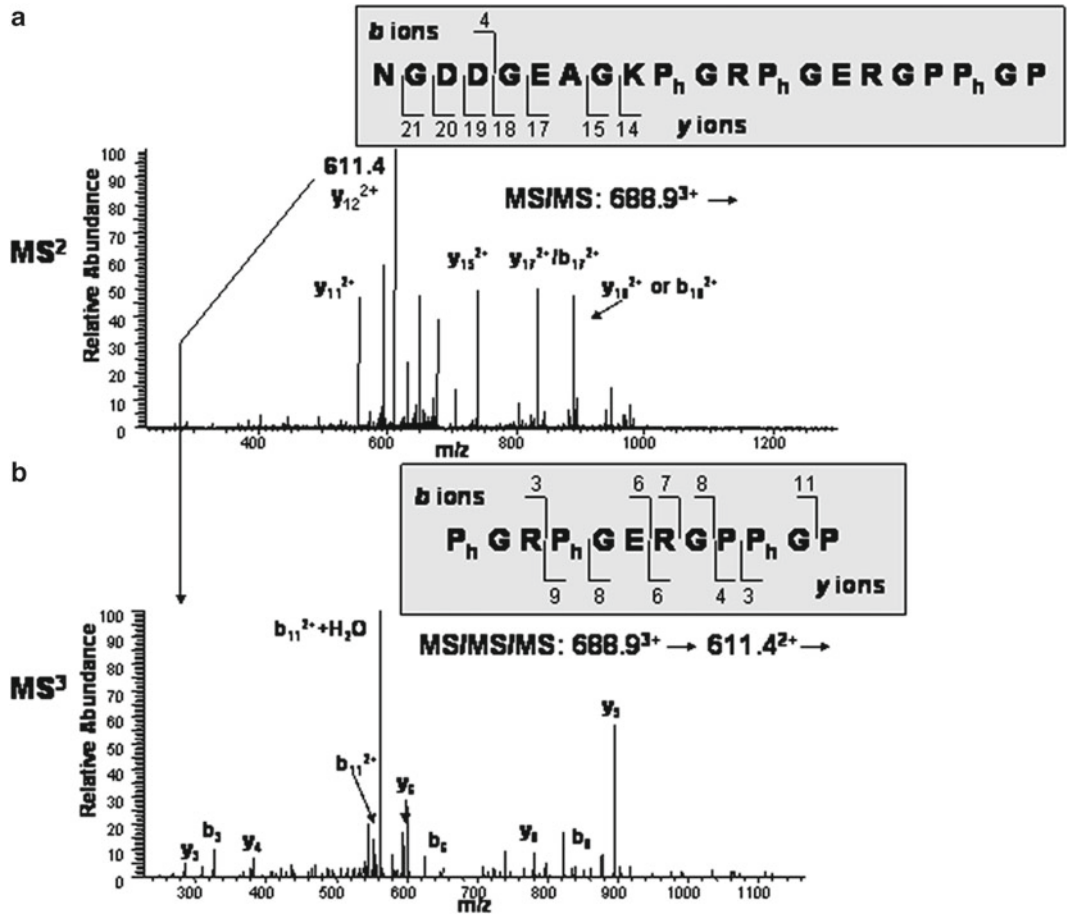


**Fig. 4** $MS^2$ and $MS^3$ analysis of a urine peptide published by Zürbig et al. [16]. (**a**) $MS^2$ of *m/z* 688.931 showing a limited number of abundant doubly charged y-ions. (**b**) $MS^3$ of the *m/z* 611.421 fragment ion from CID of 688.931 showing multiple fragment ions that allows complete sequence identification

validation of peptide identifications obtained from LC-MS/MS analysis, the strict correlation between peptide charge at the working pH of 2 and CE migration time was utilized to minimize false-positive identification rates [19]. Calculated CE migration time of the sequence candidate based on its peptide sequence (number of basic amino acids) was compared to the experimental migration time. Peptides were only accepted with a mass deviation below ±25 ppm and a CE migration time deviation below ±1 min (Fig. 4).

## 4 Notes

1. The samples must be collected under proper conditions especially when highly sensitive analysis like MS is applied. While in common proteomic techniques, such as western blotting, ELISA, or even 2D gel electrophoresis minor degradation of

the proteins generally does not cause problems, any MS-based proteomic analysis will be severely hampered by degradation. The samples require storage at least at –20 °C immediately after collection in order to prevent degradation of proteins, which would result in additional fragments of proteins that are irrelevant to the underlying disease. Immediate cooling of the samples is another way to preserve the stability. Urine is a very stable body fluid, compared to serum or plasma, and thus in our hands is preferable over the other fluids.

2. Initial experiments and also our previous data revealed that higher molecular weight proteins in the urine sample generally appear not to contain significant information but cause severe problems during the CE-MS runs, like precipitation, clogging of the capillary, and overloading. Therefore, an optimized protocol to remove the confounding large molecules using ultrafiltration has been developed. The most abundant higher molecular weight protein is albumin, a carrier protein that binds a substantial fraction of other proteins and peptides. In order to prevent binding of small fragments to albumin, we use a chaotropic agent, urea, in combination with a detergent, SDS, for the dilution of the samples. Consistently good and reproducible results and recovery of >80 % of added standard polypeptides were observed in the presence of 2 M urea and 0.1 % SDS [30].
3. Under neutral or basic conditions the silanol groups of the capillary form a negatively charged surface which interacts with the positive charge of the proteins. This leads to peak broadening especially of highly charged molecules. To circumvent these problems, several different coatings and coating protocols have been described [31–34]. Our experience using different types of coating so far was quite unsatisfactory, and the optimal approach appears to be the use of uncoated capillaries. Decreasing the pH of the background electrolyte (BGE) reduces the negative charge of the surface, thus reducing capillary–protein interaction. Additionally, hydrophobic interactions can be reduced by adding organic solvent to the BGE. Therefore, best results are obtained at low pH in the presence of acetonitrile. It is important to point out that most coatings result in a positively charged capillary wall and cause an inverse electro-osmotic flow; consequently, the electrical field must be reversed.

## References

1. Anderson NL, Anderson NG (1998) Proteome and proteomics: new technologies, new concepts, and new words. Electrophoresis 19:1853–1861
2. Kaiser T, Kamal H, Rank A et al (2004) Proteomics applied to the clinical follow-up of patients after allogeneic hematopoietic stem cell transplantation. Blood 104:340–349
3. Weissinger EM, Schiffer E, Hertenstein B et al (2007) Proteomic patterns predict acute graft-versus-host disease after allogeneic

hematopoietic stem cell transplantation. Blood 109:5511–5519

4. Decramer S, de Gonzalez PA, Breuil B et al (2008) Urine in clinical proteomics. Mol Cell Proteomics 7:1850–1862
5. Mischak H, Coon JJ, Novak J et al (2009) Capillary electrophoresis-mass spectrometry as a powerful tool in biomarker discovery and clinical diagnosis: an update of recent developments. Mass Spectrom Rev 8:703–724
6. Mullen W, Albalat A, Gonzalez J et al (2012) Performance of different separation methods interfaced in the same MS-reflection TOF detector: a comparison of performance between CE versus HPLC for biomarker analysis. Electrophoresis 33:567–574
7. Mischak H, Allmaier G, Apweiler R et al (2010) Recommendations for biomarker identification and qualification in clinical proteomics. Sci Transl Med 2:46ps42
8. Picotti P, Aebersold R (2012) Selected reaction monitoring-based proteomics: workflows, potential, pitfalls and future directions. Nat Methods 9:555–566
9. Kaiser T, Wittke S, Just I et al (2004) Capillary electrophoresis coupled to mass spectrometer for automated and robust polypeptide determination in body fluids for clinical use. Electrophoresis 25:2044–2055
10. Schiffer E, Mischak H, Novak J (2006) High resolution proteome/peptidome analysis of body fluids by capillary electrophoresis coupled with MS. Proteomics 6:5615–5627
11. Siwy J, Mullen W, Golovko I, Franke J, Zurbig P (2011) Human urinary peptide database for multiple disease biomarker discovery. Proteomics Clin Appl 5:367–374
12. Stalmach A, Albalat A, Mullen W, Mischak H (2013) Recent advances in capillary electrophoresis coupled to mass spectrometry for clinical proteomic applications. Electrophoresis 34(11):1452–1464
13. Mischak H, Schanstra JP (2011) CE-MS in biomarker discovery, validation, and clinical application. Proteomics Clin Appl 5:9–23
14. Schiffer E, Liabeuf S, Lacroix C et al (2011) Markers of vascular disease in plasma from patients with chronic kidney disease identified by proteomic analysis. J Hypertens 29:783–790
15. Jahn H, Wittke S, Zürbig P et al (2011) Peptide fingerprinting of Alzheimer's disease in cerebrospinal fluid: identification and prospective evaluation of new synaptic biomarkers. PLoS One 6:e26540
16. Kaiser T, Hermann A, Kielstein JT et al (2003) Capillary electrophoresis coupled to mass spectrometry to establish polypeptide patterns in dialysis fluids. J Chromatogr A 1013:157–171
17. Jiang H, Schiffer E, Song Z et al (2008) Proteins induced by telomere dysfunction and DNA damage represent biomarkers of human aging and disease. Proc Natl Acad Sci U S A 105:11299–11304
18. Mischak H, Vlahou A, Ioannidis JP (2013) Technical aspects and inter-laboratory variability in native peptide profiling: the CE-MS experience. Clin Biochem 46:432–443
19. Zürbig P, Renfrow MB, Schiffer E et al (2006) Biomarker discovery by CE-MS enables sequence analysis via MS/MS with platform-independent separation. Electrophoresis 27:2111–2125
20. Mischak H, Kolch W, Aivalotis M et al (2010) Comprehensive human urine standards for comparability and standardization in clinical proteome analysis. Proteomics Clin Appl 4:464–478
21. Jantos-Siwy J, Schiffer E, Brand K et al (2009) Quantitative urinary proteome analysis for biomarker evaluation in chronic kidney disease. J Proteome Res 8:268–281
22. Neuhoff N, Kaiser T, Wittke S et al (2004) Mass spectrometry for the detection of differentially expressed proteins: a comparison of surface-enhanced laser desorption/ionization and capillary electrophoresis/mass spectrometry. Rapid Commun Mass Spectrom 18:149–156
23. Good DM, Zürbig P, Argiles A et al (2010) Naturally occurring human urinary peptides for use in diagnosis of chronic kidney disease. Mol Cell Proteomics 9:2424–2437
24. Dakna M, Harris K, Kalousis A et al (2010) Addressing the challenge of defining valid proteomic biomarkers and classifiers. BMC Bioinformatics 11:594
25. Benjamini Y, Hochberg Y (1995) Controlling the false discovery rate: a practical and powerful approach to multiple testing. J Royal Stat Soc B (Methodological) 57:125–133
26. Mischak H (2012) How to get proteomics to the clinic? Issues in clinical proteomics, exemplified by CE-MS. Proteomics Clin Appl 6:437–442
27. Mischak H, Ioannidis JP, Argiles A et al (2012) Implementation of proteomic biomarkers: making it work. Eur J Clin Invest 42:1027–1036
28. Henzel WJ, Watanabe C, Stults JT (2003) Protein identification: the origins of peptide mass fingerprinting. J Am Soc Mass Spectrom 14:931–942
29. Chalmers MJ, Mackay CL, Hendrickson CL et al (2005) Combined top-down and bottom-up mass spectrometric approach to characterization of biomarkers for renal disease. Anal Chem 77:7163–7171
30. Theodorescu D, Fliser D, Wittke S et al (2005) Pilot study of capillary electrophoresis coupled

to mass spectrometry as a tool to define potential prostate cancer biomarkers in urine. Electrophoresis 26:2797–2808

31. Belder D, Deege A, Husmann H, Kohler F, Ludwig M (2001) Cross-linked poly(vinyl alcohol) as permanent hydrophilic column coating for capillary electrophoresis. Electrophoresis 22:3813–3818
32. Johannesson N, Wetterhall M, Markides KE, Bergquist J (2004) Monomer surface modifications for rapid peptide analysis by capillary electrophoresis and capillary electrochromatography coupled to electrospray ionization-mass spectrometry. Electrophoresis 25:809–816
33. Liu CY (2001) Stationary phases for capillary electrophoresis and capillary electrochromatography. Electrophoresis 22:612–628
34. Ullsten S, Zuberovic A, Wetterhall M et al (2004) A polyamine coating for enhanced capillary electrophoresis-electrospray ionization-mass spectrometry of proteins and peptides. Electrophoresis 25:2090–2099
35. Mischak H, Delles C, Klein J, Schanstra JP (2010) Urinary proteomics based on capillary electrophoresis-coupled mass spectrometry in kidney disease: discovery and validation of biomarkers, and clinical application. Adv Chronic Kidney Dis 17:493–506

# INDEX



Meral Beksaç (ed.), *Bone Marrow and Stem Cell Transplantation*, Methods in Molecular Biology, vol. 1109,
DOI 10.1007/978-1-4614-9437-9, © Springer Science+Business Media New York 2014

## D

## E



## F



## G



## H

## M



## N



## O



## P

## R



## S



## T

## U



## Z